DOCTOR OF PHILOSOPHY

An investigation of the regulation of Sialoadhesin ligands on CD4+ T cells and its potential significance in Systemic Lupus Erythematosus

Kidder, Dana

Award date:
2011

DOCTOR OF PHILOSOPHY

An investigation of the regulation of Sialoadhesin ligands on CD4+ T cells and its potential significance in Systemic Lupus Erythematosus

Dana Kidder

2011

University of Dundee

An investigation of the regulation of Sialoadhesin ligands on CD4+ T cells and its potential significance in Systemic Lupus Erythematosus

Dana Kidder

A Thesis Submitted in

Candidature for the Degree of

Doctor of Philosophy

University of Dundee

August 2011

Table of Contents

List of abbreviations

APC	antigen presenting cell
BMDM	bone marrow-derived macrophages
BWF1	New Zealand Black X New Zealand White F1
C2GnT	Core 2 β1,6 N-acetylglucosaminyltransferase
CHO	Chinese hamster ovary cells
CMP	cytidine monophosphate
CTLA-4	cytotoxic T lymphocyte antigen 4
DMNJ	1-deoxymannojirimycin
EAE	experimental allergic encephalomyelitis
EAU	experimental autoimmune uveoretinitis
Edu	5-ethynyl-2'-deoxyuridine
Foxp3	forkhead box p 3
FUT7	fucosyltransferase 7
GalNAc	*N*-acetylgalactosamine
GlcNAc	*N*-acetylglucosamine
IFN	interferon
KO	knock out
MAL	maackia amurensis lectin
M-CSF	macrophage colony stimulating factor
mDC	monocyte-derived DC
MMZ	marginal metalophilic zone
MOG	myelin oligodendrocyte glycoprotein
PAMP	pathogen-associated molecular pattern
PBMC	peripheral blood mononuclear cells
PDBu	phorbol 12,13 dibutyrate
pDC	plasmacytoid dendritic cells
PHA	phaseolus vulgaris agglutinin
PNA	pea nut agglutinin

PSGL-1	P-selectin glycoprotein ligand-1
RBMM	resident bone marrow derived macrophages
Sia	sialic acid
SLE	systemic lupus erythematosus
Sn	sialoadhesin
SNA	sambucus nigra lectin
SnL	sialoadhesin ligand
ST	sialyltransferase
TCR	T cell receptor
Teffs	CD4Foxp3- T cells
TGFβ	transforming growth factor beta
TLR	Toll like receptor
TNFα	tumor necrosis factor alpha
Tregs	CD4Foxp3+ T cells
WT	wild type
β1,4 Gal T	beta 1,4 galactosyltransferase

Table of Figures and Diagrams

List of Tables

Dedication

This thesis is dedicated to my wife Bayan for putting up with me and being ever so patient, thank you

Acknowledgments

I would first like to thank my supervisor Professor Paul Crocker for his support and guidance throughout my PhD. I would also like to thank all the past and present members of the Crocker lab for their advice and support. I wish to particularly thank Hannah, Emma, Sarah, Pierre and Ritu. Your friendship is greatly valued.

Throughout my PhD, Dr Oliver Garden (Royal Veterinary College, London) provided me with advice for which I am grateful. I would also like to appreciate the support I had from Professor Hermann Ziltener (University of British Columbia, Canada).

I wish to thank my family and friends for their love and encouragement. In particular, I would like to thank my wife, Bayan and my daughter, Masti for being my reason to carry on during difficult times. This effort would not have been possible without your unending support, love and belief in me. Finally, I would like to thank my brother for his backing and kindness over the past years.

Declaration

I, Dana Kidder, declare that: I am the sole author of the whole work presented in this thesis; I have consulted all cited references; I have carried out all of the work described unless otherwise acknowledged; the data presented within has not previously been accepted for a higher degree.

Signed: ***Dana Kidder*** Dated: 20/12/2011

Abstract

Sialoadhesin (Sn) is the prototype of Sialic acid binding Immunoglobulin-Like Lectins (SIGLECs). Sn is expressed on macrophages from metalophilic zone and subcapsular sinus in spleen and lymph nodes respectively. Under inflammatory conditions, Sn expression is upregulated on macrophages. Sn was recently found to downregulate CD4+Foxp3+ regulatory T cells (Tregs) in a mouse model of experimental autoimmune Encephalomyelitis (EAE); however the nature of the interaction between Sn and CD4+ T cells is not well characterised. The first aim of this thesis was to investigate the upregulation of Sn ligand (SnL) on CD4+ T cells *in vitro*. Both Tregs and CD4+Foxp3- T cells upregulate SnL following T cell receptor (TCR) ligation. SnL+CD4+ T cells express a higher state of activation and proliferation compared to SnL- counterparts. Furthermore, engaging SnL on activated CD4+ T cells induces cell death. Experiments performed to analyse the nature of sialylation changes and expression of glycosyltransferases on SnL+ CD4+ T cells, indicated that terminal sialic acids on N-linked glycans represent a putative ligand for Sn.

The second aim of this project was to analyse the role of Sn in a mouse model of systemic lupus erythematosus (SLE). NZB x NZW F1 (BWF1) hybrid model was used for this purpose. Examination of Sn expression on pre-diseased and diseased mice showed that Sn expression is upregulated around the disease onset and went down to pre-disease levels subsequently. This finding might suggest a role for Sn in enhancing cell death and downregulating Treg and therefore augmenting immune dysregulation. Two approaches were used to further study the role of Sn in this model. First, Sn neutralising antibodies were used prophylactically to study the effect on disease severity. Secondly, using speed congenic method, BWF1 mice deficient for Sn were generated. Data presented in this thesis suggest that Sn might play an anti-inflammatory role in murine SLE.

Introduction

The surface of all mammalian cells is covered with a dense layer of glycans (sugar chains) bound to proteins, lipids or other compounds. This is referred to as the glycocalyx. The process of attaching a glycan to a protein, lipid or another glycan is mediated by the action of glycosyltransferase enzymes and is referred to as glycosylation. Glycan synthesis reflects numerous combinatorial possibilities generated by often competing and sequential action of glycosyltransferases and glycosidases which reside in Golgi and ER. Glycosylation at these sites are referred to as secretory pathway (Marth *et al*, 2008). The glycans or glycoconjugates are subsequently transported to the cell surface. Glycosylation is not restricted to Golgi and ER as protein glycosylation in the cytoplasm and nucleus occurs through the action of the glycosyltransferase OGT (*O*-GlcNAc transferase) and is referred to as intracellular glycosylation (Marth *et al*, 2008).

Glycosylation can affect many aspects of the immune system. For example, P-selectin glycoprotein ligand-1 (PSGL-1) is a glycoprotein that carries ligands for selectins and plays a major role in leukocyte homing and trafficking. Defective glycosylation results in attenuated lymphocyte homing to peripheral lymph nodes and cell trafficking to inflamed tissues (Carlow *et al*, 2009). Proteins that bind glycans but are not enzymes (glycosyltransferases or glycosidases) are referred to as lectins. There are four major classes of mammalian lectins (Varki 2009): i) C-type lectins which require calcium for recognition. Selectins are members of this family of lectins and they mediate interactions between leukocytes and endothelial cells, ii) I-type lectins or siglecs which belong to the immunoglobulin superfamily and they bind ligands bearing sialic acid and regulate cell-cell interaction and signalling in lymphocytes and other cell types, iii) S-type (sulfhydryl-dependent) or galectins contributes to cell-cell and cell-matrix interactions and galectin signalling modulates cellular functions, iv) P-type lectins which recognizes mannose-6-phosphates which play a role in lysosomal enzymes trafficking.

The pathogen-host interactions are regulated to a great extent by glycosylation. Mammalian lectins can recognise glycans from other organisms. This evolutionary mechanism offers 'self' and 'non-self' recognition and protection from certain pathogens. For example, humans are resistant to certain influenza viruses e.g. H5N1 due to the fact the upper airways epithelium display α2,6 linked sialic acids while H5N1 recognises α2,3 linked sialic acids. Therefore, for the virus to become pathogenic a specific mutation in the sialic acid binding site in the virus hemagglutinin needs to occur. Birds can become infected because they express α2,3 sialic acids (Varki *et al*, 2007). In addition, aberrant glycosylation of endogenous glycans can result in perceiving these glycans as non-self and triggering autoimmunity. An example on this is related to deficiency in α-mannosidase that is required for the conversion of hybrid *N*-glycans to complex *N*-glycans. Hybrid *N*-glycan is a primitive form that is found in yeasts and fungi, and it is recognised by the mannose-binding –lectin (MBL) as non-self and therefore chronic activation of innate immunity with consequent autoimmunity in the form of SLE ensues (Green *et al*, 2007).Glycosylation of various classes of immunoglobulins affect antibody function, this is exemplified by the finding of truncated *O*-glycans attached to IgA in patients with IgA nephropathy. The truncated form leads to the exposure of underlying *N*-acetylgalactosamine and deposition of the aberrant form of IgA in the kidneys (Hiki *et al*, 2001).

Sialoadhesin (Sn) is the first identified member of the siglec family and is constitutively expressed on subpopulations of tissue resident macrophages (Crocker *et al*, 1989). Several studies gave support to a role for Sn in cell-cell interaction, especially in modulating T lymphocyte function (Jiang *et al*, 2006; Ip *et al*, 2007; Kobsar *et al*, 2006 and Wu *et al*, 2009). In the Wu et al study, regulatory CD4Foxp3+ T cells (Tregs) were found to express ligands for Sn. However, the requirements for the induction of these ligands, whether they are expressed solely on Tregs and the functional consequences of engaging these ligands, remain unknown. Additionally, Sn was recently shown to be a potential biomarker for the 'interferon signature' in human systemic lupus

erythematosus, SLE (Biesen *et al*, 2008). In this study, the frequency of Sn+ monocytes was found to correlate well with established markers of disease severity in SLE. However, it is unknown whether Sn contributes to the pathogenesis of SLE.

This thesis aims at identifying the characteristics of CD4 T cells bearing SnL and investigating the nature of these ligands. The second goal of this thesis is related to addressing the question of the function of Sn in SLE by using a Sn deficient murine model of SLE. In this chapter, I describe concepts of glycan and sialic acid diversity. Next, I present literature on the structure of Sn, its sialic acid-recognition properties and recent studies on Sn involvement in cell-cell interactions. In the second part of this chapter, I introduce the genetic basis of murine SLE in the New Zealand Black X New Zealand White F1 model, certain aspects of disease pathogenesis and, finally, the evidence on the role of Tregs in murine SLE.

1.1 Glycans structure and diversity

1.1.1 Types of glycans

Glycans bound to proteins or lipids are classified, based on the nature of the linkage, into *N*- , *O*-linked glycans and glycolipids. *N*-glycans are oligosaccharides that are attached to the nitrogen of the asparagine residue in the sequence Asn-X-Ser/Thr of a protein. The sugar unit that forms the link with the asparagine residue is an *N*-acetylglucosamine (GlcNAc). *O*-linked glycan, on the other hand, are oligosaccharides that are linked to the hydroxyl group of a serine or a threonine in a polypeptide chain. The linkage sugar to the serine or threonine is *N*-acetylgalactosamine (GalNAc).

The structure of *N*-glycan is generally more complex than *O*-glycan (Diagram 1.2). In vertebrates *N*-glycans are characterised by having “antennae” that are initiated by the addition of GlcNAc to mannose and the reaction is catalyzed by the enzyme GlcNAc transferase. The addition of galactose to the initiating GalNAc results in the formation

of Galβ1,4GlcNAc sequence (also known as type 2 *N*-acetyllactosamine or LacNAc). The antennae can be elongated with tandem repeats of LacNAc sequences (polyLacNAc). The termini of these antennae are capped with sialic acids in an α2,3 or α2,6 linkage.

O-glycans on the other hand can be subdivided based on their core branching. Core 1 (unbranched) *O*-glycans are synthesized by the addition of *N*-acetylgalactosamine (GalNAc) to serine or threonine residue. This is followed by the sequential addition of galactose and final capping with sialic acids in an α2,3 linkage. Sialic acids can also be attached directly to the GalNAc in an α2,6 linkage. Core 2 (branched) *O*-glycans are formed by the addition of *N*-acetylglucosamine (GlcNAc) to the GalNAc of Core 1 structures catalyzed by the glycosyltransferase, Core 2 β1,6 N-acetylglucosaminyltransferase (C2GnT). This is followed by the addition of a galactose to form Galβ1,3GlcNAc (also known as type 1 *N*-acetyllactosamine or LacNAc). Repeats of this building block lead to the extension of Core 2 *O*-glycan. Similar to Core 1, the final decoration of Core 2 *O*-glycan occurs by the addition of sialic acids in an α2,3 linkage.

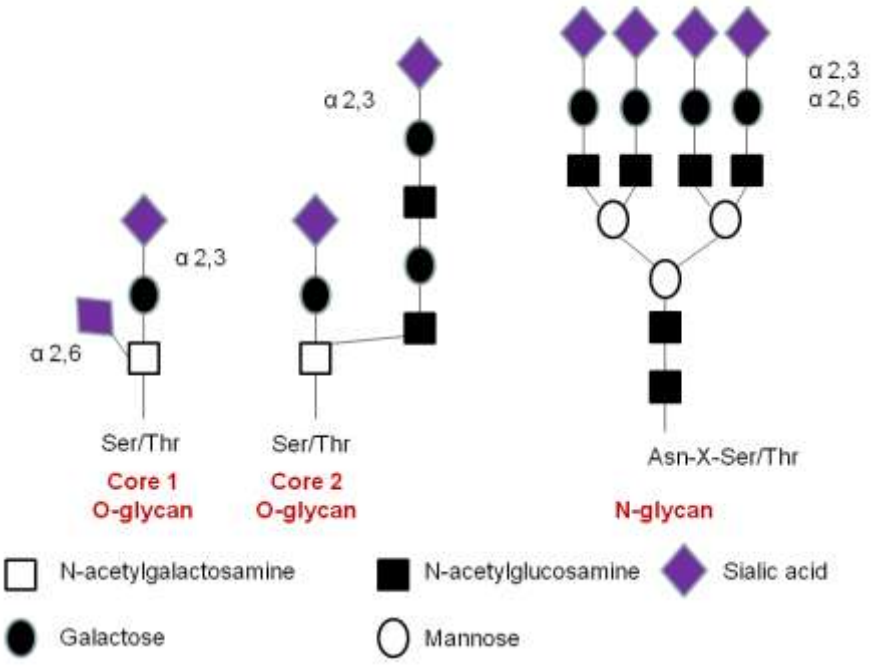

Diagram 1.1 Glycan classes and diversity

1.1.2 Sialic acids

Sialic acids (Sia) are members of a family of sugars which are primarily derived from N-acetylneuraminic acid (Neu5Ac). Sia are located at the termini of N- and O-linked glycan structures. All Sia have a 9-carbon structure (Diagram 1.2). Out of more than 50 forms of naturally occurring Sia, mammals express mainly 3 types: *N*-acetylneuraminic acid (Neu5Ac), *N*-glycolylneuraminic acid (Neu5Gc) and 5,(7)9-*N*,O-diacetylneuraminic acid (Neu5,(7)9Ac2). These three different forms of Sia represent a structural diversity that arises from natural modifications on the fifth and ninth carbon of the molecule. Hydroxylation of the *N*-acetyl group attached to the C-5 leads to the formation of Neu5Gc. Humans lack Neu5Gc due to a mutation in the enzyme cytidine monophosphate N-acetylneuraminic acid hydroxylase (CMAH) which is responsible for converting NeuAc to NeuGc (Sonnenburg *et al*, 2004). Additional substitutions can occur at the hydroxyl groups on C-4, C-7, C8 and C-9. Such substitutions include: *O*-acetylation, *O*-methylation and *O*-sulfation (Diagram 1.2).

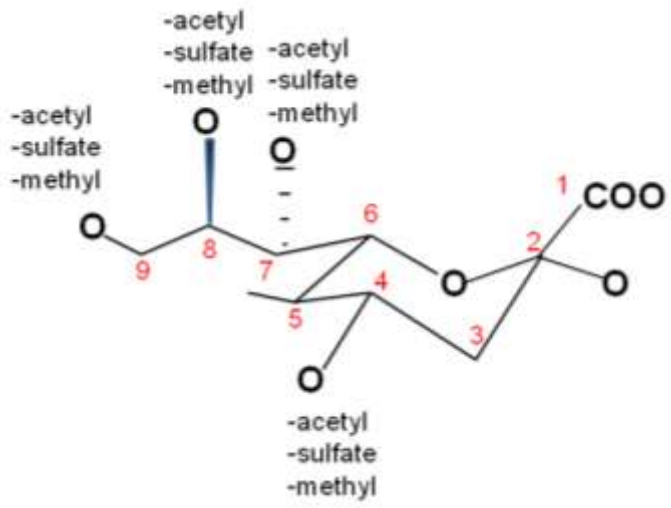

Diagram 1.2 Sialic acid structure and diversity

Another level of diversity of Sia comes from the variety of their linkages to other sugars. Sia are the outermost monosaccharide units of glycan chains and they utilize different linkages with the underlying sugars e.g. α-linkages between the second carbon (C-2) from Sia and C-3 (galactose residue) or C-6 (galactose or *N*-acetylgalactosamine residues) of the underlying sugar. Such interactions result in linkages referred to as α2,3 or α2,6. These reactions are mediated by specific sialyltransferases using cytidine monophosphate-Sia (CMP-Sia) as a high energy sugar donor. In addition, α-linkages between Sia occur via C-2 and C-8 resulting in the formation of di-, oligo- and poly-sialic acids.

The terminal position of Sia on glycan structures of glycoproteins and glycolipids can result in dual function for these sugars. The first function is related to masking the underlying sugar residue (galactose). CD8 T cells from mice lacking the specific sialyltransferase, ST3Gal I, responsible for adding Sia to the subterminal galactose undergo rapid apoptosis (Priatel *et al*, 2000). This was found to be directly related to the exposure of the underlying galactose and consequent recognition by galactose-recognising galectin-1 and ultimately induction of cell death (Priatel *et al*, 2000). Another example of the biological significance of masking underlying galactose by Sia comes from the observation of reduced platelet counts and von Willibrand factor levels in mice deficient in sialyltransferase ST3Gal IV (Ellies *et al*, 2002a). The exposure of the underlying galactose induces asialoglycoprotein clearance mechanisms resulting in these deficiencies.

The second general function of Sia is that they, together with the glycan chain they are attached to, serve as ligands (Diagram 1.3) for Sia-recognising molecules e.g. sialic-acid binding immunoglobulin-like lectins (Siglec).

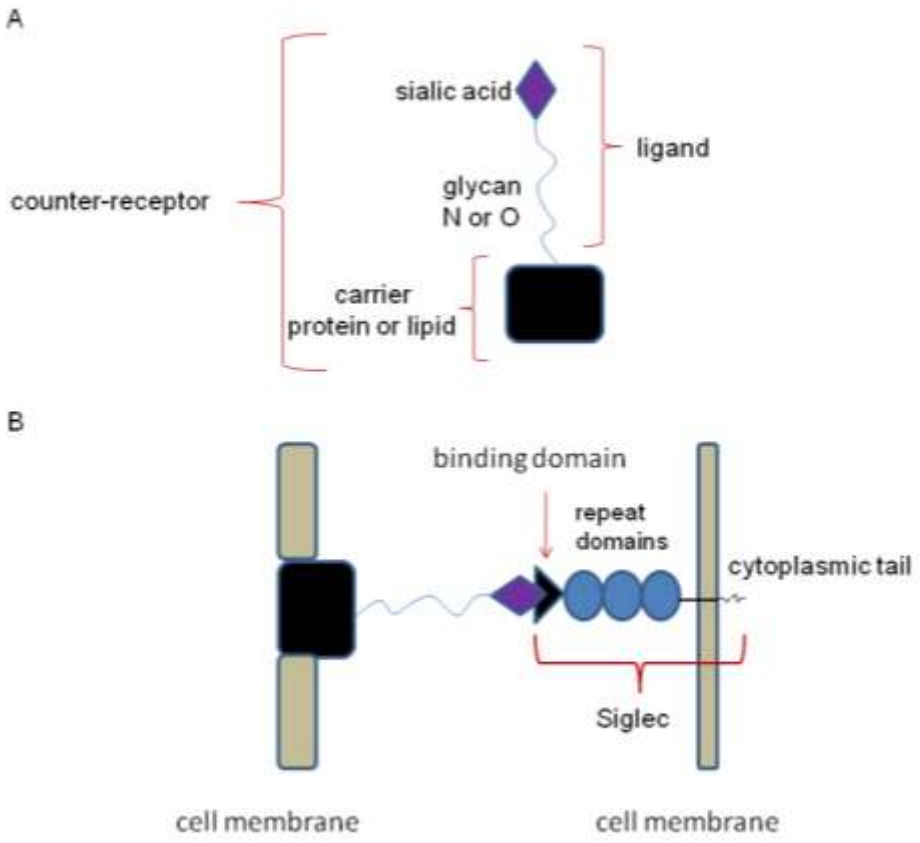

Diagram 1.3 A, The concepts of ligand and counter-receptor. A sialylated oligosaccharide works as a ligand for a sialic-acid recognising lectin e.g. siglec. When a ligand is attached to protein or lipid carriers (black box), the combination is referred to as a counter-receptor. B,lectin-carbohydrate interactions. A representative siglec expressed on the cell surface binds to the sialic acid expressed on a ligand via its distal sialic-acid recognising domain.

1.1.3 Sialyltransferases

1.1.3.1 Structure and classification

Mammalian STs are characterised by having a type II transmembrane topology (Diagram 1.4). They are composed of a short N-terminal cytoplasmic tail, a transmembrane domain, a short stem and a catalytic domain. These enzymes can be composed of 300-600 amino acid residues. This wide range of amino acid length is primarily due to the differences in the stem region length. The catalytic domain of a ST consists of highly conserved motifs which are known as sialyl motifs. These sialyl motifs are referred to a long (L), short (S), III and very short (VS). Sialyl motif L is located in the centre of the ST enzyme and mediates binding to the donor substrate

(CMP-Sia). The sialyl motif S is located towards the C-terminus and mediates both donor and acceptor substrates binding. The VS sialyl motif is primarily involved in catalytic activity. Motif III is located between VS and S motifs and, similar to VS, is involved in catalytic activity (Takishima 2008).

The family of STs consists of 20 different members. These can be categorised into 4 sub-families according to the carbohydrate linkages they catalyze:

- β-galactoside α2,3 STs (ST3Gal) with six members (ST3Gal I-VI)
- β-galactoside α2,6 STs (ST6Gal) with two members (ST6Gal I-II)
- N-acetylgalactosamine (GalNAc) α2,6 STs (ST6GalNAc) with six members (ST6GalNAc I-VI)
- α2,8 STs (ST8Sia) with six members (ST8Sia I-VI)

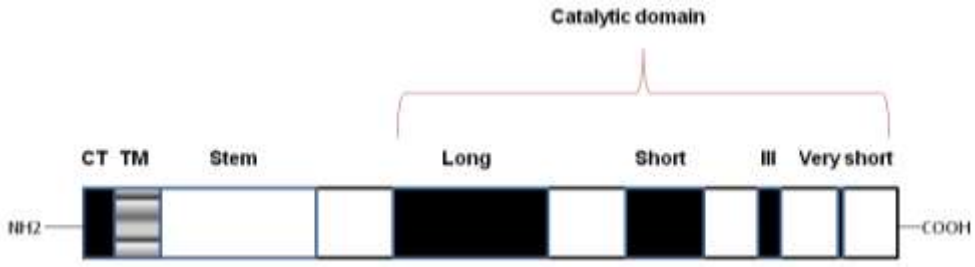

Diagram 1.4 Structure of sialyltransferases.

1.1.3.2 Functional aspects

Insights into the functions of sialyltransferases originated from the generation of knock-out models of these enzymes. The function and/or main phenotypic features resulting from deficiency in these enzymes are summarized in Table 1.1.

Table 1.1 ST3Gal and ST6Gal sialyltransferases substrate preferences, sialylconjugate structures and phenotype of sialyltransferases knock-out models.

Sialyltransferase	Substrate	Structure	Deficiency/Role	Reference
ST3Gal I	Galβ1,3GalNAc	Siaα2,3Galβ1,3GalNAc	Increased peripheral CD8 apoptosis. Thrombocytopenia	Priatel et al, 2000 Ellies et al, 2002b
ST3Gal II	Galβ1,3GalNAc	Siaα2,3Galβ1,3GalNAc	No defects in haematopoiesis. Role in ganglioside synthesis	Ellies et al, 2002b Ishii et al, 1998
ST3Gal III	Galβ1,3GlcNAc > Galβ1,4GlcNAc	Siaα2,3Galβ1,3GlcNAc Siaα2,3Galβ1,4GlcNAc	No defects in haematopoiesis	Ellies et al, 2002b
ST3Gal IV	Galβ1,4GlcNAc > Galβ1,3GlcNAc	Siaα2,3Galβ1,4GlcNAc Siaα2,3Galβ1,3GlcNAc	Thrombocytopenia and reduced Von Willibrand factor levels. Defective selectin ligand formation and impaired leukocyte rolling	Ellies et al, 2002a Ellies et al, 2002b
ST3Gal V	Galβ1,3GlcNAc Cer	Siaα2,3Galβ1,3GlcNAc Cer	Enhanced insulin sensitivity in skeletal muscles	Yamashita et al, 2003
ST3Gal VI	Galβ1,4GlcNAc	Siaα2,3Galβ1,4GlcNAc	Role in selectin ligand synthesis	Underhill, et al, 2005
ST6Gal I	Galβ1,4GlcNAc	Siaα2,6Galβ1,4GlcNAc	Marked attenuation of B cell proliferation and IgM production	Hennet et al, 1998
ST6Gal II	Galβ1,4GlcNAc	Siaα2,6Galβ1,4GlcNAc	Not reported	

1.2 Sialoadhesin

1.2.1 Structure

Sialoadhesin (Sn), also known as Siglec-1 or CD169, is the prototype of the family of sialic acid binding immunoglobulin (Ig) superfamily lectins (SIGLEC) adhesion molecules. Siglecs are type I membrane proteins containing a V-set domain that binds Sia and variable numbers of C2-set Ig domains. Sn is one of the largest members of the Ig superfamily with an extracellular region made of 17 Ig domains and this is well conserved in mammals (Diagram 1.5). Unlike many other siglecs, Sn lacks intracellular tyrosine-based signalling motifs and the cytoplasmic tail is poorly conserved. Therefore, its role might be more in cell-cell interaction rather than in signalling (Crocker, 2007).

Sn was originally described as a sheep erythrocyte receptor based on the ability of resident bone marrow derived macrophages (RBMM) to bind unopsonised sheep erythrocytes without phagocytosing them (Crocker *et al* 1986). This binding was found to be Sia-dependent as pre-treatment of sheep erythrocytes with *Vibrio cholera* neuraminidase abolished binding.

The first monoclonal antibody against Sn was referred to as SER 4 and was generated by immunizing rats with mouse serum-induced thioglycollate peritoneal macrophages expressing high levels of the molecule and screening hybridoma supernatants for their ability to inhibit RBC binding to macrophages. SER 4 was found to inhibit the binding of sheep erythrocytes to resident bone marrow macrophages. Using this monoclonal antibody, the tissue distribution of Sn was found to be on resident bone marrow, subcapsular and marginal metalophilic zone macrophages (Crocker *et al*, 1989). Subsequently, SER4 mAb was used to examine the distribution of Sn on RBMM within haematopoietic clusters. While a diffuse pattern of distribution at the contact zone between macrophages and erythroblasts was observed, the receptor displayed clustering at the points of contact between macrophages and myelomonocytic cells.

This selectivity in the interaction between Sn and myeloid cells suggested that myeloid cells (more than erythroblasts) expressed higher concentration of ligands for Sn (Crocker *et al*, 1990).

Molecular cloning of murine Sn identified the molecule as a type I transmembrane glycoprotein and a new member of the immunoglobulin superfamily with 17 Ig-like extracellular domains (Crocker *et al*, 1994). Sn was shown to be composed of 1694 amino acids with a hydrophobic leader peptide (19 amino acids), followed by an extracellular region (1619 amino acids), a hydrophobic transmembrane domain (21 amino acids) and a hydrophilic intracellular tail (35 amino acids). Domains 4-17 appear to constitute a stem region made of alternating shorter and longer C2-domains. This pattern is suggestive for an ancestral two-domain molecule that gave rise to this stem region via duplication process (Crocker *et al*, 1994).

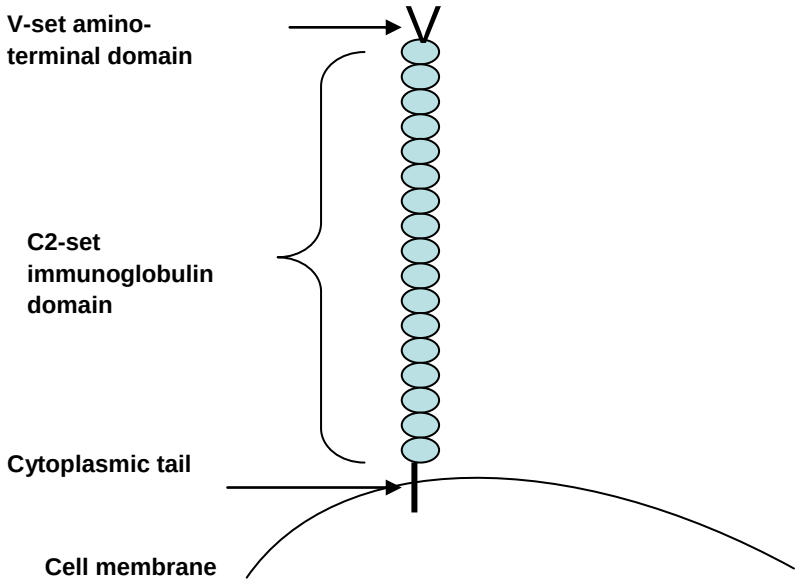

Diagram 1.5 Sialoadhesin structure and interaction with Neu5Ac.

The extracellular domain of Sn displayed a sequence similarity, extending over the first four Ig-like domains, to CD22 and myelin-associated glycoprotein (MAG) and CD33. COS cells transfected with full length of Sn cDNA showed a positive binding to human red blood cells (RBCs) in a Sia-dependent manner. In addition, monoclonal antibodies (SER4 and 3D6) against two distinct epitopes of the molecule abolished binding of COS cells to RBCs (Crocker *et al*, 1994).

1.2.2 Sialic acid recognition

The molecular basis of carbohydrate recognition by Sn was explained by examining crystal structures of the V-set Ig domain complexed with different Sia-containing glycoconjugates (May *et al*, 1998) and analysis of Sia binding properties by nuclear magnetic resonance (NMR) and affinity measurement (Crocker *et al*, 1999). The V-set domain was shown to be sufficient in mediating Sia binding and that most of the relevant interactions are made within a discrete set of amino acids within this domain. The crystal structure of the V-set domain complexed with 3'-sialyllactose has identified a highly conserved arginine residue and two well-conserved tryptophan residues which mediate interactions with Sia. The highly conserved arginine residue makes a salt bridge with the carboxyl group of Neu5Ac. Tryptophan residues make hydrophobic interactions with the N-acetyl and glycerol moieties of Neu5Ac. The importance of the arginine residue in Sia binding was evidenced by complete abrogation of binding by substitution with alanine. In addition, arginine substitution with lysine resulted in reduction of binding by 10-fold. Moreover, Sn was found to have a higher binding affinity to α2,3 sialyl-lactose (0.8 mM) compared to α2,6 sialyl-lactose (2.1mM) (Crocker *et al*, 1999).

Sn exhibits low affinity (K_d of 0.1-3mM) for Sia that are commonly found at the termini of glycans structures (Blixt *et al*, 2003). Although the binding affinity of Sn to relevant sialylconjugates is relatively weak, high-avidity can be achieved via clustering (multi-valency) of Sn and its ligand. The evidence in favour of this phenomenon comes from

binding experiments using streptavidin-based GT1b (SiaGalGalNAcSiaSiaGalGlcCer) oligosaccharides. GT1b oligosaccharides were coupled to streptavidin producing monomer form of streptavidin carrying 13 oligosaccharides. Polymers carrying more than 140 oligosaccharides were constructed using biotinylated-bovine serum albumin. The binding of different forms of GT1b to Sn expressed on Chinese hamster ovary cells (CHO) was measured by radioactive iodine labelling. The linear increase in the number of ligand residues from the monomeric to the multimeric forms of GT1b was associated with increased binding on a log scale (Hashimoto *et al*, 1998). This study illustrated that the low binding affinity of sialylated ligands to Sn can be overcome by an enhanced avidity through multivalency.

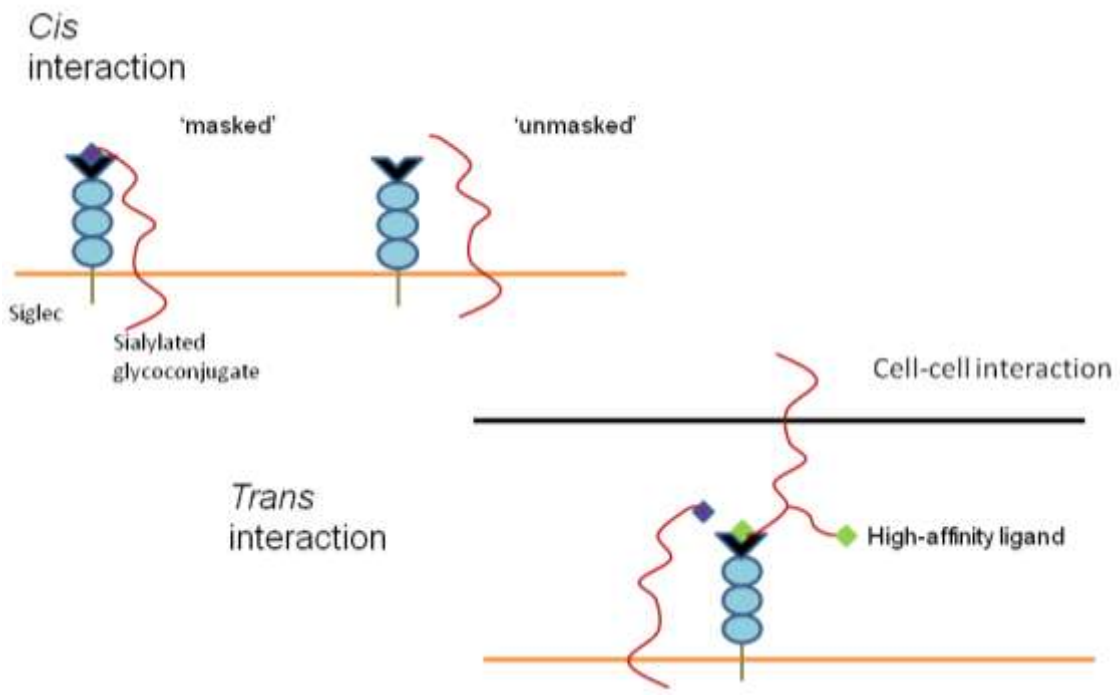

Diagram 1.6 *Cis* and *trans* interactions between siglecs and neighbouring glycoconjugates.

Sia abundance in various glycoconjugates on the surface of immune cells can result in *cis* interaction between siglecs and relevant sialoasides (Diagram 1.6). Consequently, this makes siglecs less available for cell-cell or *trans* interactions. This phenomenon is often referred to as ‘masking’ siglec binding sites. Cleavage of Sia from surface sialosides using sialidase leads to enhanced functional activity of these siglecs

(Freeman *et al*, 1995). This biased interaction towards *cis* rather than *trans* patterns can have a direct effect on biological activities of siglecs (Crocker 2007). However, cell-cell *trans* interactions are still possible when siglecs are 'masked' with *cis* interactions, as high affinity ligands on the other cell can out-compete low affinity ligands masking the siglec molecule. Sn might represent an exception to this rule due to its long extracellular region which extends the sia binding V-set domain away from the plasma membrane and thereby reducing *cis* interactions (Munday *et al*, 1999). However, Sn-expressing COS cells pre-treated with sialidase bound to human RBCs to a greater extent compared to no sialidase treatment (Barnes *et al*, 1999). This might have been related to the fact that negative charge is associated with reduced interaction and sialidase treatment reduces negative charge on the cell surface leading to enhanced interactions. Comparison of the binding potency of rat splenic and mesenteric lymph node cells to GT1b probe revealed 10-fold higher binding with the latter group (Nakamura *et al*, 2002). Only macrophage depletion (as compared to T and B cells) from these two groups led to reduction in binding by more than 90%. The enhanced binding to GT1b probe was not exclusive to mesenteric lymph nodes as axillary and inguinal lymph nodes displayed a similar trend. Interestingly, sialidase treatment of splenic cells caused an increased binding to GT1b, suggesting a differential 'masking' of Sn in spleen and lymph nodes by endogenous Sia.

1.2.3 Sn expression

Sn was originally characterised as a macrophage-restricted receptor on RBMM (Crocker *et al*, 1986). Subsequently, immunohistochemistry analysis of murine secondary lymphoid organs using SER4 mAb revealed high expression of Sn on discrete subsets of macrophages in the subcapsular sinus and medullary cords in lymph nodes and in the marginal metalophilic zone (MMZ) in spleen (Crocker *et al*, 1989). In humans, cloning of the Sn molecule and amino acid sequence analysis showed up to 72% sequence similarity with murine Sn (Hartnell *et al*, 2001). The extracellular region of the molecule revealed the greatest degree of similarity. Human

tissue expression of Sn was similar to mouse to a great extent. High Sn expression was found on resident bone marrow macrophages, splenic perifollicular region and perifollicular sinusoidal macrophages in lymph nodes. In addition, other resident macrophages found to express Sn included: Kupffer cells in liver, alveolar and interstitial macrophages and macrophages in colonic lamina propria.

Various inflammatory conditions can lead to the up-regulation of Sn expression on inflammatory macrophages. Sn positive (Sn+) inflammatory macrophages and Sn+ circulating monocytes were identified in diseases like: proliferative glomerulonephritis (Ikezumi *et al*, 2005), HIV infection (Pulliam *et al*, 2004), SLE (Biesen *et al*, 2008) systemic sclerosis (York *et al*, 2007) and rheumatoid arthritis (Hartnell *et al*, 2001).

1.2.4 Putative Sn counter-receptors

Several studies investigated potential counter-receptors for Sn. Generally, two patterns of Sn binding have been identified: Sia-dependent (mediated by the V-set domain of Sn) and Sia-independent (mediated by the C2-domains of Sn). Van den Berg and colleagues attempted to identify counter-receptors for Sn on TK-lymphoma cell line (Van den Berg *et al*, 2001). Immunoprecipitation experiments, using fusion proteins made of the membrane-distal three Ig domains of Sn and human IgG, revealed glycoproteins corresponding to CD43 and PSGL-1. The mutant form of SnFc protein (R97A) or pre-treatment of cells with sialidase were used as controls. CD43 (also called leukosialin or sialophorin) is heavily expressed on the surface of all hemopoetic cells except erythrocytes and IgM+ B cells (Fukuda *et al*, 1991). There are two major forms of CD43, a lower molecular mass (115 kDa) which is expressed under resting conditions and a higher molecular weight (130 kDa) that is also referred to as the activation-associated glycoform. This is expressed on activated T lymphocytes and is rich in Core-2 O-linked glycans (Jones 1994). CHO cells transfected with the resting (115 kDa) and activated (130 kDa) glycoforms of CD43 displayed an enhanced binding to immobilized SnFc compared to sham transfected CHO cells (Van den Berg *et al*,

2001). This study has, therefore, showed that Sn binds similarly to both isoforms of CD43.

Nath and colleagues showed that infiltrating macrophages in contact with human breast cancer cells expressed Sn. Further analysis was carried out using two breast cancer cell lines. In these experiments SnFc was found to bind cells from these lines in a Sia-dependent manner. Immunoprecipitation experiments on these cell lines identified epithelial mucin (MUC1) as a counter-receptor for Sn on breast cancer cells (Nath *et al*, 1999).

Macrophage galactose-C-type lectin (MGL-1) was also reported as a Sn counter-receptor. Dermal macrophages expressing MGL-1 migrate from skin to lymph nodes where they localize to subcapsular sinus interfollicular regions and areas surrounding high endothelial venules. Recombinant MGL-1 was found to bind to immobilized Sn. Binding was calcium and *N*-glycan dependent but Sia-independent (Kumamato *et al*, 2004). The cysteine-rich (CR) domain of the macrophage mannose receptor was also found to bind to Sn. Immunostaining of murine spleen and lymph nodes showed a positive staining in both MMZ and subcapsular sinus. The binding of Sn to CR-Fc was shown to be Sia-independent but dependent on sulphated *N*-glycan structures of Sn (Martinez-Pomares *et al*, 1999).

A general feature of all but one (Martinez-Pomeraz *et al*, 1999) of the above studies is the use of cell lines rather than primary cells for identifying the nature of counter-receptors examined. It remains to be determined whether Sn binding to primary cells requires the presence of these counter-receptors and if there is any redundancy between them. In addition, the functional consequences of these interactions remain largely unexplored.

1.2.5 Sn and autoimmunity

The above studies explored molecular features of Sn and suggested a role for Sn in cell-cell interactions. In an attempt to explore the functions of Sn, mice deficient in Sn were generated (Oetke *et al*, 2006). These mice were viable and did not show any developmental abnormalities. Sn was previously shown to cluster at contact points between RBMM and myeloid cells and not erythroblasts (Crocker *et al*, 1990). However, Sn deficient mice did not show any defect in neutrophils in the resting state or in mice stimulated with thioglycollate, compared to Sn sufficient mice. These findings indicated that Sn does not play a major non-redundant role in granulocyte production or release from bone marrow. Similarly, there were no differences in the frequency and development of thymocytes in Sn deficient mice compared to wild-type littermates. While there was no difference in CD4 T cell frequency in the periphery, Sn deficient mice had relatively more CD8 T cells. The main difference between Sn deficient and wild-type mice was a reduction in serum IgM levels in the former group. Overall, the findings suggested that Sn might be involved in the regulation of the immune system, rather than haematopoiesis.

1.2.5.1 Sn in murine models of autoimmunity

The role of Sn in a model of interphotoreceptor retinal binding peptide-induced (IRBP) experimental autoimmune uveoretinitis was examined. This disease model is mediated by CD4 T cells. The disease onset was delayed and severity was reduced in Sn deficient mice. The proliferation of total cells from spleen and draining lymph nodes from immunised Sn wild-type and deficient mice was examined by re-stimulation with IRBP *ex vivo*. Cells from Sn deficient mice displayed reduced proliferation *ex vivo* compared to those from the wild-type littermates. Furthermore, there was reduced production of IFNγ and TNFα demonstrated in the supernatant of splenocytes from Sn deficient, compared to wild-type, mice when re-stimulated with IRBP *ex vivo* (Jiang *et al*, 2006). These findings suggested a role for Sn at the beginning of the disease. The reduced proliferation capacity and production of inflammatory cytokines that were

demonstrated *ex vivo* were in agreement with overall reduced inflammatory responses in Sn deficient mice early in the disease.

It is important to mention that in this study, T lymphocytes (CD4 or CD8) frequency, activation profile or proliferation were not examined. Furthermore, it is unclear whether potential altered frequency of regulatory T cells in Sn deficient mice could have explained the differences in disease, onset, severity and cytokine production by splenocytes. Finally, the examination of *ex vivo* proliferation of total cells from spleens or draining lymph nodes might not directly reflect T cell proliferation.

Sn involvement in the pathogenesis of inherited forms of nervous system inflammation was evaluated. In one murine model of axonal degeneration and demyelination mediated by over-expression of the gene for myelin proteolipid protein (PLP), the majority of inflammatory CD11b+ macrophages showed a positive expression of Sn. Inflammation in this model is primarily related to CD8 T cells. Sn deficient mice over-expressing PLP were found to have reduced disease severity and accumulation of macrophages and CD8 T cells in disease sites (Ip *et al*, 2007). In a second model of inherited neuropathies, mice deficient in Sn and myelin component P0 showed a similar pattern of amelioration of disease and reduced cellular infiltrate, especially CD8 T cells in peripheral nerves (Kobsar *et al*, 2006). These data suggested that Sn expression on inflammatory macrophages plays a major role in disease models of central and peripheral nervous system demyelination. The fact that CD8 T cells were found to be reduced at sites of inflammation (in both models) in the Sn deficient mice is in contrast to the relative increase in the frequency of CD8 T cells that was observed in peripheral lymphoid organs under steady state conditions (Oetke *et al*, 2006). Whether, Sn deficiency in these models promoted regulatory mechanisms to down-regulate CD8 T cells at the sites of inflammation is an unexplored area.

The interaction between Sn+ macrophages and lymphocytes was further explored in a mouse model of experimental autoimmune encephalomyelitis (EAE) which resembles

human multiple sclerosis (Wu *et al*, 2009). The frequency of total CD4+ T cells but not CD8+ T cells was found to be reduced in the CNS of Sn deficient mice. Interestingly, the frequency of CD4+CD25+Foxp3+ (Tregs) was found to be increased in CNS, blood and lymphoid tissues in the Sn deficient mice. Sn+ resident and tissue-infiltrating inflammatory macrophages were found to interact directly with Tregs in inflamed CNS and in peripheral lymphoid tissues. Using SnFc fusion protein, the Tregs in active EAE, but not from normal mice, were shown to express substantial amount of ligands for Sn (SnL). Higher frequency of SnL+ Tregs was demonstrated in the inflamed CNS of Sn deficient mice. In addition, *ex vivo* stimulation of Tregs and CD4+Foxp3- (Teffs) with myelin oligodendrocyte glycoprotein in the presence of CD11b+F4/80+ macrophages from Sn wild-type or Sn deficient mice, showed that the proliferation of Tregs and not Teffs was reduced in the presence of Sn. Moreover, blocking Sn on these macrophages led to increased Tregs proliferation. This study established for the first time a direct interaction between Sn+ macrophages and Tregs with Sn negatively regulating the frequency of Tregs and consequently affecting disease severity.

1.2.5.2 Sn and autoimmune diseases in human

Sn was reported to be up-regulated on inflammatory monocytes in several chronic autoimmune disease entities. While Sn, generally, appears to be up-regulated at the time of flares or onset of disease, it is not clear whether Sn represents a marker of inflammation or plays a role in the pathogenesis of these diseases.

An investigation of the role of fractalkine and its receptor CX3CR1 in a rat model of chronic proliferative glomerulonephritis confirmed the presence of Sn+ macrophages (being ED3+ and CD68+) at the sites of glomerular injury (Ito *et al*, 2002). An influx of Sn+ macrophages and CD4+ T cells was observed in the inflamed glomeruli. The percentage of Sn+ macrophages correlated well with the disease onset and severity. Up to two thirds of these macrophages expressed the chemokine receptor CX3CR1. In vitro chemotaxis assays suggested that Sn+ macrophages can be attracted by fractalkine expressed in the glomerulus.

Sn+ macrophages were identified in human renal biopsies of patients with lupus nephritis and other forms of glomerulonephritis (Ikezumi *et al*, 2005). In this study, Sn+ macrophages were not detected in renal biopsies of normal kidneys. The frequency of these macrophages in diseased glomeruli was positively correlated with the degree of proteinuria and glomerular damage. In addition, Sn+ macrophages were found to co-localize with CD3+ T cells in the interstitium and were correlated with the degree of tubulointerstitial damage. Glucocorticoid therapy resulted in a reduction in glomerular inflammation, proteinuria and number of Sn+ macrophages in the glomeruli.

Transcriptomic analysis of peripheral blood monocytes from 9 SLE patients was undertaken to identify a potential biomarker for the type I IFN-signature. In this study, Sn was identified as a one of the most prominent type I IFN-regulated candidate genes (Biesen *et al*, 2008). This observation was in line with previous studies that have reported enhanced Sn expression on PBMCs when stimulated with IFNα and TLR3 agonist poly I:C *in vitro* (Taylor *et al*, 2004 and York *et al*, 2007). The frequency of Sn+ resident (CD14+CD16+) and inflammatory (CD14+CD16-CD32+) monocytes was significantly increased in PBMCs of SLE patients compared to those from healthy controls. While the increased frequency of both Sn+ cells on both subsets of monocytes correlated positively with disease activity index, only the frequency of Sn+ resident monocytes showed a positive correlation with anti-dsDNA. A negative correlation was also observed between Sn+ monocytes and serum C3 levels. Immunosuppression therapy (primarily glucocorticoids) and disease remission led to reduced frequency of Sn+ PBMCs. A similar analysis of type I IFN-regulated genes in systemic sclerosis (Ssc) patients reported similar findings of a positive correlation between Sn+ monocytes and type I IFN (Farina *et al*, 2010). In addition, when skin sections from patients with Ssc were compared to healthy controls a prominent staining for Sn was demonstrated. This was evident in the dermis and perivascular regions of the skin lesions. These two studies highlighted a direct link between Sn and type I IFN and a potential active role for Sn in the pathogenesis of SLE and Ssc. However, a

mechanistic approach to analyse the role of Sn in cell-cell interaction was not undertaken in either of these two studies. As the frequency of Sn+ inflammatory and resident monocytes correlated with disease flare and remission, an interaction between Sn and Tregs similar to that observed in EAE might be relevant. Another possibility is related to whether these monocytes are contributing to the pool of apoptotic cells (via defective phagocytosis or as a source of apoptotic materials) and therefore to the production of autoantibodies. Finally, evaluating the relative antigen presenting capacity of the Sn+ resident and inflammatory monocytes might explain if they play a role in inducing autoantibody production.

1.3 Systemic lupus erythematosus

1.3.1 Introduction

SLE is an autoimmune chronic inflammatory condition with multi-system pattern of involvement. SLE is the prototype of systemic autoimmunity of unknown aetiology (Kotzin *et al*, 1996). The disease is characterized by loss of self-tolerance and accelerated apoptosis with subsequent release of nucleosomal materials, which are a major target for immune responses (Bruns *et al*, 2000). Failure to clear these apoptotic materials results in expansion of autoreactive lymphocytes, with increased formation of autoantibody (Denny *et al*, 2006 and Ren *et al*, 2003). Increased levels of antigen-antibody immune-complexes lead to deposition of these in various tissues causing inflammation and damage by activation other immune pathways e.g. complement system. The kidneys are prime sites for immune complex deposition, causing glomerulonephritis (Feng *et al*, 2006). Other organs that can be involved include: haematological abnormalities, cardiovascular, pulmonary, gastrointestinal, peripheral and central nervous system.

The pathogenesis of SLE is multi-factorial. Various genetic, immunological, environmental and hormonal disturbances have been recognised to be involved in the

aetiology of the disease. As for the immune dysregulations, they appear to be secondary to loss of peripheral tolerance. An imbalance between enhanced apoptosis and reduced clearance is central in the pathogenesis of the disease (Jiang *et al*, 2003). The release of nucleosomal materials (nucleic acids complexed with proteins) from apoptotic cells in the presence of defective clearance of these by phagocytic cells lead to processing and subsequent presentation of released DNA and RNA by antigen presenting cells (APCs) to lymphocytes. Expansion of autoreactive T and B lymphocytes causes increased anti-DNA and anti-RNA antibodies with subsequent formation of immune complexes (Diagram 1.7).

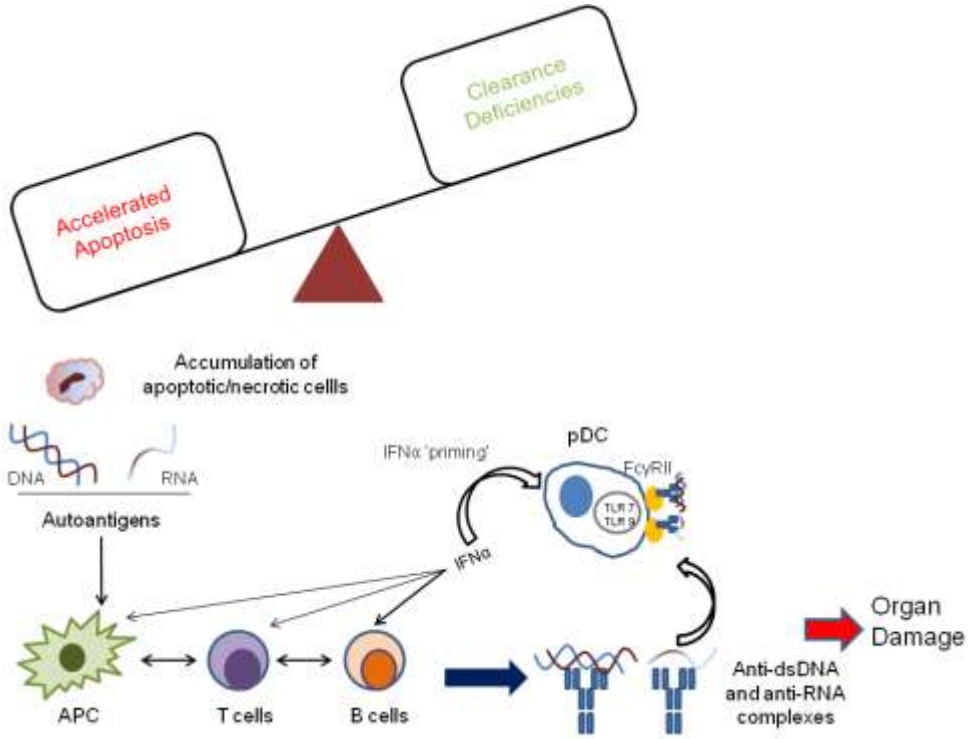

Diagram 1.7 The contribution of an imbalance between apoptosis and clearance to the pathogenesis of SLE. An imbalance between enhanced apoptosis and reduced clearance of apoptotic nucleosomal materials leads to the release of free nucleic acids. These act as autoantigens which are presented to CD4+T cells by antigen presenting cells (APC). Subsequent interaction between T and B cells leads to differentiation and maturation of B cells and the production of autoantibodies. Immune complexes formed of nucleic acids and autoantibodies are internalized by FcγRII on plasmacytoid dendritic cells (pDC) and act as ligands for endosomal Toll like receptor 7 (RNA) and 9 (DNA). This leads to activation of pDCs and production of high amount of IFNα which can further prime pDCs and other monocytes to produce more IFNα. In addition, IFNα exerts multiple biological effects on T and B cells.

1.3.2 Type I interferons

1.3.2.1 In human SLE

Type I interferon family plays a major role in the pathogenesis of murine and human SLE. Early evidence for interferon alpha as a biomarker for human SLE comes from the observation that serum titres of IFN in SLE patients with active disease were found to be considerably elevated and directly correlated to anti-dsDNA titres and disease severity and negatively correlated with C3 levels (Hooks *et al*, 1979). These were thought, initially, to be interferon gamma (IFNγ) in origin based on the fact that these were unstable at pH 2, which is a characteristic feature of IFNγ. Subsequently, sera from SLE patients were incubated with neutralising antibodies against IFNγ and interferon beta which did not have an effect on further detection of IFNα in these sera. Consistent with initial findings, interferon alpha isolated from sera of these patients was acid-labile (Preble *et al*, 1982).

Interestingly, unstimulated mononuclear cells from SLE patients with high and low serum IFNα were found to lack spontaneous production of IFNα *in vitro*. However, these cells were capable of producing interferon alpha when stimulated with interferon alpha inducers. This observation suggested that while peripheral mononuclear cells are capable of producing IFNα, they are unlikely to be a major source for this cytokine *in vivo* (Preble *et al*, 1983). In addition, the incubation of normal PBMCs from healthy donors with sera from SLE patients led to induction of IFNα production. This effect was further enhanced by the addition of IFNa2b and GM-CSF into these cultures (Vallin *et al*, 1999a). Furthermore, sera from patients in remission were less capable of inducing IFNα production in healthy donor PBMCs. This led to the hypothesis of the presence of an interferon alpha inducing factor, which was referred to as SLE-IIF, in the sera of patients with active SLE.

SLE-IIFs were found, initially, to have a molecular weight ranging between 300-1000 kDa. They appeared to consist of immunoglobulin and DNA, which suggested an anti-

dsDNA immune complex structure. Purified anti-dsDNA antibodies or immunoglobluins from sera of SLE patients showed a mild effect on IFNα production by healthy donors PBMCs *in vitro*. Similarly, plasmids with immunostimulatory DNA motifs containing unmethylated CpGs had no IFNα inducing effect on PBMCs. However, when the purified anti-dsDNA and plasmid DNA were combined they led to induction of high levels of IFNα. Interestingly, methylation of plasmid DNA abrogated this effect (Vallin *et al*, 1999b). These findings suggested that IFNα production can be induced with exposure of PBMCs to immune complexes. However, this hypothesis could not explain the natural source of IFNα *in vivo*.

Experiments carried out on stimulation of healthy donors PBMCs with herpes simplex virus (HSV) showed enhanced production of IFNα by a small subset of immature-like dendritic cells which were detected by *in situ* hybridisation. The frequency of these natural interferon alpha producing cells (NIPCs) was 10-fold higher in PBMCs from SLE patients with active disease compared to those from healthy controls, stimulated with IFNγ and GM-CSF (Cederblad *et al*, 1998). Further examination of NIPCs revealed that these cells were CD4+ CD123+ and CD11c-. Isolation and subsequent viral challenge revealed that these cells are capable of producing IFNα at 200-1000 fold higher than other PBMCs. So-called plasmacytoid dendritic cells (pDCs) were found to be a major source of IFNα in vivo (Siegal *et al*, 1999). Furthermore, stimulation of enriched pDCs with combination of apoptotic material and purified IgG from SLE patients led to induction of IFNα production. This effect was reversible with both DNase and RNase treatment (Lovgren *et al*, 2004). Taken together these observations were suggestive for immune complexes to trigger the production of IFNα production by pDCs. Surprisingly, depletion of pDCs from PBMCs of SLE patients and normal healthy controls resulted in only a reduction of 57% versus 95%, respectively, in their IFNα production following viral challenge (Blanco *et al*, 2001). This suggested that although pDCs are a major contributor to IFNα production, other monocytes can be a source of IFNα especially when these are ‘primed’ with the cytokine.

Further evidence for the role of IFNα in autoimmunity and SLE came from observations in patients receiving IFNα therapy for viral hepatitis and carcinoid tumors (Ronblom *et al*, 1991). These patients were found to develop rising anti-nuclear antibodies titres and rarely frank autoimmunity with organ involvement. In a landmark study on the contribution of IFNα to lupus pathogenesis, Baechler and colleagues utilized gene-expression profiling and microarrays of peripheral blood mononuclear cells (PBMCs) from patients with moderate to severe SLE and healthy controls. The type I interferon genes were found to be up-regulated in almost half of the patients enrolled in the study. Interestingly, there was a tendency in the IFN-high group to develop renal, haematological and CNS disease. These findings confirmed a correlation between this" interferon signature" and disease severity (Baechler *et al*, 2003).

1.3.2.2 In murine SLE

New Zealand Black (NZB) X New Zealand White (NZW) F1 hybrid, or (BWF1) mice is a classical model of spontaneous murine SLE (Xu *et al*, 2010). The disease manifestations in BWF1 mice include: rising ANAs titres, lymphosplenomegaly and glomerulonephritis. The spectrum of ANAs includes: anti-double stranded DNA (anti-dsDNA), anti-chromatin, anti-histone and anti-gp70 antibodies (Morel *et al*, 1999, Tucker *et al*, 2000). The disease often starts at 5-6 months of age manifested by increased urinary protein excretion which heralds the onset of glomerulonephritis. This is followed by progressive kidney impairment and death of >90% of these mice by the first year of age (Xu *et al*, 2010). Similar to human SLE, female BWF1 mice are more susceptible to develop disease manifestations.

Early studies in BWF1 mice injected with polyI:C (TLR9 agonist and a potent IFNα inducer) which induces IFNα and IFNβ caused acceleration of disease, enhanced autoantibody production, worsening nephritis and reduced survival (Carpenter *et al*, 1970). Similarly, treatment of 4 week old Fas deficient mice with poly I:C for 12 weeks lead to the development of IgG autoantibodies and renal immune deposits. Crossing these Fas deficient lpr mice with IFNαR KO mice abolished the detrimental effect of

poly I:C (Braun *et al*, 2003). However, a direct analysis of the role of IFNα in murine lupus came from the generation of NZB mice deficient for IFNα/β receptor. NZB mice are characterised by developing autoimmune haemolytic anemia due to the production of anti-erythrocyte antibodies, late onset renal disease and lymphoproliferative disease resembling human chronic lymphocytic leukemia. IFNα/β receptor deficient mice were found to have reduced anti-erythrocyte antibodies, haemolytic anemia and autoantibodies (Santiago-Raber *et al*, 2003). In addition, IFNαR deficiency was associated with reduced T and B cell proliferation and dendritic cell maturation, reflecting the pleotropic effect of IFNα.

The role of IFNα in BWF1 mice was examined by using a replication-deficient murine recombinant IFNα 5-containing adenovirus, given intravenously to pre-autoimmune mice and control BALB/c mice. These were compared to similar groups that received vector only. IFNα treatment caused an early rise in anti-dsDNA titres (10 days post-injection), early onset of disease (19 weeks versus 25 weeks) and increased mortality in BWF1 treated with IFNα versus those treated with vector only (Mathian *et al*, 2005).

1.3.2.3 Function of IFNα/β

Type I interferons may contribute to the pathogenesis of SLE in multiple ways. Exposure of human PBMCs to sera from SLE patients induces maturation of monocytes to dendritic cells capable of efficient antigen presentation to allogenic T lymphocytes (Blanco *et al*, 2001). This potential for DC differentiation was found to be correlative to disease activity index of patients from which sera were obtained. In addition, neutralising antibodies against IL-4, CD40L and GM-CSF did not affect this pro-maturation effect of sera from SLE patients. However, neutralising IFNα dramatically down-regulated such effects (Blanco *et al* 2001). Therefore, type I interferon can influence the disease by driving myeloid dendritic cell maturation and promoting autoantigen presentation to Th cells and augmenting autoreactivity.

Exposure of monocyte-derived DC (mDC) to type I interferon (Interferon α/β) during maturation hinders the ability of these cells to support the proliferation of naive CD4+ T cells stimulated with immobilized anti-CD3. In addition, CD4+ T cells stimulated under these conditions were found to have a reduced capacity to produce IFNγ (McRae *et al*, 2000). The mechanism of this poor co-stimulatory ability of mDCs exposed to type I interferon were found to be correlated with their reduced ability to produce IL-12. In another study on the effect of IFNβ on Th1 differentiation, the timing of type I interferon exposure was shown to be crucial in determining the outcome of Th differentiation. The presence of IFNβ during mDC maturation only versus continuous exposure during mDC maturation and subsequent CD4+ T cells stimulation can lead to paradoxical promotion versus inhibition of Th1 differentiation. Exogenous IL-12 was found to reverse the inhibitor effect of continuous IFNβ exposure of Th1 differentiation and IFNγ production (Nagai *et al*, 2003). Furthermore, healthy human PBMCs treatment with TLR9 agonist CpG, mimicking exposure of pDCs to immune complexes, and subsequent stimulation with staphylococcal enterotoxin A (SEA) in the presence of recombinant human IFNα was found to be associated with reduced production of IFNγ and IL-17. Interestingly, this negative effect was reversed by blocking type I interferon with virus-derived soluble type I interferon receptor (Meyers *et al*, 2006).

Finally, IFNα can directly affect B cells maturation and antibody production. Systemic administration of IFNα co-incidental with or following antigen stimulation was associated with augmented antibody production. In this model selective B cell deficiency in IFNα/β receptor was found to be associated with reduced antibody production and class switching (Le Bon *et al*, 2006). Moreover, pre-treatment of B cells with IFNα was found to lower B cell receptor activation threshold to unmethylated CpG-containing immune complexes (Uccellini *et al*, 2008).

1.3.3 SLE susceptibility loci in BWF1 mice

The identification of lupus susceptibility loci in murine SLE is achieved by undertaking linkage analysis of lupus-prone mouse models. The validation of the involvement of these loci in the disease process comes from introgressing a specific quantitative trait locus (QTL) or genomic interval of interest from one strain into a non-autoimmune strain e.g. C57BL/6 (B6) or BALB/c. Similarly, a combination of loci rather than one locus can be introgressed to analyse potential genetic interactions. Alternatively, locus homozygosity in a lupus-prone or a lupus-resistant background can be used to examine for dominance or recessive pattern of contribution of an individual locus.

The BWF1 hybrid model is a classic example of genetic interaction between two strains, each one having rather mild (NZW) or late (NZB) display of autoimmunity, but once crossed results in full manifestations of disease. This phenomenon is in line with epistatic mechanisms by which a gene might not be penetrant in the parental background, but in association with other genes increases disease susceptibility.

Female BWF1 mice develop fatal autoimmunity characterised by rising antinuclear antibodies (mostly IgG) and severe lupus nephritis which culminates in death in the first year of life (Morel et al, 1999). In contrast, parental NZB can occasionally develop renal manifestation within the first year of life. Instead they develop autoimmune hemolytic anemia and rising IgM ANA. As for the parental NZW mice, they don't develop features of autoimmune disease for the first 18 months of their life (Braverman *et al*, 1968). This might suggest that the contribution of the NZW genes to the mild autoimmunity of NZB strain can accelerate the process in their hybrid progeny. Evidence for this hypothesis arises from crossing BWF1 mice with NZB parental strain to examine for NZW genome contribution to the disease. The MHC class II ($H2^z$) locus on chromosome 17 was identified as a dominant gene with direct impact on the development of IgG ANAs and severe lupus nephritis (Kotzin *et al*, 1987). Heterozygosity at this locus in the BWF1 mice ($H2^d$ from NZB and $H2^z$ from NZW i.e. $H2^{d/z}$) is one of the major factors in disease

pathogenesis with a direct link to CD4 autoreactivity in the hybrid model. However, the presence of other loci (MHC-related or -unrelated) can affect the impact of the H2 locus. This was evident when PL/J non-autoimmune mice, which have the same MHC class II genes as NZW mice, or B6/H2^{z} or BALB/c/H2^{z}, were crossed with NZB strain and shown to have a much lower incidence of ANA production and nephritis compared to BWF1 mice (Schiffenbauer *et al*, 1992 and Drake *et al*, 1995).

The above findings suggested the presence of other loci from NZW mice that could contribute to disease susceptibility. In an attempt to address this point, (NZW x PL/J) F1 mice were crossed with the NZB strain, generating BWP mice. In this model, the presence of PL/J genes would have impeded the interaction of certain alleles from NZB and NZW mice, leading to disease amelioration. The BWP mice were found to develop nephritis (45%) and early mortality (25% first year), albeit to a lesser extent compared to BWF1 mice. Linkage analysis revealed two loci contributing to mortality and nephritis. The first locus was found on chromosome 2 and the second was found to be telomeric to MHC locus on chromosome 17. They were designated (NZ**W**-NZ**B** x NZ**W**) Wbw1 and Wbw2, respectively. Wbw1 locus was shown to have a high risk of early mortality (52%) and proteinuria (52%). On the other hand, mice carrying the Wbw2 locus had a mortality rate of 29% and proteinuria rate of 42%. Interestingly, mice carrying a PL/J allele of the Wbw2 locus had a lower mortality compared to those carrying the NZW allele. This was indicative of a positive influence of Wbw2 on Wbw1 with regard to mortality. In addition, mice carrying both PL/J alleles did not develop disease (Rahman *et al*, 2002).

Endogenous retroviral glycoprotein 70 is an acute-phase reactant, the level of which was found to be elevated in NZW mice. Immune complexes formed from gp70 and anti-gp70 are found to be deposited in diseased glomeruli and serum levels of anti-gp70 antibodies were found to be closely related to lupus nephritis correlative with disease severity (Vyse *et al*, 1996). Enhanced gp-70 production in New Zealand mice was found to be linked to multiple loci of NZB and NZW origins. These are referred to

as Nbwa (New Zealand Black/White autoimmunity) loci. These are located on chromosome 4, NZB-derived Nbwa2 (Drake, 1994), chromosome 12 NZW-derived Nbwa1 (Rigby *et al*, 2004) and chromosome 13 NZB-and NZW-derived Nbwa1 (Tucker *et al*, 2000 and Santiago *et al*, 1998).

Although the previous studies showed loci linkage to ANA and/or renal disease traits the association of susceptibility loci to specific immune pathways/cell subsets was not evident. In a landmark series of studies to identify new susceptibility loci, Morel and colleagues defined the genomic positions of three recessive loci termed Sle1, Sle2 and Sle3 on chromosomes 1, 4 and 7. The New Zealand Mixed ((NZB x NZW) F1 x NZW), also known as NZM2410, was used to identify these loci which were found to be strongly associated with severe lupus nephritis (worse than BWF1 disease). Subsequently, congenic strains carrying one of these segments on B6 background were examined. These models were shown to have specific defects in different immune pathways. The B6.NZMc1, carrying Sle1 segment, mediated loss of tolerance to nuclear antigens (Mohan *et al*, 1998). In the B6.NZMc4, with Sle2 locus, there was evidence of reduced activation threshold of B cell activation (Mohan *et al*, 1997). Finally, B6.NZMc7, carrying Sle3, had T cell dysregulation and reduced CD4+ T cells activation-induced cell death (Mohan *et al*, 1999). These findings raise the question of the possibility of resistance-genes in NZW mice that would prevent the development of clinical manifestations of autoimmunity in NZW mice. This led to identification of lupus-resistant loci Sles1, Sles2, Sles3 and Sles4. Crossing B6.NZMc1 to NZW mice abolished the rise in ANA. These data have further confirmed important epistatic mechanisms that keep susceptibility loci suppressed (Morel *et al*, 1999).

The **L**upus NZ**B** x NZ**W** (Lbw) set of susceptibility loci were identified by intercrossing BWF1 mice, generating BWF2 strain. Eight loci (Lbw 1-6) were found on chromosomes 17, 4, 5, 6, 7, 18, 1 and 11. Of these, Lbw1 (MHC) locus was linked to increased ANA titres, glomerulonephritis and mortality. Although, Lbw2 (NZB gene) was associated with increased early mortality in BWF2 mice; this effect was reduced in the BWF1 mice

carrying this locus. This phenomenon was likely to indicate epistatic requirements for Lbw2 to exert its pro-mortality effect. Lbw2 was also found to be significantly associated with developing glomerulonephritis. Lbw5 on chromosome 7 is an NZW locus that was found to contribute to the high mortality of the BWF1 mice. Interestingly, these loci had an additive effect when combined, with first year mortality rising from around 30% for a single locus to more than 50% when all three were combined. However, the latter figure is still short of the 90% mortality in the BWF1 mice, indicating more loci were required. Lbw3 (chromosome 5) and Lbw6 (chromosome 18) are both NZW-derived genes. Like Lbw1 locus, Lbw6 was linked to glomerulonephritis severity. The study of this group of loci suggested that although six of these loci (Lbw1-6) were associated to various extents with increased mortality, only three (Lbw1, 2 and 6) were associated with glomerulonephritis. This discrepancy suggested that the non-GN loci might increase mortality by their effect on other systems e.g. vasculopathy (Kono *et al*, 1994).

The contribution of MHC and non-MHC loci derived from the NZW genome to the BWF1 disease was examined in a study of (NZW x BALB/c) x NZW mice. The aim of this investigation was to identify NZW-derived non-MHC loci that might influence ANA production, especially as NZW mice do not develop renal disease. BALB/c mice were chosen in this study as they have the NZB haplotype for MHC locus, $H2^{d}$. The titres of IgG anti-ssDNA antibodies, characteristic for NZW strain, were found to be at least 10-fold lower in NZW x BALBc compared to NZW parental strains. Mice that were heterozygous for the MHC locus ($H2^{d/z}$) showed a higher titre of IgG anti-ssDNA compared to homozygous state ($H2^{z/z}$). This finding indicated that the contribution from the non-autoimmune genome of the BALB/c strain for the MHC locus increased the chance of having a high titre of IgG anti-ssDNA antibody. In addition, two new NZW loci on chromosomes 16 and 19 were identified. These were called **N**ew Zealand **W**hite **a**utoimmunity, Nwa1 and Nwa2 respectively. Nwa1 was found to be significantly linked

to IgG anti-ssDNA and anti-histone antibodies, while Nwa2 was linked to the production of the former antibody only (Vyse *et al*, 1996).

The contribution of NZB loci to disease in BWF1 was investigated with NZB x C57BL/6 and NZB x BALB/c crosses. First B6 and BALB/c mice were crossed with NZW mice to generate congenics for $H2^z$ MHC locus on each of the non-autoimmune strains. These were subsequently crossed with NZB mice. The effect of the $H2^z$ locus was only evident on the B6 non-autoimmune background. This finding did further suggest the influence of the genetic background on NZB-derived disease loci. Furthermore, linkage analysis of these mice identified a novel locus on the distal end of chromosome 1, **N**ew Zealand **B**lack **a**utoimmunity locus (Nba2) that was implicated in lupus nephritis in both sets (Rozzo *et al*, 1996). The characterisation of the Nba2 locus in lupus nephritis was subsequently examined by generating congenic mice of Nba2 on a B6 background (B6.Nba2). These mice were then intercrossed to generate congenic mice homozygous for Nba2. The later mice were crossed with NZW strain and found to develop severe proteinuria, lupus nephritis and rising ANA (particularly IgG anti-dsDNA and IgG anti-histone antibodies). In addition, microarray analysis of spleens from B6.Nba2 and B6 mice showed as genes with differential expression and localisation to the Nba2 region. These were Ifi202 and Ifi203, Interferon-Inducible (Ifi) in the Ifi200 cluster. Phenotypically, the B6.Nba2 mice showed a higher frequency of B cells and reduced degree of apoptosis following anti-IgM treatment, compared to B6 mice (Rozzo *et al*, 2001).

In conclusion, the disease in BWF1 mice represents complex interaction between multiple NZB and NZW susceptibility and resistance loci. These polygenic interactions contribute to different aspects of the disease process and survival. Epistatic mechanisms appear to be central in the interaction between different loci to account for a certain trait. Equally important, the genetic background in which the interactions of these loci occur appears to be central for the loci to result in a trait manifestation.

1.3.4 Tregs in SLE

1.3.4.1 Tregs characteristics

CD4+CD25+Foxp3+ T cells (Tregs) are specialized CD4+ lymphocytes that play a central role in maintaining immunological tolerance. They were initially described in the 90s by Sakaguchi and colleagues as a T lymphocyte subset expressing high levels of IL-2 receptor alpha-chain (CD25) that were able to prevent autoimmunity in neonatal thymectomised mice (Sakaguchi *et al*, 1995). Adoptive transfer of CD4+CD25+ T cells to these thymectomised mice prevented autoimmunity and multi-organ inflammation. Subsequent studies revealed that stable expression of forkhead box p3 (Foxp3) gene is restricted to Tregs and is required for their differentiation, suppressive function and proliferative potential (Fontenot *et al*, 2003 and Hori *et al*, 2003). Thus Foxp3 is regarded a master regulator and lineage specific marker of murine Tregs development and differentiation. In humans, mutation in the Foxp3 gene leads to the development of IPEX (immune dysregulation, polyendocrinopathy, enteropathy, X-linked syndrome). Scurfy is the murine analogue of IPEX (Bennett *et al*, 2001). Both syndromes are characterised by lymphoproliferation and multi-organ inflammation.

Thymic Tregs differentiate from CD4 single positive Foxp3- thymocytes. Their differentiation as defined by Foxp3 induction requires: instructive TCR stimulation with self-peptide-MHC complexes presented by thymic epithelial cells, CD28 co-stimulation by CD80/86 on APCs, high affinity IL-2 receptor and other gamma cytokines e.g. IL-7 and IL-15. Tregs homeostasis is dependent on IL-2 produced by the CD4+Foxp3- T effectors (Teffs). On the other hand, Tregs can develop outside the thymus in the secondary lymphoid tissues (Knoechel *et al*, 2005) and the gut (Ivanov *et al*, 2008). These are referred to as induced Tregs (iTregs). The differentiation of iTregs requires IL-2 and TGFβ. The mechanism by which TGFβ induces transcription of Foxp3 in iTregs involves the cooperation of transcription factors STAT3 and NFAT (Josefowicz *et al*, 2009). While TGFβ appears to be essential for the generation of iTregs, the

cytokine is redundant for the generation of thymic Tregs. T cell-specific TGF-beta receptor II deletion or TGFβ1 deficiency didn't appear to affect the development of natural Tregs (Marie *et al*, 2006, Fahlen *et al*, 2005).

Although Foxp3 transcription factor is used as a murine Tregs specific marker, transient or unstable expression of Foxp3 can occur. These cells were recently labelled as "exFoxp3" and they were found to produce inflammatory cytokines such as IFNγ and IL-17. In addition, exFoxp3 cells isolated from pancreas of new onset diabetes (NOD) mice were found to have low CD25 and high CD127 expression. Furthermore, adoptive transfer of these cells into T cell deficient NOD mice led to aggravation of disease. These data suggested that instability of Foxp3 expression in Tregs could result in the generation of pathogenic effector/memory cells. (Zhou *et al*, 2009).

In human, the search for a unique Tregs marker is still ongoing. Initially, CD4+CD25 hi were considered to represent Tregs. However, CD25 is also expressed by recently activated CD4+ T cells. Subsequently, other markers such as CTLA-4, GITR, LAG-3 and CD127 were found also not to be Tregs restricted (Roncarolo *et al*, 2008). Comparative DNA microarray analysis of freshly isolated or activated T cell subsets revealed a number of genes that were up-regulated in a Treg-specific manner. Among these Helios, a member of Ikaros transcription factor family was found to be a potential Foxp3 target gene (Sugimoto *et al*, 2006). Recently, the protein expression of Helios was investigated by means of a newly developed monoclonal antibody (Thornton *et al*, 2010). While CD4+CD8-Foxp3+ thymocytes were found to have 100% expression of Helios, only 70% of peripheral CD4+Foxp3+ T cells expressed Helios. In addition, induction of Foxp3 in naive T cells from mouse and human with TCR stimulation in the presence of IL-2 and TGFβ was not found to be associated with Helios expression. This finding meant that Helios expression is specific for thymic Tregs and not peripherally induced Tregs.

Tregs express a range of homing receptors including adhesion molecules and chemokine receptors. In lymph nodes the majority of Tregs express CCR7 at high levels. Around 30% of Tregs express CD103 which interacts with its ligand E-cadherin on epithelial cells. More than 50% of Tregs express high levels of CD62L. The pattern of expression of these homing receptors dictates Tregs localization and trafficking to various tissues and their involvement in a particular immune response (Sakaguchi *et al*, 2008).

1.3.4.2 Mechanisms of suppression

Tregs utilize multiple mechanisms to exert their suppressive function. These mechanisms might differ depending on the target cell of the Tregs. Indeed most of these mechanisms are described in vitro rather than in vivo. They can be broadly divided into those related to suppressing T effectors and those related to interaction with APCs. Contact-dependent inhibition of IL-2 mRNA production by the T responders is regarded as one of the main mechanisms of Tregs suppression of T responders. Direct evidence for this mechanism comes from the findings of low IL-2 mRNA expression in Teffs in co-culture with Tregs (Oberle *et al*, 2007). Moreover, exogenous addition of IL-2 did not affect this prominent inhibition of IL-2 mRNA production. As Tregs express high levels of IL-2Rα (CD25), there is a possibility of competition between Tregs and Teffs for IL-2 which ultimately can lead to Teffs death. However, the use of anti-CD25 blocking antibodies against human Tregs failed to have an effect on the suppressive function of these cells against mouse Teffs (Tran *et al*, 2009).

Cytolysis represents another potential contact-dependent mechanism of Tregs suppression upon Teffs. This observation was made on activated murine Tregs as they were found to up-regulate granzyme B expression and mediate death of Teffs via a granzyme B-dependent mechanism in vitro (Gondek *et al*, 2005). This cytolytic potential of Tregs was also examined in malignancy. About a third of Tregs expressed granzyme B and they induced cytolysis on NK and CTLs in a granzyme B- and perforin-dependent mechanism (Cao *et al*, 2007).

Cell cycle arrest is another possible mechanism of Tregs interaction with either Teffs or APCs. Galectin-1 is a homodimer that binds to many glycoproteins like CD45, CD43 and CD7. Galectin-1 is preferentially expressed by activated Tregs and can induce cell cycle arrest and apoptosis in a contact-dependent manner. Blocking galectin-1 or galectin-1 deficiency were both found to reduce the inhibitory effect of Tregs (Garin *et al*, 2007) Recently, IL-35 has been identified as a Tregs-related new inhibitory cytokine. IL-35 is a member of the IL-12 family and is composed of Epstein-Barr virus induced gene 3 (Ebi3) and IL12a. The mRNA of both these components is increased in Tregs suppressing T effectors (Collison *et al*, 2009). Interestingly in this study, Tregs maintained the ability to suppress Teffs across a permeable membrane when placed in the top chamber and in direct contact with Teffs. This process was IL-35 and IL-10 dependent.

Another mechanism of suppression by Tregs can occur via interaction with DCs. In co-culture of Tregs and DCs, it was shown that Tregs exert suppression by two mechanisms: an initial aggregate formation on immature DCs which is dependent on leukocyte function-associated antigen (LFA-1 or CD11a/CD18). The second mechanism is down-regulation of CD80/86 expression on DCs being dependent on both LFA-1 (Tran *et al*, 2009) and CTLA-4. Consequently, this failure of maturation affects the ability of DCs to present antigens to autoreactive naive T cells (Onishi *et al*, 2009). Further evidence to the importance of CTLA-4 in mediating Tregs suppression comes from the findings of fatal lymphoproliferative disease in mice with selective Tregs CTLA-4 deficiency. Reconstitution of immunodeficient mice with total CD4+ T cells from CTLA-4-deficient-Treg mice can maintain immune responses to transplanted tumors, suggesting defective Tregs suppression (Wing *et al*, 2008)

1.3.4.3 Tregs in murine SLE

Tregs abnormalities can be central to the aetiopathogenesis of SLE. Such abnormalities can be broadly divided into: (i) altered Tregs frequency in active disease leading to enhanced proliferation of autoreactive Teffs (ii) reduction in Tregs

suppressive function (iii) Teffs resistance to Tregs suppressive action (iv) Tregs involvement in complex scenarios with Th17 and Th1 responses. Studies on NZB x NZW F1 lupus prone mice showed mixed results in terms of the frequency of Tregs population. Tregs depletion 3 days after birth in BWF1 mice using anti-CD25 antibodies led to increased IgG2a anti-dsDNA titres and accelerated nephritis (Hayashi *et al*, 2005). Similarly, comparison of Tregs frequency among autoimmune strains such as BWF1 mice and non-autoimmune B6 and BALB/c mice showed a reduced peripheral lymph nodes frequency of these cells in young mice from BWF1 mice compared to non-autoimmune strains. Splenic frequency followed a similar trend except for comparison between BWF1 mice and B6 (Tucker *et al*, 2011).

In contrast, the prevalence of Tregs between young (8-10 weeks) and old (48-52 weeks) BWF1 mice compared to age-matched non-autoimmune BALB/c mice revealed that there was reduced frequency in pre-diseased BWF1 mice. However, there was an increase in the frequency of these cells in peripheral lymph nodes in the aged mice group. Interestingly, there was a decline in the prevalence of splenic Tregs in diseased mice. There was no difference in the proliferation or suppressive capacity of Tregs between these two groups, *in vitro*. Adoptive transfer of, in vitro expanded Tregs helped in disease amelioration (Scalapino *et al*, 2006).

Similarly, Tregs frequency was found to be increased in diseased mice between 32-40 weeks of age compared to BALB/c control mice. In addition, Tregs were found in glomerular, interstitial and perivascular infiltrates of kidneys from diseased BWF1 mice. The suppressive function of Tregs isolated from spleen and lymph nodes was not defective in the aged compared to young BWF1 mice (Abe *et al*, 2008).

These two studies indicated that Tregs frequency or suppressive functions were not affected in diseased BWF1 mice, yet Tregs failed to control disease. This might be explained by other factors that can influence Tregs function. In vitro studies of Tregs suppressive function are not necessarily a mirror image of their in vivo profile. The

presence of other inflammatory cytokines such as IL-6 and TNFα can both have a direct effect on Tregs function. IL-6 has been shown to increase Teffs resistance to Tregs suppression (Pasare *et al*, 2003). Indeed, IL-6 (in the presence of TGFβ) can convert Tregs into Th-17 cells (Xu *et al*, 2007). Similarly, TNFα was found to down-regulate Foxp3 expression in both naturally occurring CD4+CD25hi and TGFβ induced human Tregs. Interestingly, patients with rheumatoid arthritis were found to have reduced Foxp3 mRNA and protein expression. Anti-TNFα Therapy with infliximab restored both Foxp3 expression and suppressive function on Tregs from these patients (Valencia *et al*, 2006). These studies highlight the effect of the cytokine milieu on Tregs function

Another explanation for Tregs failure in controlling disease is related to Tregs repertoire. Immunizing female BWF1 mice with an artificial peptide derived from sequences within the V_H regions of several murine anti-dsDNA Ig was found to delay onset of disease and prolong survival. While the total frequency of Tregs was similar between tolerized and control mice, there was a significant expansion of peptide-specific-Tregs. This study highlights the importance of the repertoire of Tregs over the total frequency of Tregs in BWF1 mice (La Cava *et al*, 2004).

The other side of the equation in Tregs suppression is related to Teffs resistance to Tregs suppression. This was investigated in MRL/mp murine model of SLE. Crossover suppression tests between enriched Tregs from H2-matched CBA/ca mice and CD4+CD25- T cells from MRL/mp mice showed reduced sensitivity to suppression (Monk *et al*, 2005).

In conclusion, Tregs play a major role in maintaining immunological tolerance. The evidence for the negative association between Tregs frequency and disease severity in SLE is conflicting. The factors involved in this are related to the timing of the analysis of Tregs frequency in the course of the disease, the control mice used in the experiments and whether peripheral lymphoid organs are representative of targeted organs (in

BWF1 mice the kidneys). As for the suppressive function of Tregs, it appears that in vitro analysis does not necessarily reflect in vivo scenarios particularly with the complex in vivo cytokines milieu in which Tregs function.

1.4 Aims of this thesis

Sn is the prototype of the Siglec family and it has been shown to mediate cell-cell interactions of macrophage subsets (Crocker 2007). Recent evidence has suggested that in mice with autoimmune disease Tregs express abundant ligands for Sn (Wu *et al*, 2009). The interaction between Sn and Tregs was found to negatively influence the frequency of Tregs in inflamed central nervous system and peripheral lymphoid organs. It is not clear if SnL are expressed exclusively on Tregs or whether Teffs can also express these ligands under certain conditions. Indeed, the conditions leading to the up-regulation of SnL or the phenotype of this subset of cells have not been determined.

The first aim of this thesis was to explore the regulation of SnL on CD4+ T cells. To achieve this, an in vitro analysis of the expression of SnL on both Tregs and Teffs following ligation of T cell receptor (TCR) was undertaken.

The objectives of this part of the project were:

- To identify the phenotype of SnL+CD4 T cells. Experiments were designed to examine the activation, proliferation and cytokine profiles of these cells.
- The second objective was related to the analysis of the functional consequences of engaging SnL on CD4 T cells.
- Another objective was to explore the nature of SnL on CD4 T cells. This analysis was done at multiple levels. First, an investigation into the changes in sialylation and glycosylation that coincides with the up-regulation of these ligands was undertaken. Second, the glycan nature of the SnL was determined by performing glycosylation inhibition experiments. Third, the nature of the SnL carrier and potential counter-receptors for Sn on CD4 T cells were examined.

The experiments related to this part of the investigation are described in chapter 3 of this thesis.

The second aim of this project was to examine the role of Sn and SnL+ CD4 T cells in the NZB XNZW F1 (BWF1) mouse model a of spontaneous systemic lupus erythematosus. Transcriptomic analysis in human SLE revealed that Sn is a candidate gene linked to the “interferon signature” associated with disease (Biesen *et al*, 2008). In addition, the expression of Sn on monocytes was found to correlate with disease severity and other established biomarkers of the disease. However, the role of Sn in this complex polygenic disease is not understood. The correlation between Sn expression and disease severity might be suggestive for a pro-inflammatory role for the molecule as in other autoimmune disease models (Jiang *et al*, 2006;Ip *et al*, 2006; Kobsar *et al*, 2007 and Wu *et al*, 2009) but the evidence is lacking.

The aim of the second part of this project was to explore the significance of Sn and SnL in the pathogenesis of murine SLE. To achieve this aim, three objectives were set:

- To confirm the enhanced expression of Sn in murine BWF1 model of spontaneous SLE. To this end, Sn mRNA expression was examined in renal tissues of BWF1 mice. Understanding time-point in the disease course at which Sn is up-regulated is pertinent to scenarios in which the molecule may play a role. Furthermore, the cytokine microenvironment, particularly IFNα, can be directly involved in enhancing Sn expression.
- The second objective was to examine the effect of blocking the expression of Sn on the disease onset and severity. Monoclonal antibodies against two distinct epitopes of Sn were administered to BWF1 mice at a pre-nephritic stage and lupus nephritis onset and severity were examined at 32 weeks of age.
- The third objective of this study was to analyse the function of Sn in murine lupus nephritis by generating Sn deficient BWF1 mice. Sn deficient BWF1 mice were generated using speed congenics strategy. Pre-defined NZB and NZW

lupus susceptibility loci were initially introgressed into NZB and NZW mice heterozygous for Sn and then these mice were used to generate Sn deficient NZB and NZW mice. Homozygotes were generated by crosses between heterozygous or homozygous NZB and NZW mice. Due to time restrictions, Sn deficient and wild-type BWF1 mice were examined at the age of 18 weeks only and the data are considered preliminary.

The experiments related to this part of the investigation are described in chapter 4 of this thesis.

In summary, the works presented in this thesis describes investigations into the regulation of SnL, molecular aspects of up-regulating these ligands and functional consequences of engaging SnL on CD4+ T cells. The second part of this analysis examines the significance of Sn and SnL up-regulation in BWF1 murine model of SLE.

Materials and Methods

2.1 Mice

C57BL/6, New Zealand White, New Zealand Black and New Zealand Black X New Zealand White F1 (BWF1) mice purchased from Harlan (Oxford, UK) or bred and maintained at Wellcome Trust biological services (Dundee, UK). The generation of sialoadhesin deficient mice was previously reported by Dr C Oetke (Oetke *et al*, 2006). Briefly, Sn knockout mice were generated by targeted homologous recombination using the 129Sv embryonic stem cell line in which a neomycin resistance gene cassette was inserted into exon III. All Sn wild type and knockout mice used were intercross offspring of heterozygotes backcrossed for more than 20 generations onto a C57Bl/6 background. Sn WT and Sn KO mice of 8-14 weeks of age were employed in all experiments. Mice were housed under specific-pathogen-free conditions. All experiments were performed in compliance with Home Office regulations.

2.2 Sn-/- BWF1 mice

2.2.1 Generation of Sn-/-BWF1 mice

The generation of BWF1 mice deficient for Sn was done in three phases (Diagram 2.1): (1) generation of parallel NZB and NZW mice that are heterozygous for Sn. (2) Crossing Sn heterozygous mice for each strain to generate NZB and NZW mice wild-type and deficient for Sn. (3) Intercrossing wild-type (WT) or Sn sufficient or deficient male NZW mice with WT or Sn deficient NZB mice, to generate Sn WT and Sn deficient BWF1 mice. Speed congenics (Wakeland *et al*, 1997) was employed to transfer a set of pre-defined NZB and NZW susceptibility loci (Table 2.1) to recipient mice that are heterozygous for Sn. Monitoring the introgression of these loci was examined by genotyping with microsatellite markers (20 for NZB and 25 for NZW).

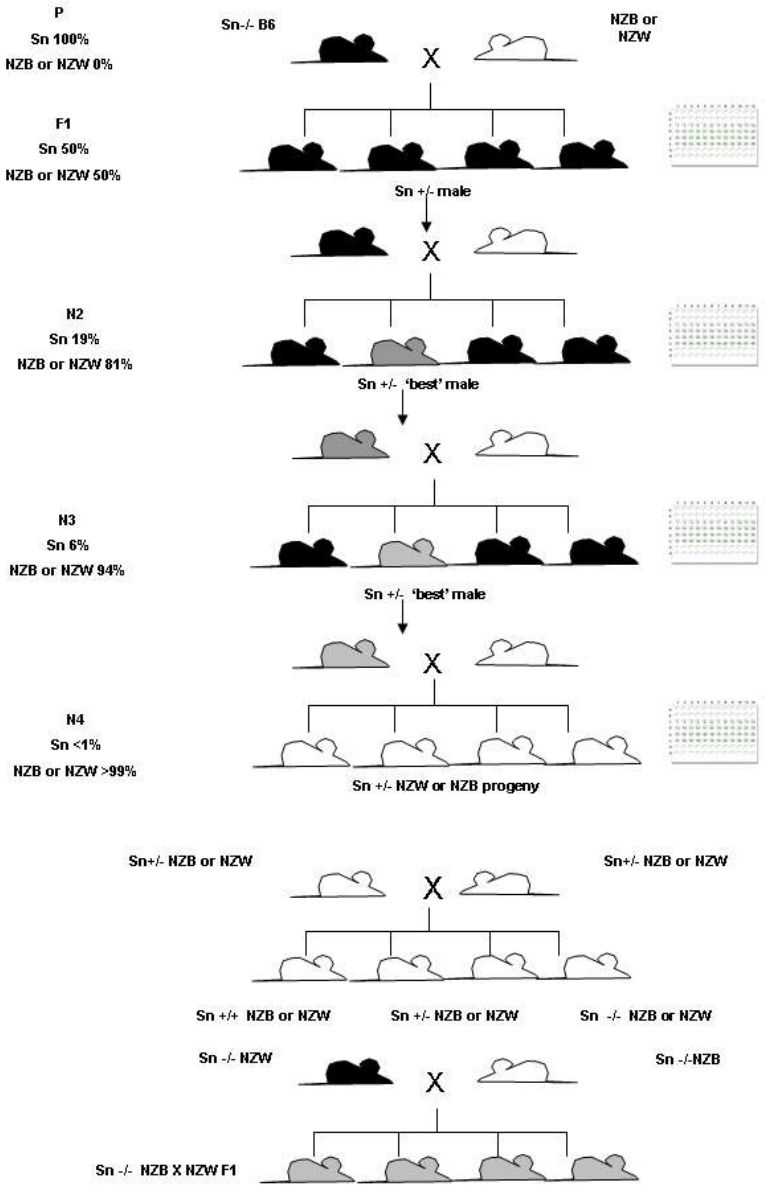

Diagram 2.1 Speed congenics schematic for generating Sn+/+ and Sn-/- BWF1 mice. P (parental mice) Sn-/- B6 mice were crossed to NZB and NZW mice to generate Sn+/- on each background. Male mice in each generation were screened with polymorphic markers (96-well plate) for NZB or NZW susceptibility loci. The best male in each generation was backcrossed to parental NZB or NZW to increase the number of required susceptibility loci in the next generation. The colour of the best male in each generation represents step-wise increase in the number of introgressed loci (NZW in this case). Sn+/- NZB and NZW mice with a full set of loci were then intercrossed to generate Sn-/- and Sn+/+ NZB and NZW mice. Subsequently, male Sn+/+ and Sn-/- NZW and female Sn+/+ and Sn-/- NZB were used as parental mice to generate Sn+/+BWF1 and Sn-/-BWF1 mice.

Table 2.1 NZW and NZB susceptibility loci and corresponding markers used in generating BWF1 mice deficient for Sn.

NZW loci and markers			NZB loci and markers		
Locus	**Chromosome**	**Marker**	**Locus**	**Chromosome**	**Marker**
Sle1	1	D1Mit1001	**Sle1**	1	D1Mit132
Sle1	1	D1Mit111	**Sle1**	1	D1Mit308
Sle1	1	D1Mit155	**Sle1**	1	D1Mit111
Wbw1	2	D2Mit66	**Sle2**	4	D4Mit193
Wbw1	2	D2Mit411	**Sle2**	4	D4Mit17
Wbw1	2	D2Mit148	**Sle2**	4	D4Mit308
Nbwa2	4	D4Mit193	**Lbw4**	6	D6Mit209
Nbwa2	4	D4Mit308	**Lbw4**	6	D6Mit36
Lbw3	5	D5Mit95	**Lbw4**	6	D6Mit328
Lxw2	6	D6Mit138	**Sle3**	7	D7Mit350
Lxw2	6	D6Mit36	**Sle3**	7	D7Mit101
Lbw5	7	D7Mit294	**Lmb4**	10	D10Mit230
Lbw5	7	D7Mit350	**Lmb4**	10	D10Mit96
Nbwa1	12	D12Mit182	**Lbw8**	11	D11Mit285
Nbwa1	12	D12Mit158	**Lbw8**	11	D11Mit333
Nw	13	D13Mit275	**B6.NZBc13**	13	D13Mit16
Nw	13	D13Mit260	**B6.NZBc13**	13	D13Mit74
Nwa1	16	D16Mit131	**H2**	17	D17Mit51
Nwa1	16	D16Mit52	**H2**	17	D17Mit10
Lbw1	17	D17Mit245	**Fas**	19	D19Mit333
Wbw2	17	D17Mit93			
Lbw6	18	D18Mit177			
Lbw6	18	D18Mit48			
Nwa2	19	D19Mit28			
Nwa2	19	D19Mit33			

2.2.2 Genotyping

Ear biopsies from mice in each progeny were genotyped initially for Sn. All Sn heterozygous NZB and NZW mice were then screened for relevant polymorphic markers (Table above). Once all required susceptibility loci were introgressed, further genotyping was done for Sn only. All polymerase chain reactions (PCR) were done using the GoTaq®Flexi DNA polymerase PCR kit (Promega). The kit includes: 5X Green GoTaq®Flexi buffer (proprietary formulation at pH8.6), $MgCl_2$ 25mM and GoTaq DNA polymerase (5U/µl). A 100mM dNTP (2'-deoxynucleoside 5'-triphosphate) was purchased from Invitrogen. PCR conditions were optimized for each marker by adjusting factors such as: annealing temperature, extension temperature, primer concentrations and polymerase concentrations (see Appendix A.3). The primer sets used in genotyping of NZB polymorphic markers were a kind gift from Dr Paul Lyons (Cambridge institute for medical research (CIMR), Cambridge). For a list of these primer sets see Table A.1. The primer sets used in genotyping of NZW polymorphic markers were designed using Primer Express software 2.0 (Applied Biosystems) and they were purchased from Eurofins MWG operons. Table A.2 lists the primers sets used in genotyping of NZW markers. In Sn genotyping, bands were visualized by ethidium bromide on a 2% agarose gel and the size of the PCR products was examined using a 1 Kb DNA ladder (Bio Labs). In NZB and NZW genotyping, bands were visualized by ethidium bromide on a NuSieve:Agarose gel 3:1 (Lonza) and the size of the PCR products was examined using a 50bp ladder (Promega).

2.3 Cell culture

Complete RPMI (RPMI 1640 (Life Technologies, UK) + 10% heat-inactivated foetal calf serum (FCS, PAA laboratory) + 2mM L-glutamine (Gibco) + 2mM mercaptoethanol (Gibco) + 10mM HEPES (Gibco) + 100 units/ml penicillin/0.1mg/ml streptomycin

(Gibco)) was used with splenocytes, CD4 T cell cultures and CD4:bone marrow-derived macrophages (BMDM) co-cultures. DMEM (Life Technologies, UK) + 10%FCS + 100units/ml penicillin/0.1mg/ml streptomycin was used in BMDM cultures (without CD4+ T cells). Serum free Ultracho (BioWhittaker, Belgium) was used in cultures of SnFc secreting CHO cells, in alternation with Glutamine –free Glasgow modified Eagle's medium (GMEM) containing 1% FCS. Chinese hamster ovary cells (CHO) secreting SnFc or R97A (mutant form of SnFc in which arginine 97 is substituted with alanine, Vinson et al, 1996) were cultured in F-12 nutrient mixture Ham's medium (Gibco) +10%FCS.

2.4 Cell isolation

2.4.1 CD4+ T cells

CD4 T cells were enriched by magnetic-activated cell sorting (MACS). Single cell suspensions from spleen were prepared by mashing the spleen through a 100 micron cell strainer (BD Bioscience). Red blood cells were removed using RBC lysis buffer (Sigma).This was followed by DNase treatment (2µg/ml) (DNase I, Roche) to remove any cell clumps. CD4 T cells were selected using a mouse CD4 T cell isolation kit (Miltenyi Biotec). In this protocol, cell populations (CD8, B cells, macrophages, B lymphocytes, NK cells and erythroid cells) except the one of interest (CD4) are labelled with a cocktail of biotinylated antibodies (CD8, CD11b, CD45R (B220), DX5 and Ter-119) in PBS+2mMEDTA+0.5%BSA for 10 minutes at 4^{o}C. This is followed by the addition of anti-biotin microbeads and further incubation for 15 minutes at 4^{o}C. Next, cells are washed and re-suspended at a density of up to 1 X 10^{8} cells/ 500µl of PBS+2mMEDTA+0.5%BSA. Cells were then resuspended in buffer. Magnetic separation was done using AutoMACS separator, by depleting antibody-labelled populations. A purity of more than 94% was obtained in all experiments.

2.4.2 CD4+CD25+ Treg cells

CD4+CD25+ T cells (Tregs) were purified using a similar protocol to the previous section (2.4.1) with some modifications. First, anti-CD25 PE antibody was added together with anti-biotin microbeads against biotin-antibody cocktail against non-CD4 T cells. Second, following CD4 enrichment, cells were washed, re-suspended in PBS+2mMEDTA+0.5%BSA and anti-PE microbeads were added to separate CD4+CD25+ and CD4+CD25- population afterwards. All the above steps were done using a mouse Tregs isolation kit (Miltenyi Biotec) and following manufacturer's instructions. Magnetic separation was done using AutoMACS separator, as per manufacturer's instructions. A purity of more than 95% was obtained in all experiments.

2.4.3 Sn+ Bone marrow-derived macrophages (BMDM)

In order to obtain a homogeneous Sn+ BMDM population, a two-phase enrichment protocol was employed. To begin with, BMDMs were prepared from bone marrow collected from femur and tibia bones of age- and sex-matched Sn+/+ and Sn-/- C57BL/6 mice between 8-16 weeks of age. Ends of bones were removed and marrow flushed out using a 25 gauge needle and syringe filled with DMEM + 10% FCS. Cells were collected by centrifugation at 350 x g for 5 minutes. A Single cell suspension was achieved by pipetting to remove clumps and passed through a 70 micron cell strainer (BD Bioscience). Cells from one mouse were suspended in 20 ml of DMEM + 10% FCS supplemented with Macrophage-Colony Stimulating Factor (25ng/ml) purchased from Peprotech. Cell suspensions were then plated at 10 ml on a 100mm bacterial Petri dish plates (BD Bioscience). Cell cultures were incubated at 37^{o}C in 8% CO2 incubator.

The second phase involved stimulation of enriched BMDMs with IFNα (R&D) to induce Sn up-regulation. On day 7, non-adherent cells were gently removed by washing with PBS twice. Adherent cells were lifted by incubation with 4mg/ml Lidocaine (Sigma) +

5mM EDTA in PBS for 2-3 minutes in 8% CO2 incubator at 37^{o}C. Cells were then harvested and washed with DMEM+10%FCS. Next, cells were counted and plated at 2 X 10^5 cells/well of a 24 well-plate in the presence of 25units/ml of mouse IFNα. On day 3 post-IFNα stimulation, dead cells were removed by gentle washing with DMEM + 10% FCS medium. Next, cells were either lifted with 4mg/ml Lidocaine + 5mM EDTA in PBS to be used for flow cytometry studies or in co-culture experiments with activated CD4 T cells.

2.5 In vitro lymphocytes activation

2.5.1 Purified CD4+ T cells and Tregs

Activation of enriched CD4 T cells and Tregs was done using anti-CD3/CD28 Dynabeads (Invitrogen). Beads were washed with PBS+2mMEDTA+0.5%FCS and then used at bead to cell ratio of 1:1 to activate cells for 48-72 hours. At the end of the activation beads were removed using a magnetic particle concentrator (Invitrogen). Activated cells were then either used for flow cytometry studies or co-cultured with BMDM. In proliferation experiments of enriched CD4 T cells in co-culture with BMDM, soluble anti-CD3 (clone 2C11, BD Bioscience) at 5µg/ml was used.

2.5.2 Splenocytes

Splenocytes were stimulated with plate-bound anti-CD3, clone 2C11 (BD Bioscience). The antibody was used at 5µg/ml unless indicated otherwise. 24- or 6-well plates were coated with 1 ml or 500 µl of the antibody diluted in carbonate bicarbonate buffer pH 7.2 (Sigma) for 2 hours at 37^{o}C. Plates were then washed with PBS to remove unbound antibody and blocked with RPMI + 10% FCS for 20 minutes. Subsequently, media was aspirated and cell splenocytes suspensions were added at 1 X 10^6/2ml (24-well plate) or 3 X 10^6/6ml (6-well plates). Activation was done for 48-72 hours unless otherwise indicated.

2.6 Proliferation assays

In vitro proliferation assays were done with Click-iT EdU (Invitrogen). For the former, enriched CD4 T cells were labelled with 2 µM CFSE in PBS for 8 minutes at room temperature and washed with PBS+10%FCS three times. Cells were activated with soluble anti-CD3 (5µg/ml) or left un-stimulated, in co-culture with BMDMs.

Proliferation assays examining differences between SnL+ and SnL- activated CD4+CD25- T cells were done using EdU DNA incorporation. EdU (5-ethynyl-2'-deoxyuridine) is a nucleoside analog to thymidine and is incorporated in DNA during active DNA synthesis. Detection of incorporated EdU is based on a click reaction, a copper catalysed reaction between an alkyne (EdU) and an azide (detection dye). Activated cells were incubated with 10mM EdU over the last 12 hours of activation. Cells were then harvested and surface labelled with SnFc pre-complexes followed by intracellular staining for nuclear incorporated EdU.

2.7 Cell death assays

Enriched BMDM from Sn+/+ and Sn-/- mice were washed three times with RPMI+10%FCS, following three days stimulation with IFNα, to remove dead cells and debris. Enriched CD4+ T cells stimulated for 48 hours with anti-CD3/CD28 Dynabeads were added at 1:1 ratio to BMDM in complete RPMI. At 12 hours, total cells were lifted with 4mg/ml Lidocaine in 5mMEDTA+PBS. The viability of CD4+ T cells was assessed after 12 hours using Yo-Pro viability dye (Invitrogen) and CD4 labelling to distinguish CD4 T cells from macrophages. Analysis was performed by flow cytometry.

Alternatively, activated CD4 T cells were co-cultured with CHO cells expressing full length Sn or the R97A mutant form of the molecule. Viability was assessed by forward and side scatter flow cytometry profile.

2.8 SnFc preparation and purification

2.8.1 SnFc preparation

SnFc is a fusion protein composed of the first three immunoglobulin domains of Sn fused to hinge CH2 and CH3 domains of the human IgG1 molecule (Crocker *et al*, 1999). CHO cells stably secreting the transfected SnFc or mutant SnFc protein were prepared using the glutamine synthetase expression system (Bebbington 1992). In this method, high SnFc CHO producers are selected using specific inhibitor of glutamine synthetase, methionine sulfoxamine (MSX) in a glutamine free medium.

SnFc CHO cells, originally stored at -80, were thawed and transferred into warm media (GMEM-glutamine free (Gibco) + 10% FBS + 100 units/ml penicillin/0.1mg/ml streptomycin + 2% glutamine synthetase expression medium + 0.1% MSX). Cells were then centrifuged at 350g for 5 minutes. Supernatant was poured and pellet was re-suspended in 30 ml of medium. Sn-Fc producing CHO cells were cultured 150cm^2 size flasks (Technology Plastic Products, Switzerland) and incubated at 5% CO2 for 5-7 days. Fresh media replacement was done when yellow colour appearance was observed. Once >70% confluent the cells were transferred into 150 ml medium supplemented with 1mM HEPES in a 490cm^2 roller-bottle (Corning, USA). The roller bottle then was placed on a roller at 0.5-1 rpm. Once the inner side of the bottle coated with cells, the medium was changed to Ultracho or (GMEM-glutamine free + 1% FBS). After 72-86 hours the media was collected and centrifuged at 3000rpm for 5 minutes. The roller bottle was rinsed with PBS to remove waste and fresh media (GMEM-glutamine free + 10% FBS + 100 units/ml penicillin/0.1mg/ml streptomycin + 2% glutathione synthase + 0.1% MSX) were added for 72-86 hours. Next, culture media were aspirated and Ultracho or GMEM+1%FCS were added to roller bottle for a further 72-86 hours as described above. This process was repeated for a total of 4 weeks. The supernatants were pooled together and Sn-Fc concentration was quantified.

Quantification of SnFc was done by an ELISA using previously purified SnFc as a control for standard curve generation. Microtitre plates were pre-coated with anti-Sn monoclonal antibody 3D6 at 5µg/ml (50µl/well) and incubated overnight at 4^{o}C. Following three washes with PBS+ 0.05% Tween (PBST), wells were blocked for non-specific binding with 2% BSA in PBS for 1 hour at 37^{o}C. Serial dilutions of purified SnFc of known concentration and supernatant SnFc were added at 100µl/well for 2 hour at 37^{o}C. Following three washes with PBST, alkaline phosphatase-conjugated goat anti-human IgG Fc specific (1:10000) dilution was added at 100µl/well for 1 hour at room temperature. Wells were washed 5 times with PBST and developed using p-nitrophenyl phosphate substrate (Sigma). Absorbance was measured at 405nm.

2.8.2 Purification of SnFc protein

SnFc protein purification was done using protein G sepharose column chromatography. The chromatography column (Biorad) was filled with 2ml of Fast-flow Protein G sepharose (Sigma) in 20% ethanol. The column was washed with 200 ml PBS over 2 hours to remove ethanol. Sterile filtered SnFc supernatant was then passed twice over the column at 1ml/min. The column was then washed with 200ml PBS over 2 hours. Purified SnFc protein was eluted with 0.1M glycine pH3. Eluted fractions were collected in 200µl of 1M Tris pH10. A total of 10 fractions were collected. Protein concentration was quantified with NanoDrop spectrophotometer (Thermo Scientific). The first three fractions with highest concentration were pooled and dialysed overnight against 1X PBS using dialysis cassettes (Thermo scientific). Aliquots of purified SnFc were stored at -80.

2.9 Sialidase treatment

Two forms of sialidase were used in this project. First, *Vibrio cholera* sialidase (Sigma) which cleaves sialic acids from α2-,3,-6 and-8 linkages. Cells were washed three times

with serum free DMEM to remove any FCS. Cells were then suspended at 1 million cells per 60 µl of serum free DMEM. Cells were then incubated with 0.1 units/ml of *Vibrio cholera* sialidase for 1 hour at 37^{o}C. Cells were the washed three times with DMEM + 10% FCS and used in further analysis. Untreated cells were kept in media alone for the duration of the incubation.

Secondly, sialidase L (V-lab, USA) from *Macrobdella leech* exhibits α2,3 specific sialidase activity. Cells were washed three times in HBSS and suspended at 1 million cells per ml of HBSS. 25 units of sialidase L was used per one million cells and for 2 hours incubation at 37^{o}C. Cells were then washed with HBSS three times and used in flow cytometry analysis of SnFc binding specificity. In addition, cells were labelled with plant lectin SNA to assess the retention of α2,6-linked sialic acids following sialidase L treatment.

2.10 Solid phase RBC binding assays

The binding properties of supernatant and purified SnFc were examined by means of solid phase RBC binding assay ELISA (Crocker et al, 1991). 96-well microtitre plates were coated with goat anti-human IgG (Sigma) at 15µg/ml in 0.1 M carbonate bicarbonate buffer pH 9.6, overnight at 4^{o}C. Wells were then washed three times and blocked with PBS+ 2% BSA for 30 minutes at room temperature and then washed three times with PBS+ 0.2% BSA (PBA). Serial dilutions of supernatant or purified SnFc were added in PBA, in triplicates. Next, wells were washed three times with PBA and blocked with 5% Marvel semi-skimmed milk in PBS for 1 hour at 37^{o}C and then washed for a further three times. To assess the effect of anti-sialoadhesin monoclonal antibodies on RBCs binding, wells were pre-incubated with 20µg/ml in PBA of SER-4 or 3D6 or combination of both for 1 hour at 37^{o}C.

For human RBCs preparation, up to 2 ml of peripheral blood was obtained from healthy donors. After extensive washing with PBS, RBCs were stored for up to 14 days in

Alsever's solution (27mM sodium citrate, 72 mM sodium chloride, 114 mM glucose and 2.6 mM citrate) and at 4-8^{o}C. RBCs were either treated with *Vibrio cholera* sialidase (Sigma) in serum free DMEM for 1 hour at 37^{o}C, or left untreated. RBCs were then suspended at 0.25% (vol/vol) in PBA. Aliquots of 100µl of RBCs suspensions were added to replicate wells and allowed to adhere for 1 hour at 4^{o}C. Unbound cells were then removed by gentle wash with PBA. Adherent RBCs were then fixed with 0.125% glutaraldehyde in PBS for 10 minutes at room temperature. RBC binding was assessed by exploiting the pseudoperoxidase activity of haemoglobin. Bound RBCs were permeabilized with methanol for 15 minutes. Wells were allowed to dry in a non-humidified incubator at 37^{o}C. 100µl TMB substrate (1:1 solution A and B, BD bioscience) was added to each well for 20 minutes at room temperature in the dark. The peroxidase reaction was then stopped with 50µl/well of 0.16M sulphuric acid. Absorbance was measured at 450nm.

2.11 Clinical evaluation of lupus nephritis

Mice were monitored for disease onset by testing urine with a test strip (Uristix, Bayer) for protein excretion on a weekly basis. Results were graded according to the extent of proteinuria as follows: 0 = negative or trace, + = 30mg/dl, ++ = 100mg/dl, +++ = 300mg/dl and ++++ = >2000 mg/dl. Onset of disease was defined as two consecutive readings equal or more than ++ (100mg/dl). Grade 2 proteinuria was defined as proteinuria of equal or more than +++ (300 mg/dl).

2.12 Analysis of serum anti-dsDNA antibodies

Sera from BWF1 mice were examined for anti-dsDNA subclasses titres using ELISA. 96-well microtitre plates were coated with 20µg/ml of poly-L lysine (Sigma) in deionised water overnight at 4^{o}C. Plates were washed three times with PBS and 100 µl/well of

20µg/ml calf thymus DNA was added for 3 hours at 37°C. Plates were washed three times with PBS + 0.05% Tween (PBST) and non-specific binding was blocked using PBS + 3% BSA for 1 hour at 37°C. Following three washes with PBST, serial dilutions of 100µl/well of sera were added in triplicates for 2 hours at 37°C. Sera dilutions were started at 1/100 to 1/6400 in PBS + 0.5% BSA. Plates were washed three times with PBS+0.5%BSA. Secondary antibodies were diluted in PBS + 0.5% BSA used for detection of anti-dsDNA subclasses included: alkaline phosphatase-conjugated goat anti-mouse IgM (1/5000, Sigma), HRP-conjugated goat anti-mouse IgG (1/5000, Sigma), alkaline phosphatase-conjugated goat anti-mouse IgG1 (1/2000, Serotec) or HRP-conjugated goat anti-mouse IgG2a (1/5000, Invitrogen). This was followed by 5 washes with PBST. Plates were developed either with p-nitrophenyl phosphate substrate (Sigma) for alkaline phsophatase-conjugated secondary antibodies and TMB substrate (BD bioscience) for HRP-conjugated secondary antibodies. Plate readings were analysed at 405nm for the former and 450nm for the latter. Pooled sera from old female BWF1 mice were used as a positive control in all experiments.

2.13 Real time-PCRs

2.13.1 Renal tissues

Renal cortical samples from left kidneys were lysed in guanidine-thiocyanate containing lysis buffer in a homogenization tube containing 1.4mm ceramic beads (Precellys homogenization kit, Peqlab). RNA extraction was done using RNeasy mini kit (Qiagen) according to manufacturer's instructions. In this protocol, samples were lysed in the presence of denaturing guanidine-thiocyanate-containing buffer to inactivate RNases. Sample homogenization was done with a rotor-stator homogenizer (Precelys, Peqlab). Lysate was then centrifuged for 3 minutes at 10000 rpm and supernatant was mixed with equal volumes of 70% ethanol to promote appropriate RNA binding conditions.

The sample was then transferred to an RNA binding spin-column. Following three washes with ethanol-containing buffers, RNA was eluted with RNase-free water.

The concentration of the extracted RNA was measured based on the absorbance at 260nm (A_{260}) in a NanoDrop spectrophotometer (Thermo Scientific). The purity of RNA was estimated by measuring the ratio of the readings at 260nm and 280nm (A_{260}/A_{280}). Samples ratios between 1.9 and 2.1 were regarded as acceptable for cDNA preparation.

cDNA synthesis was performed with QuantiTect reverse transcription kit (Qiagen). One microgram of purified template RNA was incubated in genomic-DNA wipeout buffer for 2 minutes at 42^{o}C. Next, reverse transcription was achieved using a master mix containing reverse transcriptase, reverse-transcription primer mix (oligo-deoxy-thymine nucleotides and random primers) and dNTP-containing buffer. Reverse transcription reaction was then incubated for 15 minutes at 42^{o}C, followed by incubation for 3 minutes at 95^{o}C to inactivate the reverse transcriptase. All incubations were done in a thermocycler (Bio-Rad) for the specified temperatures and durations. All cDNA samples were stored at -20^{o}C until used in RT-PCR experiments.

2.13.2 Sialyltransferases expression on SnL+ and SnL- Teffs.

Three biological replicates from spleens of 5 female C57BL/6 mice between age of 8-10 weeks were used in these experiments. CD4+CD25- T cells (purity >95%) were isolated from spleens using Tregs isolation kit (Miltenyi Biotec) as per manufacturer's instructions. CD4+CD25- T cells were then activated with anti-CD3/CD28 Dynabeads (cell: bead ratio, 1:1) for 72 hours in complete RPMI. Cells were then washed with complete RPMI and beads were removed. Cells were blocked for non-specific binding with 0.25 µg/1 million cells/100µl of azide-free low-endotoxin anti-CD16/CD32 (BD bioscience) for 20 minutes on ice and then surface labelled with SnFc pre-complexes (Alexafluor 488) for 1 hour on ice. Cells were washed three times with PBS+2 % FCS

and counter-stained with DAPI. Subsequently, viable activated cells (DAPI negative and forward scatter high) were sorted by FACS into SnL+ (Alexa fluor 488 positive) and SnL- (Alexa fluor 488 negative). Cells were counted and pelleted by centrifugation at 350 x g for 10 minutes. Supernatants were aspirated completely and samples were lysed with RLT buffer. RNA extraction was accomplished using RNeasy micro kit (Qiagen) according to manufacturer's instructions. RNA extraction procedure was accomplished similar to (2.13.1), except for an additional initial DNase treatment step. The quality and quantity of isolated RNA was measured with NanoDrop spectrophotomter. The estimation of the concentration and purity of all samples was done as in previous section. cDNA synthesis was performed with QuantiTect reverse transcription kit (Qiagen) with integrated removal of genomic DNA contamination, according to manufacturer's instructions. All cDNA samples were stored at -20^{o}C until used in RT-PCR experiments.

2.13.3 PCR reaction

Oligonucleotides were designed by using the computer software Primer Express 2.0 (Applied Biosystems), synthesized by MWG technologies. A list of all primers used in these experiments is outlined below. PCR were performed with the SYBR Green method in an ABI 7900HT sequence detection system (Applied Biosystems). The reactions were set on a 96-well-plate by mixing 12.5 µl of the SYBR Green Master Mix (Applied Biosystems) with 2 µl of a oligonucleotide solution and 2 µl of a cDNA solution corresponding to 1/50 of the cDNA synthesis product. The thermal profile for all the reactions was 2 min at 50°C, followed by 10 min at 95°C and then 40 cycles of 15 s at 95°C and 1 min at 60°C. The housekeeping gene *GAPDH* was used as endogenous reference. In BWF1 experiments including NZW control mice, mRNA fold expression was calculated by initially calculating $\Delta Ct = {}^{Ct\ gene\ of\ interest\text{-}Ct\ GAPDH}$ then following the formula fold expression = $2^{\wedge\Delta Ct\ (BWF1)\ -\ \Delta Ct\ (NZW)}$. In BWF1 experiments involving Sn+/+

and Sn-/- fold expression values are represented as ΔCt values. In RT-PCRs of sialyltransferases fold expression values represent $2^{\wedge \Delta Ct\ (SnL+) - \Delta Ct\ (SnL-)}$

2.13.4 RT primers

Primer sets were designed using Primer Express software version 2 (Applied Biosystems). Individual primer sets were examined for target gene specificity with basic local alignment tool (BLAST) for sequence identity. Optimal concentrations for primers were estimated with Ct values and melting curves of serial dilutions and compared to GAPDH endogenous control. All the primer sets used in RT-PCR experiments are outlined below.

Table 2.2 List of genes and primer sets used in RT-PCR experiments.

Gene	Forward primer	Reverse primer
SnD2	5'-CCCAGCCCCCCCACT AT-3'	5'-AAGTTCCTCTCCATGCCTTCA C-3'
SnD17	5'-AGCCCCACATCCGAGTCA-3'	5'-AGGGCCGAGCTCCTCTATGTC-3'
F4/80	5'-CTTTGGCTATGGGCTTCCAGTC-3'	5'-GCAAGGAGGACAGAGTTTATCGTG-3'
CD68	5'-CTTCCCACAGGCAGCACAG-3'	5'-AATGATGAGAGGCAGCAAGAGG-3'
CD4	5'-CAGCATGGCAAAGGTGTATTAATTAG-3'	5'-CCCATGCCCCTTTTTTGG-3'
Foxp3	5'-CCCAGGAAAGACAGCAACCTT-3'	5'-TTCTCACAAGGCCACTTG-3'
IFNαR1	5'-TGGTGGTTCTGTCTCGGTGTT-3'	5'-GCTACGGCAGGATTAAAAATCG-3'
IFNγ	5'-AGCTCTTCCTCATGGCTGTT-3'	5'-TTTGCCAGTTCCTCCAGATA-3'
IL-10	5'-TAGAGCTGCGGACTGCCTTC-3'	5'-AGTCGGTTAGCAGTATGTTGTCCAG-3'

IL-17	5’-GCCCTCAGACTACCTCAACC-3’	5’-GAATTCATGTGGTGGTCCAG-3’
TGFβ	5’-TGGAGCAACATGTGGAACTC-3’	5’-GTCAGCAGCCGGTTACCA-3’
IL-1β	5’-AAGTGATATTCTCCATGAGCTTTG-3’	5’-TTCTTCTTTGGGTATTGCTTGG-3’
ST3Gal I	5’-TCGCCTGGTGCCTGGCAATG-3’	5’-TGGTCCGGCTCCCAACGTCT-3’
ST3Gal III	5’-CATCTTCCCCAGGTTCTCCAA-3’	5’-ACTTGCGAAAGGAGTCATCCA-3’
ST3Gal IV	5’-CTGAGCCTGCCCATACAACA-3’	5’-GGCTAGCAGACCCGTGGTT-3’
ST3Gal VI	5’-CTGGTGGCCATATTCCTGAG-3’	5’-CCGGACATGGCAGCAACC-3’
ST6Gal I	5'-CTCTGAAGAACTCCCAGCTG-3’	5'-GAGTTCACTAGGCGGATGG-3’
C2GnT	5’-CTGCTGTGATTTTGGGTAGTGAGT-3’	5’-GAGCCATTCGTGCCAAACAT-3’
CMAH	5’-GGTGGTCAGGATGATTGAAACAGATG-3’	5’-CCACCCGGCTATGGATTTCTTC-3’
1,4Gal T	5’-ACAAGAAAAATGAGCCCAATCC-3’	5’-CGAAGCGCATCGTTTCCTT-3’
FUT 7	5’-CGATAGCTCAGCACCCAGTTG-3’	5’-CATGGAATCGCCCAGTAATACC-3’
Bcl2	5’-GAGGCTGGGTAGGTGCATGT-3’	5’-GCATCTTGGCCTTGAGATCAA-3’

2.14 Histology

Right kidneys were used for assessing lupus nephritis severity by light microscopy. Kidneys were fixed in 10% neutral-buffered formalin. Processing and staining of kidney sections were conducted by the Veterinary Services, University of Glasgow. Kidney sections (5µm) were stained with H&E and Masson’s trichrome stains and evaluated

by light microscopy. Scoring of nephritis severity included examining glomeruli, tubular and perivascular regions as described previously (Nozaki *et al*, 2005). Glomerular pathology was assessed by counting number of cells per glomerular cross section (gcs), of 30 glomeruli per kidney. Score 0, normal cellularity (35-40 cells/gcs); 1, mild hypercellularity (41-50 cells/gcs); 2, moderate hypercellularity (51-60 cells/gcs) with segmental or diffuse proliferative changes; 3, severe hypercellularity (>60 cells/gcs) with segmental or global sclerosis, crescent formation and severe exudation. Tubular pathology was assessed based on the percentage of tubules showing dilatation or atrophy among 200 tubules in a randomly chosen field. Perivascular cell accumulation was also evaluated by counting the number of cell layers surrounding randomly chosen inter-and intralobular arteries. Perivascular scoring included: 0, no perivascular infiltrate; 1, less than 5 layers surrounding less than half the diameter of the artery; 2, 5-10 layers surrounding more than half of the diameter of the vessel; 3, more than 10 layers surrounding more than half the diameter of the artery). Scoring of all kidney sections was done in a blinded fashion.

2.15 Flow cytometry

2.15.1 Fluorescent staining

Anti-CD4-APC (clone L3T4), -CD4-PerCpCy5.5 (clone RM4.5), -CD25-PE (clone PC61.5), - CD69 (clone H1.2F3), - CD62L-PE or-APC (clone MEL-14), - Foxp3-PE or APC (clone FJK-16), - CTLA4-APC or biotin (clone UC10-4B9), - GITR-APC (clone DTA-1), - CD95L-biotin (clone MFL3), -CD95-biotin (clone 15A7), - IL-2-PE (clone JES6-5H4),-IFNγ-PE (clone XMG1.2),- CD45RB-FITC (clone C363.16a) were purchased from eBioscience, as were their rat IgG isotype controls. Anti-CD43-FITC (clone 1B11) and rat IgG-FITC isotype control were purchased from Biolegend, USA.

Maackia amurensis lectin-biotin (MAL), Sambucus nigra lectin-biotin (SNA), Limax flavus lectin-biotin (LFA), Pea nut agglutinin-biotin and Phaseoulus vulgaris

leucoagglutinin-biotin were all purchased from Vector labs. Streptavidin-FITC and APC were purchased from eBioscience.

2.15.2 Surface labelling

All staining and washes were carried out in FACS buffer (PBS+2% FCS+2mM EDTA) and on ice to minimise antibody internalisation. Non-specific binding was limited with incubation with 0.25 µg of anti-CD16/CD32 (Fc blocking antibody 2.4G2) per 1 million cells in 25 µl for 20 minutes. Cells were then washed once. Staining with relevant antibodies was done with optimal concentrations as decided with prior antibody titrations. Surface labelling was done in all cases on ice except with LFA staining which was done at room temperature as per manufacturer's instructions. Surface labelling incubations were done for 1 hour (except LFA for 30 minutes). Cells were washed twice with FACS buffer and analysed with FACS Calibur 2. FlowJo software was employed for data analysis.

2.15.3 Intracellular staining

Foxp3 and CTLA-4 were detected with intracellular staining following surface labelling. A Foxp3 staining kit (eBioscience) was used for this purpose. Cells were first fixed in formaldehyde fixation buffer for 30 minutes to 18 hours. Cells were then washed twice in saponin-based permeabilization buffer. Pellets were then suspended in 100 µl of permeabilization buffer containing relevant concentration of the antibody against the intracellular antigen of interest. This was followed by 1 hour incubation at 4^{o}C. Cells were then washed twice with permeabilization buffer and finally suspended in FACS buffer.

Intracellular cytokines IFNγ and IL-2 were detected on MACS enriched CD4+CD25- T cells. Following enrichment cells were stimulated with anti-CD3/CD28 Dynabeads at 1:1 ratio for 48 hours. Cells were washed following the removal of beads and re-

stimulated with phorbol 12,13-dibutyrate (PdBU) 10ng/ml(Sigma) and ionomycin 10ng/ml (Sigma) for 3 hours in the presence of brefeldin (3µg/ml). Following surface labelling with SnFc pre-complexes cells were fixed and intracellular staining was done as above.

2.16 Statistical analysis

Statistical significance was determined by Student's t test, Mann-Whitney test, one-way ANOVA or two-way ANOVA based on the number of groups analysed and the number of variables included in these evaluations. P value was considered to be significant when less than 0.05. Whenever, the p value was significant, the actual value has been depicted.

Characterisation of SnL+CD4+ T cells

3.1 Introduction

Recently, Wu and colleagues (2009) studied the interaction between Sn and Tregs in a murine model of multiple sclerosis, experimental allergic encephalomyelitis (EAE). Tregs, but not Teffs, from diseased animals were shown to be bearing Sia-dependent ligands for Sn. In addition, Sn was shown to exert a negative down-regulatory effect on the frequency of Tregs in inflamed central nervous system and peripheral lymphoid tissues.

The nature of SnL on Tregs has not been explored previously. Similarly, the phenotype of SnL+ CD4+ T cells and the mechanism through which Sn affects the function and frequency of CD4+ T cells have not been determined. In this chapter, data on the characterisation of SnL+CD4+ T cells are presented. In addition, a glycomic analysis of the changes in glycosylation/sialylation that are associated with the induction of these ligands with novel findings on the nature of these ligands, is demonstrated.

3.2 Results

3.2.1 Preliminary analysis of SnFc

CD4+ T cells from C57BL/6 wild-type mice were examined for the expression of SnL in vitro. For this purpose a fusion protein, Sialoadhesin-Fc (SnFc) was used. SnFc is composed of the V-set and first 3 immunoglobulin domains of Sn molecule fused to human IgG1 molecule. As SnFc has a low binding affinity, various binding assays can be enhanced by using complexes of the SnFc protein with an anti-Fc secondary antibody. This will lead to enhanced binding by means of avidity.

The concentration of supernatant SnFc was estimated by an ELISA (Figure 3.1, A). The binding properties of the quantified SnFc were analysed by using a red blood cell (RBC) binding assay. RBCs are heavily sialylated cells that can be used to test sialic-

acid dependent binding properties of siglecs to sialic acid residues on their surface (Crocker et al, 1991). An ELISA-based solid phase RBC binding assay was utilized to examine sialic acid binding specificity of supernatant SnFc (Figure 3.1, B). The binding of titrations of SnFc protein, bound to wells of microtiter plate coated with anti-human IgG Fc specific, to RBCs was measured using the pseudoperoxidase activity of RBCs. Binding remained positive down to 2.5 µg/ml of the protein and it was sialic acid dependent as prior treatment of RBCs with *Vibrio cholerae* sialidase abolished binding.

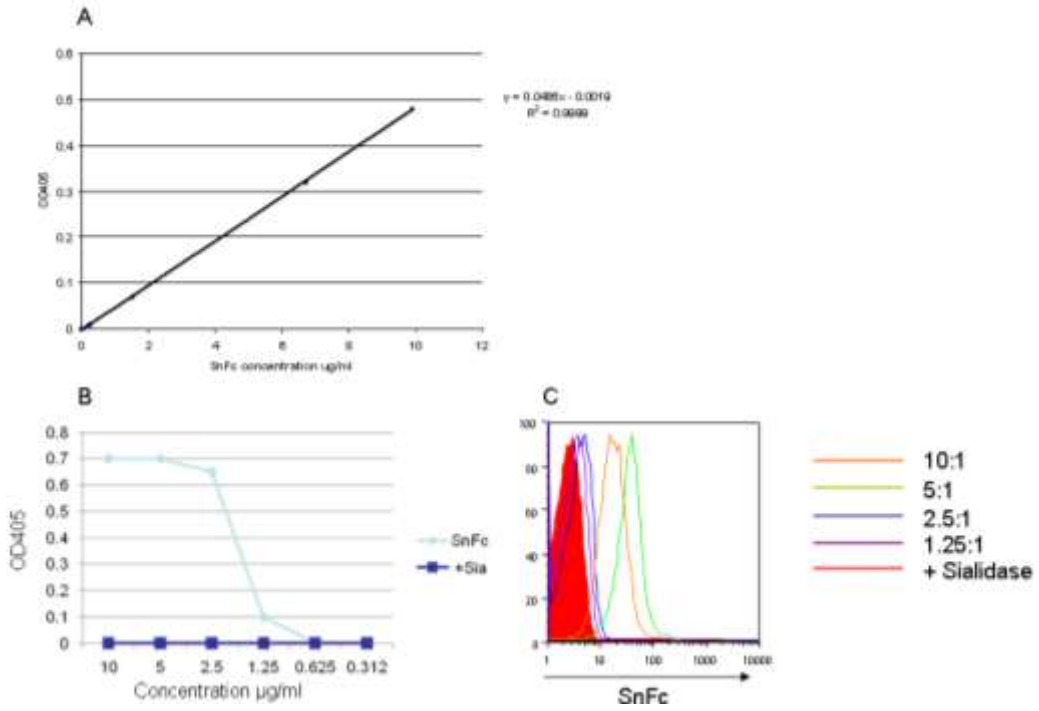

Figure 3.1 Preliminary analysis of SnFc. A,quantification of supernatant SnFc by an ELISA using purified SnFc of a known concentration as explained in Materials and Methods. B, solid phase RBC binding assay, the binding of titrations of SnFc bound to adsorbed goat anti-human IgG Fc to human RBCs was measured as explained in Materials and Methods. RBCs were either treated with sialidase (negative control) or left untreated. C, optimization of SnFc pre-complexes binding to human RBCs. SnFc complexed with goat anti-human IgG Fc specific at ratios of 10:1, 5:1, 2.5:1 and 1.25:1. Histograms demonstrate the binding of SnFc pre-complexes to human RBCs. Sialidase treated RBCs was used as a negative control (red histogram).

Subsequently, different ratios of SnFc to goat anti-human IgG Fc specific were used in pre-complexes to identify an optimal ratio for use in flow cytometry assays (Figure 5.2, C). The optimal ratio was identified as 5:1 (2.5 µg/ml of SnFc to 0.5 µg/ml of the

secondary antibody) and this combination was used in all subsequent flow cytometry experiments.

3.2.2 SnL are up-regulated on CD4+ T cells following TCR ligation

The expression of Sn ligand (SnL) on CD4 T cells was investigated following TCR triggering *in vitro*. A time-course analysis was conducted on enriched CD4+ T cells starting from day 0 (immediately following magnetic-activated cell sorting, MACS) and then 24-hourly up to 72 hours. CD4+ T cells treated with sialidase from *Vibrio cholera* were used as a negative control. There was no evidence of SnL up-regulation prior to stimulation of enriched CD4+ T cells (Figure 3.2). A step wise increase in the percentage of SnL+CD4+ T cells was observed reaching up to 30% by 72 hours. This initial examination demonstrated that resting CD4+ T cells do not express SnL and TCR ligation is required to induce SnL.

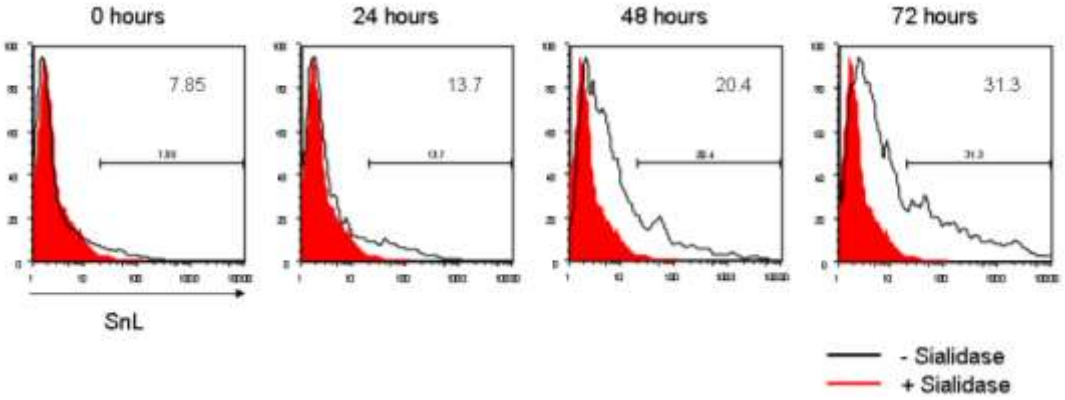

Figure 3.2 Time course of SnL induction on CD4+ T cells. MACS-enriched splenic CD4+ T cells were examined for the expression of SnL by staining with SnFc-complexes and CD4. Cells were labelled either following enrichment or at 24, 48 and 72 hours following stimulation with anti-CD3/CD28 Dynabeads at 1:1 ratio. Histograms show SnFc binding on gated CD4+ T cells with open histograms representing cells untreated with sialidase and red histograms representing sialidase treated controls.

To examine whether CD4+Foxp3+ T cells (Tregs) follow a similar pattern to total CD4+ T cells, Tregs isolated from spleens of wild-type C57BL/6 mice were examined for SnL expression. In contrast to total CD4+ T cells, there was a significant (12%) percentage of SnL+Tregs following MACS sorting (data not shown). It was not clear whether this

subset of Tregs was positive for SnL prior to sorting i.e. Tregs expressing SnL under homeostatic conditions, or they became SnL+ due to inadvertent activation while isolated by MACS.

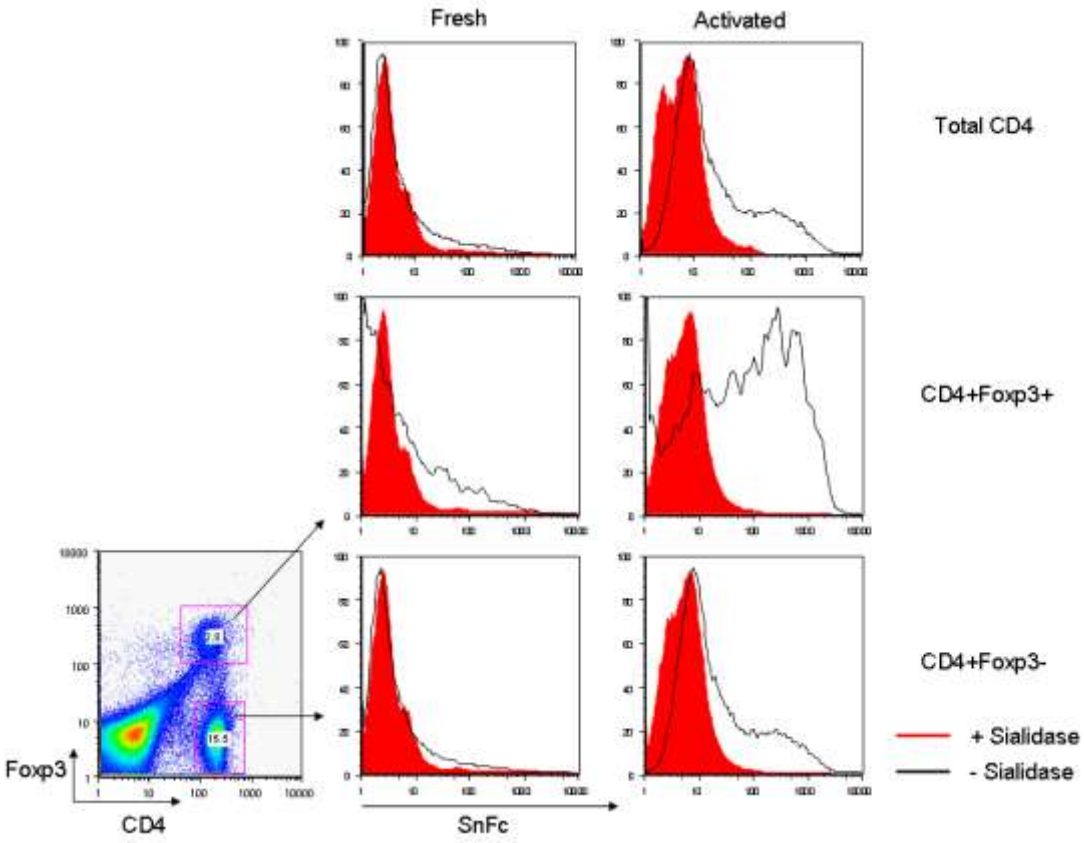

Figure 3.3 TCR ligation induces SnL up-regulation on Tregs more than Teffs. Splenocytes from wild-type mice were activated with plate-bound anti-CD3 (5ug/ml) for 72 hours and compared to freshly isolated splenocytes for the expression of SnL. Intracellular staining of Foxp3 was undertaken to examine SnL on both Tregs and Teffs cells in both freshly isolated and activated groups. Dot plots of activated splenocytes stained for CD4 and intracellular staining Foxp3. CD4+Foxp3+ (Tregs) and CD4+Foxp3- (Teffs) are gated with representative percentages out of total splenocytes analysed. Histograms of SnL expression (black histograms) and sialidase treated controls (red histograms) are presented. Data from fresh (left column) and stimulated (right column) splenocytes include analysis of total CD4 T cells (top panel), Tregs (middle panel) and Teffs (bottom panel).

To address this discrepancy, total splenocytes rather than enriched populations were used in further analysis. Splenocytes from wild-type C57BL/6 mice were activated *in vitro* with solid-phase anti-CD3/CD28 for 72 hours and compared with freshly isolated splenocytes for their SnL expression. The analysis showed that a subset of Tregs from fresh splenocytes were SnL+ (around 15%). As for the activated CD4+ T cells, Tregs

and CD4+Foxp3- (T effectors, Teffs) were both found to display SnL positivity following TCR ligation (Figure 3.3).

The binding of SnFc on both Tregs and Teffs was sialic-acid dependent. These findings suggested that SnL induction is an event that follows TCR ligation. In addition, SnL positivity was biased towards TCR-triggered Tregs compared to Teffs. The presence of SnL+Tregs in fresh splenocytes confirmed that the observation of SnL expression in MACS-enriched Tregs was not related to the process of sorting. A possible explanation to the presence of SnL+Tregs in fresh splenocytes might be that these cells might have had an antigenic exposure *in vivo* and consequently up-regulated SnL.

3.2.3 SnL+CD4+ T cells display a higher state of activation

To determine whether the up-regulation of SnL on activated CD4+ T cells was associated with an altered state of activation compared to SnL-CD4+ T cells, the expression of early activation markers was examined. It has been shown that TCR triggering of CD4+ T cells is associated with the transcription of IL-2 and surface expression of the α-chain of the IL-2 receptor (CD25) (Junghans *et al*, 1996; Powell *et al*, 1998). IL-2 secretion and subsequent binding to the high affinity IL-2 receptor (IL-2Rα (CD25), IL-2Rβ (CD122) and IL-2Rγ (CD132) was found to induce the activated cells to proliferate and differentiate.

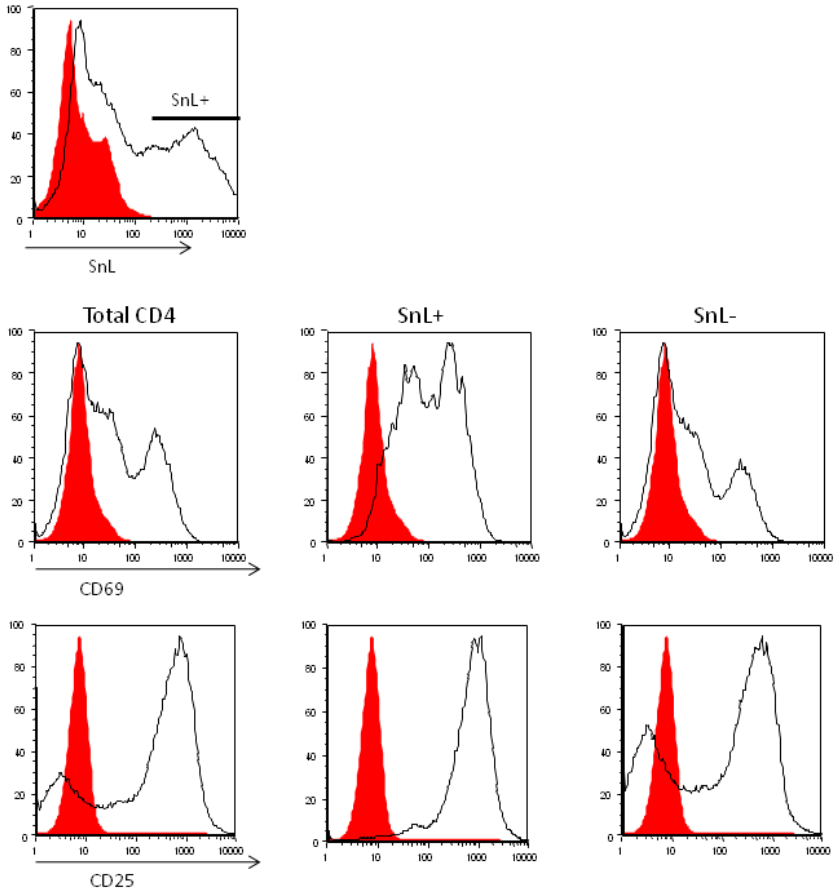

Figure 3.4 SnL+CD4+ T cells display a higher state of activation following TCR ligation compared to SnL-CD4+ T cells. Splenocytes from wild-type mice were stimulated with plate-bound anti-CD3 (5µg/ml) for 72 hours. Top, small horizontal bar outlines SnL+ population on gated CD4 T, compared to control cells treated with sialidase (red histogram). Middle panel, histograms represent the expression of activated markers CD69 on total CD4+ (left), SnL+CD4 (middle) and SnL-CD4 (right) T cell populations. Bottom panel, histograms represent the expression of activated markers CD69 on total CD4+ (left), SnL+CD4 (middle) and SnL-CD4 (right) T cell populations . Red histograms in middle and bottom panels represent CD69 and CD25 isotype controls respectively. Data are representative of three independent experiments.

CD69 also called Activation Inducer Molecule (AIM) was found to be up-regulated following TCR ligation on T cells (Testi *et al*, 1994). CD25 and CD69 were used to assess the activation status of SnL+ and SnL- CD4 T cells following TCR triggering *in vitro*. The analysis revealed a significant increase in the surface expression of both these markers on SnL+ subset of activated CD4+ T cells compared to their SnL- counterparts (Figure 3.4).

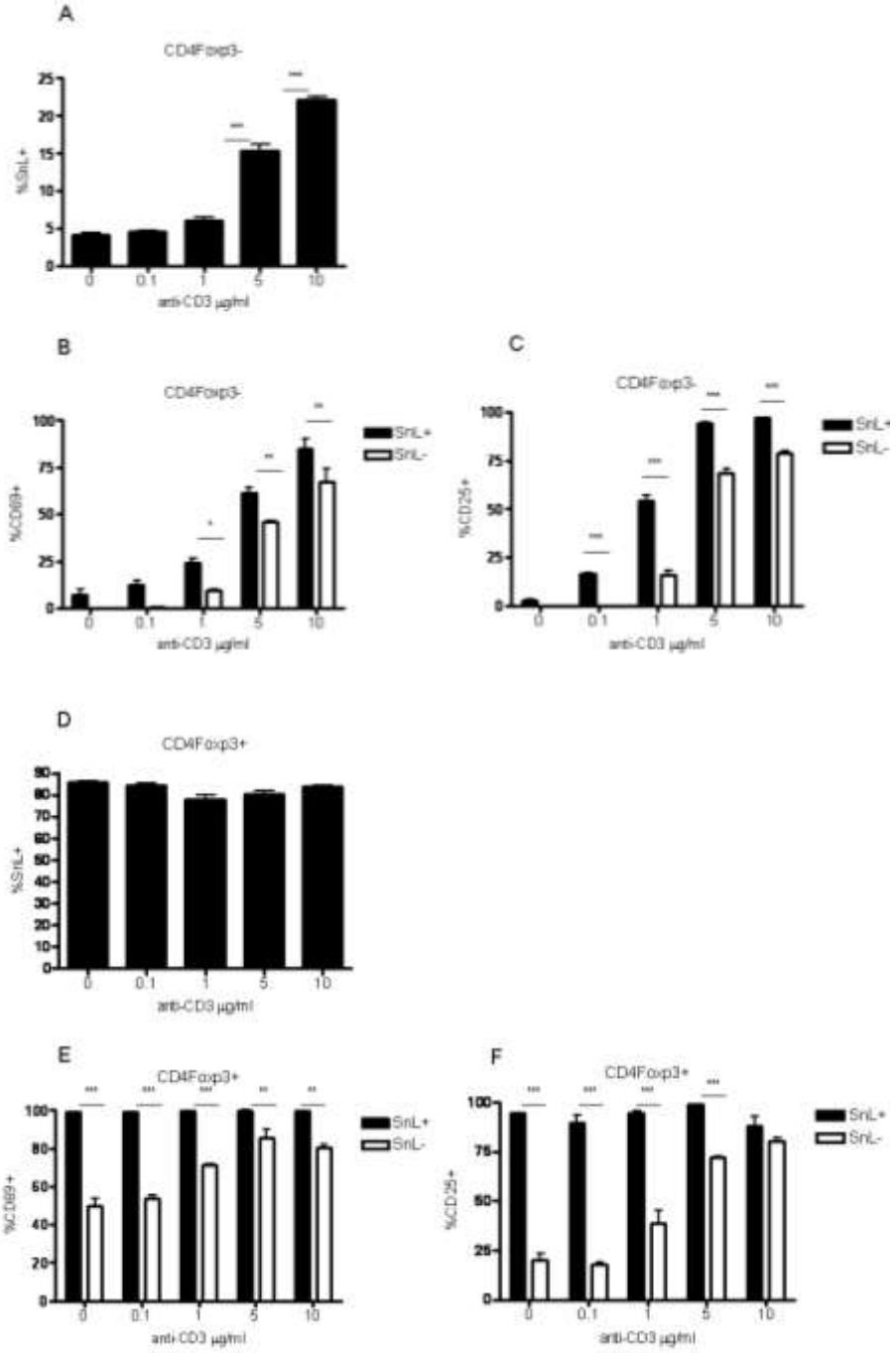

Figure 3.5 Expression of early activation markers CD69 and CD25 on SnL+ and SnL- CD4 T cells. Splenocytes from wild-type mice were stimulated with titrations of plate -bound anti-CD3 for 48 hours. Splenocytes were surface-labelled with CD69, CD25, CD4 and SnFc. Intracellular staining for Foxp3 was undertaken and percentage of CD69+ and CD25+ cells in SnL+ and SnL- CD4 T cell subsets was examined by flow cytometry. A,percentage of SnL+Teffs across various anti-CD3 titrations. B, percentage of CD69+ cells in SnL+ and SnL- Teffs. C, percentage of CD25+ cells in SnL+ and SnL- Teffs. D, percentage of SnL+Tregs across various anti-CD3 titrations. E, percentage of CD69+ cells in SnL+ and SnL- Tregs. F, percentage of CD25+ cells in SnL+ and SnL- Tregs. The bars represent means+/- SEM of triplicates samples of each CD3 concentration. Data are representative of three independent experiments. Statistical analysis was done using Two-way ANOVA with Bonferroni post-test analysis. * = $p<0.05$, ** = $p<0.01$ and *** = $p<0.001$.

As the above SnFc binding data on CD4+ T cells revealed that Tregs had a higher percentage of SnL+ cells compared to the Teffs, this could have contributed to the enhanced expression of these activation markers on the SnL+CD4+ T cells. Further analysis of these activation markers was undertaken by examining the percentage of activated Teffs that were positive for these markers in both SnL+ and SnL- subsets. Splenocytes from C57BL/6 mice were exposed to titrations of plate-coated anti-CD3 antibody for 48 hours. The extent of induction of SnL on Teffs was found to be directly associated with the TCR signal strength (Figure 3.5, A). Interestingly, the percentages of CD69+ and CD25+ cells in the Teffs cells were consistently higher in SnL+ compared to SnL- counterparts (Figure 3.5, B and C). These data identified SnL+CD4+ cells as a subset with higher state of activation compared to their SnL- counterparts. The direct correlation between the strength of TCR triggering and the percentage of SnL+Teffs suggested that SnL positivity reflects a state of hyper-responsiveness to TCR stimulation. Surprisingly, in this set of experiments the analysis of SnL expression on Tregs showed high positivity (>90%) across all anti-CD3 titrations as well as in resting cells. However, the expression of CD69 and CD25 on SnL-Tregs were found to be augmented with increasing anti-CD3 concentrations. Although it is unclear what caused the up-regulation of SnL on resting Tregs to such a high extent, but SnL positivity was again associated with higher activation status among these cells.

Having shown that SnL+Teffs display a heightened state of activation, the cytokine profile of these cells was explored. Intracellular expression of IL-2 and IFNγ on SnL+ and SnL- Teffs cells were analysed by flow cytometry. Initially, CD4CD25- T cells were sorted magnetically and activated for 48 hours to induce SnL surface expression. These cells were then re-stimulated with phorbol 12,13 dibutyrate (PDBu, a protein kinase C activator) and ionomycin (Ca^{++} ionophore) in the presence of brefeldin (protein transport inhibitor). Consistent with their higher state of activation, SnL+ Teffs

showed a higher intracellular expression of these cytokines per cell as demonstrated by higher fluorescence intensity of IFNγ and IL-2 (Figure 3.6).

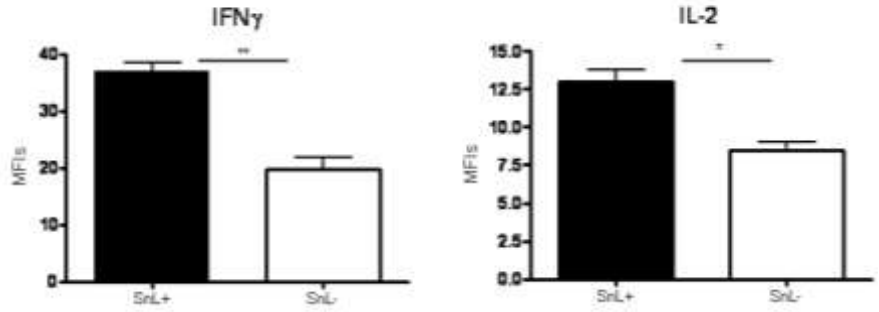

Figure 3.6 Intracellular cytokine expression in SnL+ and SnL- Teffs. MACS sorted CD4+CD25- T cells from three wild-type mice were activated with anti-CD3/CD28 Dynabeads for 48 hours to induce SnL. Activated cells were re-stimulated with PDBu and ionomycin in the presence of brefeldin for 4 hours. Subsequently, cells were surface-labelled with SnFc and intracellular staining for IFNγ and IL-2 was carried out. The bars represent means+/-SEM of mean fluorescence intensity from three samples. Statistical analysis was done using student's t test. * = $p<0.05$ and ** = $p<0.01$.

To investigate whether the heightened response to TCR triggering in the SnL+ Teffs would translate into a proliferative response the incorporation of 5-ethynyl-2'-deoxyuridine (Edu) into the DNA of activated cells was examined. Edu is a nucleoside analog to thymidine and it is incorporated into DNA during active DNA synthesis. Consistent with their activation profile, SnL+Teffs showed a higher extent of Edu incorporation compared to their SnL-Teffs as detected by flow cytometry (Figure 3.7).

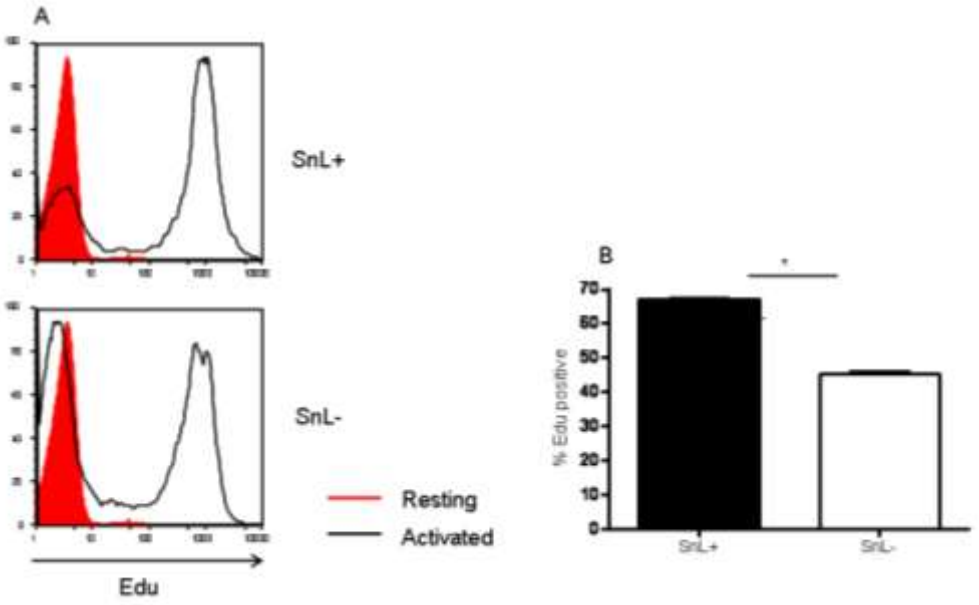

Figure 3.7 SnL+Teffs display a hyper-proliferative response following TCR ligation. MACS sorted CD4+CD25- T cells from three wild-type mice were activated with anti-CD3/CD28 Dynabeads for 72 hours. Edu 10 µg/ml was added in the last 12 hours of incubation. Intracellular staining for incorporated Edu was carried out following surface labelling with SnFc. A, Histograms represent Edu expression on SnL+ (top) and SnL- (bottom) as compared to resting un-stimulated Teffs (filled red histogram). B, The percentage of Edu+ cells in SnL+ (black bar) and SnL- (unfilled bar) cells. Bars represent means +/- SEM of triplicate samples. Statistical analysis was done using student's t test. * = $p<0.05$.

Taken together, these data indicated that SnFc identifies a subset of activated CD4+ T cells that are hyper-responsive to TCR stimulation as evidence by their higher expression of early activation markers and intracellular cytokines (IL-2 and IFNγ). In addition, SnL+Teffs cells tend to mount a higher proliferative response to polyclonal stimulation *in vitro*.

3.2.4 Engaging SnL on CD4+ T cells induces cell death

The functional consequences of Sn interaction with CD4+ T cells are not clear. Wu and colleagues observed that Sn+ macrophages, negatively affect the proliferation of Tregs only, when Tregs and Teffs were stimulated with myelin oligodendrocyte glycoprotein (MOG), *ex vivo* (Wu *et al*, 2009). However, the underlying mechanism by which Sn+ macrophages exerted such an effect remained unclear. Whether Sn+ macrophages

can affect the viability of CD4 T cells and consequently their proliferation is an unexplored possibility.

To further address this possibility, co-culture experiments of bone marrow derived macrophages (BMDM) from Sn WT (Sn+/+) or Sn deficient (Sn-/-) and activated CD4+ T cells were implemented (Diagram 3.1). BMDMs were expanded with macrophage-colony stimulating factor (M-CSF) for seven days followed by treatment with interferon alpha (IFNα) for further three days. IFNα treatment was used to enhance Sn expression on BMDMs (Figure 3.8). CD4+ T cells, on the other hand, were activated for 48 hours with bead-bound anti-CD3/CD28 antibodies to induce SnL expression and then co-cultured with BMDMs for 12 hours. Total co-cultured cells were then lifted and the viability of CD4+ T cells was examined by flow cytometry.

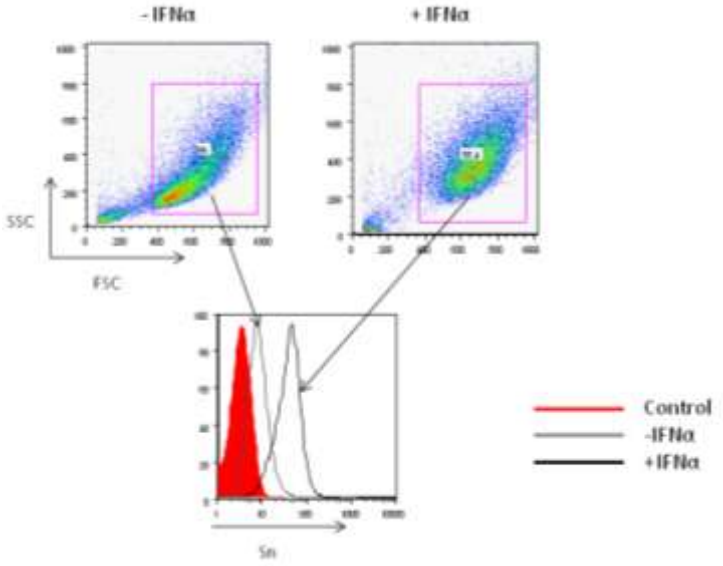

Figure 3.8 Enhanced expression of Sn on BMDM following IFNα stimulation. BMDM from Sn+/+ mice were enriched with 7 days stimulation with M-CSF.BMDM were either stimulated for 3 days with IFNα at 250IU/ml or left untreated. Sn expression was compared between the two groups using biotinylated anti-Sn monoclonal antibodies (SER4 and 3D6 at 2µg/ml each) followed by fluorescent-conjugated secondary streptavidin labelling. Cells stained with secondary antibody only were used as control.

Activated CD4+ T cells co-cultured with Sn+/+ BMDMs showed a significant reduction in viability as compared to CD4+ T cells co-cultured with Sn-/- BMDMs (Figure 3.9, A). The reduced viability was most prominent when cells were co-cultured at 1:1 ratio and

became less apparent with increasing the number of activated CD4+ T cells (Figure 3.9, B). These findings suggested that engaging SnL on CD4+ T cells induced cell death.

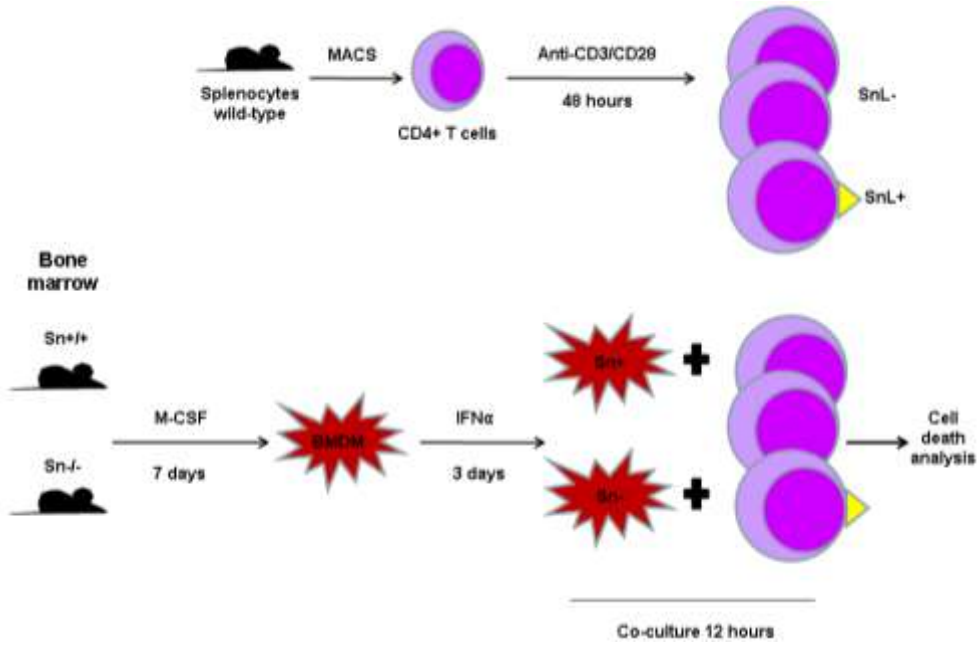

Diagram 3.1 Model for investigating engaging SnL on activated CD4+ T cells with Sn on bone marrow-derived macrophages (BMDM) from Sn+/+ and Sn-/- mice.

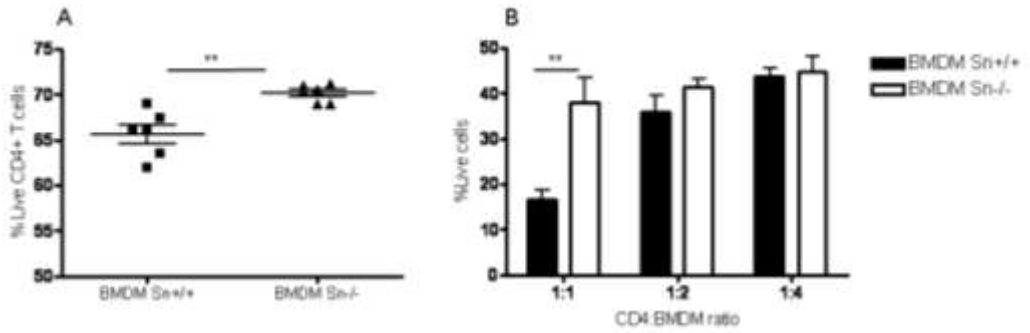

Figure 3.9 Sn induces cell death on activated CD4+ T cells. A, Activated enriched CD4+ T cells (from 3 wild-type mice) were co-cultured for 12 hours with IFNα-stimulated BMDM from Sn+/+ and Sn-/- mice, at 1:1 ratio and in triplicates. Total cells were lifted and stained for surface expression of CD4 and Yo-Pro membrane permeability dye. The percentage of live cells was defined as being negative for Yo-Pro. B, titrations of co-cultured activated CD4+ T cells and BMDM. Data are representative of three independent experiments. Statistical analysis was done using student's t test in A and Two-way ANOVA in B. * = $p<0.05$. ** = $p<0.01$.

To examine whether the reduced viability of activated CD4+ T cells was a result of Sn expression and not other phenotypic or cytokine production differences between Sn+/+ and Sn-/- macrophages, experiments were designed in which purified SnFc was used

instead of BMDM. CD4+ T cells were activated with anti-CD3/CD28 Dynabeads and then exposed to purified SnFc or similar concentration of SnFc incubated for 1 hour with anti-Sn antibodies prior to addition to the activated CD4+ T cells. Activated CD4+ T cells exposed to 50 µg of the protein showed higher percentage of 7-AAD positive cells (Figure 3.10). This effect was Sn specific as it was reversible with exposure to SnFc incubated with anti-Sn antibodies led to increased viability as compared to SnFc only. These data confirmed that SnFc interaction with activated CD4+ T cells results in cell death.

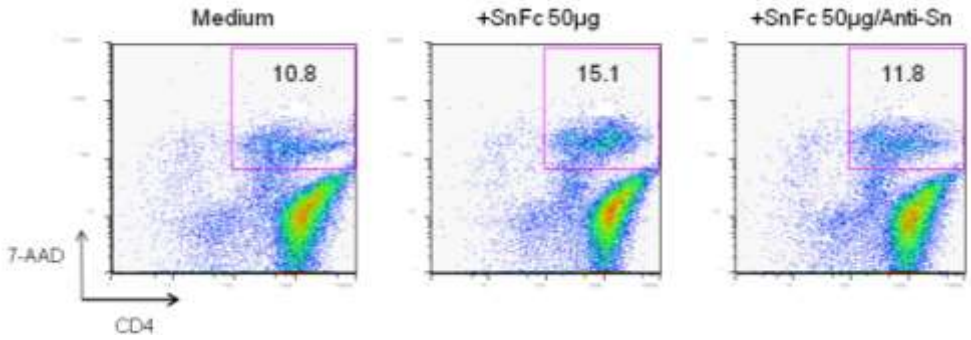

Figure 3.10 Purified SnFc induces cell death in activated CD4+ T cells. Activated CD4+ T cells were exposed to titrations of purified SnFc for 12 hours or to 50ug of SnFc pre-incubated with anti-Sn monoclonal antibodies (SER4+3D6 each at 20ug/ml) for 1 hour at 37oC. Cells were stained for CD4 and assessed for viability using 7-AAd dye. Dot plots shown are representative of samples treated with buffer alone (left), 50ug of SnFc (middle) or SnFc+anti-Sn (right). Gates on dot plots represent dead CD4+ T cells.

Furthermore, CD4+ T cells death induction by Sn was examined in co-cultures with Sn expressing CHO cells. CHO cells expressing full length of Sn or its mutant form R97A were utilized in this experiment. Consistent with the above data, there were a higher percentage of dead cells (as identified by their forward and side scatter profile) in co-cultures CD4+ T cells with Sn CHO compared to those expressing the mutant form of Sn (Figure 3.11).

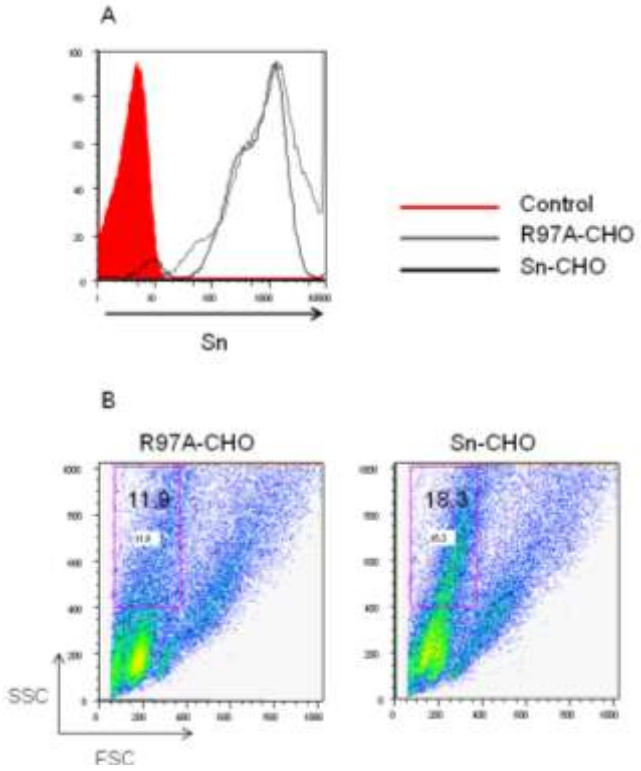

Figure 3.11 Reduced viability of activated CD4+ T cells co-cultured with Sn-CHO cells. A, Flow cytometry examination of the expression of Sn (black histogram) or mutant Sn (grey histogram) compared to secondary antibody control (red filled histogram). B, Enriched CD4+ T cells were stimulated with anti-CD3/CD28 Dynabeads for 48 hours. Following the removal of beads, CD4+ T cells were co-cultured with CHO cells for 2 hours at 37^{o}C, cells were then washed and analysed by flow cytometry.

Collectively, these data demonstrated that the exposure of activated CD4+ T cells to Sn resulted in induction of cell death. This effect was consistent when activated CD4+ T cells were exposed to Sn+ BMDM, SnFc protein and CHO cells expressing wild-type Sn. However, the mechanism by which Sn exerts its pro-apoptotic effect on these cells is unknown.

3.2.5 SnL+ CD4+ T cells express higher degree of CD95L

A preliminary analysis was undertaken to examine potential differences in SnL+ and SnL- CD4+ T cells in their expression of key members of the extrinsic and intrinsic apoptosis pathways. TCR re-stimulation of activated T cells in the presence of IL-2 is known to induce cell death by inducing the expression of FasL and subsequent interaction between Fas-FasL and induction of cell death (Brunner *et al*, 1996). This

process is known as activation induced cell death and it is regarded as an important regulatory mechanism in the contraction phase of the immune response (Green *et al*, 2003). The intrinsic pathway of apoptosis is activated by DNA damage and cytokine deprivation. The activation of the intrinsic pathway leads to loss of mitochondrial membrane integrity and release of cytochrome C which eventually results in activation of caspases and apoptosis. Members of the Bcl2 family of mitochondrial proteins are broadly divided into anti-apoptotic and pro-apoptotic. Bcl2 is an anti-apoptotic member of the family. Over expression of Bcl2 in transgenic models has been associated with reduced clearance of antigen-specific T lymphocytes (Davey *et al*, 2002), while deficiency of Bcl2 was associated with reduced lymphocyte frequency due to accelerated apoptosis (Kamada *et al*, 1995).

The surface expression of CD95 and CD95L on activated CD4+ T cells was examined by flow cytometry. While there was no significant difference in the expression of CD95 between SnL+ and SnL- subsets, CD95L expression was found to be enhanced on SnL+CD4+ T cells compared to SnL- subset (Figure 3.12, A). Such an increase might have been related to the higher activation/effector profile of these cells. The examination of Bcl2 expression on SnL+ cells was conducted at mRNA and protein level. RT-PCR analysis of three biological replicates of SnL+ and SnL- CD4+CD25- T cells showed a trend towards higher expression in SnL+Teffs but this did not reach statistical significance (Figure 3.12, B). However, intracellular staining for Bcl2 on CD4+ T cells showed a modest increase in Bcl2 expression in SnL+ subset (Figure 3.12, C).

These data suggest that SnL+CD4+ T cells can potentially induce cell death on neighbouring cells in a ‘fratricide’ manner. Although the combined CD95/CD95L and Bcl2 profile of these cells might argue against being more susceptible to self-induced cell death or ‘suicide’, further evaluation of these possibilities is needed.

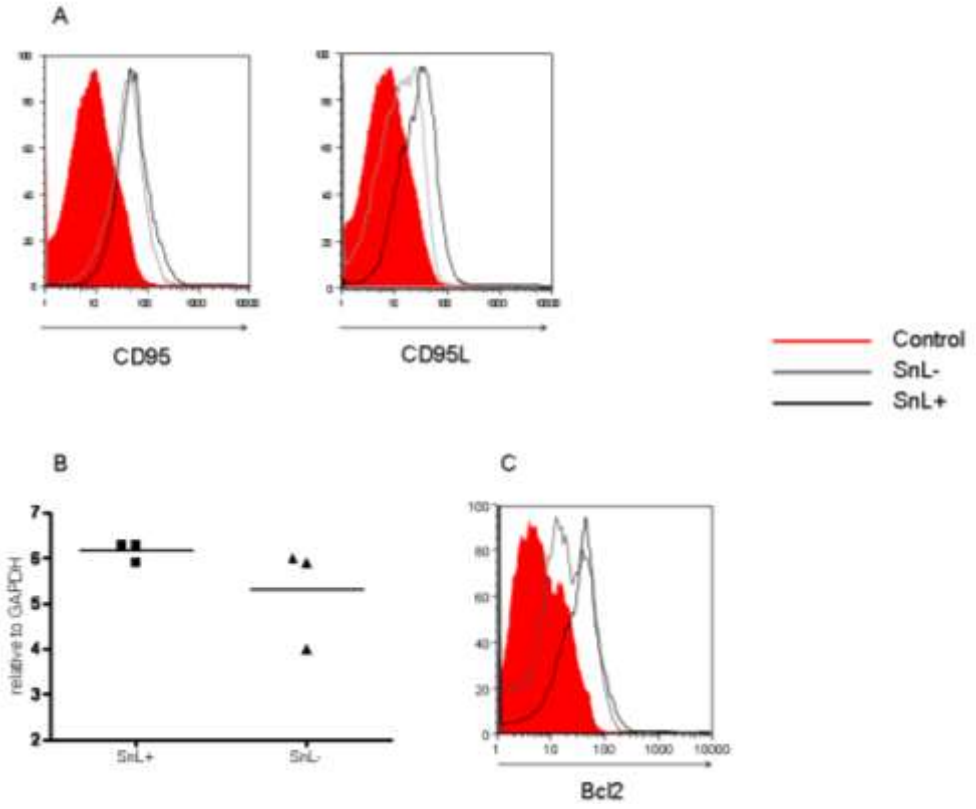

Figure 3.12 Expression of apoptosis-related factors on SnL+ and SnL- CD4+ T cells. A,flow cytometry analysis of surface expression of CD95 and CD95L on activated CD4 T cells. Splenocytes from wild-type C57BL/6 mice (n=3) were stimulated with plate coated anti-CD3 (5µg/ml) for 72 hours. Cells were then labelled with CD95 or CD95L together with SnFc-pre-complexes. Histograms represent the expression of CD95 (left) and CD95L (right) on gated SnL+CD4+ T cells (black unfilled histogram) and SnL-CD4 T cells (grey unfilled histograms) and compared to their isotype controls (red histograms). Data are representative of three independent experiments. B, RT-PCR data of Bcl2 mRNA expression in FACS sorted SnL+ and SnL- CD4+ CD25- T cells. cDNA from three biological replicates (n=5 mice/replicate) were used to examine the mRNA expression of Bcl2 in SnL+ and SnL- in these samples. Each dot represents average of triplicate measurements. Fold expression is expressed relative to GAPDH. Statistical analysis was done using student's t test. C, flow cytometry analysis of intracellular expression of Bcl2 in SnL+ CD4 (black histogram) and SnL-CD4 (grey histogram) T cells as compared to isotype control (red histogram).

3.2.6 Up-regulation of SnL on CD4+ T cells is associated with increased α2,3 sialylation

T cell activation is associated with important alterations in surface glycosylation. These changes can have a substantial effect on the binding of various lectins, their mode of action and function. In order to understand changes in sialylation that are associated

with induction of SnL on CD4+ T cells, two major patterns of sialylation were examined. These included: α2,3 and α2,6 sialylation. To this end, plant lectins with specific sialic acid-linkage recognition at the termini of *O*- and *N*-linked glycans, were used. These included: plant lectins specific for α2,3 sialylation, Maackia Amurensis Lectin (MAL) and α2,6 sialylation Sambucus Nigra Lectin (SNA), (Diagram 5.2).

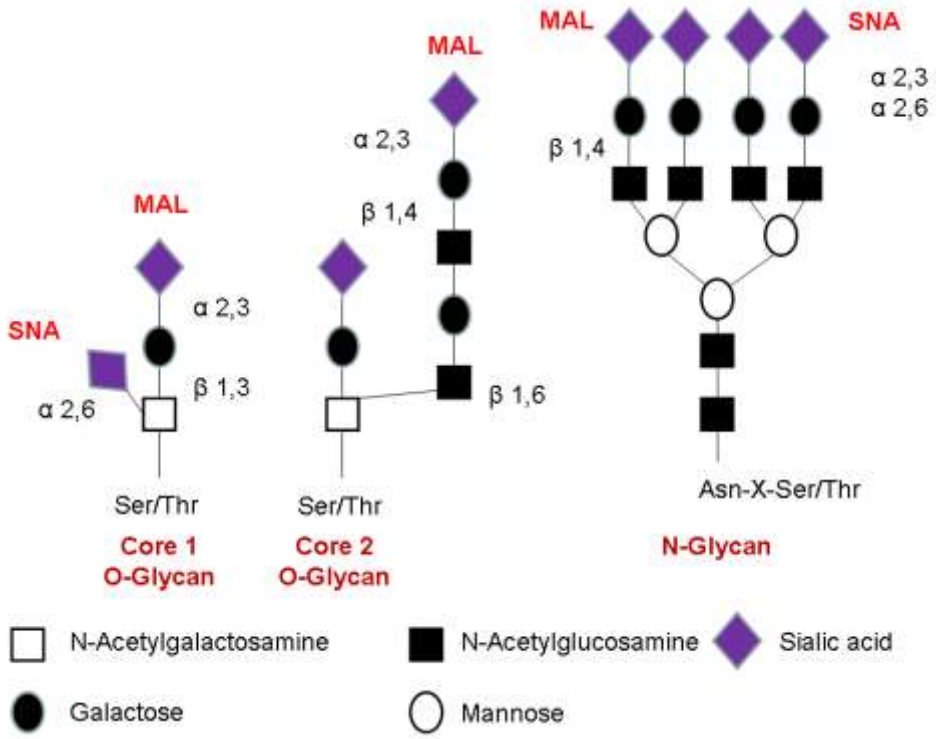

Diagram 3.2 Recognition of different patterns of sialylation by plant lectins, MAL and SNA on *N*- and *O*-linked oligosaccharides.

SnL up-regulation, on both Tregs and Teffs, was associated with up-regulation of α2,3 sialylation as evidenced by increased binding of MAL (Figure 3.13). While activated Tregs showed a modest increase in α2,6 sialylation as evidenced by increased binding to SNA, there was no significant increase in α2,6 sialylation on Teffs cells compared to unstimulated cells. The analysis of the mean fluorescence intensity (MFIs) of SnFc , MAL and SNA on unstimulated and activated Tregs and Teffs was consistent with an increase in α2,3 sialylation following TCR triggering (Figure 3.14). Activated Tregs also showed a significant increase in SNA MFIs compared to unstimulated Tregs. There was no significant difference in SNA MFIs of unstimulated and stimulated Teffs.

Together these data suggest that the up-regulation of SnL on activated CD4 T cells is associated with an overall enhanced α2,3 sialylation on Tregs and Teffs.

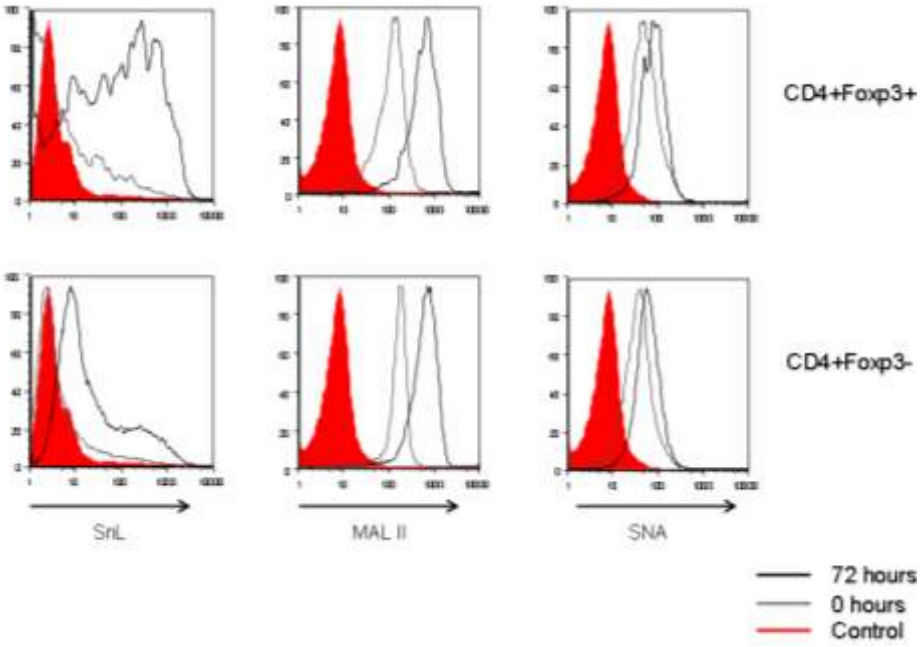

Figure 3.13 SnL up-regulation on CD4+ T cells is associated with increased α2,3 sialylation. Splenocytes from wild-type mice (n=4) were activated for 72 hours with plate-bound anti-CD3 (5ug/ml). Activated cells (black histograms) were compared with freshly isolated splenocytes (grey histograms), (n=4) for SnFc binding, α2,3 (using biotinylated MAL) and α2,6 (using biotinylated SNA) sialylation. Sialidase treatment was used as a negative control for SnFc binding (red histogram) and streptavidin as controls for (MAL and SNA). Data are representative of two independent experiments.

The specificity of MAL binding to α2,3-linked sialic acid residues was questioned previously by the finding of positive binding of this lectin to CHO cells expressing sulphated *N*-glycan oligosaccharides despite sialidase treatment (Bai *et al*, 2001). The study showed that MAL bound to sulphated group on the galactose under the α2,3-linked sialic acid (Bai *et al*, 2001). This property of MAL can explain the difference in the MFIs of MAL and SnL on Teffs (Figure 3.14). In order to ascertain the sialic acid linkage specificity of SnFc binding to activated CD4 T cells, an alternative approach was employed based on the use of α2,3-specific versus treatment with a sialidase that cleaves all sialic acid linkages.

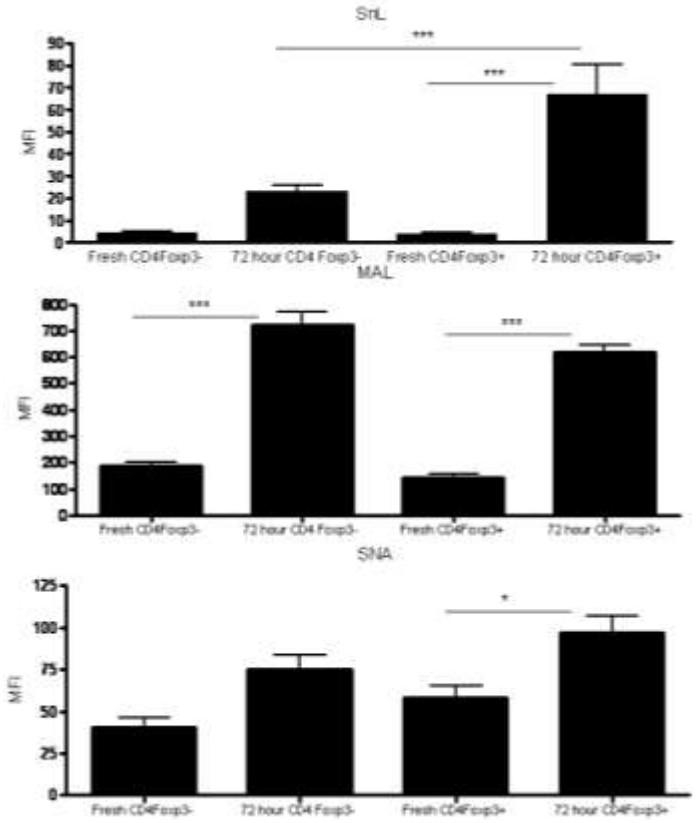

Figure 3.14 Mean Fluorescence Intensity (MFI) of SnFc (top), MAL (middle) and SNA (bottom). Bars represent means +/-SEM from 4 mice per activation status (un-stimulated (white bars) and activated (black bars). Statistical analysis was done using one-way ANOVA with Bonferroni post test. * = $p<0.05$, ***= $p<0.001$.

.

Sialidase L from *Macrobdela Leech* was previously reported to have specificity for α2,3-linked sialic acids (Hernandez *et al*, 2007). To examine the sialic acid-linkage specificity of SnL, sialidase L was compared to *Vibrio cholerae* sialidase (non-specific sialidase) and staining with SNA (α2,6 specific) was done as a control. Sialidase L was found not to affect α2,6 sialylation as evidenced with positive SNA binding (Figure 3.15). *Vibrio cholerae* sialidase treatment, on the other hand, abrogated SNA and SnFc binding. Interestingly, SnFc binding to activated CD4+ T cells was abolished with sialidase L treatment. These data further confirmed that SnFc binding to SnL+CD4 T cells is mediated by α2,3-linked sialic acids

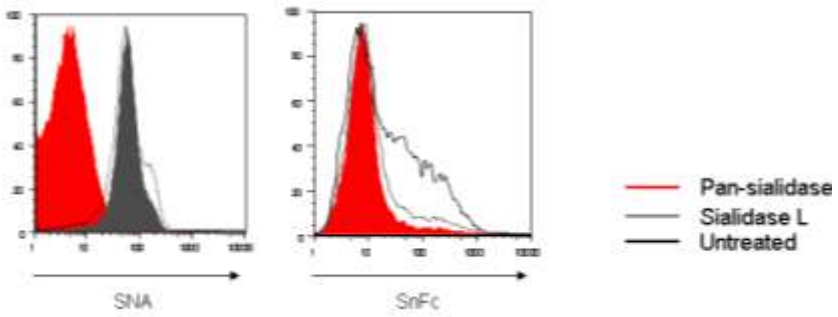

Figure 3.15 SnFc binds SnL on activated CD4+ T cells in α2,3-specific manner. Activated CD4+ T cells were treated with sialidase L, non-specific (pan-sialidase) from Vibrio cholera or left untreated. Surface labelling with SNA was performed (left) to confirm that sialidase L does not affect α2,6-linked sialic acid expression (grey filled histogram) compared to untreated (black histogram). Pan-sialidase treatment abolished SNA binding (red histogram). SnFc binding on activated CD4+ T cells (right) was equally affected by sialidase L (grey histogram) and pan-sialidase (red histogram) as compared to untreated cells (black histogram).

3.2.7 Altered glycosyltransferases expression on SnL+CD4+Foxp3- T cells

The above data showed a dominant α2,3 sialylation pattern associated with the induction of SnL on activated CD4 T cells. To explore glycosyltransferases that might be involved with SnL up-regulation, two-step enrichment approach was undertaken to sort SnL+ and SnL- CD4+Foxp3- T cells. CD4 T cells were initially enriched and further selected for CD4+CD25- and CD4+CD25+ T cells by Magnetic-Assisted Column Selection (MACS). CD4+CD25- T cells were then activated for 72 hours with anti-CD3/CD28 Dynabeads. Following activation, cells were labelled with SnFc and sorted by FACS into SnL+ and SnL- subpopulations. Afterwards, RNA was isolated from SnL+ and SnL- cells and utilized in real-time PCR experiments designed to examine the mRNA expression of specific glycosyltransferases. Three biological replicates from age and sex matched wild-type C57BL/6 mice were employed in these experiments (Diagram 3.3).

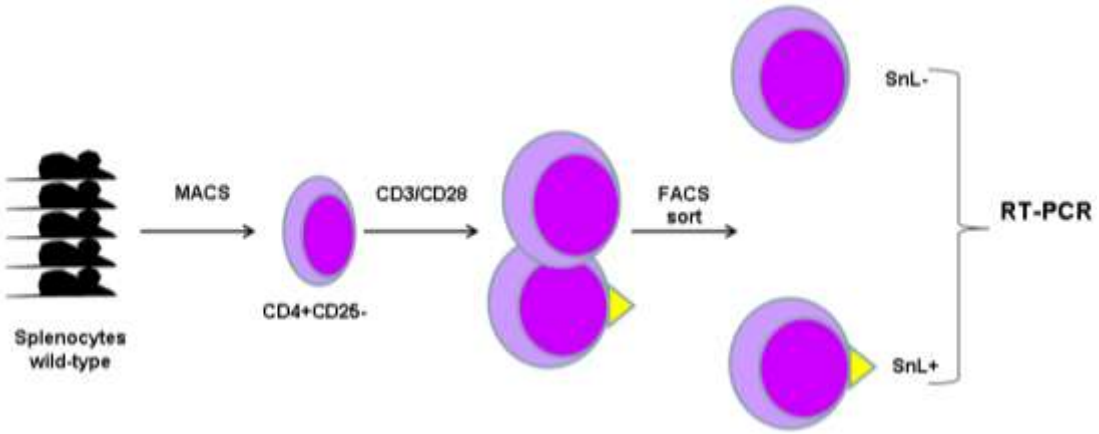

Diagram 3.3 Sorting SnL+ and SnL- Teffs cells for evaluation of altered glycosyltransferases expression with RT-PCR.

Having demonstrated that SnL induction of CD4 T cells is associated with an enhanced α2,3 sialylation and the binding of SnFc to SnL on activated CD4+ T cells being α2,3 sialic acid-linkage specific, the mRNA expression of members of the ST3Gal family of α2,3 sialyltransferases was initially examined. Of the 6 members of this family, four were included in the analysis: ST3Gal I, ST3Gal III, ST3Gal IV and ST3Gal VI. Murine ST3 Gal II and ST3Gal V were excluded from the analysis as they are both involved in gangliosides synthesis and have tissue specific distribution (brain and liver for the former and skeletal muscle for the latter), (Lee *et al*, 1994 and Takeshima, 2008).

ST3 Gal I is the first member of this family and it mediates the transfer of sialic acid to the galactose residue on Core 1 O-linked glycan structures (Diagram 3.4). It has been reported previously that T cell activation is associated with down-regulation of ST3Gal I and consequently loss of sialic acids on Core 1 oligosaccharides (Gillespie *et al*, 1993). There was no difference in the expression of ST3Gal I between SnL+ and SnL- subsets (Figure 3.16). This finding might suggest that ST3Gal I (and possibly Core 1 O-glycans) is not involved in sialylation of on SnL on activated CD4+ T cells.

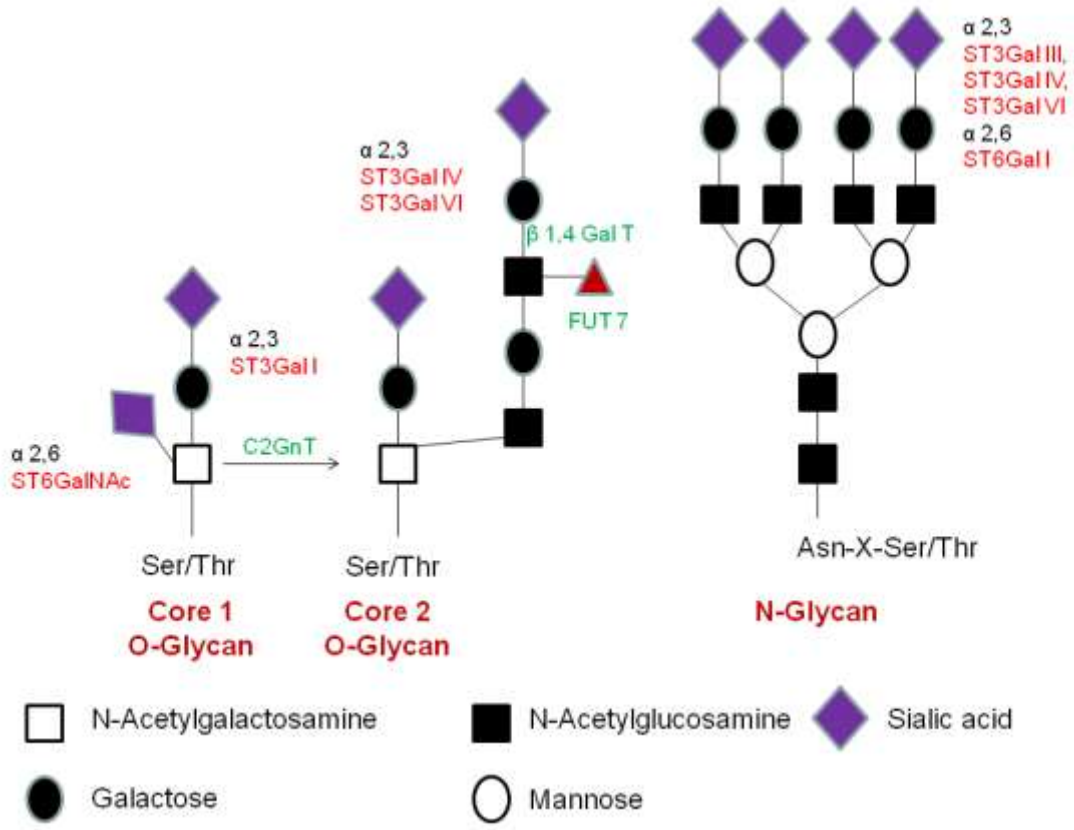

Diagram 3.4 The sites of action of examined *O*- and *N*-glycan-related glycosyltransferases.

ST3Gal III is another member of the α2,3 sialyltransferase that was shown to be primarily involved in terminal sialic acid capping on N-linked glycans (Varki, 2009 and Earl *et al*, 2010, see Diagram 3.4) . A certain degree of overlap exists between ST3Gal III and ST3Gal IV in their substrate as they can use both Galβ1,3GlcNAc and Galβ1,4GlcNAc sequences (Kono *et al*, 1997). However, ST3Gal III was found to have a preference for Galβ1,3GlcNAc and ST3Gal IV to have a preference for Galβ1,4GlcNAc (Takeshima 2008). In addition, ST3Gal IV was reported previously to be up-regulated following TCR triggering in the presence of IL-2 in both CD4 and CD8 T lymphocytes (Comelli *et al*, 2006). In this analysis the mRNA expression of ST3Gal III on SnL+ subset was found to be up-regulated by more than 1.5 fold (Figure 3.16). The difference between ST3Gal IV mRNA expression between SnL+ and SnL- Teffs did not reach 1.5 fold.

ST3Gal VI catalyzes sialic acid capping on both *N*- and *O*-glycans (Varki, 2009 and Diagram 3.4). Similar to ST3Gal IV, ST3Gal VI utilizes the substrate Galβ1,4GlcNAc. Both of these enzymes were shown to be involved in terminal sialylation of sialyl Lewis X (sLe^x) motif on *O*-glycans (Blander *et al*, 1999; Sperandio *et al*, 2006). In addition, these sialyltransferases are involved in the transfer of α2,3-linked sialic acids to the termini of *N*-glycans (Comelli *et al*, 2006). The fold difference in the mRNA expression of ST3Gal VI between SnL+ and SnL- Teffs was the highest among members of the ST3Gal family.

The flow cytometry analysis, presented earlier, were suggestive of a prominent α2,3 rather than α2,6 sialylation pattern that is associated with SnL induction on activated CD4+ T cells. ST6 Gal I is one of two members of the ST6Gal family of sialyltransferases. Both of these enzymes catalyze the transfer of sialic acids to the substrate Galβ1,4GlcNAc (Varki 2009, Diagram 3.4). ST6Gal II expression was found to be specific in brain tissues and also during embryogenesis (Takeshima 2008). ST6Gal II was therefore excluded from the analysis. Consistent with the flow cytometry data ST6Gal I expression was not different between SnL+ and SnL- Teffs.

T cell activation has been shown to be associated with an enhanced Core 2 *O*-glycosylation (Priatel *et al*, 2000). The glycosyltransferases that catalyzes the first step on Core 2 synthesis is Core 2 β1,6 N-acetylglucosaminyltransferase enzyme, or C2GnT (Jones *et al*, 1994 and see Diagram 3.4). In this analysis, the mRNA expression of C2GnT was dramatically (more than 6-fold) up-regulated in cDNA from SnL+Teffs compared to those from SnL-Teffs (Figure 3.16).

The glycosyltransferases profile of SnL+Teffs highlighted C2GnT, ST3Gal III and ST3Gal VI with more than 1.5 fold difference. Both C2GnT and ST3Gal VI were found to be critical for the biosynthesis of sLe^x motifs on activated T cells (Carlow et al, 2009). In order to evaluate whether other enzymes involved in the sLe^x (Diagram 3.4) were showing a similar trend to C2GnT and ST3Gal VI, the mRNA expression of β1,4 Gal transferase (β1,4 Gal T) and fucosyltransferase 7 (FUT 7) were examined (Figure

3.16). Interestingly, both these enzymes displayed a higher mRNA expression on SnL+ group (β1,4 Gal T >1.5 and FUT7 >3 fold). Therefore a number of the key enzymes involved in the biosynthesis of sLe^x motifs were found to be up-regulated to a higher extent on SnL+ compared to SnL-Teffs.

In summary, the RT-PCR analysis was in agreement with a dominant up-regulation of α2,3 sialylation associated with induction of SnL. Secondly, the findings were suggestive of an increase in Core 2 *O*-glycan structures on SnL+ cells. However, this association with *O*-linked sialyltransferases was not exclusive as ST3Gal III (*N*-glycan related) was also found to be up-regulated, albeit not to the same extent as ST3Gal VI, C2GnT and FUT 7.

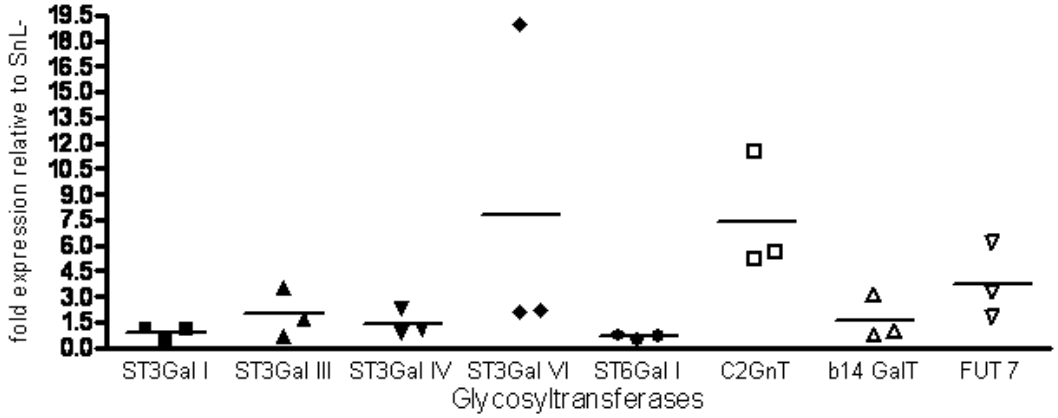

Figure 3.16 Glycosyltransferases expression profile associated with induction of SnL on Teffs. Three biological replicates (n=5 mice per replicate) were activated and sorted as explained in diagram 3.3. The expression of glycosyltransferases was compared to GAPDH as an endogenous control. Fold expression for each enzyme was calculated as explained in Materials and Methods.

3.2.8 CD43 and CD45RB expression on SnL+CD4+ T cells

The findings from the analysis of glycosyltransferase expression on SnL+ Teffs have prompted an attempt to identify the nature of carriers of SnL on CD4+ T cells. To begin with, an examination into whether the carrier is a glycoprotein or a glycolipid was undertaken using Proteinase K, an endopeptidase that cleaves peptide bonds in native proteins (Ebeling et al, 1974). Splenocytes from a wild-type C57BL/6 mouse were

activated for 48 hours with plate bound anti-CD3. The binding of SnFc to activated CD4 T cells treated with Proteinase K , but not with buffer alone, was completely abolished (Figure 3.17). This finding suggested that the nature of SnL carrier is a glycoprotein rather than a glycolipid. Next, the surface expression of two glycoproteins, CD43 and CD45RB, were examined by flow cytometery. These two glycoproteins were selected based on the abundance of Core 2 *O*-glycans in their structure (CD45RB and CD43) and published literature on potential counter-receptors for Sn (CD43, Van den Berg *et al*, 2001).

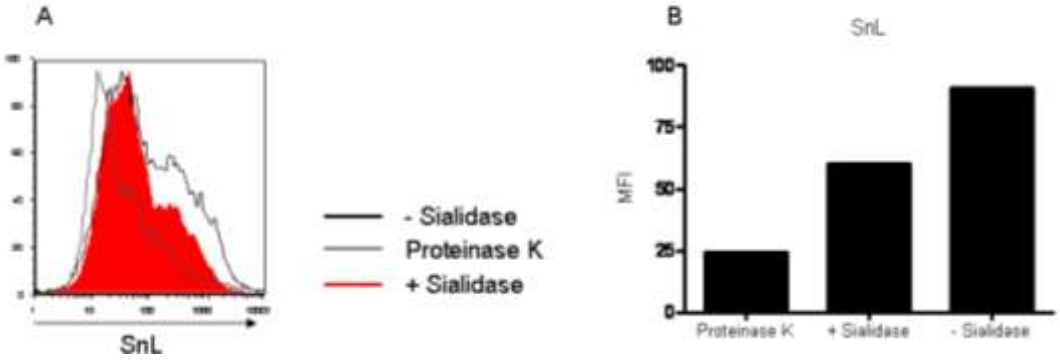

Figure 3.17 Proteinase K eliminates SnL expression on activated CD4+ T cells. Splenocytes were stimulated with plate-bound anti-CD3 (5µg/ml) for 48 hours. Harvested splenocytes were either treated with proteinase K (6mAU) or buffer for 30 minutes at 37^{o}C. Buffer treated samples were then treated with sialidase or left untreated. A, Histograms represent SnL expression on gated CD4+ T cells of buffer treated (black histogram), buffer and sialidase treated (red filled histogram) and proteinase K treated (grey histogram).B, SnL MFIs of on activated CD4 T cells under previously mentioned conditions.

There are two glycoforms of CD43, a resting glycoform (115 kDa) composed of Core 1 *O*-glycans and a higher molecular weight (130 kDa) which is composed mainly of core 2 oligosaccharides (Fukuda *et al*, 1991). The synthesis of the activated glycoform of CD43 was demonstrated to be mediated mainly by the action of C2GnT resulting in the formation of Core 2 *O*-glycans (Jones *et al*, 1994). Furthermore, the expression of this glycoform was shown to be associated with activated CD4+ T cells and being absent at the resting state, with which the resting glycoform is expressed abundantly (Jones *et al*, 1994).

The expression of the activation-associated glycoform of CD43 was examined by flow cytometry on SnL+ and SnL- subsets. Consistent with previous studies, there was no positive staining on resting CD4+ T cells. Interestingly, SnL+CD4+ T cells showed almost an exclusive expression of this molecule compared to SnL- counterparts (Figure 3.18, A and B).

CD45RB is a low molecular weight isoform of the phosphotyrosine phosphatase CD45. Resting T cells are CD45RB high and activated /memory T cells are typically CD45RB low. An up-regulation of α2,3-linked sialylation epitopes on CD45RB following T cells activation has been reported previously (Hernandez *et al*, 2007). The flow cytometry analysis showed an expected shift from CD45RB high to CD45RB low on SnL-CD4+ T cells following TCR ligation. Surprisingly, SnL+CD4+ T cells not only maintained a 'resting state' expression of CD45RB but even higher surface expression (Figure 3.18, B and C).

3.2.9 Sn binding to SnL on CD4+ T cells is independent of CD43, PSGL-1 and Core 2 O-linked glycans

The above data suggested the activated glycoform of CD43 to be a potential carrier for SnL on activated CD4+ T cells. Previously, Van den Berg and colleagues have shown that SnFc binds different glycoforms of CD43 expressed on TK-lymphoma cell line and CHO cells transfected with resting and activated glycoforms of CD43. The binding in all cases was sialic acid dependent (Van den Berg *et al*, 2001). To examine whether CD43 serves as a carrier for SnL on activated CD4 T cells, the binding of SnFc pre-complexes to activated CD4+ T cells from CD43 deficient mice was analysed by flow cytometry. Surprisingly, CD43 deficiency did not abrogate SnFc binding to activated CD4+ T cells (Figure 3.19).

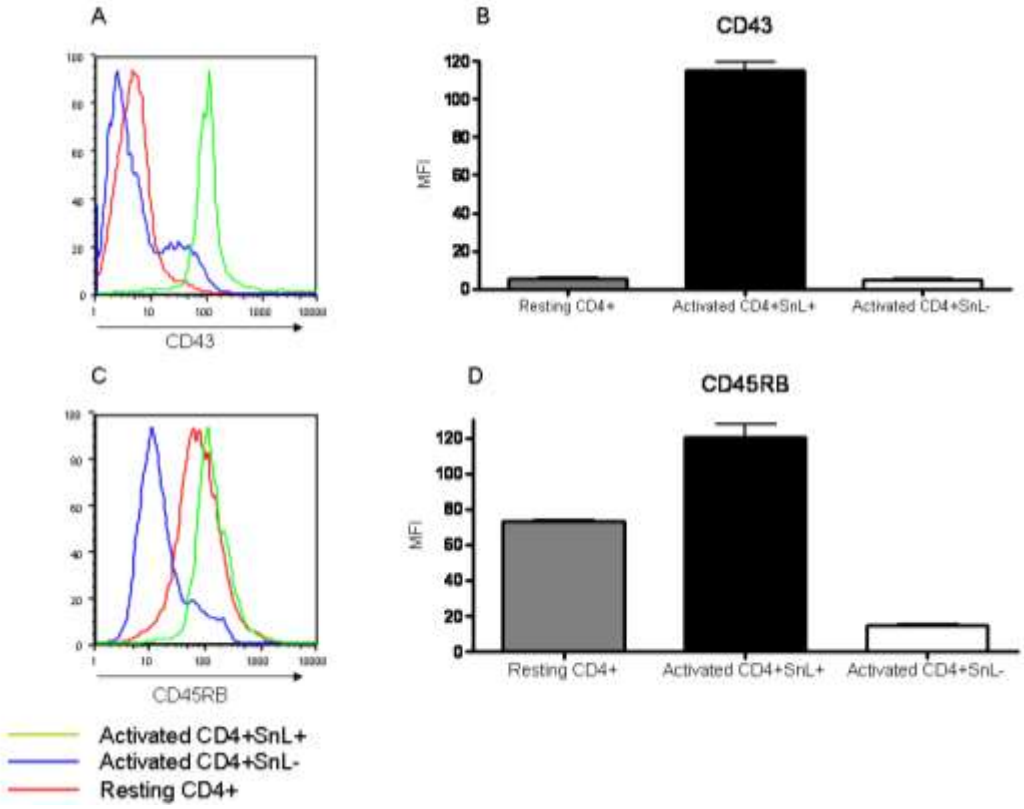

Figure 3.18 SnL+CD4+ T cells reveal a differential expression of the activation-associated glycoform of CD43 and CD45RB. Enriched CD4+ T cells were activated with anti-CD3/CD28 Dynabeads for 72 hours and compared to resting CD4+ T cells for the expression of CD43 (A and B) and CD45RB (C and D). Data are representative of three independent experiments.

The data on the glycosyltransferases expression on SnL+Teffs showed C2GnT to be dramatically up-regulated on these cells compared to their SnL- counterparts. This finding suggested the presence of abundant Core 2 oligosaccharide structures on SnL+Teffs. The question of whether Core 2 *O*-glycans are required for the formation of SnL was addressed by examining the expression of SnL on activated CD4+ T cells from splenocytes of mice deficient in all three isoforms of C2GnT. These mice are therefore lacking the capacity to synthesize Core 2 structures. Unexpectedly, CD4 T cells from these induced SnL expression following TCR ligation (Figure 3.19).

Van den Berg and colleagues found that SnFc bound to P-selectin glycoprotein ligand 1 (PSGL-1) using immunoprecipitation methods on TK-lymphoma cell lines. Similar to CD43-/- and C2GnT triple-/-, activated CD4 T cells from mice deficient in PSGL-1 maintained the ability to express SnL following activation (Figure 3.19)

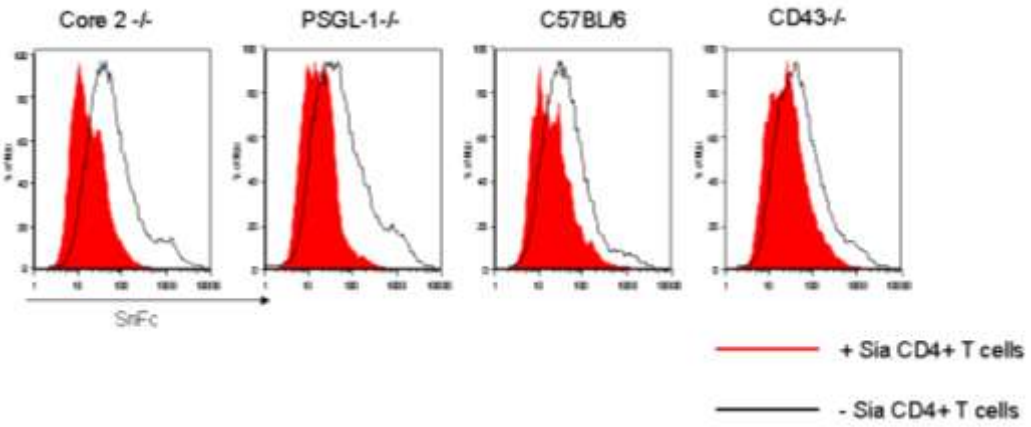

Figure 3.19 Sn binds to activated SnL+CD4+ T cells independent of CD43, Core -2 O-glycans and PSGL-1. Splenocytes from mice deficient for CD43, PSGL-1 and C2GnT (all three isoforms) were activated with plate-bound anti-CD3 (5ug/ml) for 72 hours. Activated cells were either treated with sialidase (red histograms) or left untreated. The data shown are representative of three independent experiments.

3.2.10 Sn binds *N*-glycans on activated CD4+ T cells

The activation of T cells with TCR triggering is associated with changes in the expression of both *N*- and *O*-linked glycans. In the case of *O*-linked glycans, the main changes include: loss of sialic acids on Core 1 (unbranched) structures and formation of branched Core 2 oligosaccharides. The sialylation changes occurring on *N*-glycans following TCR ligation in CD4 T cells include: a dramatic reduction in sialylated biantennary *N*-glycans carrying terminally α2,6 sialylated residues (reduced ST6Gal I expression) and an increase in N-glycans carrying galactosylated structures (up-regulation of α1,3 Gal transferase) (Comelli *et al*, 2006).

It is not known whether Sn prefers α2,3 sialic acid-linkages on *N*- or *O*-linked glycans on activated CD4+ T cells. The positive binding of SnFc pre-complexes to CD4 T cells from C2gnT deficient mice indicated that Core 2 *O*-glycans are not relevant in SnL structure. In addition, the expression of ST3Gal I, which mediates α2,3 sialylation on Core 1 *O*-glycans, was not significantly different between SnL+ and SnL-Teffs. Furthermore, ST3Gal III which mediates α2,3 sialylation primarily on *N*-glycans was expressed to a higher (>1.5 fold) level in SnL+ compared to SnL-Teffs.

To further examine the requirement of *N*- or *O*- glycans in the synthesis of SnL, splenocytes from wild-type C57BL/6 mice were activated in the presence of *N*- or *O*-glycan inhibitors. BenzylαGalNAc is an *O*-glycan inhibitor that acts as a primer competing with endogenous GalNAc for Ser/Thr residues. The efficiency of *O*-glycan inhibition can be confirmed by staining with pea nut agglutinin (PNA) which recognizes the exposed Galβ1,4GalNAc sequence (Varki 2009; Hernandez *et al*, 2007 and Earl *et al*, 2010). 1-deoxymannojirimycin (DMNJ), on the other hand, inhibits the formation of complex *N*-glycan structures. DMNJ specifically inhibits α-mannosidase I, leading to the accumulation of early highly mannosylated *N*-glycan precursors. N-glycan inhibition with DMNJ can be verified with negative staining for Phaseolus vulgaris agglutinin (PHA) (Varki, 2009 and Walzel *et al*, 2006).

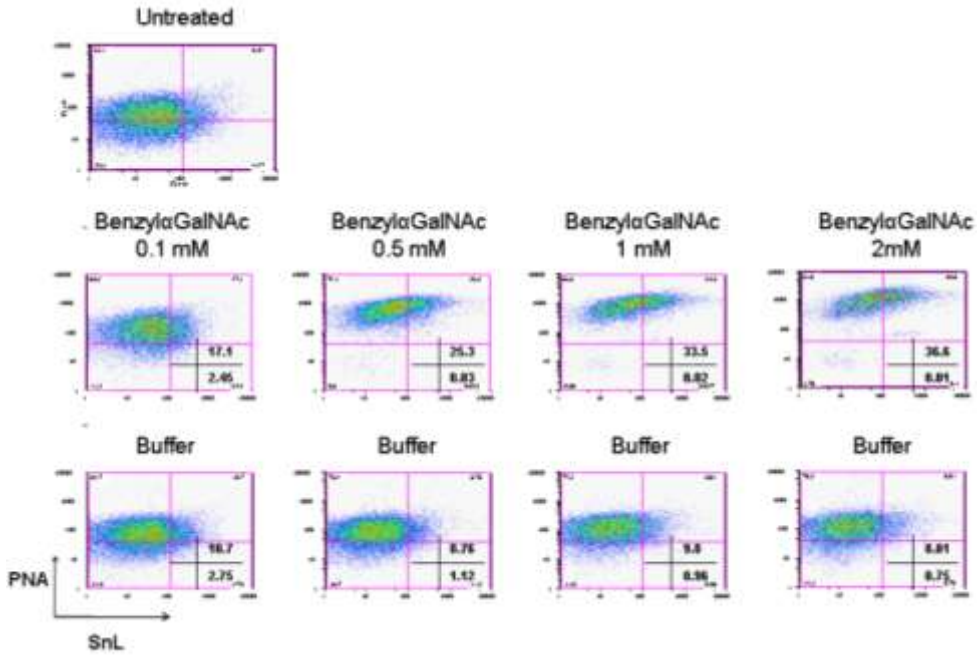

Figure 3.20 SnL expression on activated CD4+T cells in the presence of *O*-glycan inhibitor, benzylαGalNAc. Splenocytes from wild-type mice were activated with plate-bound anti-CD3 (5ug/ml) alone (top dot plot), in the presence of benzylαGalNAc (middle row) or buffer alone (bottom row). At 72 hours, cells were harvested and labelled for CD4, PNA and SnL. Dot plots represent relevant binding on gated CD4+ T cells.

O-glycan inhibition with benzylαGalNAc resulted in an increase in the percentage of SnL+CD4+ T cells and SnL expression at cell level (Figure 3.20). This effect of

benzylαGalNAc was concentration dependent. The inhibition of O-linked glycans was confirmed with enhanced PNA binding as the concentration of benzylαGalNAc was increased (Figure 3.20 and Figure 3.21). These findings suggested that *O*-glycans are not involved in the synthesis of SnL on activated CD4+ T cells.

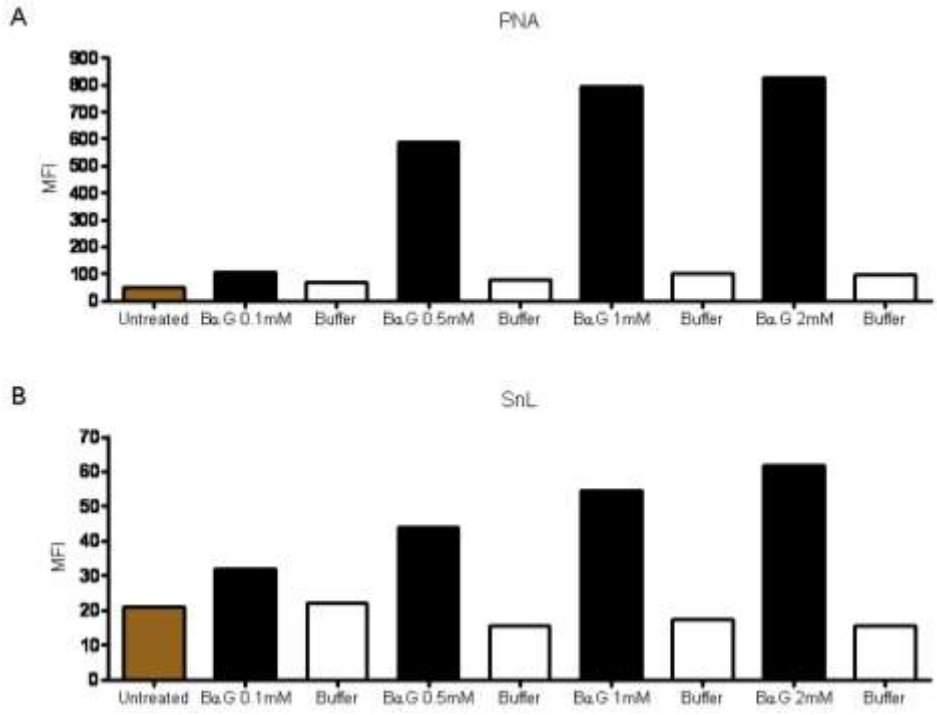

Figure 3.21 Mean fluorescent intensities (MFIs) of PNA and SnL on activated CD4 T cells from wild-type mice. A, PNA MFIs of an untreated sample (brown bar) or in the presence (black bars) of different concentrations of benzylαGalNAc (BαG), or in the presence of buffer only (white bars). B, SnL MFIs of an untreated sample (brown bar) or in the presence (black bars) of different concentrations of benzylαGalNAc (BαG), or in the presence of buffer only (white bars).

DMNJ treatment was found to be associated with cell morphology changes as evidence by the forward and side scatter profile of the treated cells (Figure 3.22, A). Interestingly, *N*-glycan maturation inhibition with DMNJ resulted in complete inhibition of SnL induction on activated CD4+ T cells. The inhibitory effect of DMNJ was confirmed with negative staining for PHA on activated CD4+ T cells (Figure 3.22, B). These findings indicated that *N*-glycans are required for the formation of SnL on CD4+ T cells.

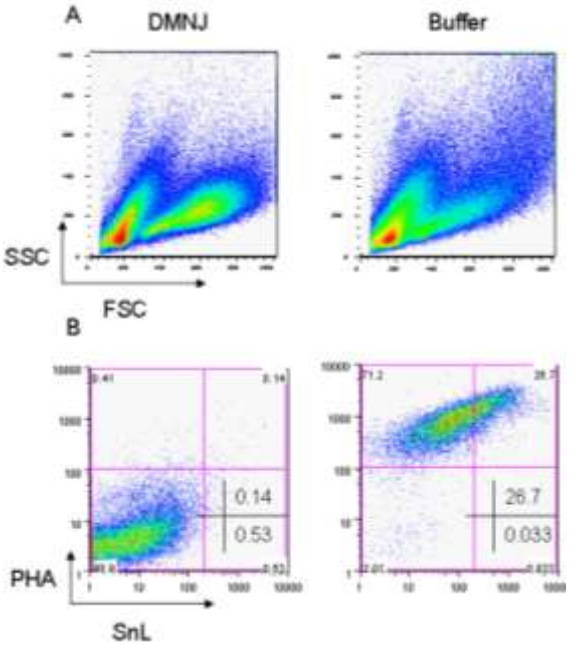

Figure 3.22 SnL expression on activated CD4+ T cells in the presence of *N*-glycan inhibitor, DMNJ. Splenocytes from wild-type mice were activated with plate-bound anti-CD3 (5ug/ml) in the presence of 2mM of DMNJ (left) or buffer (right). At 72 hours, cells were harvested and labelled for CD4, PHA and SnL. Dot plots represent relevant binding on gated CD4+ T cells.

3.2.11 Summary of the characteristics of CD4SnL+ and nature of SnL

The investigation of the SnL+CD4+ T cells revealed significant differences in phenotype and functional aspects of this subset of activated CD4+ T cells compared to their SnL- counterparts. Table 3.1 summarizes the main findings of this analysis.

Similarly, examination of the nature of SnL on CD4+ T cells demonstrated novel findings related to sialylation pattern, sialyltransferases and glycans structure of SnL. The main findings of the glycomic analysis of SnL on CD4+ T cells are summarized in Table 3.2.

Table 3.1 Summary of characteristics of SnL+CD4+ T cells and nature of SnL.

Characteristics	CD4+SnL+
Induction	TCR ligation
Expression	Higher expression in Tregs compared to Teffs
Activation	Higher levels of early activation markers CD25 and CD69
Cytokines	Higher intracellular expression of IFNγ and IL-2 in SnL+Teffs
Proliferation	Hyperproliferative in response to TCR ligation
Apoptosis markers	Extrinsic pathway: higher CD95L and similar CD95 surface expression Intrinsic pathway: higher expression of Bcl2
Other markers	Maintain expression of CD45RB following TCR ligation and almost exclusive expression of activation-associated glycoform of CD43

Table 3.2 Summary of key findings of the glycomic analysis of SnL

Characteristics	Findings
Sialic acid linkage	α2,3
Sialyltransferases associated with induction	ST3Gal VI>ST3Gal III>ST3Gal IV
Other glycosyltransferases associated with induction	C2GnT, FUT7 and β1,4Gal T
Glycan type	*N*-linked
Carrier	Glycoprotein
Nature of glycoprotein carrier	unknown but unlikely to be CD43 or PSGL-1

3.3 Discussion

The aims of the experiments outlined in this chapter were: i) to identify whether SnL are expressed exclusively on Tregs or both Tregs and Teffs; ii) to characterise the phenotype of SnL+CD4+ T cells.iii) to evaluate the functional consequences of engaging SnL on CD4+ T cells; iv) to explore the glycosylation changes that accompany the induction of SnL on activated CD4+ T cells and differential O- or N-glycan contribution to the binding of Sn to SnL; v) to examine potential candidates for SnL.

3.3.1 SnL up-regulation on CD4+ T cells

The data presented on the induction of SnL on CD4+ T cells indicate that TCR ligation is sufficient for up-regulating the expression of these ligands. However, such induction is a rather late event (24-48 hours) following TCR stimulation, as demonstrated by time course analysis. Wu and colleagues has recently demonstrated that Tregs isolated from CNS, secondary lymphoid organs and blood of EAE mice express abundant ligands for Sn. In addition, SnL expression was Tregs exclusive as Teffs were shown to be SnL-. The data presented in this chapter has confirmed that SnL induction occurs on both Tregs and Teffs following TCR triggering *in vitro*. However, there was a clear bias towards Tregs when the percentage of SnL+ cells among activated Tregs and Teffs was examined. A subset of freshly isolated Tregs or Tregs from total splenocytes of wild-type C57BL/6 mice showed SnL positivity prior to TCR stimulation *in vitro*. Peripheral Tregs comprise both thymic-derived “natural” Tregs (nTregs) and “induced-Tregs” (iTregs). The requirements for the generation of the later subset include: TCR stimulation, IL-2 and TGFβ (Fantini *et al*, 2006). iTregs can be generated in secondary lymphoid organs and other tissues, particularly the gut. They were also found in transplant tissues (Waldmann *et al*, 2004). One potential explanation for having SnL+Tregs from fresh splenocytes is that this subset could have already been

activated in the periphery *in vivo*. Furthermore, whether this SnL+ subset of Tregs belongs to nTreg or iTregs remains a possibility that warrants further investigation. Examining the expression of markers such as helios, which was found to be a marker for nTregs (Thornton *et al*, 2010), might be useful to identify the nature of these Tregs.

3.3.2 Phenotypic characteristics of SnL+CD4 T cells

SnL+CD4+ T cells constitute a subset of CD4+ T cells with higher state of activation as evidenced by their expression profile of early activation markers: CD25 and CD69. These data show heterogeneity in CD4+ T cells response following TCR ligation and SnL positivity can be used as a marker for cells at the high end of activation. This differential state of activation might be related to a certain degree of TCR-hyper-responsiveness in SnL+CD4+ T cells. This was evident when the effect of titrating TCR signal strength with various concentrations of anti-CD3 antibodies was employed. On the Teffs, even at low concentration of the anti-CD3 there was a significant difference in the expression of activation markers between SnL+ and SnL- subsets. Moreover, the percentage of SnL+ cells and the percentage of CD69+ and CD25+ cells were proportional to the degree of TCR triggering by different concentration of anti-CD3 antibody. Surprisingly, unstimulated Tregs were found to express high SnL expression. In addition, the up-regulation of SnL observed on these cells did not differ with increasing anti-CD3 concentration. These findings suggest that the majority of Tregs were already activated after 3 days in culture. However, it is not clear what caused such activation. In these experiments, plates were coated with anti-CD3 prepared in sterile-filtered carbonate bicarbonate buffer. The wells for the resting splenocytes had buffer alone. While the possibility of TLR-mediated activation cannot entirely be excluded, it does not explain that Teffs were not activated (based on their expression of CD69 and CD25) to any extent in the resting state. Therefore, the reason behind the up-regulation of SnL on Tregs in the absence of TCR stimulation remains unclear.

The analysis of intracellular cytokine expression, especially with IFNγ, was also in agreement with the higher state of activation of SnL+Teffs. While the hyperproliferative state of these cells can be related to their response to TCR stimulation, it can also be related to these cells being able to utilize more endogenous IL-2 by the virtue of their higher extent of CD25 expression compared to SnL-Teffs. This possibility could be investigated further by analysing the expression of an IL-2R-related protein such as phosphorylated signal transducer and activator of transcription 5 (pSTAT5) following exposure of SnL+ and SnL- Teffs to exogenous IL-2.

3.3.4 SnL ligation on CD4 T cells induces cell death

Experiments performed on the functional outcome of ligating SnL on activated CD4+ T cells by Sn revealed a novel function of Sn. The interaction between Sn+/+BMDM and activated CD4+ T cells revealed a reduced cell viability compared to co-cultures with Sn-/-BMDMs. Similar results were obtained with exposure to SnFc protein (consisting of the first three immunoglobulin domains of the molecule) and with CHO cells expressing full length of the molecule. The mechanism of inducing cell death is not clear. CD95L surface expression was found to be significantly higher in SnL+ versus SnL- CD4+ T cells. CD95L has been shown to play a key role in mediating cell death in activated T cells, and other cells, via its interaction with CD95 and therefore activating the extrinsic apoptosis pathway (Brunner *et al*, 2003). In addition, stimulation of resting CD4+ T cells was found to induce less expression of FasL compared to stimulation of primed CD4+ T cells (Pawelec *et al*, 1996). Studies of activation-induced cell death, in which T cells are re-stimulated with anti-CD3 or by specific antigens, revealed that FasL can induce cell death on neighbouring cells and in a cell autonomous manner (Dhein *et al*, 1995). TCR signalling plays a key role in activating various downstream signalling pathways that would result in the transcription of FasL gene (Brunner *et al*, 2003). Therefore, it is also possible that the heightened expression of CD95L on SnL+CD4+ T cells is related to the enhanced activation status of these cells. The

enhanced expression of CD95L on SnL+CD4+ T cells might be related to an important cytotoxicity potential of these cells. The analysis of Bcl2 expression on SnL+CD4+ T cells was inconclusive as there was no statistical difference between SnL+ and SnL- Teffs at mRNA level while there was difference at protein level. Repeating these experiments with inclusion of more biological replicates might help to determine if there is a significant difference between the two subsets. In addition, analysis of other members of the Bcl2 family, especially the closely related BclxL might be useful. In conclusion, although this analysis has further identified the phenotype of SnL+CD4 T cells, it did not provide an explanation to how SnL ligation with Sn induces cell death.

3.3.5 Enhanced α2,3-sialylation associated with induction of SnL on CD4 T cells

The induction of SnL on activated CD4 T cells was associated with an increase in α2,3 versus α2,6 sialylation as evidenced by increased binding to plant lectins MAL compared to SNA. This pattern is relevant to Sn preferences of recognising α2,3-linked sialic acid residues that has been reported previously (Crocker, 2007). This was further confirmed by the use of α2,3 specific sialidase L treatment. Such a treatment led to abolishing SnFc binding to activated CD4+ T cells to a similar extent to cells that received ‘pan-sialidase’ treatment. In addition, these findings were useful in directing the search for sialyltransferases that might be involved in sialylation of SnL. Comparison of SnFc and MAL binding to activated Tregs and Teffs revealed an interesting discrepancy. While MAL binding to Tregs versus Teffs was similar, the binding of SnFc Tregs was much higher than Teffs. These findings meant that even for a similar extent of α2,3 sialic acid availability on Tregs and Teffs as represented by similar MAL binding, there is a higher binding to SnFc on Tregs versus Teffs. This observation suggests the presence of additional features of SnL on Tregs that result in higher SnFc binding compared to Teffs.

The investigation of the expression of sialyltransferase on SnL+ and SnL- CD4+ T cells relied on the use of enriched Teffs. The rationale behind this was primarily related to

the limitations in having sufficient numbers of enriched Tregs to use in subsequent FACS sorting and RNA isolation. While in vitro expansion of Tregs was a possible choice, but it would have reflected a different spectrum of changes with other factors involved including exposure to high concentrations of IL-2. Consistent with the pattern of sialylation observed with plant lectins, there was a dominant increase in α2,3 sialyltransferases mRNA expression. Among these, a significant increase was observed in the expression of ST3 Gal VI and a modest increase of ST3 Gal III (>1.5 fold) compared to SnL-Teffs. The former has been reported to mediate terminal sialic acid capping on *N*- glycans and Core 2 *O*-glycans (Comelli *et al*, 2006; Underhill *et al*, 2005) and the latter being involved with the same process but on N-linked glycans only (Earl *et al*, 2010). Based on the data showing the higher activation status of the SnL+CD4+ T cells, it was expected that there would be an increase in C2GnT, which mediates the synthesis of Core 2 structures, and reduced expression of ST3 Gal I (related to reduced sialylation of Core 1 structures). These findings were in line with previous studies of a shift in the *O*-glycan pattern from Core 1 to Core 2 structure following T cell activation (Priatel *et al*, 2000). In addition, the increased mRNA expression of FUT7 and β1,4 Gal T were further evidence for the dominant Core 2 rather than Core 1 O-glycosylation on SnL+Teffs.

The data on the binding of SnFc to activated CD4+ T cells from mice deficient for all three isoforms of C2GnT and therefore defective in the synthesis of Core 2 *O*-glycans, indicated that Core 2 structures are not required for the synthesis of SnL. Consequently, the up-regulation of mRNA expression of Core 2 related sialyl- and glycosyltransferases observed on SnL- Teffs reflected global changes related to the heightened state of activation in these cells. Collectively, these data suggested that the glycan nature of SnL on activated CD4+ T cells is that of an *N*- rather than *O*-linked glycan.

3.3.6 SnL are made of *N*-glycans

Specific inhibitors of *O*- and *N*-linked glycans demonstrated that Sn binds N-glycans structures on activated CD4+ T cells. DMNJ completely abolished binding of SnFc to these cells, while benzylαGalNAc did not exert an inhibitory effect on the binding of SnFc. Moreover, *O*-glycan inhibition enhanced SnL induction (percentage of SnL+CD4 T cells) and per cell expression (MFIs). A possible explanation for this effect is that changes in the glycan distribution and expression on numerous glycoproteins might affect the threshold of TCR stimulation leading to more activated CD4+ T cells and therefore a higher percentage of SnL+ population. In addition, benzylαGalNAc may compete for Gal T and shunt *N*-glycan to more complete α2,3 sialylation. The findings from these glycans inhibition experiments together with the data on altered expression of sialyltransferases associated with induction of SnL, suggest that two *N*-glycan related sialyltransferases (ST3Gal III and ST3Gal VI) to be mediating the transfer of sialic acid to the termini of *N*-glycan structures of SnL. Ultimately the contribution or redundancy of each of these enzymes can be examined in mice deficient for one or both of these sialyltransferases.

3.3.7 CD45RB and CD43 are both differentially expressed on SnL+CD4 T cells

The search for surface markers to distinguish SnL+ from SnL- CD4+ T cells revealed that CD45RB and activated glycoform-CD43 were expressed primarily on SnL+ versus SnL- activated CD4+ T cells. As for the former marker, SnL+ cells not only maintained CD45RB high status but also had an increased expression compared to the resting state. This interesting observation might help to explain certain aspects of SnL+CD4+ T cells phenotype. CD45 can act as a negative and positive regulator of TCR signalling by dephosphorylating different tyrosine residues in the Src-family of kinases (Mcneill *et al*, 2007). Transgenic mice expressing less than 3% of wild-type CD45 showed a high

threshold of TCR triggering. In contrast, around 60% expression of CD45 caused heightened sensitivity to TCR signalling. These properties of CD45 were found to be independent on isoform (Salmond *et al*, 2008). Whether the maintenance of CD45RB high status in the SnL+ subset leads to a state of hyper-responsiveness to TCR ligation, remains to be determined.

Another interesting aspect of CD45RB is related to its interaction with galectin-1. Galectin 1 is a prototypic member of the galectin family which are characterized by having a carbohydrate-recognition-domain that is responsible for their βgalactoside-binding activity. The molecule is produced and secreted by activated T and B cells and levels of expression are significantly up-regulated in Tregs and NK cells (Rabinovitch *et al*, 2009). Galectin 1 has been found to bind different surface glycoproteins e.g. CD45, CD43 and CD7 (Earl *et al*, 2010). One of the main regulatory functions of the molecule is related to apoptosis of immature thymocytes and activated peripheral T cell. This function of galectin 1 was found to be highly dependent on the glycosylation state of binding glycoprotein. For example, T cell lines expressing CD45RB but being deficient in C2GnT (high affinity ligand for galectin 1) are resistant to cell death induction by galectin 1 (Nguyen *et al*, 2001).

The binding of galectin 1 to *N*-glycans on CD45RB was found to be directly related to the types of sialic acid linkage at the termini of the *N*-glycans. The expression of ST6Gal I, which results in the addition of α2,6-linked sialic acid to the terminal galactose, resulted in reduced binding of galectin 1. In contrast, overexpression of ST3Gal III, which results in the addition of α2,3- linked sialic acids led to enhanced galectin 1 binding and cell death induction. Interestingly, the RT-PCR data on SnL+Teffs showed an increase in the mRNA expression of ST3Gal III and no change in the expression level of ST6Gal I compared to SnL-Teffs. In addition, *N*-glycan inhibition abolishes the induction of SnL on activated CD4+ T cells. Collectively, the similarities between Sn and galectin 1 in their preferences for sialic acid-linkages on *N*-glycans raise an important question. As there is an overlap between Sn and galectin 1

in their glycosylations preferences, would this translate into a competition or a synergy in their binding to *N*-glycan structures and what the functional consequences of such an interaction could be?

CD43, both resting and activated glycoforms, have been reported previously to constitute a putative counter-receptor for Sn on TK-lymphoma cell lines, based on immunoprecipitation experiments (Van den Berg *et al*, 2001). The extracellular domain of CD43 consists primarily of *O*-linked glycans with only one N-glycosylation site (Carlsson *et al*, 1986). The activated glycoform of CD43 consists to a greater extent of Core 2 *O*-linked glycans the synthesis of which is mediated by C2GnT. In addition, Van den Berg and colleagues reported a positive binding between Sn and both resting and activated glycoforms of CD43. These observations are in contrast to the data on the induction of SnL on activated CD4 T cells and the absence of SnL on freshly isolated CD4+ T cells. Yet, the activated glycoform of CD43 was found to be differentially expressed on SnL+CD4+ T cells compared to their SnL- counterparts, a finding that was consistent with C2GnT up-regulation on SnL+Teffs. In order to explain these discrepancies, SnFc binding on activated CD4+ T cells from spleens of CD43-/- was analysed. The absence of CD43 did not affect the binding of SnFc to activated CD4 T cells. This finding was in agreement with the data presented on glycan inhibition in which *O*-glycan inhibition (and therefore formation of the activated glycoform of CD43) resulted in an increase in SnL expression on activated CD4 T cells.

In summary, SnL+CD4+ T cells represent a subset of highly activated CD4+ T cells. SnL+Teffs appear to be hyper-proliferative and produce higher levels of inflammatory cytokines e.g. IFNγ, compared to SnL-Teffs. Engaging SnL with Sn or SnFc leads to induction of cell death. The binding of SnFc to SnL is sialic acid-dependent in an α2,3-specific manner. Two members (ST3Gal III and ST3Gal VI) of the α2,3 family of sialyltransferases have been identified as candidates to mediate sialylation of SnL. The binding of SnFc to activated CD4+ T cells is dependent on *N*-glycan and not *O*-linked glycans, indicating that the former contributes to the synthesis of SnL on activated

CD4+ T cells. Finally, the investigation of finding putative Sn counter-receptor on murine activated CD4 T cells ruled out CD43 and PSGL-1 as potential candidates.

Potential function for Sn in NZB X NZW F1 lupus nephritis

4.1 Introduction

Sn+ macrophages were shown previously to be present in glomerulonephritis of different aetiologies in rodents (Ito *et al*, 2007) and in human (Ikezumi *et al*, 2008). In addition, Sn+ resident and inflammatory monocytes were found in PBMCs of patients with SLE and correlated to disease severity and other established biomarkers of the disease (Biesen *et al*, 2008). In this chapter, the evidence for expression of Sn in the kidneys of spontaneous murine lupus nephritis model NZB X NZW F1 (BWF1) mice will be discussed. Secondly, the effect of pre-disease blocking of Sn, using anti-Sn monoclonal antibodies, on disease onset and severity will be presented. Finally, the generation of Sn deficient BWF1 mice and preliminary data on the effect of such a deficiency at an early time point of the disease will be presented.

4.2 Sn expression in BWF1 mice

4.2.1 Disease manifestations in BWF1 mice

The main disease manifestations in BWF1 mice are: overproduction of autoantibodies against nucleosomal materials (particularly dsDNA), proteinuria and glomerulonephritis caused by the deposition of immune complexes in the glomeruli. BWF1 mice tend to develop proteinuria, as first manifestation of nephritis, around 24-28 weeks of age (Werwitzke *et al*, 2005; Hayashi *et al*, 2007; Mathian *et al*, 2005 and Kasagi *et al*, 2010). The strategy employed in this investigation for examining the expression of Sn included examining mice at a pre-disease stage (16 weeks of age) and at the onset of lupus nephritis (24-28 weeks). A total of 16 mice were included in this analysis (4 at 16 weeks of age and 12 at 28 weeks). To begin with, mice were examined for urinary protein excretion and serum anti-dsDNA titres (n=12, age 28 weeks). Subsequently,

the mRNA expression of Sn, CD4, Foxp3, macrophages lineage markers (CD68 and F4/80) and other relevant cytokines were examined by real-time PCR in kidney tissues (n=19, 4 BWF1 and 3 NZW mice at the age of 16 weeks and 8 BWF1 and 4 NZW mice at the age of 28 weeks).

At 28 weeks of age, eight mice had proteinuria of less than 300mg/dl (< grade 2) and four mice had proteinuria of >300mg/dl (> grade 2). Dividing the BWF1 mice into high and low grade of proteinuria might be useful in determining whether there is a difference in Sn mRNA expression between early and late nephritis. In order to examine whether this strategy can distinguish between mice with different degrees of disease severity, serum anti-dsDNA levels were used as a marker of disease severity.

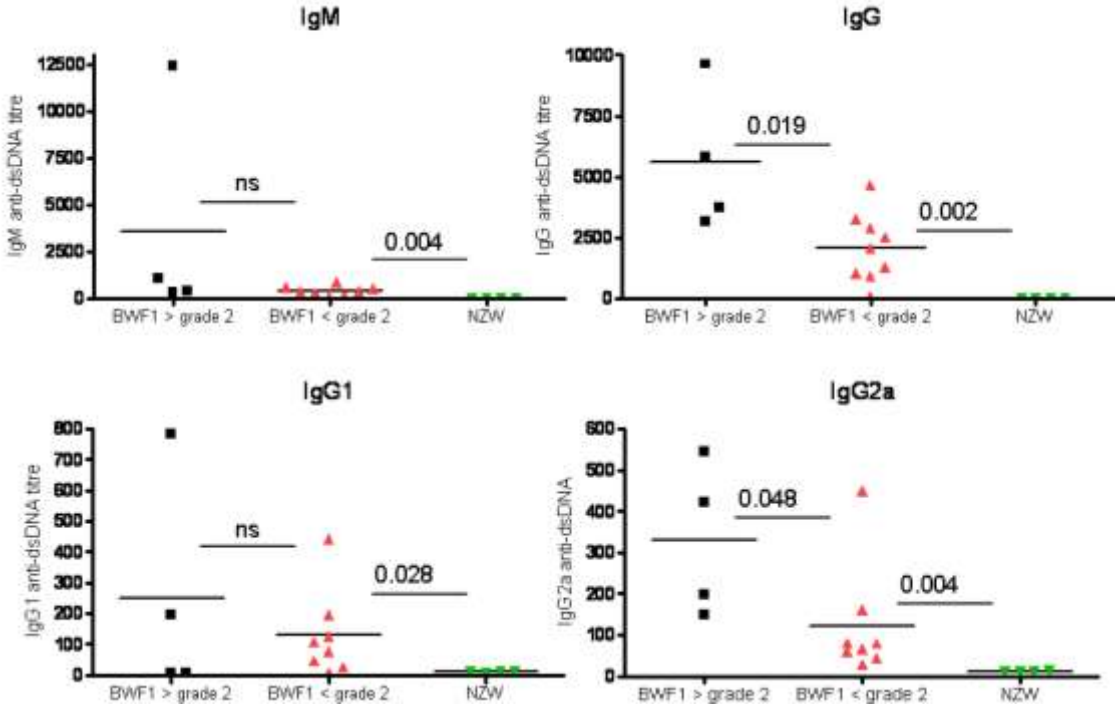

Figure 4.1 Serum anti-dsDNA titres of BWF1 mice at the age of 28 weeks according to their grade of proteinuria. Sera from 12 mice, 4 with >grade 2 proteinuria and 8 with detectable (>100mg/dl) proteinuria were examined for anti-dsDNA titres by ELISA. Pooled sera from 32 weeks old BWF1 mice were used as a positive control. Statistical analysis was done using student's t test. Exact p values of significant differences appear on the small horizontal bar between the groups examined.

Sera from all mice at 28 weeks of age were examined for anti-dsDNA classes IgM, IgG, IgG2a and IgG1 (Figure 4.1). There were significant differences between BWF1 mice

with high and low grade proteinuria in IgG and IgG2a anti-dsDNA titres. In contrast serum IgM and IgG1 anti-dsDNA titres showed no difference between these two groups. These findings suggested that mice with high grade of proteinuria exhibit higher levels of IgG and IgG2a anti-dsDNA and therefore higher tendency to have more severe nephritis compared to those with low grade of proteinuria.

4.2.2 Sn is expressed around the onset of lupus nephritis

To examine the expression of Sn in renal tissues, primers were designed to identify two extracellular Ig domains of Sn (domains 2 and 17). Two distant domains of the molecule were used due to the possibility of alternative splicing of Sn that might affect the detection by real-time PCR. The primers were initially examined for sequence similarity against Sn using basic local alignment search tool (BLAST). Subsequently, the primers were tested on cDNA of splenic tissues from WT and Sn-deficient C57BL/6 mice (Figure 4.2).

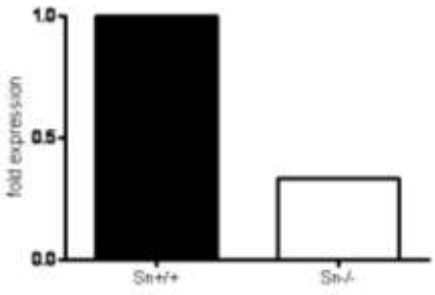

Figure 4.2 Sn expression by RT-PCR on splenic tissues from Sn WT (filled bar) and Sn-deficient (open bar). Sn mRNA expression was normalized for endogenous GAPDH mRNA expression. Fold expression was calculated by setting the value of Sn ΔCt on Sn+/+ sample as 0 and using this value in the equation $2^{-\Delta Ct}$ Sn yielding 1 as maximum expression. The mRNA expression of Sn in Sn-/- was calculated following the formula $2^{Sn-/-\Delta Ct-Sn+/+\Delta Ct}$.

Sn mRNA expression remained detectable in Sn deficient mice albeit to one third of the level in the wild-type mice. This finding was consistent with the literature on Sn deficient mice (Oetke *et al*, 2006). The reason behind this phenomenon is not entirely clear. The generation of Sn deficient mice was achieved by disrupting the Sn gene by insertion of a neomycin cassette into exon III. One might speculate that RNA

transcription of other exons can occur but the resulting mRNA is unstable, degradable and does not translate into protein.

The pre-diseased kidneys from 16 weeks BWF1 and control NZW mice were examined for the expression of Sn and macrophage lineage markers: CD68 (pan-macrophage marker) and F4/80. RT-PCR analysis revealed no statistically significant difference between pre-disease BWF1 and control NZW mice in the mRNA expression of Sn and CD68 (Figure 4.3). Although there was a trend towards a higher mRNA expression of F4/80 in BWF1 mice, but this did not reach statistical significance.

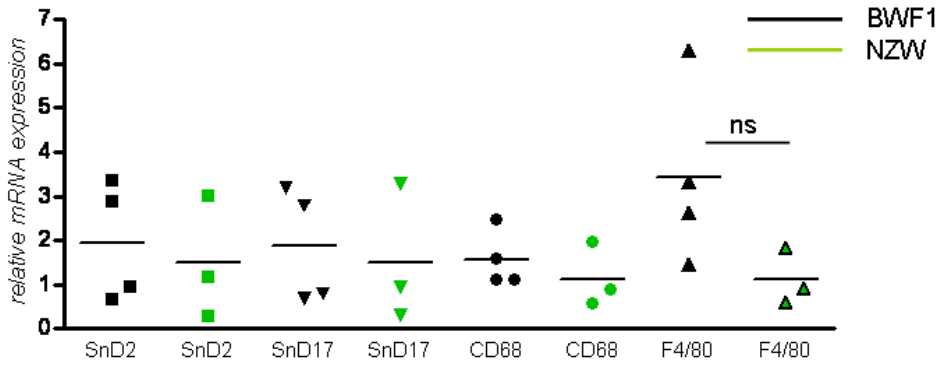

Figure 4.3 Expression of Sn and macrophage markers in pre-diseased kidneys. The expression of Sn and macrophage lineage markers in kidney samples 16 weeks BWF1 mice (n=4) and control NZW mice (n=3). Each dot represents mean of triplicate from an individual mouse. Statistical analysis was done using student's t test.

Mice at 28 weeks of age showed an enhanced mRNA expression of Sn compared to age-matched NZW control mice (Figure 4.4). When the contribution of mice with > grade 2 and < grade 2 of proteinuria were analyzed, it was evident that mice with less than grade 2 of proteinuria did primarily contribute to the difference in Sn mRNA expression between BWF1 and NZW mice (Figure 4.5). These findings were further confirmed by using a different set of primers designed to identify sequences in the extracellular domain 17 of Sn (Figure 4.4). A similar expression pattern was observed for CD68 and F4/80 macrophage markers (Figure 4.4 and 4.5).

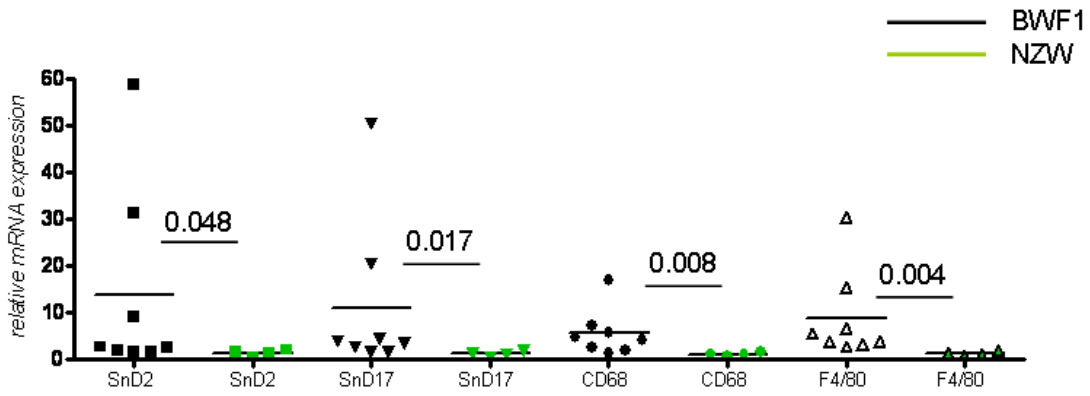

Figure 4.4 The mRNA expression of Sn, CD68 and F4/80 in 28 weeks BWF1 mice (at 28 weeks of age) analyzed by RT-PCR. The BWF1 group (n=8, black symbols) includes all mice with detectable proteinuria, regardless of the grade, at 28 weeks of age. Age matched NZW mice (n=4) appear as green symbols. Each symbol represents an individual mouse. Statistical analysis was done using student's t test. Exact p values of significant differences appear on the small horizontal bar between the groups examined.

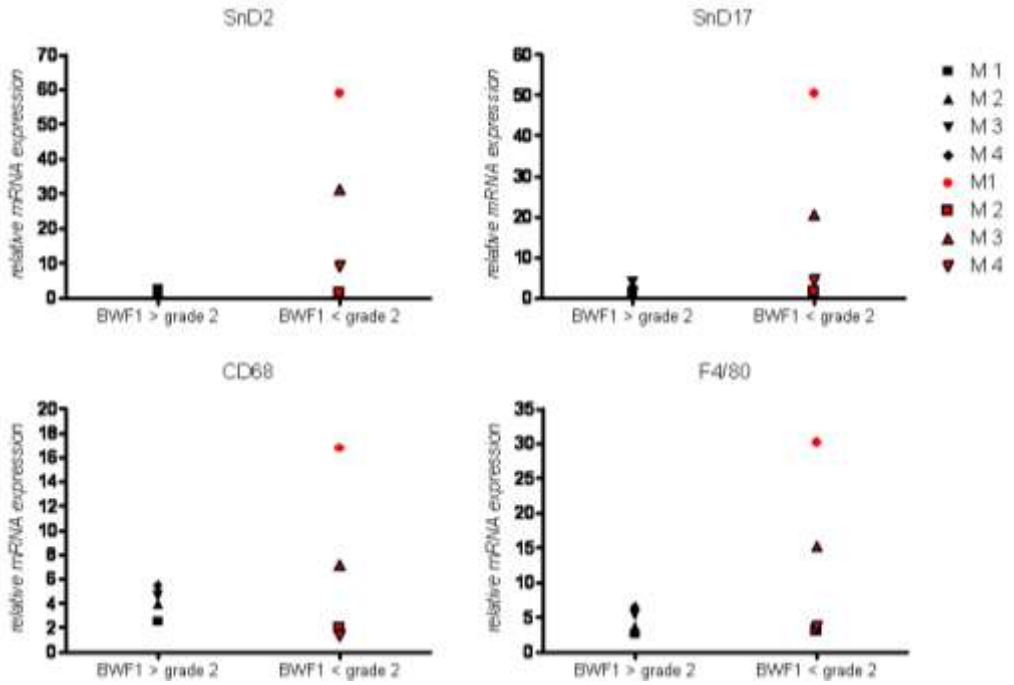

Figure 4.5 The mRNA expression of Sn, CD68 and F4/80 in individual BWF1 mice based on their grade of proteinuria. Mice with > grade 2 (n=4) appear as black symbols and those with < grade 2 (n=4) appear as red symbols.

This pattern of enhanced co-expression of Sn and other macrophage markers suggested a possible influx of macrophages that are positive for Sn into the renal cortical tissues of BWF1 mice. In addition, it appears that the mRNA expression of all

of these markers increased at an early (< grade 2) rather than late (> grade 2) stage of lupus nephritis in diseased BWF1 mice.

The analysis of CD4 and Foxp3 mRNA expression in diseased kidneys revealed that both were significantly up-regulated in lupus nephritis (Figure 4.6). Similar to Sn and other macrophage markers studied, mice with < grade 2 of proteinuria were the main contributors to the enhanced mRNA expression of CD4 and Foxp3 in diseased BWF1 mice compared to NZW controls (Figure 4.7, A). Furthermore, there was a statistically significant fold difference in the mRNA expression of CD4 and Foxp3 in BWF1 mice based on their grade of proteinuria (Figure 4.7, B).

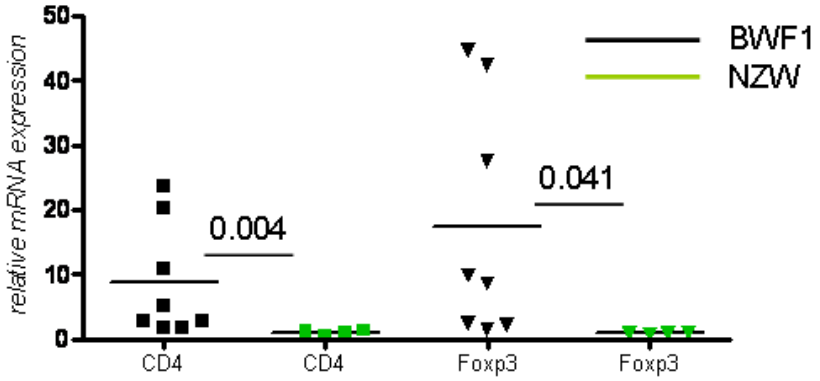

Figure 4.6 CD4 and Foxp3 mRNA expression in BWF1 mice (at 28 weeks of age) by RT-PCR. CD4 and Foxp3 mRNA fold change expression between BWF1 (black symbols) and control NZW mice (green symbols) and according to grade of proteinuria of BWF1 mice. Each dot represents an individual mouse. Statistical analysis was done using student's t test. Exact p values of significant differences appear on the small horizontal bar between the groups examined.

Taken together, these data suggest a difference in the mRNA expression of the markers studied is biased towards the early rather than later stages of lupus nephritis based on the grade of proteinuria.

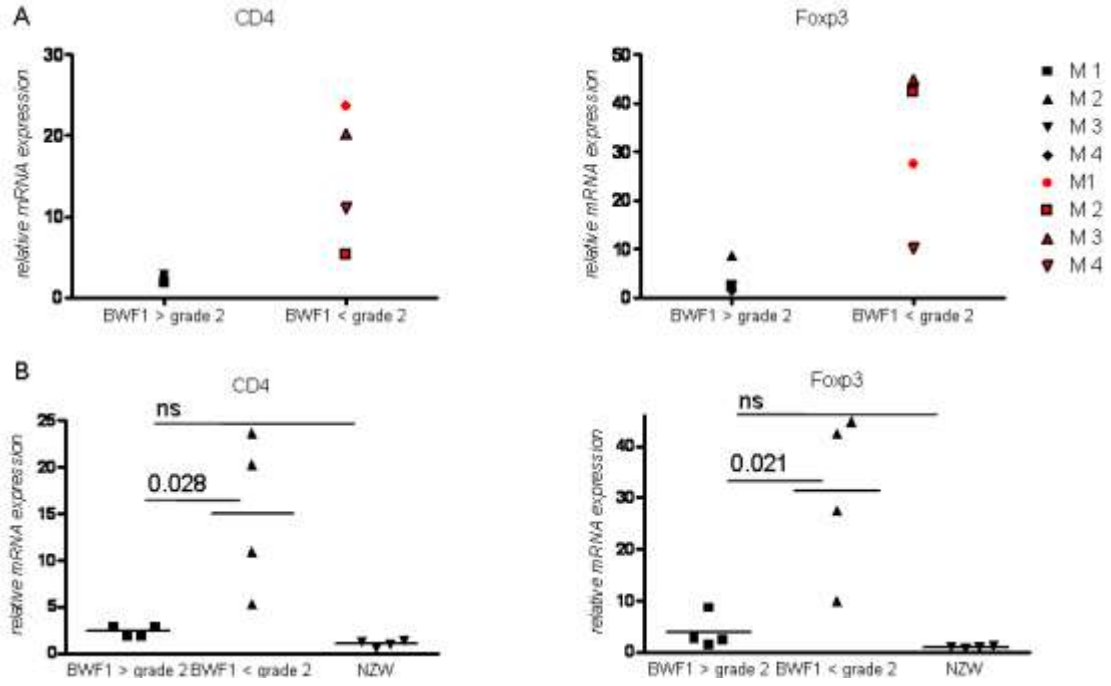

Figure 4.7 The mRNA expression of CD4 and Foxp3 in diseased BWF1 mice based on the degree of proteinuria. A,CD4 (left) and Foxp3 (right) mRNA expression in individual mice. Mice with > grade 2 (n=4) appear as black symbols and those with < grade 2 (n=4) appear as red symbols. Symbols refer to the same individual mice as in Figure 4.5. B, analysis of fold differences of mRNA expression of CD4 and Foxp3 between mice with > grade 2 and < grade 2 of proteinuria and compared to NZW controls. Statistical analysis was done using student's t test. Exact p values of significant differences appear on the small horizontal bar between the groups examined.

4.2.3 Cytokines and nephritis in BWF1 mice

In human SLE, Sn was identified as a biomarker for the "IFN signature" and patients with active disease were found to have increased frequency of circulating Sn+ monocytes (Biesen *et al*, 2008). Increased Sn mRNA expression in renal cortices of diseased BWF1 prompted the study of renal IFNα mRNA expression in the mice. IFNα/β family consists of 14 IFNα/β genes and 3 pseudogenes in the mouse genome (Pesh *et al*, 2004). It remains unclear which IFNα subtype(s) predominate in the pathogenesis of SLE. An alternative way to examine the expression of IFNα is to use surrogate markers for IFNα such as interferon inducible genes

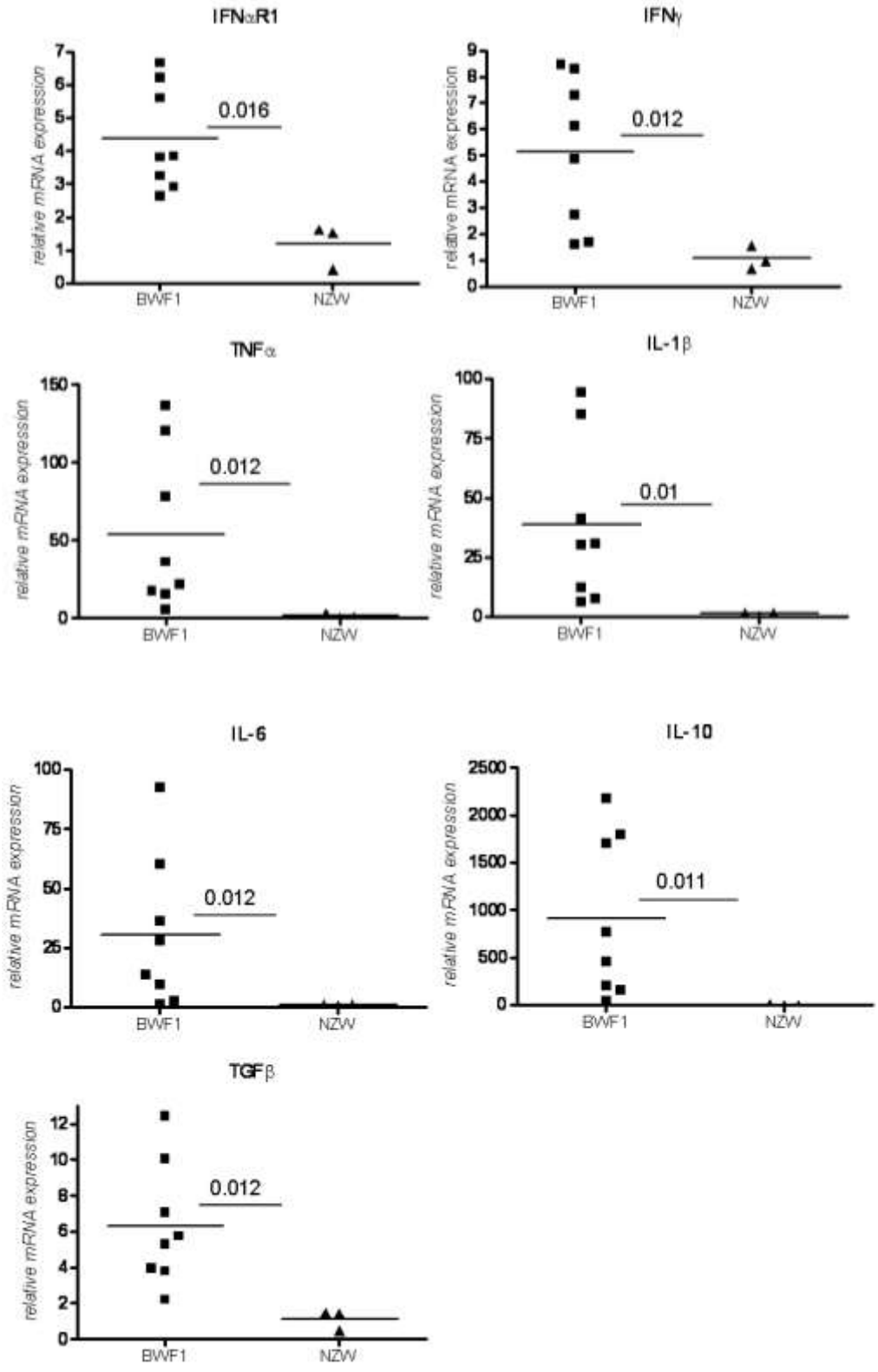

Figure 4.8 The mRNA expression of IFNαR1 and other inflammatory cytokines in diseased BWF1 mice (at 28 weeks of age). The cytokines examined included: IFNγ (top panel, right), TNFα (middle panel, left), IL-1β (middle panel, right), IL-10 (bottom panel, left) and IL-6 (bottom panel, right). Each dot represents an individual mouse. Statistical analysis was done using Student's t test. Exact p values of significant differences appear on the small horizontal bar between the groups examined.

or IFNα receptor (IFNαR). The mRNA expression of domain 1 of the IFNαR (IFNαR1) has been used previously to examine IFNα expression in MRL/lpr model of lupus nephritis (Hadj-Slimane *et al*, 2004). In this analysis, mRNA expression of IFNαR1 was therefore used as surrogate for IFNα expression. There was more than fourfold increase in IFNαR1 mRNA in diseased mice compared to NZW controls (Figure 4.8, top panel). However, there was no significant difference in the mRNA expression of this cytokine between mice based on the grade of proteinuria (Figure 4.9, top panel).

In addition to interferons, other pro-inflammatory cytokines were reported to contribute to the pathogenesis of both murine and human SLE. TNFα and IL-1β are two cytokines that were found to be abundantly expressed in the renal cortices of BWF1 mice (Brennan *et al*, 1989). Macrophages are one of the main sources of production of these two cytokines among other cells. Brennan and colleagues showed that the expression of both cytokines, as evidenced by northern blot analysis, appeared to be enhanced between 3-4 months of age and continues to increase as nephritis ensues. Systemic administration of these two cytokine led to acceleration of nephritis and increased mortality, only if these were given beyond 4 months of age. Early exposure (2-4 months) did not affect disease progression compared to control mice (Brennan *et al*, 1989).

IL-6 has been implicated in the pathogenesis of both murine and human SLE. Elevated levels of IL-6 were found in the glomeruli of patients with lupus nephritis (Iwano *et al*, 1993). Similarly, elevated IL-6 mRNA was found in PBMCs from active SLE patients (Linker-Israeli *et al*, 1991). In addition, *in vitro* proliferation and IgG production of B cells from SLE patients were shown to be positively regulated by IL-6 (Kitani *et al*, 1992). Moreover, anti-IL-6 monoclonal antibody treatment of BWF1 mice was associated with delayed disease onset and severity (Finck *et al*, 1994). Interestingly, IFNα administration to BWF1 mice was recently shown to be associated with increased serum levels of IL-6 (Liu *et al*, 2011).

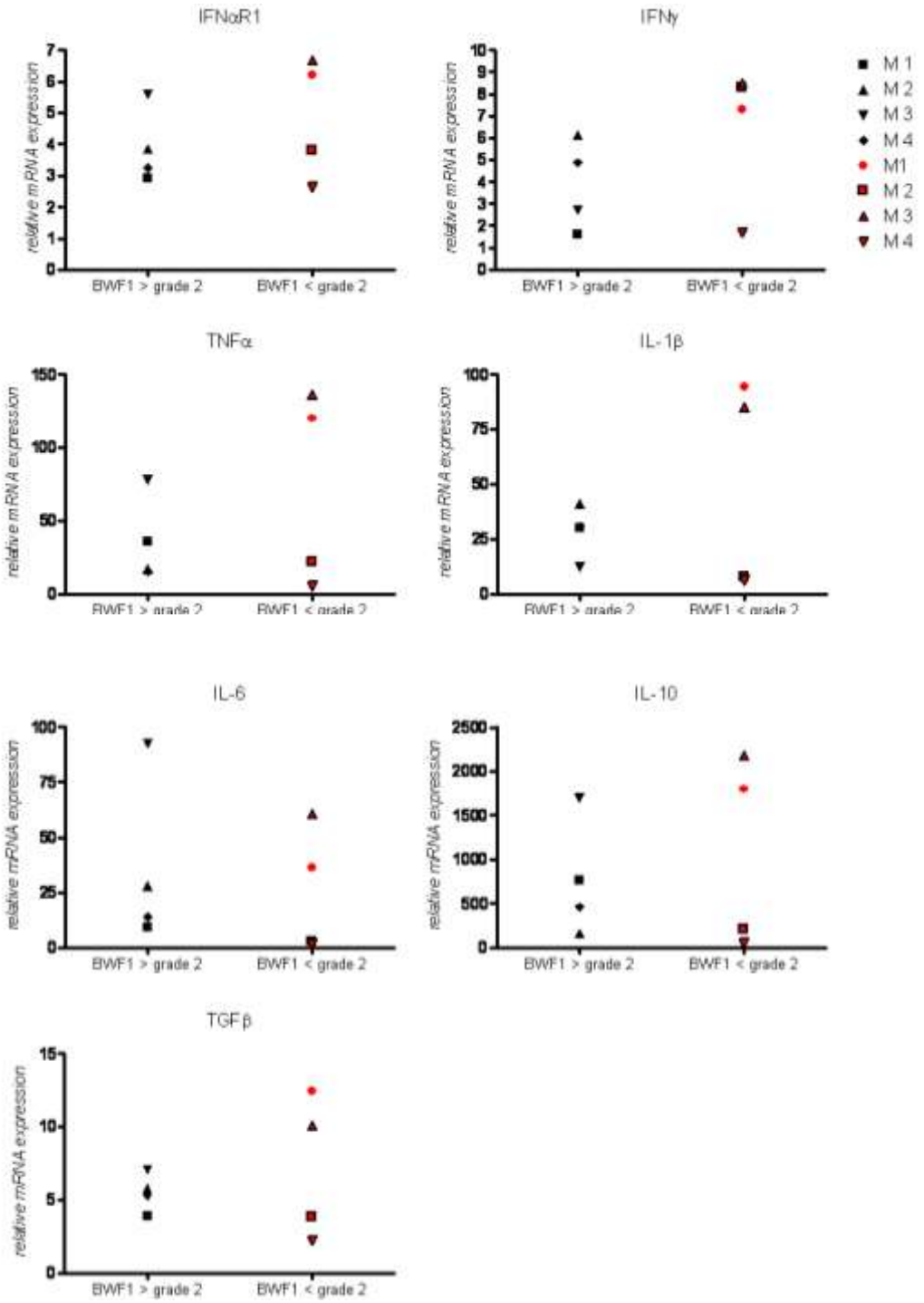

Figure 4.9 The mRNA expression of IFNαR1, IFNγ, TNFα, IL-1β, IL-10, IL-6 and TGFβ in individual BWF1 mice based on their grade of proteinuria. Mice with > grade 2 (n=4) appear as black symbols and those with < grade 2 (n=4) appear as red symbols.

IL-10 is an important immunoregulatory cytokine with pleiotropic and sometimes contrasting biological functions. IL-10 can down-regulate the production of pro-inflammatory cytokines by activated T cells. In addition, the cytokine can negatively regulate the expression of MHC class II and B7 family of co-stimulatory molecules on

APCs (Lopez *et al*, 2010). In contrast, IL-10 can also promote B cell proliferation and antibody production *in vitro* (Rousset *et al*, 1992). While administration of IL-10 to BWF1 mice at the age of 4 months was found to be associated with accelerated disease and poor survival, long-term anti-IL10 treatment was associated with a significant reduction in autoantibody production, disease severity and favourable survival (Ishida *et al*, 1994).

4.2.4 Assessment of renal disease in BWF1 mice

In order to confirm the disease severity in kidneys from mice included in the RT-PCR analysis, paraffin embedded renal sections were stained with H&E and Masson's trichrome stain and examined by microscopy. The latter stain was employed to assess the degree of fibrosis in diseased kidneys. The severity of disease was assessed using a scoring system that includes: glomerular hypercellularity, tubular pathology (tubular atrophy and dilatation) and perivascular infiltration (Figure 4.10).

The degree of glomerular hypercellularity was in line with the state of proteinuria and anti-dsDNA titres. Mice with high grade proteinuria displayed increased percentage of hypercellular glomeruli (Figure 4.10, C and D and Figure 4.11). Tubular damage was assessed by calculating the percentage of tubules showing thinning of the epithelium and /or dilatation (Figure 4.10, E). A total of 200 tubules were examined per sample. As expected, the frequency of tubular damage was higher in the group of mice with more than grade 2 of proteinuria compared to NZW control mice (Figure 4.11). No significant difference in tubular pathology was observed between low and high grade proteinuria mice. This can be explained by the fact that, generally, the extent of tubular damage and fibrosis was not high, due to the fact that these mice were still not old enough to have features of advanced renal failure. Perivascular infiltration was scored based on the number of cellular layers, and circumference distribution, surrounding arterial blood vessels (Figure 4.10, F). Increased perivascular infiltration was noted in the mice with more than grade two proteinuria compared to NZW control mice (Figure 4.11). Similar

to tubular pathology, no difference between mice with low and high grade of proteinuria was detected.

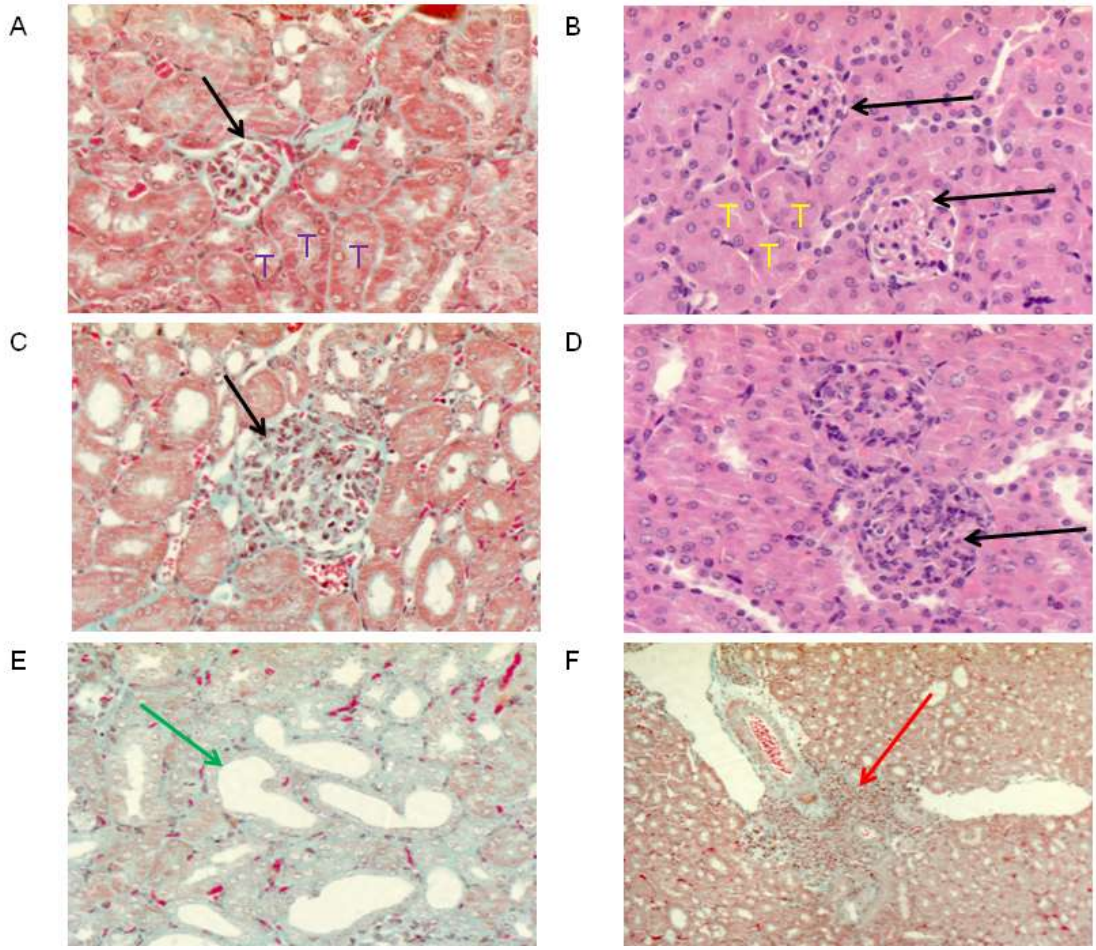

Figure 4.10 Glomerulonephritis scoring system. A and B, normal glomerular (black arrows) and tubular (T letters) histology in a paraffin-embedded section from a NZW mouse (28 weeks) stained with Masson's trichrome and H&E respectively. The cell count in the glomerular cross section is less than 30 (cells). The tubules surrounding the glomerulus are packed together and display a 'back-to-back' appearance i.e. no spaces can be identified between the tubules. In addition, there is no evidence of dilatation or loss of height in the tubular epithelium. C, glomerular hypercellularity in a renal section from a BWF1 mouse (28 weeks) with < grade 2 of proteinuria. Note the increased number of cells and the overlapping pattern of the nuclei (black arrow). D, hypercellular glomerulus (black arrow) in a renal section stained with H&E. E, marked tubular dilatation and thinning of the tubular epithelium (green arrow) in a renal section from a BWF1 mouse (28 weeks) with > grade 2 of proteinuria, staining was done with Masson's trichrome stain. Note that the tubules are now more separated and have lost their normal 'back-to-back' appearance. F, perivascular infiltration in a renal section from a BWF1 mouse (28 weeks) with > 2 of proteinuria with an artery surrounded by multiple layers of cellular infiltrate enveloping less than 50% of the artery's diameter.

Collectively, these findings suggested a correlation between the grade of proteinuria and the degree of glomerular hypercellularity but not with tubular or perivascular parameters of disease severity.

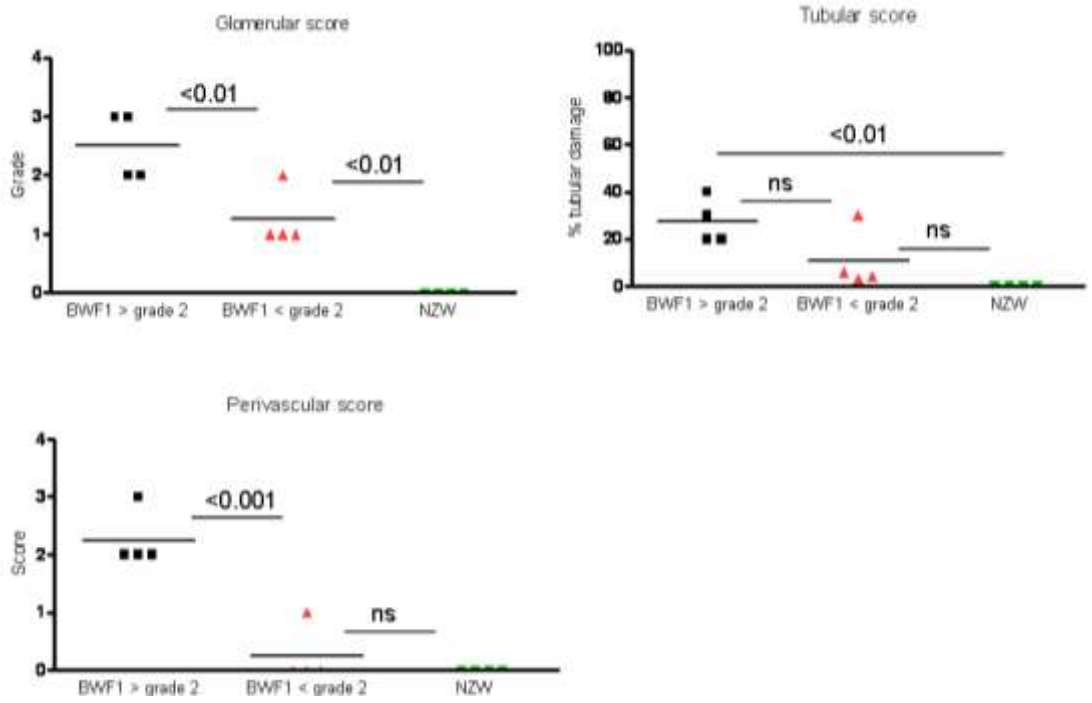

Figure 4.11 Renal histology scoring of diseased BWF1 and control NZW mice. Histology scoring in BWF1 mice was stratified based on the degree of proteinuria. The severity of disease was scored as explained in the Materials and Methods. Statistical analysis was done using student's t test, when significant exact p values are depicted above horizontal bars.

4.3 The effect of administering anti-Sn monoclonal antibodies on lupus nephritis in BWF1 mice

4.3.1 Introduction

The above RT-PCR data revealed an enhanced expression of Sn (and other macrophage markers) at the onset of disease in BWF1 mice. To evaluate the contribution of Sn to lupus nephritis in BWF1 mice, anti-Sn antibodies were administered weekly from 10 weeks of age for 6 weeks (Diagram 4.1). A total of 21 age matched female BWF1 mice were divided into three treatment groups. The first

group (n=8) received rat anti-Sn blocking antibodies (SER4 and 3D6 at 1:1 ratio) at 100µg total in 200µl PBS/mouse/week. The second group (n=8) received 100µg in 200µl PBS/mouse/week of rat IgG2a isotype control. The third group (n=5) received 200µl PBS/mouse/week.

Disease monitoring started at the age of 12 weeks with monitoring proteinuria levels in a spot urine sample on a weekly basis. In addition, body weight was monitored on a weekly basis. A spot urine sample was considered positive when more than 100mg/dl (++) of protein was detected on two consecutive occasions. The end point of the experiment was defined as any of these groups having more than 50% of the mice with >100mg/dl of proteinuria.

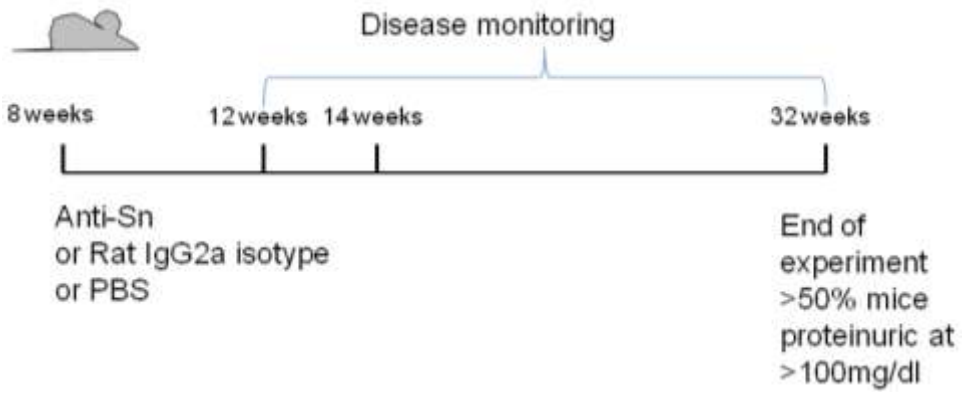

Diagram 4.1 Administration of anti-Sn antibodies to BWF1 mice.

4.3.2 Anti-Sn antibodies

SER4 and 3D6 are two monoclonal rat IgG2a antibodies directed against two different epitopes of Sn. SER-4 recognises domains 2 and/or 3 and 3D6 recognises domain 1 of the molecule (Crocker *et al*, 1994). Prior to in vivo blocking experiments in BWF1 mice, the inhibitory capacity of these monoclonal antibodies was evaluated. This was done by ELISA analysis of human RBC binding to SnFc protein immobilized to plastic in the presence of each or combination of both monoclonal antibodies (Figure 4.12). Consistent with previous observations, incubation with either 3D6 or SER-4 had a

partial inhibitory effect on RBC binding. However, when they were combined a synergistic inhibition on RBC binding to immobilized SnFc was noted.

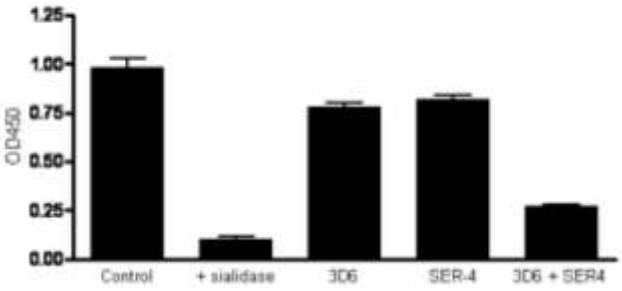

Figure 4.12 The inhibitory effect of anti-Sn antibodies on SnFc binding to human RBCs. SnFc protein was immobilized in flat bottom 96-well plate. Human RBCs were either treated with sialidase (negative control) or left untreated (positive control) prior to incubation with immobilized SnFc. Monoclonal antibodies 3D6 and SER-4 were either incubated alone or in combination with immobilized SnFc prior to the addition of human RBCs. Data represent mean + SEM of quadruples for each condition.

4.3.3 Disease onset following anti-Sn treatment

All three mice groups were monitored weekly for proteinuria which heralds the onset of lupus nephritis. Isotype control antibody mice started to develop significant proteinuria at the age of 23 weeks (Figure 4.13). Although the onset of proteinuria in mice treated with anti-Sn

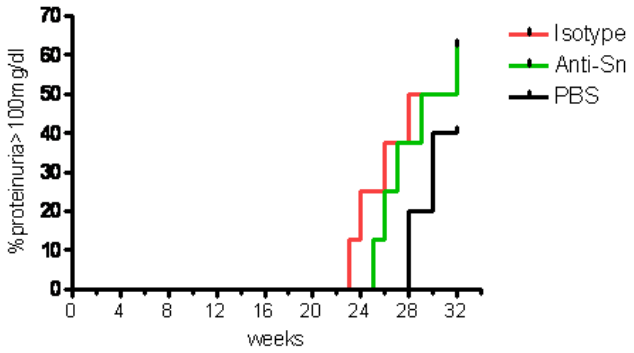

Figure 4.13 Development of proteinuria in BWF1 mice treated with anti-Sn antibodies. Three groups of mice received weekly anti-Sn antibodies, isotype control antibody or PBS for 6 weeks from 8 weeks of age. Urinary protein excretion was measured weekly with Uristix from 12 weeks of age. Data show the proportion of mice with more than 100mg/dl of proteinuria.

was delayed by two weeks from the isotype control group, a higher percentage of mice was proteinuric by 32 weeks of age (4/8 versus 5/8). In contrast, mice that received PBS only started to develop proteinuria at 28 weeks of age and only 2 out of 5 mice were proteinuric by the age of 32 weeks.

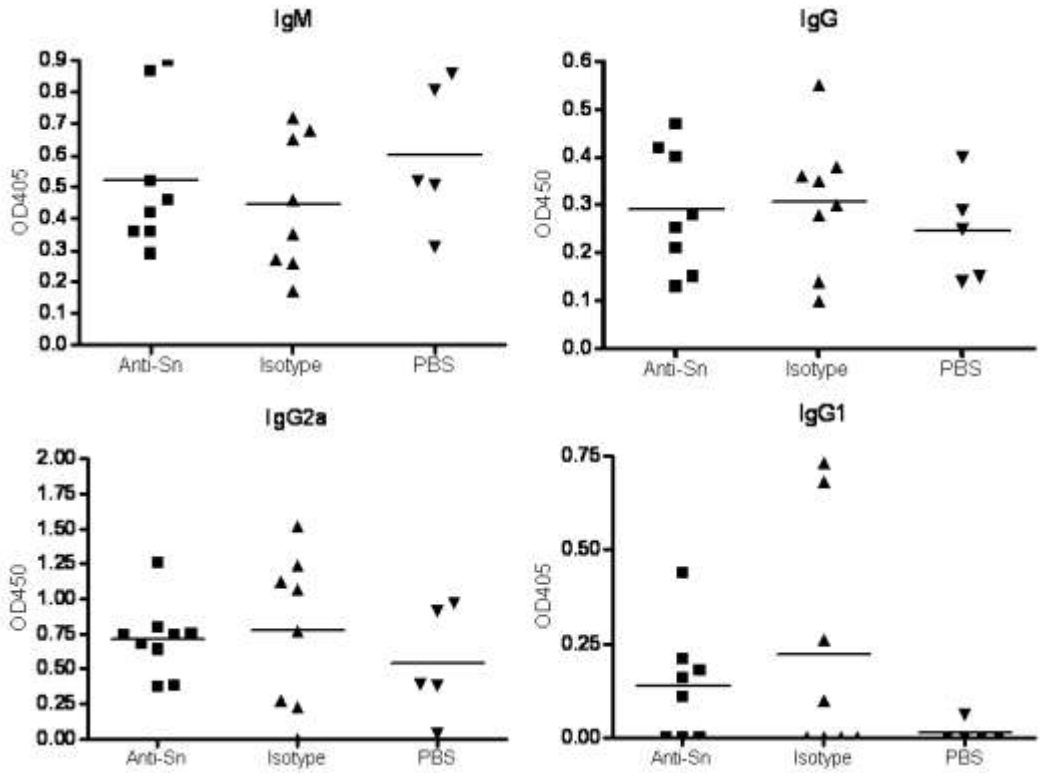

Figure 4.14 Autoantibodies production in anti-Sn treated BWF1 mice. Sera collected from anti-Sn (n=8), isotype control (n=8) and PBS (n=5) treated mice at 32 weeks of age. Samples were examined for content of IgM,IgG, IgG2a and IgG1 anti-dsDNA using an ELISA as described in Materials and Methods. Statistical analysis was done with One-way ANOVA test with Bonferroni post-test.

In order to assess the impact of administering anti-Sn antibodies on the production of autoantibodies by BWF1 mice, sera were collected from mice in all three groups and examined for anti-dsDNA titres (Figure 4.14). No significant differences were observed in the levels of IgM, IgG, IgG2a and IgG1 anti-dsDNA in all groups. These data suggest that blocking Sn at an early pre-nephritic stage of the disease does not influence the development of anti-dsDNA titres. In addition, these data indicate that the small difference observed in the onset of the disease between anti-Sn and isotype control

groups was not reflecting a difference in disease severity as evidenced by levels of anti-dsDNA titres.

4.3.3 Increased percentage of Tregs in diseased mice treated with anti-Sn antibodies

In order to examine whether early blocking Sn in BWF1 mice would influence Treg frequency, the percentage of Tregs in the spleens of all mice (diseased and non-diseased) in all treatment groups were analysed by flow cytometry. Tregs were identified with combined CD4 surface labelling and intracellular staining for Foxp3 (Figure 4.16, A).

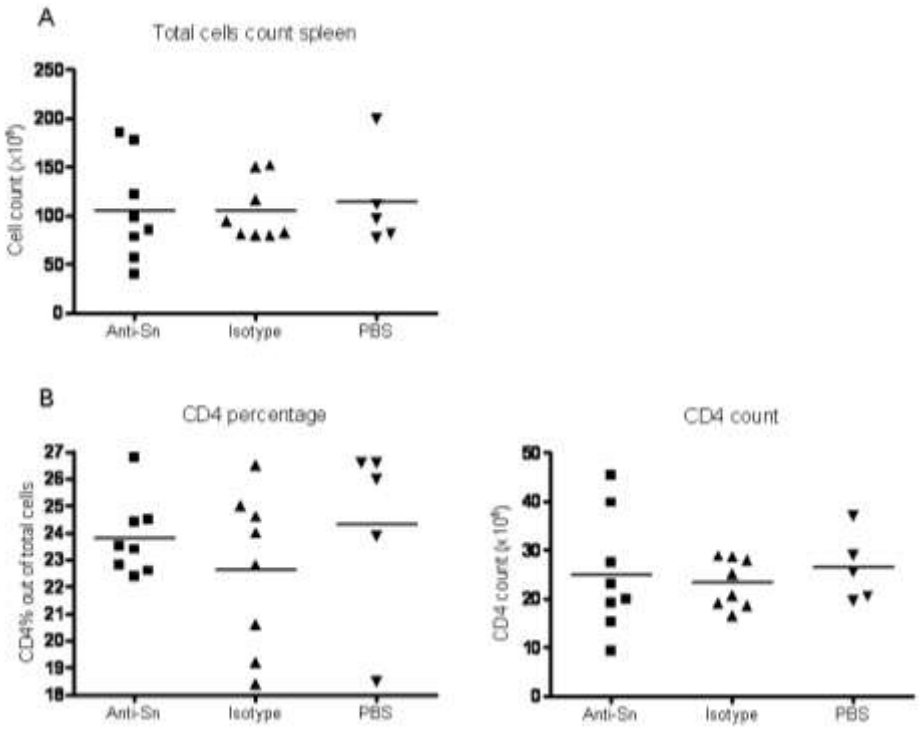

Figure 4.15 Total splenocyte count and CD4 T cell frequency in all mice included in the study. A, total splenocytes were counted, following RBC lysis, from each mouse. Each dot represents splenocyte count from one mouse. B, CD4 percentage out of total splenocytes (left) and CD4 counts (right) as calculated from CD4 percentage and the total number of splenocytes. Statistical analysis was done using one-way ANOVA with Bonferroni post test.

There were no significant differences in the total splenocyte count between the three groups of mice (Figure 4.15, A). Similarly, evaluation of the percentage and number of CD4 cells was not altered between the three groups (Figure 4.15, B). Interestingly,

mice in the anti-Sn treated groups showed a higher percentage of Tregs compared to the isotype control group (Figure 4.16). However, there was no difference in the percentage of Tregs between the anti-Sn and PBS group. In addition, there was no difference in the number of Tregs between mice in all three groups.

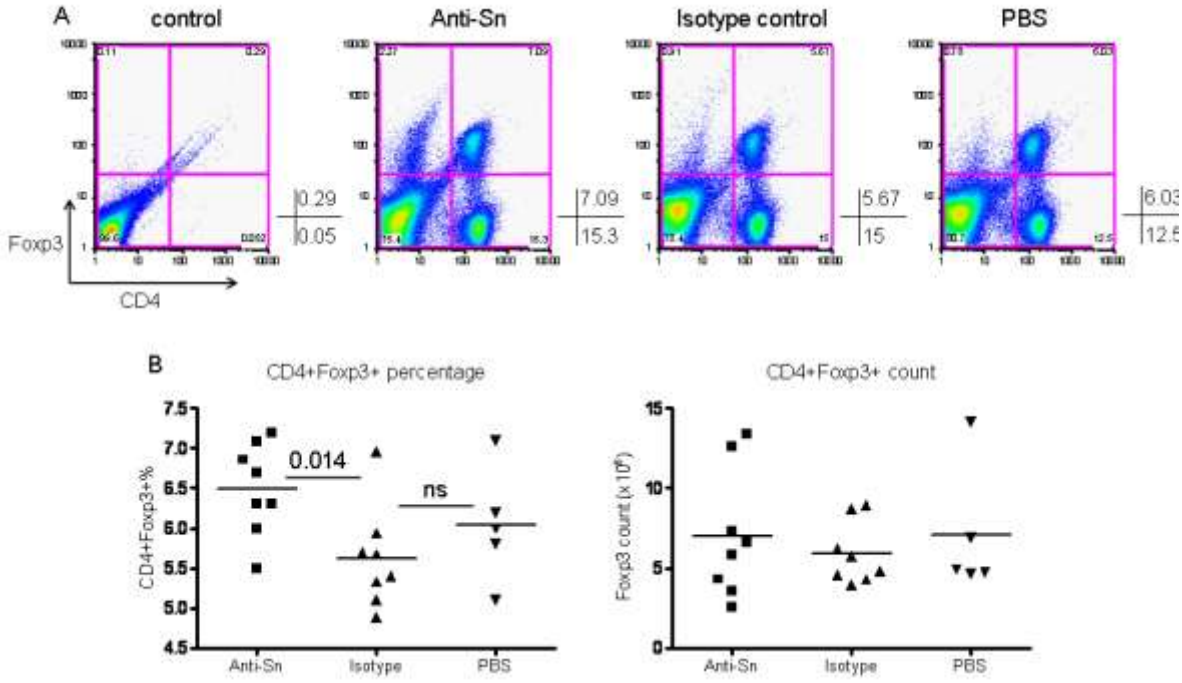

Figure 4.16 Frequency of Tregs in splenocytes of mice from all treatment groups. Splenocytes were surface-labelled for CD4 and stained for intracellular Foxp3, as explained in Materials and Methods. A, flow cytomtery dot plots of splenocytes from anti-Sn, isotype control and PBS mice (one mouse per group), compared to splenocytes stained with isotype antibodies for CD4 and Foxp3. B, analysis of the percentage (left) and number (right) of Tregs in all mice included in the experiment. Each dot represents an individual mouse. Statistical analysis was done using one-way ANOVA with Bonferroni post-test. Exact p value, when significant, is depicted above horizontal line between compared groups.

4.3.4 The frequency of SnL+Teffs correlates with proteinuria

The data on the characterisation of SnL on CD4+ T cells were indicative of high state of activated/effector profile on SnL+Teffs following TCR ligation *in vitro*. Whether increased prevalence of SnL+Teffs is related to proteinuria as a hallmark of the disease is unknown. First the expression of SnL on Tregs and Teffs in all mice was

examined. Consistent with the in vitro data, Tregs displayed higher expression of SnL compared to Teffs (Figure 4.17, A and B). The frequency of splenic SnL+Teffs was highly variable among these mice (ranging between 1 to more than 10%). The frequencies of SnL+Tregs and SnL+Teffs were analysed in view of state of proteinuria i.e. proteinuria versus non proteinuric. This analysis showed a differential increase in SnL+Teffs but not SnL+Tregs in all proteinuric mice (Figure 4.17, B).

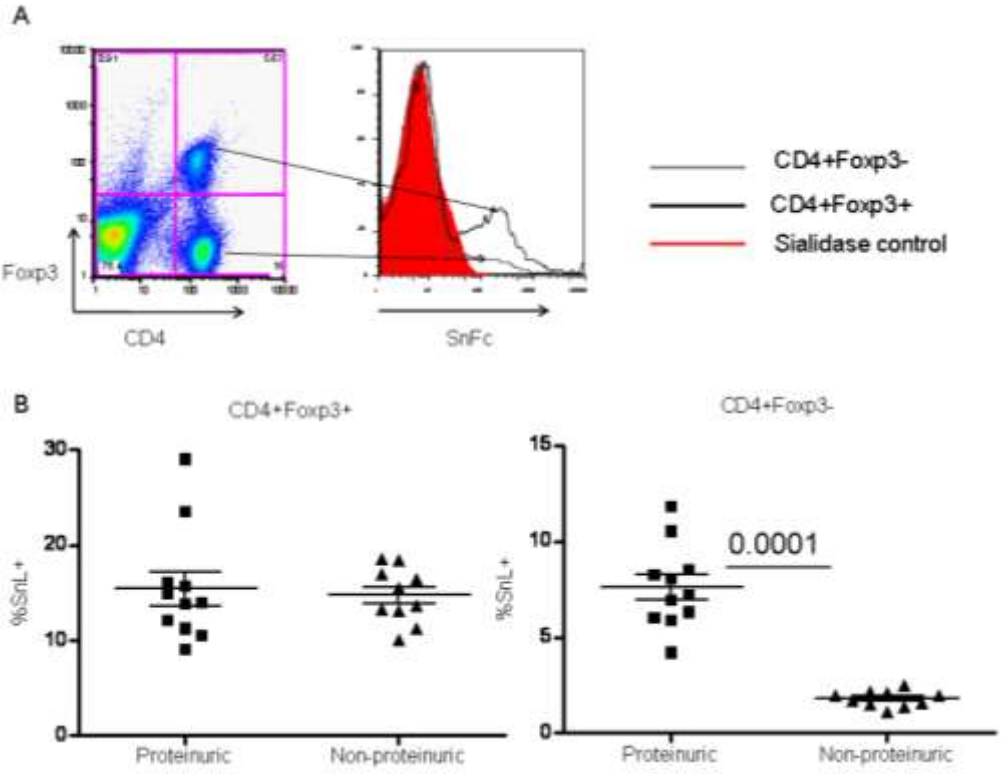

Figure 4.17 SnL+ Tregs and Teffs and correlation with proteinuria. A, left, dot plot of CD4+Foxp3+ (Tregs) and CD4+Foxp3- (Teffs) in splenocytes from an isotype control mouse. A, right, histograms of SnL expression on Tregs (black histogram) and Teffs (grey histogram), compared to sialidase treated splenocytes as a negative control (filled red histogram).B, correlation between, SnL+Tregs and proteinuria (left) and SnL+Teffs and proteinuria (right). Statistical analysis was done using student's t test. Exact p value, when significant, is depicted above horizontal line between compared groups.

4.3.5 Assessment of renal disease

Parrafin embedded renal sections from formalin-fixed left kidneys of all mice were examined for severity of lupus nephritis using H&E and Masson's trichrome stains.

Glomerular hypercellularity and glomerular wall thickening were observed in the majority of mice across the three groups. Interestingly, diseased mice from anti-Sn group showed a higher tendency for extra-capillary proliferation (Figure 4.18). The latter refers to proliferation occurring outside the capillaries of the glomerulus but within the Bowman space (Figure 4.18). This pattern of proliferation leads to the formation of a 'crescent' which could be either cellular (active), fibrous (chronic), or fibrocellular. Extra-capillary proliferation often indicates a more aggressive from of nephritis. The number of mice with crescentic glomeruli was: 4/8 in anti-Sn; 2/8 in isotype antibody control and 2/5 in the PBS groups. This pattern was suggestive for aggressive disease in this group compared to isotype antibody control and PBS groups. However, the glomerular scores were not statistically different among the three groups of mice (Figure 4.19).

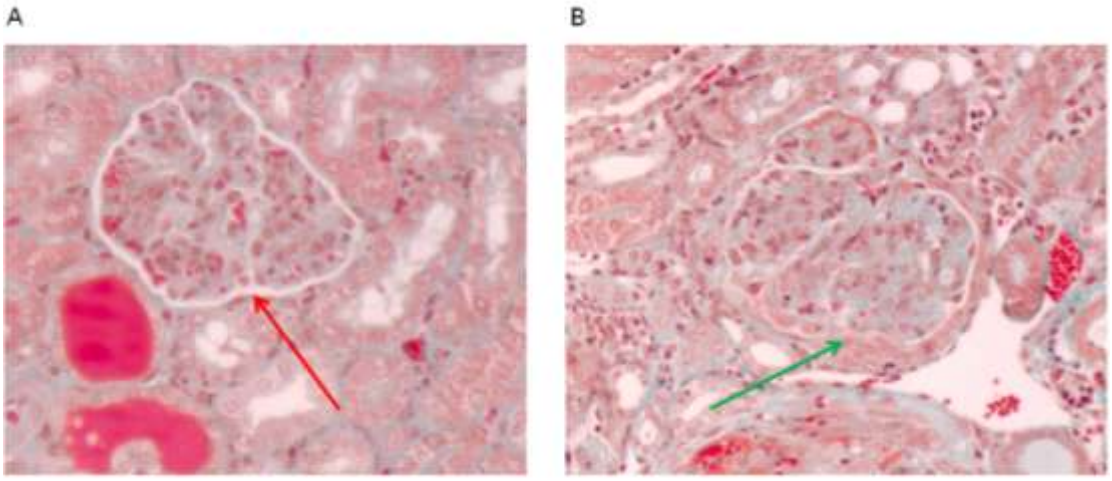

Figure 4.18 Endo- and extra-capillary proliferation patterns. A, endo-capillary proliferation pattern: in proliferation (hypercellularity) remains confined to the capillaries of the glomerulus of an isotype control-treated mouse. Note the Bowman space (red arrow) surrounding the capillaries are devoid of proliferation. B,extra-capillary (crescentic) proliferation pattern in a glomerulus from an anti-Sn-treated mouse. In addition to increased endo-capillary proliferative changes there is a significant proliferation occurring in the Bowman space, leading to a crescent formation (green arrow).

Tubular atrophy, dilatation and cell necrosis are all features of tubular damage and disease chronicity. The analysis of the percentage of damaged tubules (out of 200) revealed increased tubular damage and fibrosis in the anti-Sn group (Figure 4.19, B).

At least 3 kidney sections from three of these mice were showing evidence of more than 40% tubular injury and fibrosis. Only one sample from each of the other two treatment groups revealed a similar degree of tubular pathology. As for perivascular inflammation, the number of mice with high degree of perivascular infiltration was consistently predominant in the group that received anti-Sn antibodies (Figure 4.19, C). Together these data revealed that systemic administration of anti-Sn antibodies between 8 and 14 weeks of age might worsen lupus nephritis compared to isotype antibody and PBS controls.

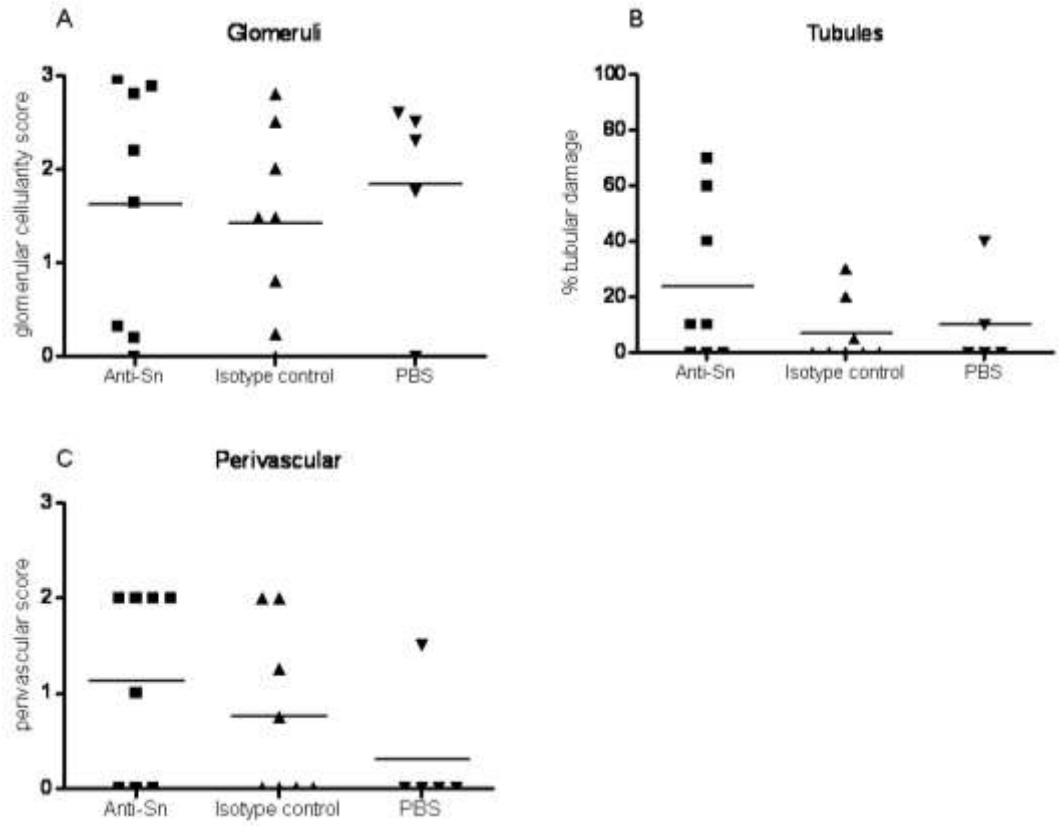

Figure 4.19 Renal histology scoring of BWF1 mice in all three groups. A, glomerular score, B, tubular score and C, perivascular infiltration were scored as explained Materials and Methods. Statistical analysis was done using one-way ANOVA with Bonferroni post-test.

4.4 SLE in Sn-/- BWF1 mice

4.4.1 Generation of Sn-/-BWF1 mice

Sn-/-BWF1 mice were generated using speed congenics. In this strategy, parallel breeding lines of Sn heterozygous NZB and NZW mice were employed to introgress a pre-defined set of SLE susceptibility loci into each of these two backgrounds. Sn heterozygous NZB or NZW mice were then intercrossed to generate Sn deficient NZB and NZW mice. Finally, Sn-/- BWF1 mice were generated by crossing female Sn deficient or heterozygous NZB with male Sn deficient or heterozygous NZW mice. Below is a detailed description of these phases of generating Sn-/- BWF1 mice with particular attention to factors that can affect a successful implementation of speed congenics in a polygenic disease such as SLE.

1. Generation of Sn+/- NZB and NZW mice: The aim of the first round of mating was to generate Sn+/- mice by crossing parental Sn-/- C57BL/6 male and NZB or NZW female mice. The mice generated in this initial round were not screened with microsatellite markers for the pre-defined set of susceptibility loci. Sn+/- male mice (11 in NZB and 8 in NZW breeding line) were then backcrossed to female NZB or NZW mice to introgress further susceptibility loci in the recipient mice genome. The progeny (N2) of the NZB line had 123 mice (8 dead pups) with 73 male mice. Of these male mice, 32 were Sn+/-. Statistically, the higher number of male carriers in each generation results in having not only a higher probability of having more than one best male but also having a greater reduction in donor/recipient genome. Consequently, there were three best male(s) harbouring 18/20 loci (90% of total loci). On the other hand, the total N2 progeny of NZW breeding line was 67 (5 dead pups) with 43 total males.

Among these, 16 males were Sn+/- with only one male achieving 15/25 loci (60% of total loci).

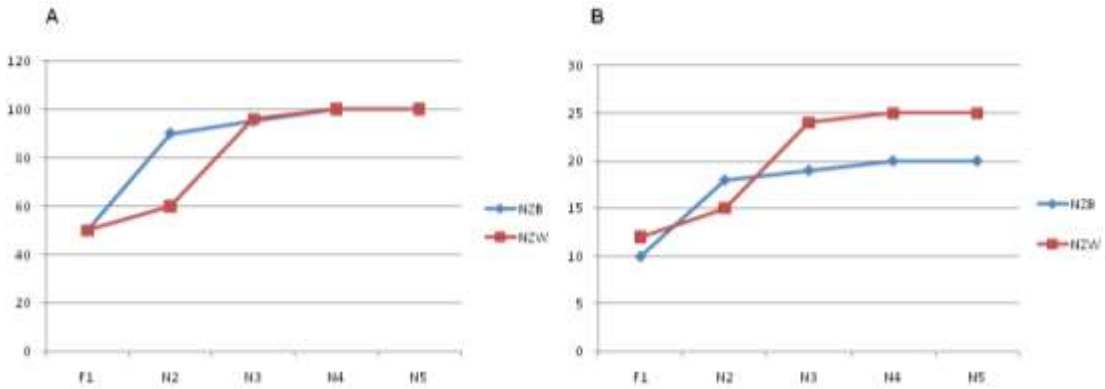

Figure 4.20 Frequency of susceptibility loci introgression in the best male genome in each generation. A, Percentage and B, frequency of introgressed loci per generation out of total required. F1 generation were presumed (based on Mendelian ratios) to have 50% genomic contributions from each parental mice. The number of introgressed loci in each generation is depicted. Both NZB (blue line) and NZW (red line) breeding lines reached 'full-house' set of loci by N4. An extra round of breeding was carried out to ensure introgression and increase future parental mice numbers.

In the third round of matings, 'best male(s)' (3 for NZB line and 1 for NZW line) from N2 were backcrossed to parental NZB or NZW female mice. In N3, the progeny for NZB line were 48 mice (14 dead pups) with 13 total males. There were 6 heterozygous male carriers for Sn gene with only one locus gain in four of them, compared to the previous round. In contrast, the NZW line had a progeny of 43 (4 dead pups) mice with 30 males. Half of these males were Sn+/- with 4 males carrying 24/25 (96%) of total loci. Therefore, in this round there was a reduction of donor/recipient segment of the best male(s) in the NZW breeding line that was again due to the relatively higher number of carrier male(s).

The fourth round of matings achieved the target number of susceptibility loci in both breeding lines. The NZB progeny were 86 mice (19 dead pups) with 24 males, 12 of which were Sn+/- and six of these had the full set of NZB susceptibility loci. In addition, there were four female carriers with full-house set

of loci. As for the NZW line, 72 mice were born (6 died) with 36 males and 21 of them were Sn+/-. In the later group only one male had the full set of NZW loci and a further 14 males were carrying 24/25 of the loci. Furthermore, there were 4 female Sn+/- mice with full set of loci.

At this stage of breeding, an additional round of backcrossing was done to increase the number of male and female Sn+/- carrying all the required NZB and NZW lupus-susceptibility loci. In N5, the number of NZW best males went up to 4 with another 3 'best' females. Expectedly, the number of the NZB 'best' males and females were much higher, 16 and 17 respectively.

1. Generation of Sn+/+ and Sn-/- NZB and NZW mice: Intercross matings of male and female Sn+/- NZB or NZW with full set of loci were carried out. This phase of breeding strategy was repeated to increase the frequency of Sn+/+ and Sn-/- on each line. In addition, Sn+/- mice (50% frequency per progeny) as parental mice to continue the breeding lines.

2. Generation of Sn+/+ and Sn-/- BWF1 mice: Male NZW and female NZB mice from the progeny of Sn+/- intercrosses were used to generate BWF1 mice. The frequency of male NZW was a limiting factor in these breedings. The first round of these matings were carried out using the available 2 male Sn-/- NZW mice.

4.4.2 Increased early post-natal mortality in BWF1 progeny from Sn-/- parental NZB and NZW mice

To further explore the role of Sn in murine SLE, Sn deficient BWF1 mice were generated using speed congenics strategy (see Materials and Methods). In this protocol, parallel lines of Sn+/- NZB and NZW mice were generated by repeated backcrossings of best male Sn+/- (harbouring the highest number of a pre-defined set of susceptibility loci, see Introduction chapter) mice to NZB and NZW strains. In total,

four rounds of backcrossings were required to achieve this goal. An extra round was performed to ensure having parental mice harbouring a full-set of loci.

Generation of Sn+/+ and Sn-/- BWF1 mice: Male NZW and female NZB mice from the progeny of Sn+/- intercrosses were used to generate BWF1 mice. Similar numbers of breeding sets were used for each genotype. However, the frequency of male Sn-/- NZW was a limiting factor in these crosses. Consequently, these mice were used in more than one set of breeding. The first round of these matings was carried out using the two available male Sn-/- NZW mice in 3 sets of matings. There was a marked reduction in the viability and frequency of the Sn-/-BWF1 mice compared to Sn+/+ BWF1 mice (Figure 4.21, A). This phenomenon has not been observed previously in our lab with the generation of Sn-/- on both C57B/L6 and BALBc backgrounds, compared to Sn+/+ mice. Furthermore, Sn-/- C57B/L6 mice were not shown to display an adverse phenotype (Oetke et al, 2006).

As it wasn't clear whether maternal or foetal factors accounted for early postnatal mortality in the Sn deficient crosses, additional Sn+/- NZW and NZB mice were used in the second round. Two sets of crosses were used per genotype. A similar pattern of reduced viability and small litter size was observed in the Sn deficient groups (Figure 4.21, B). However, viability was dramatically increased with the use of heterozygous mice. In addition, the distribution of Sn+/+ and Sn-/- pups in the progeny of the heterozygous mice was the same, suggesting that maternal NZB Sn deficiency rather than foetal lethality could have contributed to the early postnatal mortality observed with using Sn deficient parental mice.

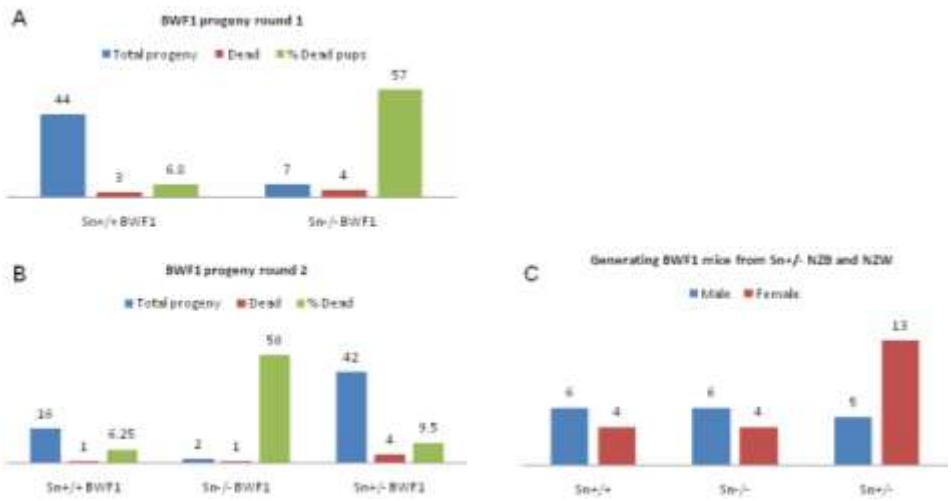

Figure 4.21 Generation of Sn deficient BWF1 mice. A, the outcomes of the first round of breeding based on Sn genotype. Progeny numbers are total of three sets of crosses per genotype. B, Second round of breeding using Sn+/+ (2 sets), Sn-/- (2 sets) and Sn+/- (3 sets) parental mice. Blue bars represent total number of progeny for each genotype, red bars represent the number of dead pups out of total progeny and green bars represent the percentage of dead pups for each genotype. C, the distribution of Sn+/+, Sn-/- and Sn+/- in the progeny of Sn+/- parental mice. Blue and red bars represent male and female gender, respectively.

4.4.3 Sn deficiency is associated with early onset disease

The effect of Sn deficiency in BWF1 mice was examined in a cohort of 8 female mice including: 4 Sn+/+ and 4 Sn-/- . These mice were included in an early pre-nephritic time point (18 weeks of age) analysis when all mice were culled. Disease monitoring was started from 12 weeks of age with semi-quantitative measurement of proteinuria on a spot urine sample on a weekly basis. Surprisingly, one Sn-/- mouse had two consecutive positive results of ++ (100mg/dl) proteinuria, by the age of 16 weeks. Proteinuria continued to be positive and by the age of 18 weeks there were two sequential readings of +++ (300mg/dl) of proteinuria. The rest of the cohort continued to be negative for proteinuria. Developing significant proteinuria at this early time-point was unexpected, especially as BWF1 mice usually start to become nephritic at 24 weeks of age.

To further investigate the differences in proteinuria between Sn+/+ and Sn-/- mice, serum levels of anti-dsDNA were examined (Figure 4.22). There was no statistical

difference in serum IgM, IgG, IgG1 and IgG2a anti-dsDNA between Sn sufficient and deficient groups. As expected, the individual high readings of anti-dsDNA titres corresponded to the Sn deficient mouse which developed an early onset significant proteinuria.

4.4.4 Treg frequency in Sn deficient BWF1 mice

Previously, induction of EAE in Sn deficient mice was found to be associated with reduced disease severity which correlated to an increase in Tregs in CNS and peripheral lymphoid tissues (Wu *et al*, 2009). I showed that there is no difference in Tregs frequency under homeostatic conditions (Figure 4.23). These findings suggest a regulatory role for Sn under inflammatory conditions.

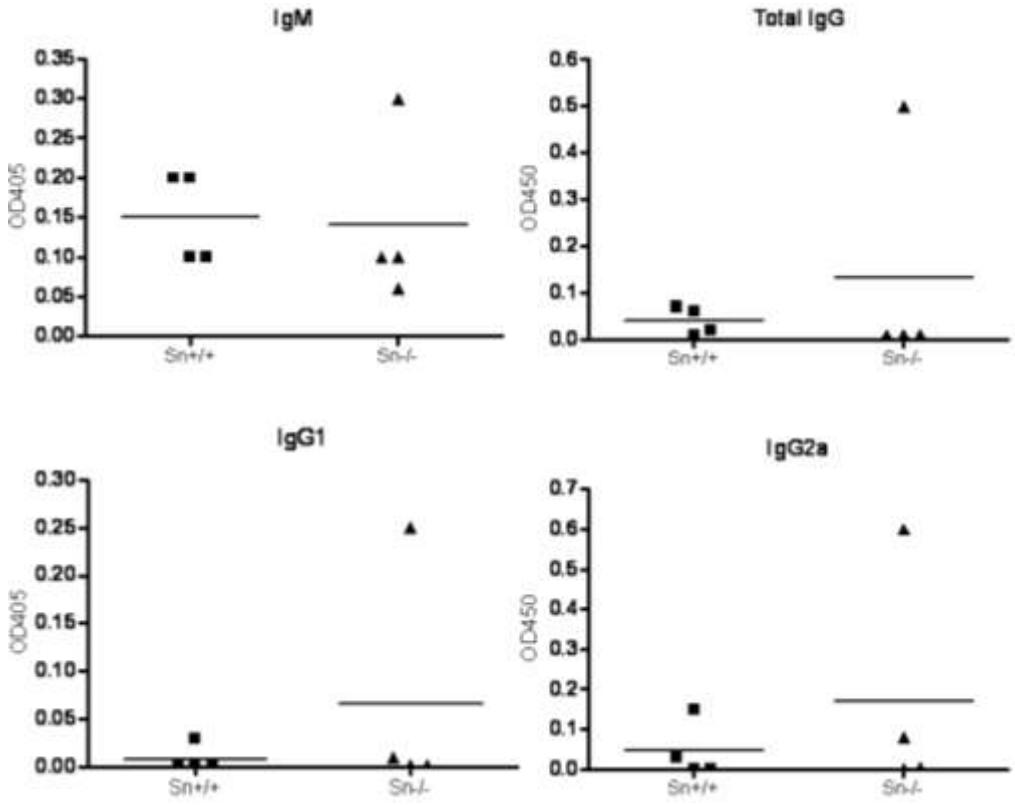

Figure 4.22 Serum anti-dsDNA titres in Sn+/+ and Sn-/- mice at 18 weeks of age. Sera were serially diluted and analysed for anti-dsDNA titres subclasses using ELISA as explained in materials and methods. Serum dilution at 1:400 was used arbitrarily to compare titres. Each dot represents an individual mouse. Statistical analysis was done using student's t test.

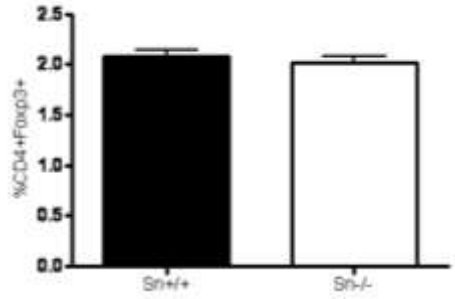

Figure 4.23 Frequency of CD4+Foxp3+ Tregs in splenocytes of Sn+/+ and Sn-/- under homeostatic conditions. Splenocytes from Sn+/+ and Sn-/- (n=5 per C57BL/6 group) were surface labelled with anti-CD4 followed by intracellular staining for Foxp3. Samples were analysed by FACS. Data represent means +SEM. Statistical analysis was done using student's t test.

Whether Sn deficiency in BWF1 mice is associated with increase Treg frequency is unknown. Spleens and peripheral lymph nodes (PLN) from young Sn sufficient and deficient mice were analysed by flow cytometry for the percentage of Tregs (Figure 4.24 and Figure 4.25). There were no differences between the total number of splenocytes or PLN cells between Sn-/- and Sn+/+ BWF1 mice (Figure 4.24, A, Figure 4.25, A). Similarly, the frequency of CD4 T cells in spleen and PLN was not altered between both groups (Figure 4.24,B and Figure 4.25,B). Interestingly, there was a trend towards an increased percentage of Tregs in splenocytes from Sn-/- compared to Sn+/+ BWF1 mice (Figure 4.24, C). However, there was no difference in the number of Tregs between the two genotypes. The frequency of Tregs in PLN showed a trend towards higher Tregs percentage and numbers in Sn-/- BWF1 mice (Figure 4.25, C).

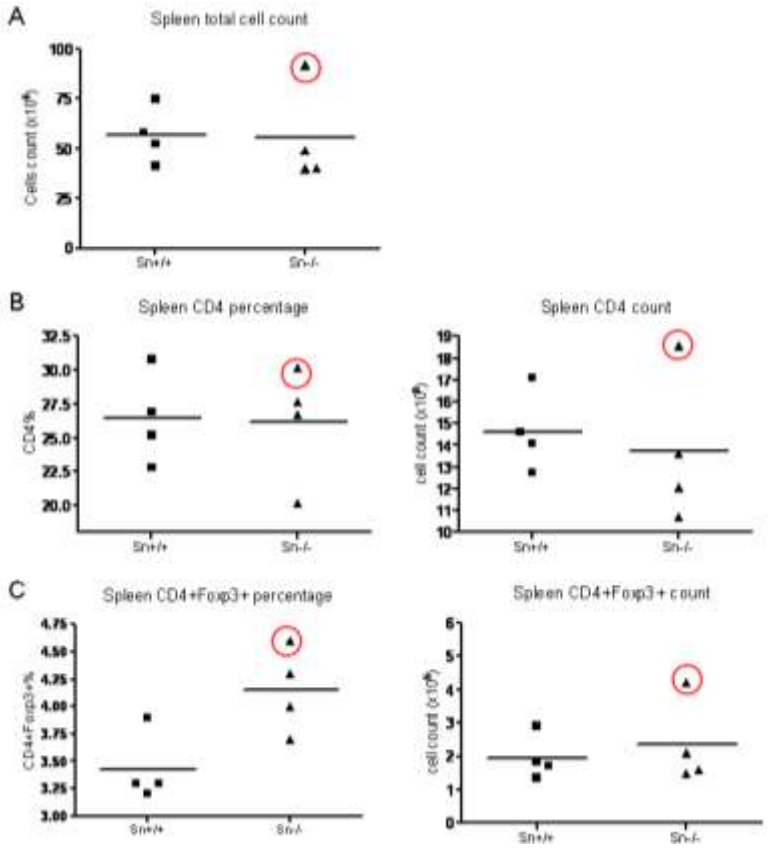

Figure 4.24 Total splenocyte count, CD4 and Tregs frequency in Sn-/- and Sn+/+ mice at 18 weeks of age. A, total splenocytes were counted, following RBC lysis, from each mouse. Each dot represents splenocyte count from an individual mouse. B, CD4 percentage out of total splenocytes (left) and CD4 counts right) as calculated from CD4 percentage and the total number of splenocytes. C, Treg percentage out of total splenocytes (left) and Tregs counts (right) as calculated from Tregs percentage and the total number of splenocytes. The red circled-dot indicates the proteinuric Sn-/- mouse. Statistical analysis was done using student's t test.

Interestingly, the individual proteinuric Sn-/- BWF1 mouse had the highest percentage and number of Tregs in spleen and PLN. This finding might suggest that the effect of Sn deficiency on Tregs frequency becomes more apparent under inflammatory conditions. However, the lack of sufficient number of Sn-/-BWF1 mice makes this hypothesis difficult to prove.

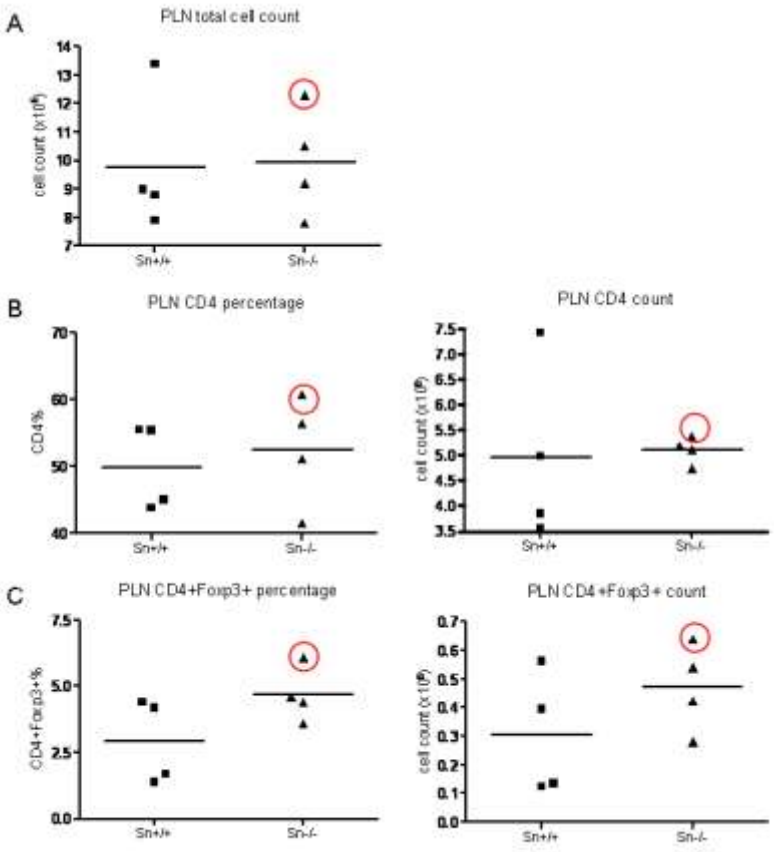

Figure 4.25 Total PLN cells count, CD4 and Tregs frequency in Sn-/- and Sn+/+ mice at 18 weeks of age. A, total PLN cells from inguinal, axillary and brachial lymph nodes were counted from each mouse. Each dot represents PLN count from an individual mouse. B, CD4 percentage out of total cells (left) and CD4 counts right) as calculated from CD4 percentage and the total number of cells. C, Tregs percentage out of total cells (left) and Tregs counts (right) as calculated from Tregs percentage and the total number of cells. The red-circled dot represents the proteinuric Sn-/- mouse. Statistical analysis was done using student's t test.

Tregs are known to have a constitutive expression of the IL-2Rα chain (CD25) and high levels of surface and intracellular cytotoxic T lymphocyte antigen 4 (CTLA-4). The expression of these markers on Sn sufficient and deficient splenic Tregs from both groups was similar (Figure 4.26).

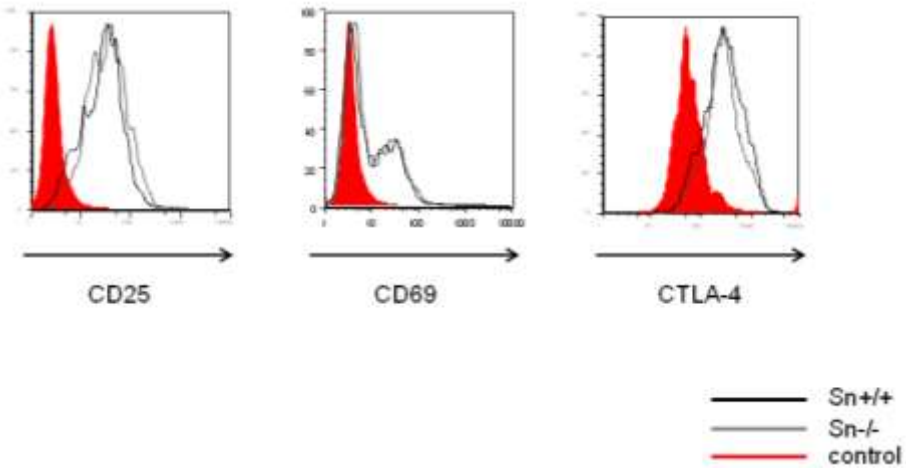

Figure 4.26 Expression of CD25, CD69 and intracellular CTLA-4 on Sn+/+ (black histograms) and Sn-/- (grey histograms) compared to isotype controls (red filled histograms), on splenic Tregs. Data are representative of 4 mice per group.

4.4.5 Renal disease in young Sn deficient BWF1 mice

In order to explore whether there is any differential up-regulation in pro-inflammatory cytokines involved in the pathogenesis of lupus nephritis in young Sn deficient mice, the mRNA expression of IFNα, IFNγ, TNFα , IL1β and TGFβ in renal cortices were examined. Interestingly, Sn deficient mice showed a trend towards increased up-regulation of IFNαR1 mRNA compared to Sn sufficient group (Figure 4.27, A). The expression of other inflammatory cytokines such as: IFNγ, TNFα and IL1β were not different between the two groups. Similarly, Sn deficient and sufficient mice showed similar expression of TGFβ in their renal cortices. The up-regulation of IFNαR1 only among the rest of these cytokines might be due to the fact that these mice were at an early time-point of the disease.

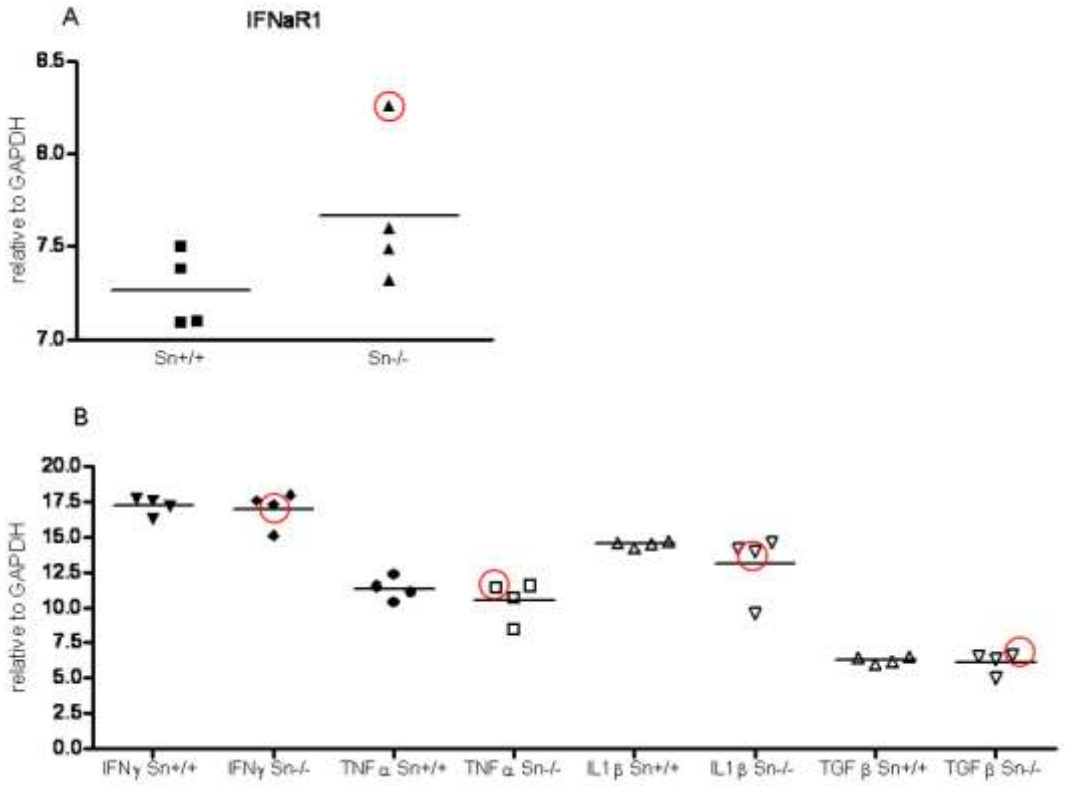

Figure 4.27 Cytokine mRNA expression in young Sn+/+ and Sn-/- BWF1 mice at 18 weeks of age. RNA was extracted from the renal cortices of each mouse, quantified and transcribed to cDNA. A, IFNαR1 was used as a surrogate for IFNα expression. B, Fold increase in mRNA of IFNγ, TNFα , IL1β and TGFβ in both groups relative to endogenous GAPDH. Each dot represents the mean of triplicates from an individual mouse. The red-circled dot represents the diseased Sn-/- BWF1 mouse. Data are presented as mean of fold change in each group of mice. Statistical analysis was done using student's t test.

4.4.6 Renal histology examination

Consistent with the data on serum anti-dsDNA, scoring of the renal histology in Sn sufficient mice revealed no evidence of glomerular hypercellularity, tubular pathology or perivascular inflammation. As for the Sn deficient group, glomerular pathology in the form of increased glomerular hypercellularity and mesangial deposition was observed in the proteinuric mouse only (Figure 4.28). The tubular and perivascular histology were both normal in this particular mouse. These features were in keeping with the development of proliferative glomerulonephritis. The renal histology in the rest of the WT and Sn-deficient group was unremarkable.

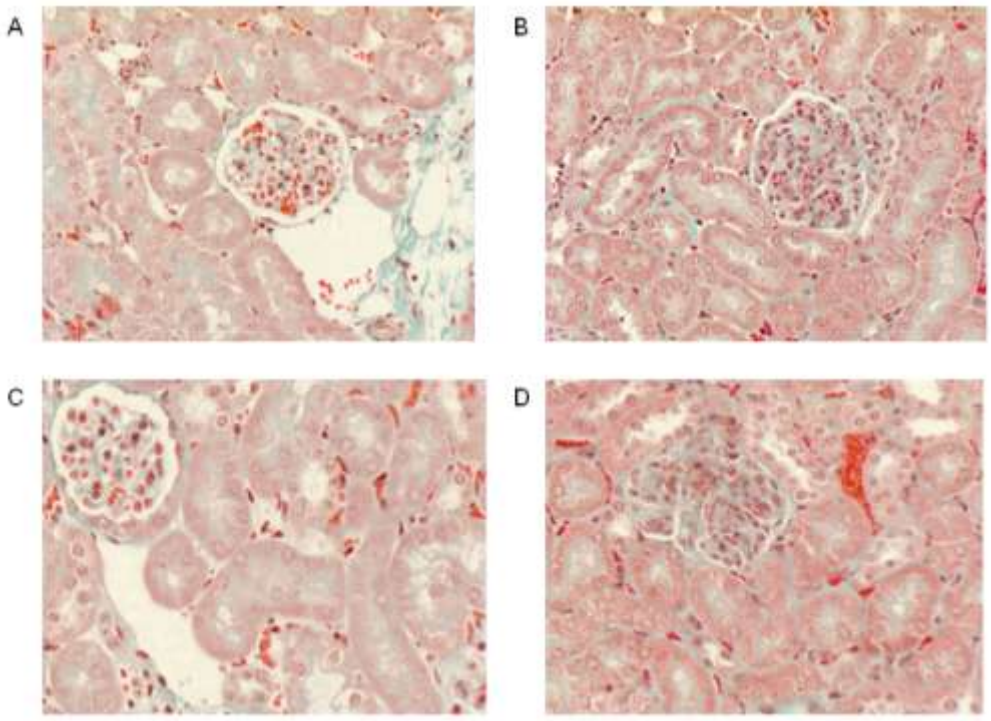

Figure 4.28 Renal histology in young Sn+/+ and Sn-/- BWF1 mice. Trichrome staining of renal sections from random fields in a representative Sn+/+ BWF1 samples (A and C) showing normal glomerular cellularity with less than 35 cells per glomerular cross section. B, and D, representative glomeruli from random fields of a renal section from the diseased Sn-/- BWF1 mouse. Note glomerular enlargement and hypercellularity.

4.5 Discussion

One of the aims of this thesis was to address the role of Sn in murine SLE. In order to achieve this aim the investigation was based on three distinct steps. The first step included an evaluation of the expression of Sn in pre-nephritic and nephritic BWF1 mice utilizing RT-PCR. The second phase was related to exploring the effect of blocking Sn, at a pre-nephritic stage, on disease severity. The final part of this investigation was to generate BWF1 mice deficient for Sn and to compare the severity of lupus nephritis between the two groups.

4.5.1 Sn expression in BWF1 mice

The evaluation of Sn expression in BWF1 mice was accomplished by means of RT-PCR analysis of renal tissues from these mice. The specificity of designed Sn primers

was validated by examining Sn expression in splenic tissues from Sn sufficient and Sn deficient mice. This finding was consistent with the original data on the generation of Sn deficient mice in which similar levels of mRNA expression was noted but with no detectable expression at protein level. Subsequently, Sn mRNA expression was assessed in pre-disease and diseased mice and also compared to NZW mice as a negative control. The results of these experiments revealed that there was no increase in Sn mRNA expression in pre-nephritic BWF1 when compared to control NZW mice. These data were in agreement with initial characterisation and tissue expression of Sn in which no evidence for Sn expression in kidneys of C57BL/6 mice was observed (Crocker *et al*, 1989).

The analysis of Sn mRNA expression in diseased BWF1 mice showed an enhanced Sn mRNA expression and to a similar extent those of CD68 and F4/80 in nephritic kidneys compared to those of age matched NZW mice. This pattern of up-regulation was more prominent in BWF1 mice with < grade 2 of proteinuria. Therefore, these data were suggestive of an influx of macrophages expressing Sn into the kidneys of BWF1 mice at early stages of the disease. An immunohistochemistry analysis would have been useful in confirming this co-expression pattern of Sn, CD68 and F4/80 as well as to identify the location(s) of macrophages expressing Sn.

Interestingly, the increase of Sn mRNA expression was associated with increased expression of IFNαR1. This finding is in agreement with the evidence of the role of IFNα in up-regulating Sn expression. Firstly, bone marrow derived macrophages exposed to IFNα for 3 days in vitro display a homogenous expression of the molecule. Indeed this method was used in the analysis of the effect of engaging SnL on activated CD4+ T cells described in the previous chapter. Secondly, in vivo evidence for this up-regulation effect of IFNα/β on Sn expression comes from the investigation into the use of Sn as a biomarker in human SLE (Biesen *et al*, 2007). In this study Sn was identified as a prominent type I IFN-regulated candidate gene and increased frequency of Sn+ monocytes was positively correlated with disease activity index. Similarly, analysis of

Sn protein expression in human renal biopsies suggested absence of Sn+ macrophages in normal biopsies and increased glomerular and interstitial Sn+ macrophages in renal biopsies of patients with mesangioproliferative glomerulonephritis including SLE (Ikezumi *et al*, 2005).

It is not known whether the expression of Sn in murine and human lupus nephritis is related to the onset of disease and whether there is any difference in expression between early and late disease. In this investigation, mice with < grade 2 proteinuria displayed a higher level of Sn mRNA expression compared to mice with higher degree of urinary protein excretion. This might suggest a role of Sn+ macrophages early in the disease. However, the lack of sufficient number of mice and the heterogeneity of disease made it difficult to ascertain a statistical significance of this trend despite fold expression difference between mice with low and high grade proteinuria.

The examination of Foxp3 and CD4 by RT-PCR in renal cortices of disease BWF1 mice showed a dramatic up-regulation compared to control NZW mice. In addition, there was a significant difference in fold expression between mice with low and high grade proteinuria. This trend would suggest a possible influx of Tregs and CD4+ T cells in early nephritis with possibility of other cells e.g. B cells predominating as progressive proteinuria ensues afterwards. The analysis of renal histology from the other kidney of the mice included in the RT-PCR experiments showed an increase in glomerular cellularity in mice with higher grade of proteinuria. This finding would argue against a possibility of total reduction of cell numbers being responsible for the decrease in CD4 and foxp3 expression in these mice.

4.5.2 Administration of anti-Sn antibodies worsens lupus nephritis in BWF1 mice

Having established the induction of Sn expression around disease onset in lupus nephritis, the potential role of Sn in the disease pathogenesis was next explored by means of blocking antibodies. The aims of this experiment were: a) to examine the

effect of blocking Sn on disease onset and severity of nephritis. b) to explore the correlation between Sn and frequency of Tregs in BWF1 mice. C) to analyse the correlation between SnL+CD4+ T cells and pathogenesis of nephritis in these mice. A combination of two monoclonal antibodies against distinct epitopes of Sn was used. The use of this combination was based on the evidence that each of these would offer a partial inhibition of Sn binding to heavily sialylated human RBCs, while synergy between both leads to a higher level of Sn blocking.

The onset of proteinuria was first evident in mice treated with isotype rat IgG2a control antibody. This was followed 2 weeks later by mice from the anti-Sn treated group. The onset of disease in the group of mice which received PBS only followed the anti-Sn group by one week. However, the anti-Sn group of mice were first to reach the end point of more than 50% of mice becoming proteinuric. Therefore, prophylactic blocking Sn does not significantly influence the course of lupus nephritis in BWF1 mice when compared to isotype antibody or PBS controls. Further evidence for this argument comes from the analysis of serum titres of anti-dsDNA antibodies which showed no significant differences between the treatment groups. Whether prolonged administration of anti-Sn antibodies or altering the timing of introducing the treatment could have affected the disease onset and/or severity are both relevant issues.

The next question in this experiment was related to whether blocking Sn can affect the frequency of Tregs in BWF1 mice. Recently, Sn was found to bind directly to Tregs and down-regulate their frequency in peripheral lymphoid organs and inflamed central nervous system in experimental autoimmune encephalomyelitis (Wu *et al*, 2009). The evaluation of the percentage of Tregs in splenocytes from mice (proteinuric and non-proteinuric) in all three groups revealed an increase in the percentage of splenic Tregs in the anti-Sn group. Such an increase was even more evident in the diseased mice. However, the number of Tregs was similar between all groups. This can be explained by the differences in the total splenocytes count in the proteinuric mice in the anti-Sn

group as there was a general tendency towards a relatively lower counts compared to isotype and PBS control groups.

SLE is characterised by increased CD4, among other innate and adaptive immune cells, autoreactivity and expansion. The expression of SnL on both CD4+ T cells subsets was examined by means of flow cytometry. Similar to the *in vitro* data on the characterization of SnL+CD4 T cells presented in the previous chapter, there was a higher percentage of SnL+ Tregs than SnL+ Teffs. Interestingly, the frequency of SnL+Teffs showed a highly significant direct correlation with proteinuria. This finding was specific for SnL+Teffs as the frequency of SnL+Tregs remained similar between proteinuric and non-proteinuric mice. These findings suggested that increased SnL+Teffs frequency is associated with inflammation and tissue injury. In addition, this observation could be exploited for the use as a 'biomarker' of disease activity in human SLE.

The assessment of renal histology in mice from all three groups showed a trend in diseased anti-Sn treated mice towards more severe forms of nephritis. This was evident with the higher number of glomeruli in renal sections from these mice with extra-capillary proliferation and crescent formation. In addition features of tubular and perivascular pathology were both predominant in the diseased mice that received anti-Sn. These findings were in agreement with a trend towards more severe and advanced disease in the anti-Sn group of mice.

In conclusion, the data on blocking Sn at a pre-nephritic stage suggested a potential negative regulatory role for Sn in the disease pathogenesis.

4.5.3 Lupus nephritis in Sn-/- BWF1 mice

The generation of Sn deficient BWF1 mice was accomplished using a speed congenics strategy. This method consists of introgressing specific genomic intervals into a particular recipient background and thus generating mice strains which lack one or more genes of interest. The strategy has been employed previously in the analysis of

complex polygenic diseases e.g. diabetes and SLE (Serreze *et al*, 1996; Winer *et al*, 2002 and Mohan *et al*, 1999).

The progeny of Sn deficient NZW XNZB crosses were observed to have small litter size and high rate of early-postnatal mortality. In human SLE, neonatal mortality can occur due to the presence of antibodies against protein-RNA complexes. Autoantibodies against an RNA-binding protein known as Ro autoantigen are associated with photosensitivity and subacute cutaneous lupus erythematosus (Provost *et al*, 1996). These anti-Ro antibodies can cross the placenta and cause cardiac conduction defects (Silverman *et al*, 1995). The fact that the use of heterozygous parental NZB and NZW overcame this pronounced postnatal mortality suggested that maternal factors might be involved in this observation. Further support against neonatal disease comes from the fact there was no evidence of sub-mendelian distribution between Sn deficient and sufficient progeny of Sn heterozygous parental mice. In addition, there was no evidence of major disease manifestations up to 16 weeks of age in the Sn deficient mice.

The main aim of the analysis of this cohort of Sn deficient mice was to examine an early time point of the disease at 16 weeks of age. Based on the experiment on blocking Sn major disease manifestations were not expected at this early time point. Surprisingly, one of the Sn deficient mice started to develop proteinuria (100mg/dl) by the age of 15 weeks. The analysis was extended to the age of 18 weeks as there was evidence of progressive increase in proteinuria. All the other mice in the cohort showed no evidence of proteinuria. Serum anti-dsDNA titres were consistent with the proteinuria observation. These data indicated that Sn deficiency is associated with early onset disease in BWF1 mice.

The data presented on the frequency of Tregs in Sn-/- and Sn+/+ mice demonstrated a trend towards a higher percentage of Tregs (spleen and PLN) and a higher number of Tregs (PLN only). This observation was even more prominent in the proteinuric mouse

in the Sn-/- group. A similar trend was observed in the previous experiment in mice that received anti-Sn antibodies, but these mice were 10 weeks older and at a later stage of the disease. In addition, the data presented on the frequency of Tregs in Sn-/- C57BL/6 mice did not show any differences compared to their wild-type littermates. In contrast, Sn-/- mice in EAE were shown to have a higher frequency of Tregs (Wu *et al*, 2009). Taken together, these observations highlight an important aspect of Sn interaction with Tregs, the requirement for an inflammatory state for Sn to down-regulate Tregs frequency. Inflammatory conditions and particularly IFNα have been demonstrated to affect Sn expression on BMDMs in vitro (data from previous chapter), in human with active SLE (Biesen *et al*, 2008) and to a certain extent in the EAE model as IFNα/β plays a major role in the pathogenesis of the disease. Furthermore, such an inflammatory microenvironment indicates activation of CD4+ T cells and Tregs which means inducing SnL on these cells and consequently optimizing the conditions for interactions between Sn and Tregs. However, a trend towards a higher frequency of Tregs was observed in Sn-/- BWF1 mice although only one of these mice had evidence of nephritis. This is an interesting observation and the possible influence of genetic background (C57BL/6 versus BWF1) on the expression of Sn cannot be ruled out.

The investigation of inflammatory cytokines involved in the pathogenesis of lupus nephritis did not reveal statistical differences between the two groups of mice. The fact that this analysis was conducted at rather an early stage of the disease and with only one diseased mouse in the cohort had a direct influence on detecting difference in mRNA expression of the cytokines studied. The examination of renal histology from Sn+/+ and all but one Sn-/- mice were normal. This examination confirmed the onset of lupus nephritis and is in favour of a regulatory role for Sn in BWF1 nephritis.

4.5.4 Potential role of Sn in SLE

One interesting question that arises from the experiments on administering anti-Sn blocking antibodies and the early time point analysis in Sn-/- BWF1 mice, is why the

relative increase in Tregs in Sn-/-BWF1 mice did not protect or delay the onset of disease? In the previous chapter, in vitro analysis of the phenotype of SnL+Teffs demonstrated this subset of activated CD4+ T cells as TCR-hyper-responsive, hyper-proliferative and expressing higher levels of IFNγ compared to their SnL- counterparts. This phenotype is relevant to the ability of these cells to be highly inflammatory Th1 cells. In addition, the data presented on the interaction between Sn and SnL *in vitro* showed that engaging SnL with Sn on activated CD4+ T cells results in cell death. This function of Sn might suggest a mechanism by which Sn negatively influences the frequency of Tregs and Teffs under inflammatory conditions. Under these conditions, especially in the presence of IFNα, Sn expression is up-regulated on macrophages other than those that constitutively express Sn i.e. in the subcapsular sinus of lymph nodes and in the MMZ of the spleen. Secondly, Tregs express abundant SnL more than Teffs especially following TCR stimulation, *in vitro* as demonstrated in the previous chapter, and *in vivo* as shown in the analysis of BWF1 mice treated with anti-Sn, isotype control or PBS.

Therefore, Sn might influence the frequency of Tregs by inducing death of SnL+Tregs under certain inflammatory conditions (Diagram 4.6, A). Similar to its interaction with SnL+Tregs, Sn might play a regulatory role on SnL+Teffs. This means that under conditions where the suppressive function of Tregs is intact, Sn deficiency results in higher frequency of Tregs and better control of inflammation (Diagram 4.6, B, top). However, under inflammatory conditions where Tregs are dysfunctional Sn deficiency might result in potentiating inflammation due to the persistence of SnL+Teffs.

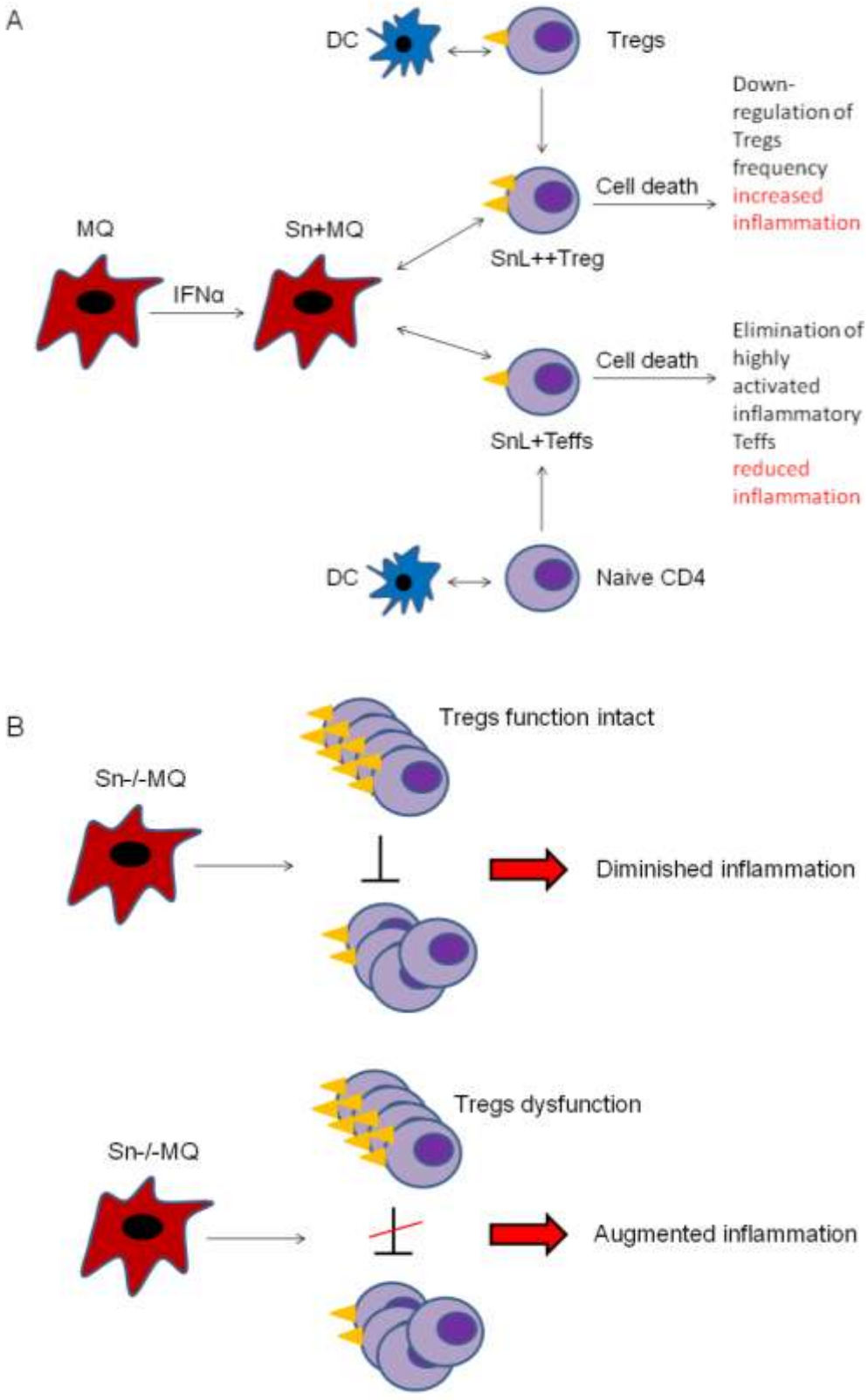

Diagram 4.6 Model for Sn interaction with SnL+Tregs and SnL+Teffs and potential outcomes depending on the functional status of Tregs.

In conclusion, this analysis was consistent with the data on blocking Sn at pre-nephritic stage. In both experiments Sn deficiency was associated with adverse renal pathology. However, blocking experiments did not lead to an early disease onset similar to that seen in Sn deficient mice. This might be explained by the fact that the use of monoclonal antibody albeit inhibit Sn but does not equate to a sustained absence of Sn in the knock out model. In both experiments, Sn inhibition/deficiency was associated with increased Tregs frequency indicating a negative regulatory role for Sn on Tregs expansion. However, this increase in Tregs frequency was not sufficient to provide a better disease control.

Final discussion

Sn is the largest member of the siglec family (Crocker, 2007). The extracellular region of Sn consists of 17 Ig domains, a distal V-set domain and 16 C2-domains. The membrane proximal 14 domains can be grouped into seven tandemly-arranged homologous pairs of domains. Each of these pairs consists of a short and a long domain. Statistical analysis of these domains suggested that all long domains are related (Mucklow *et al*, 1997). The same is applicable to the short domains. However, the long and short domains are unlikely to be related to each other. This pattern suggests that this region of Sn might have evolved by sequential duplication of a two-exon module consisting of long and a short domain. In addition, this evolutionary extension of the molecule and consequently its V-set domain is of functional relevance for cell-cell interactions and reduction of cis interactions with sialic acids expressed on neighbouring glyconjugates.

Sn is involved in ‘self’, ‘non-self’ and ‘altered-self’ recognition. Under homeostatic conditions, high-level Sn expression is restricted to macrophages in the MMZ of the spleen and the subcapsular sinus of lymph nodes. Under these conditions, sialylated ligands for Sn are expressed on granulocytes but not resting T lymphocytes. The extended structure of Sn and the low affinity of its binding with these sialylated ligands offer selectivity in Sn interactions with other cells (Crocker *et al*, 1997).

The expression of α2,3-linked sialic acids by certain pathogens such as *Neisseria meningitidis*, *Campylobactor jejuni*, group B streptococcus and *Trypanosoma cruzi* offers a mechanism of ‘non-self’ recognition. The recognition of ‘altered-self’ by Sn is evidenced by the observation of high numbers of infiltrating Sn+ macrophages in contact with breast cancer cells in human. In this regard Sn was found to interact with mucin structures expressed on the surface of human breast cancer cells (Nath *et al*, 1999). Chronic inflammatory conditions are associated with an enhanced expression of Sn on inflammatory monocytes/macrophages, indicating a role in modulating immune

responses (Ip *et al*, 2007; Hiang *et al*, 2006; Wu *et al*, 2009; Hartnell *et al*, 2001; York *et al*, 2007 and Biesen *et al*, 2009).

In this chapter, I discuss the main findings in this thesis and potential mechanisms by which Sn might contribute to murine SLE.

5.1 Characterization of SnL on CD4 T cells

Recent studies have indicated that Sn can modulate the function of T lymphocytes under inflammatory conditions (Jiang *et al*, 2006; Ip *et al*, 2007; Kobsar *et al*, 2006 and Wu *et al*, 2009). This concept arose from the findings of disease amelioration and altered frequencies of T lymphocytes at the sites of inflammation in Sn deficient mice. However, a mechanistic interpretation of these interactions remained unclear. The identification of SnL expressed on Tregs in EAE was a major step towards identifying a mechanism via which Sn can modulate CD4+ T cells responses under inflammatory conditions (Wu *et al*, 2009). Although, a function of Sn in down-regulating the proliferation of Tregs helped to explain the disease amelioration observed in Sn deficient mice, the nature of SnL on Tregs and the mechanisms by which negative regulation of Tregs is achieved remained unknown.

5.1.1 Possible explanations to the phenotype of SnL+Teffs

The data presented in the third chapter of this thesis demonstrated that SnL expression on CD4+ T cells is not exclusive to Tregs. Teffs, albeit to a lesser extent compared to Tregs, express SnL following TCR ligation *in vitro*. The phenotype of SnL+Teffs cells is that of higher state of activation, Th1 cytokine production and proliferation compared to SnL-Teffs. These findings indicate that SnL expression can be used to examine the heterogeneity of CD4+ Teffs responses to TCR ligation and identify Teffs that are at an extreme of activation. A hypothesis that might explain this altered state of activation is that SnL positivity identifies a subset of CD4+ Teffs that are hyper-responsive to TCR ligation resulting in higher expression of early activation

markers. The enhanced expression of CD25 on these cells suggests that they can utilize endogenous IL-2 more than SnL-Teffs and therefore have the high affinity IL-2 receptor which supports higher state of proliferation.

The maintained CD45RB high surface expression of SnL+Teffs is in contrast to the high activation status of these cells. T cell activation is known to be associated with a shift from CD45RB high to CD45RB low (Holmes 2006). CD45 (phosphotyrosine phosphatase) is heavily expressed on T and B lymphocytes. Alternative splicing of CD45 mRNA gives rise to different isoforms of the glycoprotein. These are referred to as A, B and C, encoded by exons 4, 5 and 6 of CD45 gene (Holmes 2006). In addition, CD45 plays a crucial and complex role in TCR signalling (Hermiston *et al*, 2002, Salmond *et al*, 2008). TCR ligation results in phosphorylation of CD3 and ζ chain immunoreceptor tyrosine-based activation motifs by Src-family kinases (SFK) initiating signalling pathways that result in T cell differentiation and proliferation. (Zamoyska *et al*, 2003). CD45 regulates TCR signalling via its ability to de-phosphorylate critical tyrosine residues in the SFK p56 (lck) and p59 (fyn) (Holmes 2006). Regulation can occur in a positive and a negative way depending on which of two $p56^{lck}$ tyrosine residues are de-phosphorylated (McNeill *et al*, 2007). A positive regulatory effect of CD45 on TCR signalling happens when it de-phosphorylates the negative regulatory $p56^{lck}$ pTyr505 site thereby initiating kinase activity and promoting enhanced TCR signalling (Hemirston *et al*, 2002). On the other hand, CD45 can negatively influence TCR signalling by de-phosphorylation of the activatory $p56^{lck}$ pTyr394 site leading to suppression of kinase activity and down-regulation of TCR signalling (Zhau *et al*, 2004). Evidence for this dual function of CD45 comes from the findings of different levels of TCR responsiveness in CD4 T cells from mice expressing intermediate or low levels of CD45RO (McNeill *et al*, 2007). While low CD45RO expression level leads to reduced TCR signalling and hypo-responsiveness, intermediate expression leads to hyper-responsiveness to TCR ligation in peripheral CD4 T cells (McNeill *et al*, 2007). These findings appear to be independent of the CD45 isoform as intermediate

expression of CD45RB resulted in CD4 T cells hyperproliferation and hyper-responsiveness (Salmond *et al*, 2008). The data presented on the surface expression of CD45RB on SnL+Teffs showed a maintained or even heightened expression of CD45RB on these cells. It is not ytentirely clear to what extent the flow cytometry analysis correlates with the phosphatase activity of CD45RB. Such an evaluation might be useful in determining whether the CD45RB high status contributed at a molecular level to the high state of activation in SnL+Teffs.

5.1.2 Nature of SnL

The data presented have shown that induction of SnL on activated CD4 T cells is associated with increased α2,3- rather than α2,6 sialylation. Further evidence for the α2,3-specific binding of SnFc to activated CD4+ T cells was obtained using α2,3-specific slialidase which led to loss of SnFc binding. In order to explore the nature of SnL on CD4 T cells the mRNA expression of four α2,3 sialyltransferases and other glycosyltransferases on FACS sorted SnL- and SnL+ Teffs was examined. Several of these enzymes were found to be up-regulated to a higher extent on SnL+Teffs compared to their SnL- counterparts. Among α2,3 sialyltransferases, ST3Gal VI (>7 fold), ST3Gal III (>1.5 fold) and to a lesser extent ST3Gal IV(1.5 fold) were found to be up-regulated more on SnL+ compared to SnL- subsets. While ST3Gal IV and ST3 Gal VI catalyzes sialylation of *N*- and *O*-linked glycans (Comelli *et al*, 2006), ST3Gal III is more specific for *N*-glycans (Earl *et al*, 2010). However, the enhanced mRNA expression of C2GnT (>7 fold) shifted the balance towards Core 2 *O*- more than *N*-linked glycans. In addition, the mRNA expression of key glycosyltransferases involved in the synthesis of sialyl Lewis x motifs (Carlow *et al*, 2009) on Core 2 *O*-glycans (β1,4 Gal T and FUT7) were also up-regulated. Sialyltransferases associated with the transfer of α2,3-linked sialic acids to Core 1 (ST3Gal I) or catalyzing the transfer of α2,6-linked sialic acid to *N*-glycans (ST6Gal I) were not found to be up-regulated on SnL+ compared to SnL- Teffs. Although these findings identified at least two α2,3

sialyltransferases (ST3Gal VI and ST3Gal III) with more than 1.5 fold difference in SnL+Teffs, but they did not discriminate between *N*- or Core 2 *O*-glycan structures.

The fact that SnL was found to be induced on activated CD4 T cells from mice deficient in all three isoforms of C2GnT, ruled out contribution of Core 2 *O*-glycan in the structure of SnL. This finding was further confirmed with the glycan inhibition data in which inhibition of *O*-glycan extension led to increased induction of SnL on activated CD4 T cells. N-glycan inhibition, on the other hand, resulted in abrogation of SnL induction. Taken together, these findings confirmed that SnL are composed of *N*-glycans with terminal capping by α2,3-linked sialic acids catalyzed by ST3Gal III or ST3Gal VI.

5.1.3 Functional consequences of engaging SnL with Sn

Sn was previously found to interact with T lymphocytes (Crocker *et al*, 1997; Van den Berg *et al*, 2001 and Wu *et al*, 2009). In the latter study, specific interaction between Sn and Tregs in autoimmune mouse model of central nervous system inflammation was identified. In addition, this interaction was found to be associated with reduced Tregs proliferation and augmented disease severity. The data on engaging SnL on activated CD4+ T cells by Sn expressed on BMDMs showed that Sn induces cell death. This novel function of Sn can explain the down-regulation of Tregs observed by Wu and colleagues. Furthermore, different functional consequences can ensue from the interactions between Sn and Tregs or Teffs. Sn interaction with Tregs can be associated with reduced frequency of Tregs and accelerated inflammation. On the other hand, contact between Sn and Teffs can contribute to amelioration of inflammation. The mechanism by which Sn induces cell death is unknown. Whether such a process is caspase-dependent or -independent remains to be determined.

The findings of heightened surface expression of CD95L and intracellular expression of Bcl2 in SnL+Teffs further suggest the potential of this subset of Teffs to induce cell

death on neighbouring cells and their contribution to inflammation compared to SnL-subset.

5.1.4 Potential synergy between Sn and galectin 1

There are a number of findings in this analysis that points towards a potential link between Sn and galectin 1. Galectins are a family of glycans-binding proteins that share a consensus amino acid sequence and a carbohydrate-recognition domain (CRD) that is responsible for their β-galactoside-binding activity (Yang *et al*, 2008). Galectin 1 is the first member of this family and it has been shown to regulate innate and adaptive immune responses including TCR signalling, modulation of cytokine production, cell trafficking, and T cell survival (Rabinovich *et al*, 2009). It is synthesized and secreted by activated but not resting T (Blaser *et al*, 1998). In addition it is significantly up-regulated on Tregs (Garin *et al*, 2007).

CD45 is a major receptor for galectin 1 (Nguyen et al, 2001). Galectin 1-induced cell death on cell lines transfected with CD45RB was found to be mediated by binding to both *N*- and *O*-linked glycans (Earl *et al*, 2010). Core 2 glycans represents the high affinity ligand for galectin 1 on CD45. However, in the absence of Core 2 structures galectin 1 binding to the low affinity Core 1 glycans is still possible via multivalency. Interestingly, the binding of galectin 1 to N-glycans on CD45RB was found to be dependent on the balance between α2,3- and α2,6-sialylation. Expression of α2,6-linked sialic acids on *N*-glycans of CD45 protects from galectin 1 induced cell death. On the other hand, enhanced α2,3 sialylation mediated by ST3Gal III promotes galectin 1 binding to *N*-glycans and consequent cell death (Earl *et al*, 2010).

As shown in chapter 3, SnL+Teffs maintain their surface expression of CD45RB following TCR ligation. In addition, the above glycomic analysis of SnL indicates that *N*-glycans, but not *O*-glycans, are contributing to the structure of the ligand. Furthermore, terminal sialylation is likely to be mediated by ST3Gal III or ST3Gal VI. Taken together, these findings suggest a potential synergy between Sn and galectin 1 in inducing cell

death. Such a possibility is based on the binding of galectin 1 to Core 2 (high affinity ligand) expressed on CD45RB and Sn to *N*-glycans of SnL and inducing cell death. Similarly, a potential synergy between these two lectins is also possible depending on which of the two α2,3 sialylaltransferases (ST3Gal III or ST3Gal VI) is used (or indeed if there is a degree of redundancy between these two enzymes) for the sialylation of *N*-glycans on SnL. Identifying the nature of the glycoprotein carrier of the SnL on activated CD4 T cells would be useful in further analysis of this potential synergy between Sn and galectin 1. It is tempting to suggest CD45RB as a carrier for SnL, however, no evidence supporting this possibility is available currently. Finally, examining the contribution of ST3Gal III and ST3Gal VI to the sialylation of SnL would be useful in explaining any potential synergy between Sn and galectin 1 in inducing CD4 cell death. Such an analysis can be accomplished using ST3Gal III and/or ST3Gal VI KO (Ellies *et al*, 2007).

5.2 Potential function for Sn in NZB X NZW F1 lupus nephritis

The data presented in chapter four of this thesis highlighted a potential role for Sn in the pathogenesis of murine lupus nephritis. To begin with, data on the mRNA expression of Sn and other macrophage lineage markers (CD68 and F4/80) showed an up-regulation in the expression of all these genes in mice with early stages of lupus nephritis but not at pre-nephritic stage. This pattern was suggestive for an increase in inflammatory macrophages bearing Sn as the enhanced mRNA expression of Sn was in parallel with those of CD68 and F4/80.

The use of anti-Sn blocking antibodies at a pre-nephritic stage of the disease showed that these did not affect the onset of disease. Indeed, the percentage of mice with proteinuria was higher in anti-Sn antibodies treated compared to control mice. However, there were no differences in the serum titres of anti-dsDNA antibodies between all three treatment groups. The potential adverse effect of blocking Sn expression was more evident in the histological findings of diseased mice. Mice treated

with anti-Sn antibodies tend to have a higher percentage of glomeruli with extra-capillary proliferation, higher extent of tubular damage and more perivascular infiltration. Surprisingly, these mice also had a higher percentage of Tregs compared to mice in the isotype control group. While this finding was consistent with the down-regulatory effect of Sn on Tregs observed in another model of autoimmunity (Wu *et al*, 2009), it raised the question of why the higher percentage of Tregs in these mice did not protect from aggressive disease? Much of interest was focused recently on the frequency of Tregs in murine (Hayashi *et al*, 2005; Scalapino *et al*, 2006; Abe *et al*, 2008) and human SLE (Scheinecker *et al*, 2010) with often conflicting findings especially in human SLE. However, other factors such as resistance of Teffs to suppression by Tregs (Monk *et al*, 2005), Tregs repertoire (La Cava *et al*, 2004) adverse cytokine milieu e.g.IL-6 (Pasare *et al*, 2003) and homing defects (Abe *et al*, 2008) can all contribute to the failure of Tregs to maintain peripheral tolerance.

Another likely explanation comes from the observation that the percentage of SnL+Teffs, in mice from all treatment groups, was directly correlated to proteinuria. As discussed in chapter 3, the phenotype of this subset of Teffs, *in vitro*, was indicative of high pathogenic potential of these cells (higher state of activation, increased production of IFNγ and hyper-proliferative compared to SnL-Teffs). The hypothesis arising from these findings is that SnL+Teffs are highly inflammatory subset of Teffs that are capable of inducing tissue damage (IFNγ) and cell death (high CD95L expression). Sn, therefore, plays a protective role in inducing cell death on SnL+Teffs and reducing tissue injury and inflammation. Further support to this protective role of Sn comes from the observation that one out of four Sn deficient BWF1 mice started to develop proteinuria, rise in anti-dsDNA and histological evidence of lupus nephritis at 16 weeks of age. As expected the Treg frequency in this diseased Sn deficient mouse was higher than the rest of the non-diseased Sn deficient and their wild-type littermates.

Overall, these findings suggested a potential function for Sn in diseased BWF1 mice under certain conditions depending on its binding to SnL+Tregs or SnL+Teffs. Under

complex inflammatory conditions that render Tregs dysfunctional, Sn deficiency can have a deleterious effect on inflammation and tissue injury despite an increase in the frequency of Tregs. Such an effect is due to the tissue injury caused by the unopposed SnL+Teffs.

Another possible mode of action for Sn in immune-complex mediated autoimmune disease such as lupus nephritis is related to whether it plays a role in clearance of apoptotic cells. Sn on resident macrophages has been shown previously to bind, without phagocytosis, preferentially to neutrophils, both apoptotic and non-apoptotic (Crocker *et al*, 1995). In addition, the data on the mRNA expression of Sn at early stages of lupus nephritis suggested an influx of inflammatory macrophages expressing. It is possible that the Sn can bind to apoptotic cells and potentiating phagocytosis by other phagocytic receptors expressed on these macrophages. In this regard, deficiency in Sn can result in defective clearance of apoptotic materials and consequently enhancing the formation of autoantibodies and immune-complexes. Recently, resident Sn+ macrophages in the subcapsular sinus of lymph nodes were shown to play an important role in the uptake of subcutaneously injected apoptotic cells and activating anti-tumor immunity (Asano *et al*, 2011).

5.3 Conclusion

The data presented in chapter 3 of this investigation revealed that SnL are expressed on Tregs and Teffs CD4 T cells. In addition, the phenotype of SnL+Teffs indicates a highly inflammatory potential for these cells. Furthermore, this investigation uncovered a novel function for Sn in the form of inducing cell death on activated CD4 T cells. Collectively, these suggest that Sn can modulate CD4 T cell responses at different levels under certain inflammatory conditions. The analysis of mRNA expression of different glycosyltransferases together with using chemical inhibitors against *O*- and *N*-glycans established the sialylation and glycan nature of SnL on activated CD4+ T cells.

Finally, while Sn binding to activated CD4+ T cells was found to be independent on CD43 and PSGL-1, two counter-receptors that have been identified previously to mediate Sn binding to CD4 T cells, the nature of the glycoprotein carrier of SnL remains to be determined.

The data presented in chapter 4 of this thesis indicate that Sn is expressed on inflammatory macrophages in renal tissues of BWF1 mice at an early stage of lupus nephritis. In addition, blocking Sn expression or Sn deficiency might negatively influence the severity and course of disease. These data suggest an anti-inflammatory role for Sn in murine lupus nephritis. Further validation of this novel function of Sn is warranted by examining nephritis onset and severity in a larger cohort of Sn deficient and wild type BWF1 mice and extending the analysis to later stages of the disease.

Appendix

Table A.1 NZB polymorphic markers and their corresponding primer sets used in genotyping. Markers and primer sets are colour coded to black and red, depending on polymerase reaction conditions (See Table A.3).

Marker	Forward Primer	Reverse Primer
D1Mit132	5'-TATTGTTTATGGAAATTGGACCC-3'	5'-CATCTCTGAAGGAAAAAGTGCA-3'
D1Mit308	5'-GAGGCTATGAGTCAAATGGACC-3'	5'-TTTATGAGGTGCTGAGATGCA-3'
D1Mit111	5'-ATTGCCTGACTCCAGTATTCTACC-3'	5'-TTAGGTGTGTGAAAGACATTCCC-3'
D4Mit193	5'-TATTTTAATTTTAGCCCATCAGGG-3'	5'-AAAGACATACAATTGATCCACAGG-3'
D4Mit17	5'-TGGCCAACCTCTGTGCTTCC-3'	5'-ACAGTTGTCCTCTGACATCC-3'
D4Mit308	5'-TATGGATCCACTCTCCAGAAA-3'	5'-CAAAGTCTCCTCCAAGGCTG-3'
D6Mit209	5'-CTCCCCCTCTGTGTGATTGT-3'	5'-TTATTACACCAGACCCATGTGG-3'
D6Mit36	5'-ACCATCTGCATGGACTCACA-3'	5'-GTTGAAGAGGACGACCAAGTG-3'
D6Mit328	5'-ACCTGGGTAAACAGGGAAGC-3'	5'-ACATCTTTGTCTGGATTTTGGG-3'
D7Mit350	5'-TCTGCATCTCACTGTCCCAG-3'	5'-ATCTACAAATGAGTTTCTAAGGACTGC-3'
D7Mit101	5'-TACAGTGTGAACATGTAGGGGTG-3'	5'-TCCCAACATGGATGTGCTAA-3'
D10Mit230	5'-AGATAGCCTAGGGGGTGCAT-3'	5'-ATCAGTTTCCAATCGCTGCT-3'
D10Mit96	5'-CTTCTTTGAAGTTAGATGCAGCC-3'	5'-TACGGAGAAGGGAACACCTG-3'
D11Mit285	5'-CATGAATCCATCACCAGCAG-3'	5'-TTTTTCAGTCATGCAGGCAG-3'
D11Mit333	5'-CATGTGGTTATTTTCTAGCCCC-3'	5'-AGGCATCAATAACTATTTTTCAGTG-3'
D13Mit16	5'-CCAGCTGAAGGCTTACTCGT-3'	5'-AAAGTTAGAATCAGCCATTCAAGG-3'
D13Mit74	5'-TATTGAAGACCAGACAGTGAAGAA-3'	5'-TTCTCATGAACGTTAGAGAAGCC-3'
D17Mit51	5'-TCTGCCCTGTAACAGGAGCT-3'	5'-CTTCTGGAATCAGAGGATCCC-3'
D17Mit10	5'-TGCACTTGCATAAGGAAAAC-3'	5'-GACTTTGGGGCCTACTTATG-3'
D19Mit333	5'-CCTTTTCAAGAGCATCCTTAAA-3'	5'-GGTGGGACTTGAGAGATGCA-3'

Table A.2 NZW polymorphic markers and their corresponding primer sets used in genotyping. Markers and primer sets are colour-coded to black, red, purple and green, depending on polymerase reaction conditions (See Table A.3).

Marker	Forward Primer	Reverse Primer
D1Mit111	5'-ATTGCCTGACTCCAGTATTCTACC-3'	5'-TTAGGTGTGTGAAAGACATTCCC-3'
D1Mit155	5'-ATGCATGCATGCACACGT-3'	5'-ACCGTGAAATGTTCACCCAT-3'
D1Mit1001	5'-TTGTGTGTAGTACAGTGTTGGTGG-3'	5'-TGGTTGCTGACATCAATCTCC-3'
D2Mit66	5'-GTTGCACAGGCAATCAACC-3'	5'-ATCTATCACTGGGGCTGTGC-3'
D2Mit148	5'-GTTCTCTGATCTACGGGCATG-3'	5'-TTCACTTCTACAAGTTCTACAAGTTCC-3'
D2Mit411	5'-ACACTCACAACTACGAGATAAAGCC-3'	5'-AGGTCATTAGGGCTGTCTTCC-3'
D4Mit193	5'-AAAGACATACAATTGATCCACAGG-3'	5'-TATTTTAATTTTAGCCCATCAGGG-3'
D4Mit308	5'-TATGGATCCACTCTCCAGAAA-3'	5'-CAAAGTCTCCTCCAAGGCTG-3'
D5Mit95	5'-TGTTCTTGTCCATGTCTGATCC-3'	5'-AACCAAAGCATGAAACAGCC-3'
D6Mit36	5'-AACATCTGCATGGACTCACA-3'	5'-GTTGAAGAGGACGACCAAGTG-3'
D6Mit138	5'-GCTCTTATTAATGAAGAAGAAGGAGG-3'	5'-CAAAGAAAGCATTTCAAGACTGC-3'
D7Mit294	5'-TAGTGGGAAAGAGAGAAACAATCC-3'	5'-TAATGTTAAATCTTGTCGTCTTAGTGG-3'
D7Mit350	5'-TCTGCATCTCACTGTCCCAG-3'	5'-ATCTACAAATGAGTTTCTAAGGACTGC-3'
D12Mit158	5'-CATTGGGCAATGGAATTTG-3'	5'-ATGAGAGAAAACCAGAAACAAAGG-3'
D12Mit182	5'GTACATACAATACATCACACAAACGG-3'	5'-GGCAAGAAAACAGACCAATAGG-3'
D13Mit260	5'-TAAATTTGGATGCAGACAATGG-3'	5'TTAAAAATAGAAATGGCTCTGTGTG-3'
D13Mit275	5'-TTAGCAAGGGAACAGAGAGAGG-3'	5'-CAATCAAGGTATCCCTGTCTCC-3'
D16Mit52	5'-ACACATGTGCAAGCCTAACC-3'	5'-TTATCCCTGGAATCTGGGG-3'
D16Mit131	5'-TGGTGGTGGTGTTGATGGTA-3'	5'-AAGACCATTTCTAATAAACAACACCC-3'
D17Mit93	5'-TGTCCTTCGAGTGTTTGTGTG-3'	5'-TCCCCGGTGAATGAGTTATC-3'
D17Mit245	5'-TGTGCTCTGGCTAGGGAGTT-3'	5'-CACATTCATATGTACACACACATGC-3'
D18Mit48	5'-TTGCACTCACAGGGCACAT-3'	5'-TCAGAGTTTCCAGAAGACACCA-3'
D18Mit77	5'-CTGTAGTTTATCAGTTCACCCTGTG-3'	5'-TGTGCTGTTAAACAAATATCTCTG-3'
D19Mit28	5'-TCTTCATGCCCAAAAGAGCT-3'	5'-GCATCCTGAATCTCCTGCC-3'
D19Mit33	5'-CCTTTTCAAGAGCATCCTTAAA-3'	5'-GGTGGGACTTGAGAGATGCA-3'

Table A.3 Genotyping reaction mixes and thermo-cycler conditions per set of markers. NZB markers (Table A.1) are divided into two groups that appear as NZB 1(black-coloured markers) and NZB 2 (red-coloured markers). NZW markers are divided into 4 groups that appear as NZW 1(black-coloured markers), NZW 2 (red-coloured markers), NZW 3 (purple-coloured markers) and NZW 4 (green-coloured markers).

	DNA	5XGoTaq Green buffer	MgCl2	dNTP	Forward Primer	Reverse Primer	GoTaq polymerase	MilliQ H2O	Thermocycler conditions
Sn	1µl 1µg	10µl	3µl 1.5mM	0.2µl 0.2mM	1µl 1.5µg/ul	1µl 1.5µg/ul	0.25µl 1.25U	33.55µl	1. 95°C 2min 2. 95°C 30sec 3. 55°C 30sec 4. 72°C 1min step 2 to 4 repeat x29 5. 72°C 5min
NZB 1	1µl 1µg	10µl	3ul 1.5mM	0.2 ul 0.2mM	1ul 1ug/ul	1ul 1ug/ul	0.25µl 1.25U	33.55µl	1. 95°C 2min 2. 95°C 30sec 3. 60°C 30sec 4. 72°C 1min step 2 to 4 repeat x29 5. 72°C 5min
NZB 2	1µl 1µg	10µl	3ul 1.5mM	0.2 ul 0.2mM	1ul 1ug/ul	1ul 1ug/ul	0.25µl 1.25U	33.55µl	1. 95°C 2min 2. 95°C 30sec 3. 56°C 30sec 4. 72°C 1min step 2 to 4 repeat x29 5. 72°C 5min
NZW 1	1µl 1µg	10µl	3ul 1.5mM	0.2 ul 0.2mM	1ul 1ug/ul	1ul 1ug/ul	0.25µl 1.25U	33.55µl	1. 95°C 2min 2. 95°C 30sec 3. 60°C 30sec 4. 72°C 1min step 2 to 4 repeat x29 5. 72°C 5min
NZW 2	1µl 1µg	10µl	3ul 1.5mM	0.2 ul 0.2mM	1ul 1ug/ul	1ul 1ug/ul	0.5µl 2.5U	33.30µl	1. 95°C 2min 2. 95°C 30sec 3. 63°C 30sec 4. 72°C 1min step 2 to 4 repeat x29 5. 72°C 5min
NZW 3	1µl 1µg	10µl	3ul 1.5mM	0.2 ul 0.2mM	1ul 1ug/ul	1ul 1ug/ul	0.5µl 2.5U	33.30µl	1. 95°C 2min 2. 95°C 30sec 3. 55°C 30sec 4. 72°C 1min step 2 to 4 repeat x29 5. 72°C 5min
NZW 4	1µl 1µg	10µl	3ul 1.5mM	0.2 ul 0.2mM	1.5ul 1ug/ul	1.5ul 1ug/ul	0.5µl 2.5U	32.30µl	1. 95°C 2min 2. 95°C 30sec 3. 55°C 30sec 4. 72°C 1min step 2 to 4 repeat x29 5. 72°C 5min

References

Abe, J., Ueha, S., Suzuki, J., Tokano, Y., Matsushima, K., and Ishikawa, S. (2008). Increased Foxp3(+) CD4(+) regulatory T cells with intact suppressive activity but altered cellular localization in murine lupus. Am J Pathol *173*, 1682-1692.

Amado, M., Yan, Q., Comelli, E.M., Collins, B.E., and Paulson, J.C. (2004). Peanut agglutinin high phenotype of activated CD8+ T cells results from de novo synthesis of CD45 glycans. J Biol Chem *279*, 36689-36697.

Asano, K., Nabeyama, A., Miyake, Y., Qiu, C.H., Kurita, A., Tomura, M., Kanagawa, O., Fujii, S., and Tanaka, M. (2011). CD169-positive macrophages dominate antitumor immunity by crosspresenting dead cell-associated antigens. Immunity *34*, 85-95.

Baechler, E.C., Batliwalla, F.M., Karypis, G., Gaffney, P.M., Ortmann, W.A., Espe, K.J., Shark, K.B., Grande, W.J., Hughes, K.M., Kapur, V.*, et al.* (2003). Interferon-inducible gene expression signature in peripheral blood cells of patients with severe lupus. Proc Natl Acad Sci U S A *100*, 2610-2615.

Bai, X., Brown, J.R., Varki, A., and Esko, J.D. (2001). Enhanced 3-O-sulfation of galactose in Asn-linked glycans and Maackia amurensis lectin binding in a new Chinese hamster ovary cell line. Glycobiology *11*, 621-632.

Barnes, Y.C., Skelton, T.P., Stamenkovic, I., and Sgroi, D.C. (1999). Sialylation of the sialic acid binding lectin sialoadhesin regulates its ability to mediate cell adhesion. Blood *93*, 1245-1252.

Bebbington, C.R., Renner, G., Thomson, S., King, D., Abrams, D., and Yarranton, G.T. (1992). High-level expression of a recombinant antibody from myeloma cells using a glutamine synthetase gene as an amplifiable selectable marker. Biotechnology (N Y) *10*, 169-175.

Bennett, C.L., Brunkow, M.E., Ramsdell, F., O'Briant, K.C., Zhu, Q., Fuleihan, R.L., Shigeoka, A.O., Ochs, H.D., and Chance, P.F. (2001). A rare polyadenylation signal mutation of the FOXP3 gene (AAUAAA-->AAUGAA) leads to the IPEX syndrome. Immunogenetics *53*, 435-439.

Biesen, R., Demir, C., Barkhudarova, F., Grun, J.R., Steinbrich-Zollner, M., Backhaus, M., Haupl, T., Rudwaleit, M., Riemekasten, G., Radbruch, A.*, et al.* (2008). Sialic acid-binding Ig-like lectin 1 expression in inflammatory and resident monocytes is a potential biomarker for monitoring disease activity and success of therapy in systemic lupus erythematosus. Arthritis Rheum *58*, 1136-1145.

Blanco, P., Palucka, A.K., Gill, M., Pascual, V., and Banchereau, J. (2001). Induction of dendritic cell differentiation by IFN-alpha in systemic lupus erythematosus. Science *294*, 1540-1543.

Blander, J.M., Visintin, I., Janeway, C.A., Jr., and Medzhitov, R. (1999). Alpha(1,3)-fucosyltransferase VII and alpha(2,3)-sialyltransferase IV are up-regulated in activated CD4 T cells and maintained after their differentiation into Th1 and migration into inflammatory sites. J Immunol *163*, 3746-3752.

Blaser, C., Kaufmann, M., Muller, C., Zimmermann, C., Wells, V., Mallucci, L., and Pircher, H. (1998). Beta-galactoside-binding protein secreted by activated T cells inhibits antigen-induced proliferation of T cells. Eur J Immunol *28*, 2311-2319.

Blixt, O., Collins, B.E., van den Nieuwenhof, I.M., Crocker, P.R., and Paulson, J.C. (2003). Sialoside specificity of the siglec family assessed using novel multivalent probes: identification of potent inhibitors of myelin-associated glycoprotein. J Biol Chem *278*, 31007-31019.

Braun, D., Geraldes, P., and Demengeot, J. (2003). Type I Interferon controls the onset and severity of autoimmune manifestations in lpr mice. J Autoimmun *20*, 15-25.

Braverman, I.M. (1968). Study of autoimmune disease in New Zealand mice. I. Genetic features and natural history of NZB, NZY and NZW strains and NZB-NZW hybrids. J Invest Dermatol *50*, 483-499.

Brennan, F.M., Chantry, D., Jackson, A., Maini, R., and Feldmann, M. (1989). Inhibitory effect of TNF alpha antibodies on synovial cell interleukin-1 production in rheumatoid arthritis. Lancet *2*, 244-247.

Brunner, T., Wasem, C., Torgler, R., Cima, I., Jakob, S., and Corazza, N. (2003). Fas (CD95/Apo-1) ligand regulation in T cell homeostasis, cell-mediated cytotoxicity and immune pathology. Semin Immunol *15*, 167-176.

Brunner, T., Yoo, N.J., LaFace, D., Ware, C.F., and Green, D.R. (1996). Activation-induced cell death in murine T cell hybridomas. Differential regulation of Fas (CD95) versus Fas ligand expression by cyclosporin A and FK506. Int Immunol *8*, 1017-1026.

Bruns, A., Blass, S., Hausdorf, G., Burmester, G.R., and Hiepe, F. (2000). Nucleosomes are major T and B cell autoantigens in systemic lupus erythematosus. Arthritis Rheum *43*, 2307-2315.

Cao, X., Cai, S.F., Fehniger, T.A., Song, J., Collins, L.I., Piwnica-Worms, D.R., and Ley, T.J. (2007). Granzyme B and perforin are important for regulatory T cell-mediated suppression of tumor clearance. Immunity *27*, 635-646.

Carlow, D.A., Gossens, K., Naus, S., Veerman, K.M., Seo, W., and Ziltener, H.J. (2009). PSGL-1 function in immunity and steady state homeostasis. Immunol Rev *230*, 75-96.

Carlsson, S.R., and Fukuda, M. (1986). Isolation and characterization of leukosialin, a major sialoglycoprotein on human leukocytes. J Biol Chem *261*, 12779-12786.

Carpenter, D.F., Steinberg, A.D., Schur, P.H., and Talal, N. (1970). The pathogenesis of autoimmunity in New Zealand mice. II. Acceleration of glomerulonephritis by polyinosinic-polycytidylic acid. Lab Invest *23*, 628-634.

Cederblad, B., Blomberg, S., Vallin, H., Perers, A., Alm, G.V., and Ronnblom, L. (1998). Patients with systemic lupus erythematosus have reduced numbers of circulating natural interferon-alpha- producing cells. J Autoimmun *11*, 465-470.

Cella, M., Facchetti, F., Lanzavecchia, A., and Colonna, M. (2000). Plasmacytoid dendritic cells activated by influenza virus and CD40L drive a potent TH1 polarization. Nat Immunol *1*, 305-310.

Chambers, S.T., Powell, K.F., Croxson, M.C., Krishnan, S., and Weir, R.P. (1994). Demonstration of herpes simplex type 2 in the cerebrospinal fluid of two patients with recurrent lymphocytic meningitis. N Z Med J *107*, 367-369.

Collison, L.W., Pillai, M.R., Chaturvedi, V., and Vignali, D.A. (2009). Regulatory T cell suppression is potentiated by target T cells in a cell contact, IL-35- and IL-10-dependent manner. J Immunol *182*, 6121-6128.

Colonna, M., Krug, A., and Cella, M. (2002). Interferon-producing cells: on the front line in immune responses against pathogens. Curr Opin Immunol *14*, 373-379.

Comelli, E.M., Sutton-Smith, M., Yan, Q., Amado, M., Panico, M., Gilmartin, T., Whisenant, T., Lanigan, C.M., Head, S.R., Goldberg, D.*, et al.* (2006). Activation of murine CD4+ and CD8+ T lymphocytes leads to dramatic remodeling of N-linked glycans. J Immunol *177*, 2431-2440.

Crocker, P.R., and Gordon, S. (1986). Properties and distribution of a lectin-like hemagglutinin differentially expressed by murine stromal tissue macrophages. J Exp Med *164*, 1862-1875.
Crocker, P.R., and Gordon, S. (1989). Mouse macrophage hemagglutinin (sheep erythrocyte receptor) with specificity for sialylated glycoconjugates characterized by a monoclonal antibody. J Exp Med *169*, 1333-1346.

Crocker, P.R., Kelm, S., Dubois, C., Martin, B., McWilliam, A.S., Shotton, D.M., Paulson, J.C., and Gordon, S. (1991). Purification and properties of sialoadhesin, a sialic acid-binding receptor of murine tissue macrophages. Embo J *10*, 1661-1669.

Crocker, P.R., Mucklow, S., Bouckson, V., McWilliam, A., Willis, A.C., Gordon, S., Milon, G., Kelm, S., and Bradfield, P. (1994). Sialoadhesin, a macrophage sialic acid binding receptor for haemopoietic cells with 17 immunoglobulin-like domains. Embo J *13*, 4490-4503.

Crocker, P.R., Paulson, J.C., and Varki, A. (2007). Siglecs and their roles in the immune system. Nat Rev Immunol *7*, 255-266.

Crocker, P.R., Vinson, M., Kelm, S., and Drickamer, K. (1999). Molecular analysis of sialoside binding to sialoadhesin by NMR and site-directed mutagenesis. Biochem J *341 (Pt 2)*, 355-361.

Crocker, P.R., Werb, Z., Gordon, S., and Bainton, D.F. (1990). Ultrastructural localization of a macrophage-restricted sialic acid binding hemagglutinin, SER, in macrophage-hematopoietic cell clusters. Blood *76*, 1131-1138.

Davey, G.M., Kurts, C., Miller, J.F., Bouillet, P., Strasser, A., Brooks, A.G., Carbone, F.R., and Heath, W.R. (2002). Peripheral deletion of autoreactive CD8 T cells by cross presentation of self-antigen occurs by a Bcl-2-inhibitable pathway mediated by Bim. J Exp Med *196*, 947-955.

Denny, M.F., Chandaroy, P., Killen, P.D., Caricchio, R., Lewis, E.E., Richardson, B.C., Lee, K.D., Gavalchin, J., and Kaplan, M.J. (2006). Accelerated macrophage apoptosis induces autoantibody formation and organ damage in systemic lupus erythematosus. J Immunol *176*, 2095-2104.

Dhein, J., Walczak, H., Baumler, C., Debatin, K.M., and Krammer, P.H. (1995). Autocrine T-cell suicide mediated by APO-1/(Fas/CD95). Nature *373*, 438-441.

Diebold, S.S., Montoya, M., Unger, H., Alexopoulou, L., Roy, P., Haswell, L.E., Al-Shamkhani, A., Flavell, R., Borrow, P., and Reis e Sousa, C. (2003). Viral infection switches non-plasmacytoid dendritic cells into high interferon producers. Nature *424*, 324-328.

Drake, C.G., Babcock, S.K., Palmer, E., and Kotzin, B.L. (1994). Genetic analysis of the NZB contribution to lupus-like autoimmune disease in (NZB x NZW)F1 mice. Proc Natl Acad Sci U S A *91*, 4062-4066.

Drake, C.G., Rozzo, S.J., Vyse, T.J., Palmer, E., and Kotzin, B.L. (1995). Genetic contributions to lupus-like disease in (NZB x NZW)F1 mice. Immunol Rev *144*, 51-74.

Earl, L.A., Bi, S., and Baum, L.G. (2010). N- and O-glycans modulate galectin-1 binding, CD45 signaling, and T cell death. J Biol Chem *285*, 2232-2244.

Ebeling, W., Hennrich, N., Klockow, M., Metz, H., Orth, H.D., and Lang, H. (1974). Proteinase K from Tritirachium album Limber. Eur J Biochem *47*, 91-97.

Ellies, L.G., Ditto, D., Levy, G.G., Wahrenbrock, M., Ginsburg, D., Varki, A., Le, D.T., and Marth, J.D. (2002a). Sialyltransferase ST3Gal-IV operates as a dominant modifier of hemostasis by concealing asialoglycoprotein receptor ligands. Proc Natl Acad Sci U S A *99*, 10042-10047.

Ellies, L.G., Sperandio, M., Underhill, G.H., Yousif, J., Smith, M., Priatel, J.J., Kansas, G.S., Ley, K., and Marth, J.D. (2002b). Sialyltransferase specificity in selectin ligand formation. Blood *100*, 3618-3625.

Ellies, L.G., Tsuboi, S., Petryniak, B., Lowe, J.B., Fukuda, M., and Marth, J.D. (1998). Core 2 oligosaccharide biosynthesis distinguishes between selectin ligands essential for leukocyte homing and inflammation. Immunity *9*, 881-890.

Ellis, A.J., Curry, V.A., Powell, E.K., and Cawston, T.E. (1994). The prevention of collagen breakdown in bovine nasal cartilage by TIMP, TIMP-2 and a low molecular weight synthetic inhibitor. Biochem Biophys Res Commun *201*, 94-101.

Fahlen, L., Read, S., Gorelik, L., Hurst, S.D., Coffman, R.L., Flavell, R.A., and Powrie, F. (2005). T cells that cannot respond to TGF-beta escape control by CD4(+)CD25(+) regulatory T cells. J Exp Med *201*, 737-746.

Fantini, M.C., Becker, C., Tubbe, I., Nikolaev, A., Lehr, H.A., Galle, P., and Neurath, M.F. (2006). Transforming growth factor beta induced FoxP3+ regulatory T cells suppress Th1 mediated experimental colitis. Gut *55*, 671-680.

Farina, G., Lafyatis, D., Lemaire, R., and Lafyatis, R. (2010). A four-gene biomarker predicts skin disease in patients with diffuse cutaneous systemic sclerosis. Arthritis Rheum *62*, 580-588.

Feng, X., Wu, H., Grossman, J.M., Hanvivadhanakul, P., FitzGerald, J.D., Park, G.S., Dong, X., Chen, W., Kim, M.H., Weng, H.H*., et al.* (2006). Association of increased interferon-inducible gene expression with disease activity and lupus nephritis in patients with systemic lupus erythematosus. Arthritis Rheum *54*, 2951-2962.

Finck, B.K., Chan, B., and Wofsy, D. (1994). Interleukin 6 promotes murine lupus in NZB/NZW F1 mice. J Clin Invest *94*, 585-591.

Fontenot, J.D., Gavin, M.A., and Rudensky, A.Y. (2003). Foxp3 programs the development and function of CD4+CD25+ regulatory T cells. Nat Immunol *4*, 330-336.

Freeman, S.D., Kelm, S., Barber, E.K., and Crocker, P.R. (1995). Characterization of CD33 as a new member of the sialoadhesin family of cellular interaction molecules. Blood *85*, 2005-2012.

Fukuda, M. (1991). Leukosialin, a major O-glycan-containing sialoglycoprotein defining leukocyte differentiation and malignancy. Glycobiology *1*, 347-356.

Gallagher, K.M., Lauder, S., Rees, I.W., Gallimore, A.M., and Godkin, A.J. (2009). Type I interferon (IFN alpha) acts directly on human memory CD4+ T cells altering their response to antigen. J Immunol *183*, 2915-2920.

Garin, M.I., Chu, C.C., Golshayan, D., Cernuda-Morollon, E., Wait, R., and Lechler, R.I. (2007). Galectin-1: a key effector of regulation mediated by CD4+CD25+ T cells. Blood *109*, 2058-2065.

Gillespie, W., Paulson, J.C., Kelm, S., Pang, M., and Baum, L.G. (1993). Regulation of alpha 2,3-sialyltransferase expression correlates with conversion of peanut agglutinin (PNA)+ to PNA- phenotype in developing thymocytes. J Biol Chem *268*, 3801-3804.

Gondek, D.C., Lu, L.F., Quezada, S.A., Sakaguchi, S., and Noelle, R.J. (2005). Cutting edge: contact-mediated suppression by CD4+CD25+ regulatory cells involves a granzyme B-dependent, perforin-independent mechanism. J Immunol *174*, 1783-1786.

Grabie, N., Delfs, M.W., Lim, Y.C., Westrich, J.R., Luscinskas, F.W., and Lichtman, A.H. (2002). Beta-galactoside alpha2,3-sialyltransferase-I gene expression during Th2 but not Th1 differentiation: implications for core2-glycan formation on cell surface proteins. Eur J Immunol *32*, 2766-2772.

Green, D.R., Droin, N., and Pinkoski, M. (2003). Activation-induced cell death in T cells. Immunol Rev *193*, 70-81.

Green, R.S., Stone, E.L., Tenno, M., Lehtonen, E., Farquhar, M.G., and Marth, J.D. (2007). Mammalian N-glycan branching protects against innate immune self-recognition and inflammation in autoimmune disease pathogenesis. Immunity *27*, 308-320.

Hartnell, A., Steel, J., Turley, H., Jones, M., Jackson, D.G., and Crocker, P.R. (2001). Characterization of human sialoadhesin, a sialic acid binding receptor expressed by resident and inflammatory macrophage populations. Blood *97*, 288-296.

Hashimoto, Y., Suzuki, M., Crocker, P.R., and Suzuki, A. (1998). A streptavidin-based neoglycoprotein carrying more than 140 GT1b oligosaccharides: quantitative estimation of the binding specificity of murine sialoadhesin expressed on CHO cells. J Biochem *123*, 468-478.

Hayashi, T., Hasegawa, K., and Adachi, C. (2005). Elimination of CD4(+)CD25(+) T cell accelerates the development of glomerulonephritis during the preactive phase in autoimmune-prone female NZB x NZW F mice. Int J Exp Pathol *86*, 289-296.

Hayes, M.J., Khemani, L., and Powell, M.L. (1994). Quantitative determination of the NMDA antagonist cis-4-phosphonomethyl-2-piperidine carboxylic acid (CGS 19755) in human plasma using capillary gas chromatography/mass spectrometry. Biol Mass Spectrom *23*, 555-561.

Hennet, T., Chui, D., Paulson, J.C., and Marth, J.D. (1998). Immune regulation by the ST6Gal sialyltransferase. Proc Natl Acad Sci U S A *95*, 4504-4509.

Hermiston, M.L., Xu, Z., and Weiss, A. (2003). CD45: a critical regulator of signaling thresholds in immune cells. Annu Rev Immunol *21*, 107-137.

Hernandez, J.D., Klein, J., Van Dyken, S.J., Marth, J.D., and Baum, L.G. (2007). T-cell activation results in microheterogeneous changes in glycosylation of CD45. Int Immunol *19*, 847-856.

Hiki, Y., Odani, H., Takahashi, M., Yasuda, Y., Nishimoto, A., Iwase, H., Shinzato, T., Kobayashi, Y., and Maeda, K. (2001). Mass spectrometry proves under-O-glycosylation of glomerular IgA1 in IgA nephropathy. Kidney Int *59*, 1077-1085.

Holmes, N. (2006). CD45: all is not yet crystal clear. Immunology *117*, 145-155.
Hooks, J.J., Moutsopoulos, H.M., Geis, S.A., Stahl, N.I., Decker, J.L., and Notkins, A.L. (1979). Immune interferon in the circulation of patients with autoimmune disease. N Engl J Med *301*, 5-8.

Hori, S., Nomura, T., and Sakaguchi, S. (2003). Control of regulatory T cell development by the transcription factor Foxp3. Science *299*, 1057-1061.

Ikezumi, Y., Suzuki, T., Hayafuji, S., Okubo, S., Nikolic-Paterson, D.J., Kawachi, H., Shimizu, F., and Uchiyama, M. (2005). The sialoadhesin (CD169) expressing a macrophage subset in human proliferative glomerulonephritis. Nephrol Dial Transplant *20*, 2704-2713.

Inoue, T., Tsuzuki, Y., Matsuzaki, K., Matsunaga, H., Miyazaki, J., Hokari, R., Okada, Y., Kawaguchi, A., Nagao, S., Itoh, K.*, et al.* (2005). Blockade of PSGL-1 attenuates CD14+ monocytic cell recruitment in intestinal mucosa and ameliorates ileitis in SAMP1/Yit mice. J Leukoc Biol *77*, 287-295.

Ip, C.W., Kroner, A., Crocker, P.R., Nave, K.A., and Martini, R. (2007). Sialoadhesin deficiency ameliorates myelin degeneration and axonopathic changes in the CNS of PLP overexpressing mice. Neurobiol Dis *25*, 105-111.

Ishida, H., Muchamuel, T., Sakaguchi, S., Andrade, S., Menon, S., and Howard, M. (1994). Continuous administration of anti-interleukin 10 antibodies delays onset of autoimmunity in NZB/W F1 mice. J Exp Med *179*, 305-310.

Ito, Y., Kawachi, H., Morioka, Y., Nakatsue, T., Koike, H., Ikezumi, Y., Oyanagi, A., Natori, Y., Nakamura, T., Gejyo, F., and Shimizu, F. (2002). Fractalkine expression and the recruitment of CX3CR1+ cells in the prolonged mesangial proliferative glomerulonephritis. Kidney Int *61*, 2044-2057.

Ivanov, II, Frutos Rde, L., Manel, N., Yoshinaga, K., Rifkin, D.B., Sartor, R.B., Finlay, B.B., and Littman, D.R. (2008). Specific microbiota direct the differentiation of IL-17-producing T-helper cells in the mucosa of the small intestine. Cell Host Microbe *4*, 337-349.

Iwano, M., Dohi, K., Hirata, E., Kurumatani, N., Horii, Y., Shiiki, H., Fukatsu, A., Matsuda, T., Hirano, T., Kishimoto, T., and et al. (1993). Urinary levels of IL-6 in patients with active lupus nephritis. Clin Nephrol *40*, 16-21.

Jiang, H.R., Hwenda, L., Makinen, K., Oetke, C., Crocker, P.R., and Forrester, J.V. (2006). Sialoadhesin promotes the inflammatory response in experimental autoimmune uveoretinitis. J Immunol *177*, 2258-2264.

Jiang, N., Reich, C.F., 3rd, and Pisetsky, D.S. (2003). Role of macrophages in the generation of circulating blood nucleosomes from dead and dying cells. Blood *102*, 2243-2250.

Johnson, G.G., Mikulowska, A., Butcher, E.C., McEvoy, L.M., and Michie, S.A. (1999). Anti-CD43 monoclonal antibody L11 blocks migration of T cells to inflamed pancreatic islets and prevents development of diabetes in nonobese diabetic mice. J Immunol *163*, 5678-5685.

Jones, A.T., Fedorsppiel, B., Ellies, L.G., Williams, M.J., Burgener, R., Duronio, V., Smith, C.A., Takei, F., and Ziltener, H.J. (1994). Characterization of the activation-associated isoform of CD43 on murine T lymphocytes. J Immunol *153*, 3426-3439.

Josefowicz, S.Z., and Rudensky, A. (2009). Control of regulatory T cell lineage commitment and maintenance. Immunity *30*, 616-625.

Junghans, R.P., and Waldmann, T.A. (1996). Metabolism of Tac (IL2Ralpha): physiology of cell surface shedding and renal catabolism, and suppression of catabolism by antibody binding. J Exp Med *183*, 1587-1602.

Kalkner, K.M., Ronnblom, L., Karlsson Parra, A.K., Bengtsson, M., Olsson, Y., and Oberg, K. (1998). Antibodies against double-stranded DNA and development of polymyositis during treatment with interferon. Qjm *91*, 393-399.

Kamada, S., Shimono, A., Shinto, Y., Tsujimura, T., Takahashi, T., Noda, T., Kitamura, Y., Kondoh, H., and Tsujimoto, Y. (1995). bcl-2 deficiency in mice leads to pleiotropic abnormalities: accelerated lymphoid cell death in thymus and spleen, polycystic kidney, hair hypopigmentation, and distorted small intestine. Cancer Res *55*, 354-359.

Kasagi, S., Kawano, S., Okazaki, T., Honjo, T., Morinobu, A., Hatachi, S., Shimatani, K., Tanaka, Y., Minato, N., and Kumagai, S. (2010). Anti-programmed cell death 1 antibody reduces CD4+PD-1+ T cells and relieves the lupus-like nephritis of NZB/W F1 mice. J Immunol *184*, 2337-2347.

Kelm, S., Schauer, R., Manuguerra, J.C., Gross, H.J., and Crocker, P.R. (1994). Modifications of cell surface sialic acids modulate cell adhesion mediated by sialoadhesin and CD22. Glycoconj J *11*, 576-585.

Kitani, A., Hara, M., Hirose, T., Harigai, M., Suzuki, K., Kawakami, M., Kawaguchi, Y., Hidaka, T., Kawagoe, M., and Nakamura, H. (1992). Autostimulatory effects of IL-6 on excessive B cell differentiation in patients with systemic lupus erythematosus: analysis of IL-6 production and IL-6R expression. Clin Exp Immunol *88*, 75-83.

Knoechel, B., Lohr, J., Kahn, E., Bluestone, J.A., and Abbas, A.K. (2005). Sequential development of interleukin 2-dependent effector and regulatory T cells in response to endogenous systemic antigen. J Exp Med *202*, 1375-1386.

Kobsar, I., Oetke, C., Kroner, A., Wessig, C., Crocker, P., and Martini, R. (2006). Attenuated demyelination in the absence of the macrophage-restricted adhesion molecule sialoadhesin (Siglec-1) in mice heterozygously deficient in P0. Mol Cell Neurosci *31*, 685-691.

Kono, D.H., Burlingame, R.W., Owens, D.G., Kuramochi, A., Balderas, R.S., Balomenos, D., and Theofilopoulos, A.N. (1994). Lupus susceptibility loci in New Zealand mice. Proc Natl Acad Sci U S A *91*, 10168-10172.

Kono, M., Ohyama, Y., Lee, Y.C., Hamamoto, T., Kojima, N., and Tsuji, S. (1997). Mouse beta-galactoside alpha 2,3-sialyltransferases: comparison of in vitro substrate specificities and tissue specific expression. Glycobiology *7*, 469-479.

Kotzin, B.L. (1996). Systemic lupus erythematosus. Cell *85*, 303-306.

Kotzin, B.L., and Palmer, E. (1987). The contribution of NZW genes to lupus-like disease in (NZB x NZW)F1 mice. J Exp Med *165*, 1237-1251.

Krug, A., Rothenfusser, S., Hornung, V., Jahrsdorfer, B., Blackwell, S., Ballas, Z.K., Endres, S., Krieg, A.M., and Hartmann, G. (2001). Identification of CpG oligonucleotide sequences with high induction of IFN-alpha/beta in plasmacytoid dendritic cells. Eur J Immunol *31*, 2154-2163.

Kumamoto, Y., Higashi, N., Denda-Nagai, K., Tsuiji, M., Sato, K., Crocker, P.R., and Irimura, T. (2004). Identification of sialoadhesin as a dominant lymph node counter-receptor for mouse macrophage galactose-type C-type lectin 1. J Biol Chem *279*, 49274-49280.

La Cava, A., Ebling, F.M., and Hahn, B.H. (2004). Ig-reactive CD4+CD25+ T cells from tolerized (New Zealand Black x New Zealand White)F1 mice suppress in vitro production of antibodies to DNA. J Immunol *173*, 3542-3548.

Le Bon, A., Thompson, C., Kamphuis, E., Durand, V., Rossmann, C., Kalinke, U., and Tough, D.F. (2006). Cutting edge: enhancement of antibody responses through direct stimulation of B and T cells by type I IFN. J Immunol *176*, 2074-2078.

Lee, Y.C., Kojima, N., Wada, E., Kurosawa, N., Nakaoka, T., Hamamoto, T., and Tsuji, S. (1994). Cloning and expression of cDNA for a new type of Gal beta 1,3GalNAc alpha 2,3-sialyltransferase. J Biol Chem *269*, 10028-10033.

Linker-Israeli, M., Deans, R.J., Wallace, D.J., Prehn, J., Ozeri-Chen, T., and Klinenberg, J.R. (1991). Elevated levels of endogenous IL-6 in systemic lupus erythematosus. A putative role in pathogenesis. J Immunol *147*, 117-123.

Liu, J.P., Powell, K.A., Sudhof, T.C., and Robinson, P.J. (1994). Dynamin I is a Ca(2+)-sensitive phospholipid-binding protein with very high affinity for protein kinase C. J Biol Chem *269*, 21043-21050.

Liu, Z., Bethunaickan, R., Huang, W., Lodhi, U., Solano, I., Madaio, M.P., and Davidson, A. (2011). Interferon-alpha accelerates murine systemic lupus erythematosus in a T cell-dependent manner. Arthritis Rheum *63*, 219-229.

Lopez, P., Gutierrez, C., and Suarez, A. (2010). IL-10 and TNFalpha genotypes in SLE. J Biomed Biotechnol *2010*, 838390.

Lovgren, T., Eloranta, M.L., Bave, U., Alm, G.V., and Ronnblom, L. (2004). Induction of interferon-alpha production in plasmacytoid dendritic cells by immune complexes containing nucleic acid released by necrotic or late apoptotic cells and lupus IgG. Arthritis Rheum *50*, 1861-1872.

Marie, J.C., Liggitt, D., and Rudensky, A.Y. (2006). Cellular mechanisms of fatal early-onset autoimmunity in mice with the T cell-specific targeting of transforming growth factor-beta receptor. Immunity *25*, 441-454.

Marth, J.D., and Grewal, P.K. (2008). Mammalian glycosylation in immunity. Nat Rev Immunol *8*, 874-887.

Martinez-Pomares, L., Crocker, P.R., Da Silva, R., Holmes, N., Colominas, C., Rudd, P., Dwek, R., and Gordon, S. (1999). Cell-specific glycoforms of sialoadhesin and CD45 are counter-receptors for the cysteine-rich domain of the mannose receptor. J Biol Chem *274*, 35211-35218.

Mathian, A., Weinberg, A., Gallegos, M., Banchereau, J., and Koutouzov, S. (2005). IFN-alpha induces early lethal lupus in preautoimmune (New Zealand Black x New Zealand White) F1 but not in BALB/c mice. J Immunol *174*, 2499-2506.

May, A.P., Robinson, R.C., Vinson, M., Crocker, P.R., and Jones, E.Y. (1998). Crystal structure of the N-terminal domain of sialoadhesin in complex with 3' sialyllactose at 1.85 A resolution. Mol Cell *1*, 719-728.

McNeill, L., Salmond, R.J., Cooper, J.C., Carret, C.K., Cassady-Cain, R.L., Roche-Molina, M., Tandon, P., Holmes, N., and Alexander, D.R. (2007). The differential regulation of Lck kinase phosphorylation sites by CD45 is critical for T cell receptor signaling responses. Immunity *27*, 425-437.

McRae, B.L., Nagai, T., Semnani, R.T., van Seventer, J.M., and van Seventer, G.A. (2000). Interferon-alpha and -beta inhibit the in vitro differentiation of immunocompetent human dendritic cells from CD14(+) precursors. Blood *96*, 210-217.

Merzaban, J.S., Zuccolo, J., Corbel, S.Y., Williams, M.J., and Ziltener, H.J. (2005). An alternate core 2 beta1,6-N-acetylglucosaminyltransferase selectively contributes to P-selectin ligand formation in activated CD8 T cells. J Immunol *174*, 4051-4059.

Meyers, J.A., Mangini, A.J., Nagai, T., Roff, C.F., Sehy, D., van Seventer, G.A., and van Seventer, J.M. (2006). Blockade of TLR9 agonist-induced type I interferons promotes inflammatory cytokine IFN-gamma and IL-17 secretion by activated human PBMC. Cytokine *35*, 235-246.

Mohan, C., Morel, L., Yang, P., and Wakeland, E.K. (1997). Genetic dissection of systemic lupus erythematosus pathogenesis: Sle2 on murine chromosome 4 leads to B cell hyperactivity. J Immunol *159*, 454-465.

Mohan, C., Morel, L., Yang, P., and Wakeland, E.K. (1998). Accumulation of splenic B1a cells with potent antigen-presenting capability in NZM2410 lupus-prone mice. Arthritis Rheum *41*, 1652-1662.

Mohan, C., Morel, L., Yang, P., Watanabe, H., Croker, B., Gilkeson, G., and Wakeland, E.K. (1999). Genetic dissection of lupus pathogenesis: a recipe for nephrophilic autoantibodies. J Clin Invest *103*, 1685-1695.

Monk, C.R., Spachidou, M., Rovis, F., Leung, E., Botto, M., Lechler, R.I., and Garden, O.A. (2005). MRL/Mp CD4+,CD25- T cells show reduced sensitivity to suppression by CD4+,CD25+ regulatory T cells in vitro: a novel defect of T cell regulation in systemic lupus erythematosus. Arthritis Rheum *52*, 1180-1184.

Morel, L., Tian, X.H., Croker, B.P., and Wakeland, E.K. (1999). Epistatic modifiers of autoimmunity in a murine model of lupus nephritis. Immunity *11*, 131-139.

Mucklow, S., Gordon, S., and Crocker, P.R. (1997). Characterization of the mouse sialoadhesin gene, Sn. Mamm Genome *8*, 934-937.

Munday, J., Floyd, H., and Crocker, P.R. (1999). Sialic acid binding receptors (siglecs) expressed by macrophages. J Leukoc Biol *66*, 705-711.

Nagai, T., Devergne, O., Mueller, T.F., Perkins, D.L., van Seventer, J.M., and van Seventer, G.A. (2003). Timing of IFN-beta exposure during human dendritic cell maturation and naive Th cell stimulation has contrasting effects on Th1 subset generation: a role for IFN-beta-mediated regulation of IL-12 family cytokines and IL-18 in naive Th cell differentiation. J Immunol *171*, 5233-5243.

Nakamura, K., Yamaji, T., Crocker, P.R., Suzuki, A., and Hashimoto, Y. (2002). Lymph node macrophages, but not spleen macrophages, express high levels of unmasked sialoadhesin: implication for the adhesive properties of macrophages in vivo. Glycobiology *12*, 209-216.

Nath, D., Hartnell, A., Happerfield, L., Miles, D.W., Burchell, J., Taylor-Papadimitriou, J., and Crocker, P.R. (1999). Macrophage-tumour cell interactions: identification of MUC1 on breast cancer cells as a potential counter-receptor for the macrophage-restricted receptor, sialoadhesin. Immunology *98*, 213-219.

Nguyen, J.T., Evans, D.P., Galvan, M., Pace, K.E., Leitenberg, D., Bui, T.N., and Baum, L.G. (2001). CD45 modulates galectin-1-induced T cell death: regulation by expression of core 2 O-glycans. J Immunol *167*, 5697-5707.

Oberle, N., Eberhardt, N., Falk, C.S., Krammer, P.H., and Suri-Payer, E. (2007). Rapid suppression of cytokine transcription in human CD4+CD25 T cells by CD4+Foxp3+ regulatory T cells: independence of IL-2 consumption, TGF-beta, and various inhibitors of TCR signaling. J Immunol *179*, 3578-3587.

Oetke, C., Vinson, M.C., Jones, C., and Crocker, P.R. (2006). Sialoadhesin-deficient mice exhibit subtle changes in B- and T-cell populations and reduced immunoglobulin M levels. Mol Cell Biol *26*, 1549-1557.

Onami, T.M., Harrington, L.E., Williams, M.A., Galvan, M., Larsen, C.P., Pearson, T.C., Manjunath, N., Baum, L.G., Pearce, B.D., and Ahmed, R. (2002). Dynamic regulation of T cell immunity by CD43. J Immunol *168*, 6022-6031.

Pasare, C., and Medzhitov, R. (2003). Toll pathway-dependent blockade of CD4+CD25+ T cell-mediated suppression by dendritic cells. Science *299*, 1033-1036.

Pillemer, B.B., Xu, H., Oriss, T.B., Qi, Z., and Ray, A. (2007). Deficient SOCS3 expression in CD4+CD25+FoxP3+ regulatory T cells and SOCS3-mediated suppression of Treg function. Eur J Immunol *37*, 2082-2089.

Powell, E.E., Wicker, L.S., Peterson, L.B., and Todd, J.A. (1994a). Allelic variation of the type 2 tumor necrosis factor receptor gene. Mamm Genome *5*, 726-727.

Powell, F.C., Spooner, K.M., Shawker, T.H., Premkumar, A., Thakore, K.N., Vogel, S.E., Kovacs, J.A., Masur, H., and Feuerstein, I.M. (1994b). Symptomatic interleukin-2-induced cholecystopathy in patients with HIV infection. AJR Am J Roentgenol *163*, 117-121.

Powell, J.D., Ragheb, J.A., Kitagawa-Sakakida, S., and Schwartz, R.H. (1998). Molecular regulation of interleukin-2 expression by CD28 co-stimulation and anergy. Immunol Rev *165*, 287-300.

Preble, O.T., Black, R.J., Friedman, R.M., Klippel, J.H., and Vilcek, J. (1982). Systemic lupus erythematosus: presence in human serum of an unusual acid-labile leukocyte interferon. Science *216*, 429-431.

Preble, O.T., Rothko, K., Klippel, J.H., Friedman, R.M., and Johnston, M.I. (1983). Interferon-induced 2'-5' adenylate synthetase in vivo and interferon production in vitro by lymphocytes from systemic lupus erythematosus patients with and without circulating interferon. J Exp Med *157*, 2140-2146.

Priatel, J.J., Chui, D., Hiraoka, N., Simmons, C.J., Richardson, K.B., Page, D.M., Fukuda, M., Varki, N.M., and Marth, J.D. (2000). The ST3Gal-I sialyltransferase controls CD8+ T lymphocyte homeostasis by modulating O-glycan biosynthesis. Immunity *12*, 273-283.

Provost, T.T., Watson, R., and Simmons-O'Brien, E. (1996). Significance of the anti-Ro (SS-A) antibody in evaluation of patients with cutaneous manifestations of a connective tissue disease. J Am Acad Dermatol *35*, 147-169; quiz 170-142.

Pulliam, L., Sun, B., and Rempel, H. (2004). Invasive chronic inflammatory monocyte phenotype in subjects with high HIV-1 viral load. J Neuroimmunol *157*, 93-98.

Rabinovich, G.A., and Toscano, M.A. (2009). Turning 'sweet' on immunity: galectin-glycan interactions in immune tolerance and inflammation. Nat Rev Immunol *9*, 338-352.

Rahman, Z.S., Tin, S.K., Buenaventura, P.N., Ho, C.H., Yap, E.P., Yong, R.Y., and Koh, D.R. (2002). A novel susceptibility locus on chromosome 2 in the (New Zealand Black x New Zealand White)F1 hybrid mouse model of systemic lupus erythematosus. J Immunol *168*, 3042-3049.

Ren, Y., Tang, J., Mok, M.Y., Chan, A.W., Wu, A., and Lau, C.S. (2003). Increased apoptotic neutrophils and macrophages and impaired macrophage phagocytic clearance of apoptotic neutrophils in systemic lupus erythematosus. Arthritis Rheum *48*, 2888-2897.

Rigby, R.J., Rozzo, S.J., Boyle, J.J., Lewis, M., Kotzin, B.L., and Vyse, T.J. (2004). New loci from New Zealand Black and New Zealand White mice on chromosomes 4 and 12 contribute to lupus-like disease in the context of BALB/c. J Immunol *172*, 4609-4617.

Rini, J., Esko, J., and Varki, A. (2009). Glycosyltransferases and Glycan-processing Enzymes. In Essentials of Glycobiology, A. Varki, R.D. Cummings, J.D. Esko, H.H. Freeze, P. Stanley, C.R. Bertozzi, G.W. Hart, and M.E. Etzler, eds. (Cold Spring Harbor (NY)).

Roncarolo, M.G., and Gregori, S. (2008). Is FOXP3 a bona fide marker for human regulatory T cells? Eur J Immunol *38*, 925-927.

Ronnblom, L., and Alm, G.V. (2001). A pivotal role for the natural interferon alpha-producing cells (plasmacytoid dendritic cells) in the pathogenesis of lupus. J Exp Med *194*, F59-63.

Ronnblom, L.E., Alm, G.V., and Oberg, K. (1991). Autoimmune phenomena in patients with malignant carcinoid tumors during interferon-alpha treatment. Acta Oncol *30*, 537-540.

Rousset, F., Garcia, E., Defrance, T., Peronne, C., Vezzio, N., Hsu, D.H., Kastelein, R., Moore, K.W., and Banchereau, J. (1992). Interleukin 10 is a potent growth and differentiation factor for activated human B lymphocytes. Proc Natl Acad Sci U S A *89*, 1890-1893.

Rozzo, S.J., Allard, J.D., Choubey, D., Vyse, T.J., Izui, S., Peltz, G., and Kotzin, B.L. (2001). Evidence for an interferon-inducible gene, Ifi202, in the susceptibility to systemic lupus. Immunity *15*, 435-443.

Rozzo, S.J., Vyse, T.J., Drake, C.G., and Kotzin, B.L. (1996). Effect of genetic background on the contribution of New Zealand black loci to autoimmune lupus nephritis. Proc Natl Acad Sci U S A *93*, 15164-15168.

Sakaguchi, S., Sakaguchi, N., Asano, M., Itoh, M., and Toda, M. (1995). Immunologic self-tolerance maintained by activated T cells expressing IL-2 receptor alpha-chains (CD25). Breakdown of a single mechanism of self-tolerance causes various autoimmune diseases. J Immunol *155*, 1151-1164.

Sakaguchi, S., Yamaguchi, T., Nomura, T., and Ono, M. (2008). Regulatory T cells and immune tolerance. Cell *133*, 775-787.

Salmond, R.J., McNeill, L., Holmes, N., and Alexander, D.R. (2008). CD4+ T cell hyper-responsiveness in CD45 transgenic mice is independent of isoform. Int Immunol *20*, 819-827.

Santiago-Raber, M.L., Baccala, R., Haraldsson, K.M., Choubey, D., Stewart, T.A., Kono, D.H., and Theofilopoulos, A.N. (2003). Type-I interferon receptor deficiency reduces lupus-like disease in NZB mice. J Exp Med *197*, 777-788.

Santiago, M.L., Mary, C., Parzy, D., Jacquet, C., Montagutelli, X., Parkhouse, R.M., Lemoine, R., Izui, S., and Reininger, L. (1998). Linkage of a major quantitative trait locus to Yaa gene-induced lupus-like nephritis in (NZW x C57BL/6)F1 mice. Eur J Immunol *28*, 4257-4267.

Scalapino, K.J., Tang, Q., Bluestone, J.A., Bonyhadi, M.L., and Daikh, D.I. (2006). Suppression of disease in New Zealand Black/New Zealand White lupus-prone mice by adoptive transfer of ex vivo expanded regulatory T cells. J Immunol *177*, 1451-1459.

Scheinecker, C., Bonelli, M., and Smolen, J.S. (2010). Pathogenetic aspects of systemic lupus erythematosus with an emphasis on regulatory T cells. J Autoimmun *35*, 269-275.

Schiffenbauer, J., Wegrzyn, L., and Croker, B.P. (1992). Background genes mediate the development of autoimmunity in (NZB x PL/J)F1 or (NZB x BIO.PL)F1 mice. Clin Immunol Immunopathol *62*, 227-234.

Schwientek, T., Nomoto, M., Levery, S.B., Merkx, G., van Kessel, A.G., Bennett, E.P., Hollingsworth, M.A., and Clausen, H. (1999). Control of O-glycan branch formation. Molecular cloning of human cDNA encoding a novel beta1,6-N-acetylglucosaminyltransferase forming core 2 and core 4. J Biol Chem *274*, 4504-4512.

Schwientek, T., Yeh, J.C., Levery, S.B., Keck, B., Merkx, G., van Kessel, A.G., Fukuda, M., and Clausen, H. (2000). Control of O-glycan branch formation. Molecular cloning and characterization of a novel thymus-associated core 2 beta1, 6-n-acetylglucosaminyltransferase. J Biol Chem *275*, 11106-11113.

Seo, W., and Ziltener, H.J. (2009). CD43 processing and nuclear translocation of CD43 cytoplasmic tail are required for cell homeostasis. Blood *114*, 3567-3577.

Serreze, D.V., Chapman, H.D., Varnum, D.S., Hanson, M.S., Reifsnyder, P.C., Richard, S.D., Fleming, S.A., Leiter, E.H., and Shultz, L.D. (1996). B lymphocytes are essential for the initiation of T cell-mediated autoimmune diabetes: analysis of a new "speed congenic" stock of NOD.Ig mu null mice. J Exp Med *184*, 2049-2053.

Siegal, F.P., Kadowaki, N., Shodell, M., Fitzgerald-Bocarsly, P.A., Shah, K., Ho, S., Antonenko, S., and Liu, Y.J. (1999). The nature of the principal type 1 interferon-producing cells in human blood. Science *284*, 1835-1837.

Silverman, E.D., Buyon, J., Laxer, R.M., Hamilton, R., Bini, P., Chu, J.L., and Elkon, K.B. (1995). Autoantibody response to the Ro/La particle may predict outcome in neonatal lupus erythematosus. Clin Exp Immunol *100*, 499-505.

Snapp, K.R., Heitzig, C.E., Ellies, L.G., Marth, J.D., and Kansas, G.S. (2001). Differential requirements for the O-linked branching enzyme core 2 beta1-6-N-glucosaminyltransferase in biosynthesis of ligands for E-selectin and P-selectin. Blood *97*, 3806-3811.

Sonnenburg, J.L., Altheide, T.K., and Varki, A. (2004). A uniquely human consequence of domain-specific functional adaptation in a sialic acid-binding receptor. Glycobiology *14*, 339-346.

Sperandio, M., Frommhold, D., Babushkina, I., Ellies, L.G., Olson, T.S., Smith, M.L., Fritzsching, B., Pauly, E., Smith, D.F., Nobiling, R.*, et al.* (2006). Alpha 2,3-sialyltransferase-IV is essential for L-selectin ligand function in inflammation. Eur J Immunol *36*, 3207-3215.

Sperandio, M., Thatte, A., Foy, D., Ellies, L.G., Marth, J.D., and Ley, K. (2001). Severe impairment of leukocyte rolling in venules of core 2 glucosaminyltransferase-deficient mice. Blood *97*, 3812-3819.

Sperling, A.I., Green, J.M., Mosley, R.L., Smith, P.L., DiPaolo, R.J., Klein, J.R., Bluestone, J.A., and Thompson, C.B. (1995). CD43 is a murine T cell costimulatory receptor that functions independently of CD28. J Exp Med *182*, 139-146.

Sugimoto, N., Oida, T., Hirota, K., Nakamura, K., Nomura, T., Uchiyama, T., and Sakaguchi, S. (2006). Foxp3-dependent and -independent molecules specific for CD25+CD4+ natural regulatory T cells revealed by DNA microarray analysis. Int Immunol *18*, 1197-1209.

Takashima, S. (2008). Characterization of mouse sialyltransferase genes: their evolution and diversity. Biosci Biotechnol Biochem *72*, 1155-1167.

Taylor, M.W., Grosse, W.M., Schaley, J.E., Sanda, C., Wu, X., Chien, S.C., Smith, F., Wu, T.G., Stephens, M., Ferris, M.W.*, et al.* (2004). Global effect of PEG-IFN-alpha and ribavirin on gene expression in PBMC in vitro. J Interferon Cytokine Res *24*, 107-118.

Testi, R., D'Ambrosio, D., De Maria, R., and Santoni, A. (1994). The CD69 receptor: a multipurpose cell-surface trigger for hematopoietic cells. Immunol Today *15*, 479-483.

Thomas, M.L. (1989). The leukocyte common antigen family. Annu Rev Immunol *7*, 339-369.

Thornton, A.M., Korty, P.E., Tran, D.Q., Wohlfert, E.A., Murray, P.E., Belkaid, Y., and Shevach, E.M. (2010). Expression of Helios, an Ikaros transcription factor family member, differentiates thymic-derived from peripherally induced Foxp3+ T regulatory cells. J Immunol *184*, 3433-3441.

Thurman, E.C., Walker, J., Jayaraman, S., Manjunath, N., Ardman, B., and Green, J.M. (1998). Regulation of in vitro and in vivo T cell activation by CD43. Int Immunol *10*, 691-701.

Tran, D.Q., Glass, D.D., Uzel, G., Darnell, D.A., Spalding, C., Holland, S.M., and Shevach, E.M. (2009). Analysis of adhesion molecules, target cells, and role of IL-2 in human FOXP3+ regulatory T cell suppressor function. J Immunol *182*, 2929-2938.

Tucker, C.F., Nebane-Ambe, D.L., Chhabra, A., Parnell, S.A., Zhao, Y., Alard, P., and Kosiewicz, M.M. (2011). Decreased frequencies of CD4(+)CD25(+)Foxp3(+) cells and the potent CD103(+) subset in peripheral lymph nodes correlate with autoimmune disease predisposition in some strains of mice. Autoimmunity.

Tucker, R.M., Vyse, T.J., Rozzo, S., Roark, C.L., Izui, S., and Kotzin, B.L. (2000). Genetic control of glycoprotein 70 autoantigen production and its influence on immune complex levels and nephritis in murine lupus. J Immunol *165*, 1665-1672.

Uccellini, M.B., Busconi, L., Green, N.M., Busto, P., Christensen, S.R., Shlomchik, M.J., Marshak-Rothstein, A., and Viglianti, G.A. (2008). Autoreactive B cells discriminate CpG-rich and CpG-poor DNA and this response is modulated by IFN-alpha. J Immunol *181*, 5875-5884.

Underhill, G.H., Zisoulis, D.G., Kolli, K.P., Ellies, L.G., Marth, J.D., and Kansas, G.S. (2005). A crucial role for T-bet in selectin ligand expression in T helper 1 (Th1) cells. Blood *106*, 3867-3873.

Valencia, X., Stephens, G., Goldbach-Mansky, R., Wilson, M., Shevach, E.M., and Lipsky, P.E. (2006). TNF downmodulates the function of human CD4+CD25hi T-regulatory cells. Blood *108*, 253-261.

Vallin, H., Blomberg, S., Alm, G.V., Cederblad, B., and Ronnblom, L. (1999a). Patients with systemic lupus erythematosus (SLE) have a circulating inducer of interferon-alpha (IFN-alpha) production acting on leucocytes resembling immature dendritic cells. Clin Exp Immunol *115*, 196-202.

Vallin, H., Perers, A., Alm, G.V., and Ronnblom, L. (1999b). Anti-double-stranded DNA antibodies and immunostimulatory plasmid DNA in combination mimic the endogenous IFN-alpha inducer in systemic lupus erythematosus. J Immunol *163*, 6306-6313.

van den Berg, T.K., Breve, J.J., Damoiseaux, J.G., Dopp, E.A., Kelm, S., Crocker, P.R., Dijkstra, C.D., and Kraal, G. (1992). Sialoadhesin on macrophages: its identification as a lymphocyte adhesion molecule. J Exp Med *176*, 647-655.

van den Berg, T.K., Nath, D., Ziltener, H.J., Vestweber, D., Fukuda, M., van Die, I., and Crocker, P.R. (2001). Cutting edge: CD43 functions as a T cell counterreceptor for the macrophage adhesion receptor sialoadhesin (Siglec-1). J Immunol *166*, 3637-3640.

Varki, A., and Crocker, P.R. (2009). I-type Lectins. In Essentials of Glycobiology, A. Varki, R.D. Cummings, J.D. Esko, H.H. Freeze, P. Stanley, C.R. Bertozzi, G.W. Hart, and M.E. Etzler, eds. (Cold Spring Harbor (NY)).

Varki, A., Esko, J.D., and Colley, K.J. (2009a). Cellular Organization of Glycosylation. In Essentials of Glycobiology, A. Varki, R.D. Cummings, J.D. Esko, H.H. Freeze, P. Stanley, C.R. Bertozzi, G.W. Hart, and M.E. Etzler, eds. (Cold Spring Harbor (NY)).

Varki, A., Etzler, M.E., Cummings, R.D., and Esko, J.D. (2009b). Discovery and Classification of Glycan-Binding Proteins. In Essentials of Glycobiology, A. Varki, R.D. Cummings, J.D. Esko, H.H. Freeze, P. Stanley, C.R. Bertozzi, G.W. Hart, and M.E. Etzler, eds. (Cold Spring Harbor (NY)).

Varki, A., Freeze, H.H., and Gagneux, P. (2009c). Evolution of Glycan Diversity. In Essentials of Glycobiology, A. Varki, R.D. Cummings, J.D. Esko, H.H. Freeze, P. Stanley, C.R. Bertozzi, G.W. Hart, and M.E. Etzler, eds. (Cold Spring Harbor (NY)).

Varki, A., and Schauer, R. (2009). Sialic Acids. In Essentials of Glycobiology, A. Varki, R.D. Cummings, J.D. Esko, H.H. Freeze, P. Stanley, C.R. Bertozzi, G.W. Hart, and M.E. Etzler, eds. (Cold Spring Harbor (NY)).

Varki, N.M., and Varki, A. (2007). Diversity in cell surface sialic acid presentations: implications for biology and disease. Lab Invest *87*, 851-857.

Verma, N.D., Plain, K.M., Nomura, M., Tran, G.T., Robinson, C., Boyd, R., Hodgkinson, S.J., and Hall, B.M. (2009). CD4+CD25+ T cells alloactivated ex vivo by IL-2 or IL-4 become potent alloantigen-specific inhibitors of rejection with different phenotypes, suggesting separate pathways of activation by Th1 and Th2 responses. Blood *113*, 479-487.

Vyse, T.J., Drake, C.G., Rozzo, S.J., Roper, E., Izui, S., and Kotzin, B.L. (1996). Genetic linkage of IgG autoantibody production in relation to lupus nephritis in New Zealand hybrid mice. J Clin Invest *98*, 1762-1772.

Wakeland, E., Morel, L., Achey, K., Yui, M., and Longmate, J. (1997). Speed congenics: a classic technique in the fast lane (relatively speaking). Immunol Today *18*, 472-477.

Waldmann, H., Graca, L., Cobbold, S., Adams, E., Tone, M., and Tone, Y. (2004). Regulatory T cells and organ transplantation. Semin Immunol *16*, 119-126.

Waldmann, T.A. (1993). The IL-2/IL-2 receptor system: a target for rational immune intervention. Immunol Today *14*, 264-270.

Walzel, H., Fahmi, A.A., Eldesouky, M.A., Abou-Eladab, E.F., Waitz, G., Brock, J., and Tiedge, M. (2006). Effects of N-glycan processing inhibitors on signaling events and induction of apoptosis in galectin-1-stimulated Jurkat T lymphocytes. Glycobiology *16*, 1262-1271.

Werwitzke, S., Trick, D., Kamino, K., Matthias, T., Kniesch, K., Schlegelberger, B., Schmidt, R.E., and Witte, T. (2005). Inhibition of lupus disease by anti-double-stranded DNA antibodies of the IgM isotype in the (NZB x NZW)F1 mouse. Arthritis Rheum *52*, 3629-3638.

Winer, S., Astsaturov, I., Gaedigk, R., Hammond-McKibben, D., Pilon, M., Song, A., Kubiak, V., Karges, W., Arpaia, E., McKerlie, C.*, et al.* (2002). ICA69(null) nonobese

diabetic mice develop diabetes, but resist disease acceleration by cyclophosphamide. J Immunol *168*, 475-482.

Wing, K., Onishi, Y., Prieto-Martin, P., Yamaguchi, T., Miyara, M., Fehervari, Z., Nomura, T., and Sakaguchi, S. (2008). CTLA-4 control over Foxp3+ regulatory T cell function. Science *322*, 271-275.

Wu, C., Rauch, U., Korpos, E., Song, J., Loser, K., Crocker, P.R., and Sorokin, L.M. (2009). Sialoadhesin-positive macrophages bind regulatory T cells, negatively controlling their expansion and autoimmune disease progression. J Immunol *182*, 6508-6516.

Xu, L., Kitani, A., Fuss, I., and Strober, W. (2007). Cutting edge: regulatory T cells induce CD4+CD25-Foxp3- T cells or are self-induced to become Th17 cells in the absence of exogenous TGF-beta. J Immunol *178*, 6725-6729.

Xu, Z., and Morel, L. (2010). Genetics of systemic lupus erythematosus: contributions of mouse models in the era of human genome-wide association studies. Discov Med *10*, 71-78.

Yamashita, T., Hashiramoto, A., Haluzik, M., Mizukami, H., Beck, S., Norton, A., Kono, M., Tsuji, S., Daniotti, J.L., Werth, N.*, et al.* (2003). Enhanced insulin sensitivity in mice lacking ganglioside GM3. Proc Natl Acad Sci U S A *100*, 3445-3449.

Yang, R.Y., Rabinovich, G.A., and Liu, F.T. (2008). Galectins: structure, function and therapeutic potential. Expert Rev Mol Med *10*, e17.

York, M.R., Nagai, T., Mangini, A.J., Lemaire, R., van Seventer, J.M., and Lafyatis, R. (2007). A macrophage marker, Siglec-1, is increased on circulating monocytes in patients with systemic sclerosis and induced by type I interferons and toll-like receptor agonists. Arthritis Rheum *56*, 1010-1020.

Zamoyska, R., Basson, A., Filby, A., Legname, G., Lovatt, M., and Seddon, B. (2003). The influence of the src-family kinases, Lck and Fyn, on T cell differentiation, survival and activation. Immunol Rev *191*, 107-118.

Zhou, X., Bailey-Bucktrout, S.L., Jeker, L.T., Penaranda, C., Martinez-Llordella, M., Ashby, M., Nakayama, M., Rosenthal, W., and Bluestone, J.A. (2009). Instability of the transcription factor Foxp3 leads to the generation of pathogenic memory T cells in vivo. Nat Immunol *10*, 1000-1007.